

Tolerance analysis and synthesis of assemblies subject to loading with process integration and design optimization tools

By

Maciej Mazur

B. Eng. Mechatronic (Hons.)

A thesis submitted in fulfilment of the requirements
of the degree of Doctor of Philosophy

April 2013

School of Aerospace, Mechanical and Manufacturing Engineering
RMIT University
Melbourne, Australia

ABSTRACT

Manufacturing variation results in uncertainty in the functionality and performance of mechanical assemblies. Management of this uncertainty is of paramount importance for manufacturing efficiency. Methods focused on the management of uncertainty and variation in the design of mechanical assemblies, such as tolerance analysis and synthesis, have been subject to extensive research and development to date. However, due to the challenges involved, limitations in the capability of these methods remain. These limitations are associated with the following problems:

- The identification of Key Product Characteristics (KPCs) in mechanical assemblies (which are required for measuring functional performance) without imposing significant modelling demands.
- Accommodation of the high computational cost of traditional statistical tolerance analysis in early design where analysis budgets are limited.
- Efficient identification of feasible regions and optimum performance within the large design spaces associated with early design stages.
- The ability to comprehensively accommodate tolerance analysis problems in which assembly functionality is dependent on the effects of loading (such as compliance or multi-body dynamics). Current Computer Aided Tolerancing (CAT) is limited by: the ability to accommodate only specific loading effects; reliance on custom simulation codes with limited practical implementation in accessible software tools; and, the need for additional expertise in formulating specific assembly tolerance models and interpreting results.
- Accommodation of the often impractically high computational cost of tolerance synthesis involving demanding assembly models (particularly assemblies under loading). The high computational cost is associated with traditional statistical tolerancing Uncertainty Quantification (UQ) methods reliant on low-efficiency Monte Carlo (MC) sampling.

This research is focused on addressing these limitations, by developing novel methods for enhancing the engineering design of mechanical assemblies involving uncertainty or variation in design parameters. This is achieved by utilising the emerging design analysis and refinement capabilities of Process Integration and Design Optimization (PIDO) tools.

The main contributions of this research are in three main themes:

- Design analysis and refinement accommodating uncertainty in early design;
- Tolerancing of assemblies subject to loading; and,
- Efficient Uncertainty Quantification (UQ) in tolerance analysis and synthesis.

The research outcomes present a number of contributions within each research theme, as outlined below.

Design analysis and refinement accommodating uncertainty in early design:

- A PIDO tool based visualization method to aid designers in identifying assembly KPCs in early design stages. The developed method integrates CAD software functionally with the process integration, UQ, data logging and statistical analysis capabilities of PIDO tools, to simulate manufacturing variation in an assembly and visualise assembly clearances, contacts or interferences. The visualization capability subsequently assists the designer in specifying critical assembly dimensions as KPCs.
- Computationally efficient method for manufacturing sensitivity analysis of assemblies with linear-compliant elements. Reduction in computational cost are achieved by utilising linear-compliant assembly stiffness measures, reuse of CAD models created in early design stages, and PIDO tool based tolerance analysis. The associated increase in computational efficiency, allows an estimate of sensitivity to manufacturing variation to be made earlier in the design process with low effort.
- Refinement of concept design embodiments through PIDO based DOE analysis and optimization. PIDO tools are utilised to allow CAE tool integration, and efficient reuse of models created in early design stages, to rapidly identify feasible and optimal regions in the design space. A case study focused on the conceptual design of automotive seat kinematics is presented, in which an optimal design is identified and subsequently selected for commercialisation in the Tesla Motors Model S full-sized electric sedan.

These contributions can be directly applied to improve the design of mechanical assemblies involving uncertainty or variation in design parameters in the early stages of design. The use of native CAD/E models developed as part of an established design modelling procedure imposes low additional modelling effort.

Tolerancing of assemblies subject to loading:

- A novel tolerance analysis platform is developed which integrates CAD/E and statistical analysis tools using PIDO tool capabilities to facilitate tolerance analysis of assemblies subject to loading. The proposed platform extends the capabilities of traditional CAT tools and methods by enabling tolerance analysis of assemblies which are dependent on

the effects of loads. The ability to accommodate the effects of loading in tolerance analysis allows for an increased level of capability in estimating the effects of variation on functionality.

- The interdisciplinary integration capabilities of the PIDO based platform allow for CAD/E models created as part of the standard design process to be used for tolerance analysis. The need for additional modelling tools and expertise is subsequently reduced.
- Application of the developed platform resulted in effective solutions to practical, industry based tolerance analysis problems, including: an automotive actuator mechanism assembly consisting of rigid and compliant components subject to external forces; and a rotary switch and spring loaded radial detent assembly in which functionality is defined by external forces and internal multi-body dynamics. In both case studies the tolerance analysis platform was applied to specify nominal dimensions and required tolerances to achieve the desired assembly yield.

The computational platform offers an accessible tolerance analysis approach for accommodating assemblies subject to loading with low implementation demands.

Efficient Uncertainty Quantification (UQ) in tolerance analysis and synthesis:

- A novel approach is developed for addressing the high computational cost of Monte Carlo (MC) sampling in statistical tolerance analysis and synthesis, with Polynomial Chaos Expansion (PCE) uncertainty quantification. Compared to MC sampling, PCE offers significantly higher efficiency.
- The feasibility of PCE based UQ in tolerance synthesis is established through: theoretical analysis of the PCE method identifying working principles, implementation requirements, advantages and limitations; identification of a preferred method for determining PCE expansion coefficients in tolerance analysis; and, formulation of an approach for the validation of PCE statistical moment estimates.
- PCE based UQ is subsequently implemented in a PIDO based tolerance synthesis platform for assemblies subject to loading. The resultant PIDO based tolerance synthesis platform integrates: highly efficient sparse grid based PCE UQ, parametric CAD/E models accommodating the effects of loading, cost-tolerance modelling, yield quantification with Process Capability Indices (PCI), optimization of tolerance cost and yield with multi-objective Genetic Algorithm (GA).
- To demonstrate the capabilities of the developed platform, two industry based case studies are used for validation, including: an automotive seat rail assembly consisting of compliant components subject to loading; and an automotive switch assembly in which

functionality is defined by external forces and multi-body dynamics. In both case studies optimal tolerances were identified which satisfied desired yield and tolerance cost objectives. The addition of PCE to the tolerance synthesis platform resulted in large computational cost reductions without compromising accuracy compared to traditional MC methods. With traditional MC sampling UQ the required computational expense is impractically high.

The resulting tolerance synthesis platform can be applied to tolerance analysis and synthesis with significantly reduced computation time while maintaining accuracy.

DECLARATIONS

I certify that except where due acknowledgement has been made, the work is that of the author alone; the work has not been submitted previously, in whole or in part, to qualify for any other academic award; the content of the thesis is the result of work which has been carried out since the official commencement date of the approved research program; any editorial work, paid or unpaid, carried out by a third party is acknowledged; and, ethics procedures and guidelines have been followed.

Maciej Mazur

April 2013

ACKNOWLEDGEMENTS

I would primarily like to show my gratitude for the extensive support of my supervisors Dr. Martin Leary and Prof. Aleksandar Subic. Their expertise, input and advice have been critically valuable throughout this research program.

Additionally, I would also like to acknowledge the support of the project Industry partners SMR Automotive Australia and Futuris Automotive Interiors. Their assistance has provided valuable industry relevant input into this research.

I would also acknowledge the financial support provided by the Commonwealth of Australia, through the Cooperative Research Centre for Advanced Automotive Technology (AutoCRC).

I am particularly thankful to my family and friends for their continued support and encouragement.

PUBLICATIONS

The following publications are associated with this research:

- Mazur M., Leary M., and Subic A. 2011. Computer Aided Tolerancing (CAT) platform for the design of assemblies under external and internal forces. *Journal of Computer-Aided Design*. Volume 43, Issue 6 (June 2011), p707-719.
- Mazur, M., M. Leary, S. Huang, T. Baxter and A. Subic (2011). Benchmarking study of automotive seat track sensitivity to manufacturing variation. *Proceedings of the 18th International Conference on Engineering Design (ICED11)*. S. J. H. Culley, B.J.; McAloone, T.C.; Copenhagen, Denmark, The Design Society. Vol. 10: 456-465.
- Mazur, M., M. Leary and A. Subic (2010). Automated simulation of stochastic part variation to identify key performance characteristics of assemblies. *6th Innovative Production Machines and Systems 2010 (IPROMS 2010) Conference*.
- Leary M., Mazur M., and Subic A. 2009. An integrated case study of material selection, testing and optimization. *Proceedings of the 17th International Conference on Engineering Design (ICED09)*. Norell Bergendahl, M.; Grimheden, M.; Stanford University, USA. The Design Society. Vol. 8: 345-356.
- Leary M., Mazur M., and Subic A. 2009. The integration of algebraic material selection and numeric optimization. *Machine Design, Monograph University of Novi Sad, 2009*.
- Leary, M., M. Mazur, T. Mild and A. Subic (2011). Optimization of automotive seat kinematics. *Sustainable Automotive Technologies 2010: Proceedings of the 2nd International Conference*. S. Hung. Greenville, South Carolina, USA, Springer: 139-144.
- Leary, M., M. Mazur, J. Gruijters and A. Subic (2010). Benchmarking and optimization of automotive seat structures. *Sustainable Automotive Technologies 2010: Proceedings of the 2nd International Conference*. J. Wellnitz, Springer: 63-70.
- Leary, M, Mac, J, Mazur, M, Schiavone, F and Subic, A 2010, Enhanced shape memory alloy actuators. *J. Wellnitz, Sustainable Automotive Technologies 2010: Proceedings of the 2nd International Conference, Springer-Verlag, Berlin Heidelberg, pp. 183-190*.
- Leary, M., J. Gruijters, M. Mazur, A. Subic, M. Burton and F. Fuss (2012). A fundamental model of quasi-static wheelchair biomechanics. *Journal of Medical Engineering & Physics* 34(9): 1278-1286.

TABLE OF CONTENTS

Abstract	i
Declarations	v
Acknowledgements	vi
Publications	vii
Table of Contents	viii
List of Figures	xiii
List of Tables	xvii
Nomenclature	xix
List of Symbols	xx
1 Introduction	1
1.1 Background and industry collaboration.....	1
1.2 Introduction and motivation.....	1
1.3 Research scope and objectives	5
1.4 Research questions	10
1.5 Methodology.....	10
1.6 Key outcomes and contributions:	12
1.7 Thesis Outline.....	14
2 Literature Review	15
2.1 Chapter summary.....	15
2.2 Stochastic manufacturing systems	19
2.2.1 Uncertainty	19
2.2.2 Quality.....	21
2.2.3 Quality loss and cost-tolerance relationships	22
2.2.3.1 Cost-Tolerance models	24
2.2.3.2 Cost of quality loss	25
2.3 Tolerance analysis.....	25
2.3.1 Worst-case and statistical tolerancing	27
2.3.2 Tolerancing schemes	27
2.3.3 Manufacturing variation distributions	28
2.3.4 Process Capability Indices (PCI)	29
2.4 Tolerance modelling.....	30
2.4.1 Manual tolerance charts.....	30
2.4.2 Parametric CAD based CAT.....	32
2.4.3 Abstracted geometry CAT and multi-variate regions.....	34
2.5 Uncertainty Quantification (UQ) methods	36

2.5.1	Sampling based methods	38
2.5.1.1	Monte Carlo (MC) simulation	38
2.5.1.2	Latin hypercube (LHC) simulation.....	39
2.5.2	Analytical methods - Elementary	40
2.5.2.1	Root Sum of Squares (RSS) method.....	40
2.5.2.2	Taguchi method	41
2.5.2.3	Other elementary analytical methods.....	42
2.5.3	Analytical methods - Advanced	42
2.6	Tolerance synthesis.....	43
2.6.1	Optimization	45
2.6.2	Optimization algorithms	47
2.6.2.1	Genetic algorithm (GA)	48
2.7	Computer Aided Tolerancing (CAT) tools	49
2.8	Process Integration and Design Optimization (PIDO)	52
2.9	Tolerance analysis and synthesis of assemblies subject to loads.....	54
2.10	Summary of outcomes and opportunities for further work.....	58
3	Development of enhanced PIDO methods for design analysis and refinement.....	61
3.1	Chapter summary.....	61
3.2	Introduction	61
3.2.1	PIDO tools	67
3.2.2	Accommodating manufacturing variation in conceptual and embodiment design.....	67
3.2.3	Assembly complexity	68
3.2.4	Key Product Characteristics (KPCs).....	68
3.2.5	Assembly response function modelling.....	70
3.2.6	CAD tools	70
3.2.7	Uncertainty quantification strategy	71
3.3	Visualization method for the identification of KPCs based on sensitivity analysis	72
3.3.1	Potential limitations	74
3.3.2	Case Study 3.1 – Visualization method for identification of KPCs in a conceptual embodiment design of an automotive actuator assembly	75
3.3.2.1	Process data	75
3.3.2.2	PIDO integration	76
3.3.2.3	Results.....	78
3.3.3	Discussion of results	81
3.4	Computationally efficient manufacturing sensitivity analysis for assemblies with linear-compliant elements	82
3.4.1	Manufacturing sensitivity analysis of automotive seat rail assemblies	83
3.4.2	Variation in coefficient of rolling resistance.....	86
3.4.3	Variation in rolling element contact force	86

3.4.3.1	Linear-compliant rail representation	87
3.4.3.2	FE contact force model	88
3.4.4	Variation in rolling element clearance	90
3.4.5	Assumptions	92
3.4.6	Results.....	92
3.4.6.1	Rail assembly A	92
3.4.6.2	Rail assembly B.....	93
3.4.6.3	Rail assemblies C, D and E.....	94
3.4.7	Benchmarking of designs.....	95
3.4.8	Discussion of results	97
3.5	Refinement of concept design embodiments through PIDO based DOE analysis and optimization	99
3.5.1	Automotive seat kinematics	99
3.5.2	PIDO based DOE analysis and optimization of the conceptual design of automotive seat kinematics	101
3.5.2.1	Results.....	103
3.5.3	Other applications	105
3.5.4	Discussion of results	106
3.6	Summary of research outcomes	108
4	Novel approach for PIDO based tolerance analysis of assemblies subject to loading	111
4.1	Chapter summary.....	111
4.2	Introduction	111
4.3	Effects of loads in tolerance analysis	113
4.4	PIDO based tolerance analysis platform.....	115
4.4.1	Platform flowchart.....	116
4.4.2	Parametric CAD model	119
4.4.3	Physical model simulation	120
4.4.4	Uncertainty quantification strategy	121
4.4.5	Variation database.....	121
4.4.6	Yield estimation	122
4.5	Case study 4.1 - Assembly design subject to external forces	123
4.5.1	Problem definition.....	123
4.5.2	Sources of variation	124
4.5.2.1	Variation in injection moulding	124
4.5.2.2	Variation in spring wire.....	125
4.5.3	Variation data used in simulation.....	125
4.5.4	Simulation model.....	126
4.5.5	Simulation results	128
4.5.6	Outcomes.....	131
4.5.7	Potential sources of error.....	131

4.6	Case study 4.2 - Assembly design subject to both external and internal forces	133
4.6.1	Problem definition	133
4.6.2	Sources of variation	134
4.6.3	Variation data used in simulation.....	134
4.6.4	Simulation model.....	135
4.6.5	Simulation results and outcomes	137
4.6.5.1	Initial simulation	137
4.6.5.2	Second simulation.....	138
4.7	Summary of research outcomes	140
5	PIDO based tolerance synthesis in assemblies subject to loading using polynomial chaos expansion	143
5.1	Chapter summary.....	143
5.2	Introduction	144
5.3	Tolerance synthesis.....	145
5.4	PIDO based tolerance synthesis.....	146
5.5	Quantification of quality and cost.....	148
5.5.1	Cost-tolerance modelling	149
5.5.2	Quality loss and process capability.....	150
5.6	Yield estimation by uncertainty quantification	151
5.6.1	Sampling based UQ methods	152
5.6.2	Analytical UQ methods.....	152
5.7	Polynomial Chaos Expansion (PCE)	153
5.7.1	Unidimensional Polynomial Chaos Expansion – Derivation of moment expressions	154
5.7.2	Multidimensional PCE.....	158
5.7.3	Higher order moments	159
5.7.4	Non-normal distributions and correlated variables	160
5.7.5	Methods for calculating PCE coefficients	161
5.7.5.1	Collocation	161
5.7.5.2	Stochastic projection	163
5.7.5.3	Complete product grid quadrature.....	164
5.7.5.4	Sparse grid quadrature	166
5.7.5.5	Anisotropic sparse grids and adaptive PCE.....	170
5.7.6	Recommendations for calculating PCE coefficients	171
5.7.7	PCE error estimates	172
5.8	Case study 5.1	173
5.8.1	Problem definition	173
5.8.2	Variation in rail geometry and tolerance costs	176
5.8.3	Simulation models	180
5.8.4	UQ strategy.....	183

5.8.5	Optimization strategy	184
5.8.6	Assumptions	184
5.8.7	Simulation results and outcomes	185
5.9	Case study 5.2	188
5.9.1	Problem definition	188
5.9.2	Simulation model and optimization	190
5.9.3	UQ strategy	191
5.9.4	Optimization strategy	192
5.9.5	Simulation results and outcomes	192
5.10	Summary of research outcomes	195
6	Conclusion.....	197
6.1	Chapter Summary	197
6.2	Contributions	198
	The contributions of this work are presented below according to the associated research theme.	198
6.2.1	Design analysis and refinement accommodating uncertainty in early design (Chapter 3)	198
6.2.2	Tolerancing of assemblies subject to loading (Chapter 4)	203
6.2.3	Efficient uncertainty quantification in tolerance analysis and synthesis (Chapter 5)	206
6.3	Future work.....	210
	Appendices.....	213
A.	Tolerancing schemes.....	214
A.1	Dimensional tolerancing	214
A.2	Geometric Dimensioning and Tolerancing (GD&T).....	214
A.3	Vectorial tolerancing	218
B.	Process capability.....	220
B.1	Process capability index – C_p	220
B.2	Process capability index – C_{pk}	220
B.3	Process capability index – C_{pm}	221
B.4	Process capability indices – Non-normal distributions	222
	References.....	223

LIST OF FIGURES

Figure 1.1 – Thesis map	9
Figure 2.1 – Literature review topic outline	16
Figure 2.2 - Classification of costs associated with poor quality (Feigenbaum 2012).....	23
Figure 2.3 – Relationship between quality control and cost (Juran 1992).....	24
Figure 2.4 - Normal distribution and confidence intervals.....	28
Figure 2.5 - Simple mechanical assembly example with all parameters X1 to X5 subject to a dimensional tolerance of +/- 0.1mm	31
Figure 2.6 - Changing assembly contact conditions due to manufacturing variation of parts. CAD systems can be limited in ability to automatically modify part mating conditions to reflect certain realistic part contacts within an assembly.....	33
Figure 2.7 - Normal distribution with LHC sampling strata of equal probability (N=8).....	39
Figure 3.1 - Steps of planning and design process. Reproduced from Pahl and Beitz 2007 (Pahl et al. 2007). Contributions of this chapter are identified in red.....	63
Figure 3.2 - (i) Design flexibility and knowledge versus project timeline (ii) Cost commitment and accrument during phases of the design process, after (Ullman 2003).....	64
Figure 3.3 - Visualization approach for the identification of KPCs within the native CAD design environment using PIDO tools.....	73
Figure 3.4 - Histogram of measured production component used to establish PCIs.....	76
Figure 3.5 - Parametric CAD assembly model of concept actuator design	77
Figure 3.6 - PIDO workflow for visualization methodology for identification of KPCs - Actuator assembly.	77
Figure 3.7 - Frequency of interference between assembly parts.....	78
Figure 3.8 - Part parameter sensitivity to interference	79
Figure 3.9 - Assembly regions identified as being prone to unwanted part interference. KPCs were defined to avoid the identified interference scenarios.	80
Figure 3.10 - (i) Automotive seat (ii) seat rail assembly (iii) - (vii) Alternative rail assembly section views.....	85
Figure 3.11 - Linear compliant rail simplification.	87
Figure 3.12 - FE model details (rail assembly B). All dimensions in mm.	89
Figure 3.13 - Rail deflection due to interference fit of rolling element (rail assembly B). Contact area shown in detail.	90
Figure 3.14 - PIDO workflow associated with seat rail benchmarking study.	91
Figure 3.15 - Rail assembly A rolling element clearance distribution. (i) Upper ball (ii) Lower ball.....	93

Figure 3.16 - Rail assembly A rolling element specification limits. Shaded profile corresponds to nominal rail dimensions. Upper Ball (UB), Lower Ball (LB).....	93
Figure 3.17 - Rail assembly B rolling element clearance distributions. (i) Left roller (ii) Bottom roller (iii) Right ball.....	94
Figure 3.18 - Rail assembly B rolling element specification limits. Shaded profile corresponds to nominal rail dimensions. Left Roller (LR), Bottom Roller (BR), Right Ball (RB).	94
Figure 3.19 - Rolling element contact force versus local rail displacement. Gradient indicates stiffness.	95
Figure 3.20 - Magnitude of variation in nominal rolling element clearance versus rail assembly design.	96
Figure 3.21 - Four-bar linkage and associated nomenclature (Leary et al. 2011).	101
Figure 3.22 - PIDO workflow associated with the second phase of design refinement and optimization of automotive seat kinematic concept designs.....	102
Figure 3.23 - Four-dimensional chart indicating performance of Pareto-optimal solutions in the conceptual design of automotive seat kinematics. Designs referred to in the discussion have been labelled with associated identification numbers.	104
Figure 3.24 - (i) Quasi-static model of users arm and wheelchair wheel interaction (Leary et al. 2012).....	106
Figure 4.1 - General tolerance analysis of a mechanical assembly. Stages are identified as per Section 4.2.....	113
Figure 4.2 - PIDO based tolerance analysis platform.....	118
Figure 4.3 - Spring and spigot assembly.	123
Figure 4.4 - Spring spigot assembly and FE model of spring.	127
Figure 4.5 - PIDO tolerance analysis workflow for Case study 4.1.	128
Figure 4.6 - Histogram of clearance measurements for spigot outer diameter ($OD_{measure}$). (Note: Solid line indicates estimated population distribution based on sample results. The initial analysis provided a yield of approximately 96.8 % for the spring outside diameter.).....	129
Figure 4.7 - Histogram of clearance measurements for spigot inner diameter ($ID_{measure}$). (Note: Solid line indicates estimated population distribution based on sample results. The initial analysis provided a yield of approximately 97.1 % for the spring inside diameter.)	129
Figure 4.8 - Student chart of $ID_{measure}$	130
Figure 4.9 - Student chart of $OD_{measure}$	130
Figure 4.10 - Histogram of clearance measurement error	132
Figure 4.11 - Comparison of original and meshed spring geometry. Light shade indicates a difference of mesh geometry from original by 50.00×10^{-3} mm (smallest tolerance used in simulation)	132

Figure 4.12 - Rotary switch and spring loaded radial detent assembly model used in Case study 4.2.....	134
Figure 4.13 - Transient resistive torque for 1000 assembly variants resulting from initial simulation.....	136
Figure 4.14 - PIDO tolerance analysis workflow for Case study 4.2.	137
Figure 4.15 - Histogram of peak resistive torques obtained from initial simulation	138
Figure 4.16 - Student chart of peak resistive torque for initial simulation	138
Figure 4.17 - Histogram of peak resistive torques for second simulation.....	139
Figure 4.18 - Student chart of peak resistive torque for second simulation.....	139
Figure 5.1 - PIDO based tolerance synthesis platform. Extension of the PIDO based tolerance analysis platform presented in Section 4.4. (Figure 4.2).	148
Figure 5.2 - (i) Exponential cost-tolerance relationship, (ii) Chain of cost-tolerance curves for multiple manufacturing processes of varying precision ($V=3$).	150
Figure 5.3 - Multidimensional full product and sparse grid Gauss-Hermite Quadrature with level 2 for 2 dimensions and $O = 2l + 1 - 1$ growth rule.....	169
Figure 5.4 - (i) Automotive seat and rail assembly (black) (ii) seat rail assembly section view including die-press folding sequence for upper and lower rails.....	174
Figure 5.5 - Measured rail assembly (i) CMM mounting jig and sample rails under measurement (ii) general jig dimensions (ii) section measurement locations (iii) section view including folding sequence for upper and lower rails (iv) sample upper rail variation (v) sample lower rail variation.	178
Figure 5.6 - Influence of additional samples to the change in overall standard deviation for a total of 24 measured rail sets.	179
Figure 5.7 - Cost-tolerance curves for rail bend angles for varying levels of variation control difficulty. The process curves are plotted only within the feasible limits of the associated process.	179
Figure 5.8 - Cost-tolerance curves for rail radii angles for varying levels of variation control difficulty. The process curves are plotted only within the feasible limits of the associated processes.....	180
Figure 5.9 - (i) Rail section parameters (alpha numeric label designates stochastic variable – see Table 5.8)	181
Figure 5.10 - PIDO tolerance synthesis workflow for Case study 5.1.....	183
Figure 5.11 - Objectives space of tolerance synthesis for Case study 5.1.....	186
Figure 5.12 - Rotary switch and spring loaded radial detent assembly model used in Case study 5.2.....	189
Figure 5.13 - Cost-tolerance curves for part parameters of radial detent assembly	190
Figure 5.14 - PIDO tolerance synthesis workflow for Case study 5.2.....	191

Figure 5.15 - Objectives space of tolerance synthesis for Case study 5.2.....	194
Figure A.1 - GD&T tolerance control frame.....	217
Figure A.2 - Traditional dimensional tolerancing (i). Traditional tolerancing involves datum ambiguity in manufactured parts (ii). GD&T tolerancing including alphabetical datums precedence specification (iii) eliminates ambiguity.	218
Figure A.3 - Process output distributions with decreasing standard deviation. C_p increasing from left to right with decreasing standard deviation.	220
Figure A.4 - Process output distributions of equal standard deviation and increasing centring. C_p is equal for all distributions. C_{pk} increases from left to right with increasing centring.....	221
Figure A.5 - Process distributions with non-symmetric specification limits. C_{pm} increasing from left to right:	221

LIST OF TABLES

Table 2.1 - Proposed cost-tolerance functions (Wu et al. 1988; Dong et al. 1994).	24
Table 2.2 - Comparison of various Tolerance Analysis methods.....	30
Table 2.3 - Tolerance chart for simple assembly example in Figure 2.5.	31
Table 2.4 - Classification of optimization algorithms	47
Table 2.5 - Comparison of commercial CAT tools. Limitations in current CAT tools are identified in bold.....	51
Table 3.1 - Process capability data of measured component (Figure 3.4). Results based on combined measurements across all locations and from all moulding cavities. ...	76
Table 3.2 - Rail assembly designs considered in benchmarking analysis.	86
Table 3.3 - Rail section parameter variation specified by industry partner and used in statistical tolerance analysis	91
Table 3.4 - Ball dimensions used for contact force simulation in rail assembly A	92
Table 3.5 - Ball dimensions used for contact force simulation in rail assembly B.....	94
Table 3.6 - Performance ranking of conceptual rail assembly designs.	97
Table 3.7 - Classification of four-bar mechanisms.....	101
Table 3.8 - Model input parameters.....	103
Table 3.9 - Model output parameters, dimension and objective.....	103
Table 3.10 - Benchmarking results against other competing products.....	104
Table 4.1 - Process capability data of measured component in Test Case 4.1.	126
Table 4.2 - Spigot and spring assembly parameters and associated variation.	126
Table 4.3 - Initial and required nominal spigot wall dimensions based on simulated clearance measurements.	131
Table 4.4 - Case study 4.2 rotary switch assembly parameters and associated variation....	135
Table 5.1 - Generalized polynomial chaos expansion (gPCE) basis and weighting functions for various parameter distributions (Xiu et al. 2003; Eldred et al. 2008)	160
Table 5.2 - Minimum number of simulations N required for point collocation based PCE with various expansion order k, and dimensionality d. Oversampling ratio $s = 2$ (as recommended in (Hosder et al. 2007)).....	162
Table 5.3 - Monomials for $d = 2$ complete product grid with excess monomials highlighted	167
Table 5.4 - Number of points required for isotropic sparse grids and full product grids based on Gauss-Hermite quadrature rules with growth rule $O = 2l + 1 - 1$, for multiple dimensions and grid levels. Precision indicates the maximum	

polynomial degree which can be exactly represented by the associated quadrature.	170
Table 5.5 - Case study 5.1 objectives and constraints.	176
Table 5.6 - Standard deviation in measured rail folds. Classification of the level of difficulty in controlling associated variation for both the case study rail (Figure 5.4 (ii)) and the measured rail (Figure 5.5 (iii))	177
Table 5.7 - Combined averaged standard deviation associated with low and high difficulty folds for measured rail.....	177
Table 5.8 - Rail assembly parameters and associated variation for initial design and selected optimum.....	187
Table 5.9 - Case study 5.2 objectives and constraints	189
Table 5.10 - Case study 5.2 assembly parameters, associated variation and tolerance synthesis outcomes.....	193
Table A.1 - GD&T variation types and standardised symbols (after ANSI Y14.5).....	216

NOMENCLATURE

Term	Definition
<i>BR</i>	Bottom Roller
<i>CAD</i>	Computer Aided Design
<i>CAE</i>	Computer Aided Engineering
<i>CAT</i>	Computer Aided Tolerancing
<i>CFD</i>	Computational Fluid Dynamics
<i>CMM</i>	Coordinate measurement machine
<i>CPU</i>	Central Processing Unit
<i>DOE</i>	Design of experiments
<i>DoF</i>	Degree of freedom
<i>FE</i>	Finite Element
<i>FEA</i>	Finite Element Analysis
<i>FEM</i>	Finite Element Modelling
<i>GD&T</i>	Geometric Dimensioning and Tolerancing
<i>gPCE</i>	generalized Polynomial Chaos Expansion
<i>KPC</i>	Key Product Characteristic. A parameter of relevance to functionality.
<i>LB</i>	Lower Ball
<i>LHC</i>	Latin Hypercube
<i>LMC</i>	Least Material Condition.
<i>LR</i>	Left Roller
<i>LSL</i>	Lower Specification Limit. The minimum limit of a parameter or KPC.
<i>MC</i>	Monte Carlo
<i>MDO</i>	Multi-disciplinary Design Optimization
<i>MMC</i>	Maximum Material Condition.
<i>MOGA</i>	Multi-Objective Genetic Algorithm
<i>Parameter</i>	Any variable of a part or an assembly
<i>PC</i>	Point Collocation
<i>PCE</i>	Polynomial Chaos Expansion
<i>PCI</i>	Process Capability Index.
<i>PIDO</i>	Process Integration and Design Optimization
<i>QLF</i>	Quality loss function
<i>Quality</i>	The degree to which a manufactured assembly fulfils specified KPCs
<i>RB</i>	Right Ball
<i>RSM</i>	Response Surface Modelling
<i>RSS</i>	Root Sum of Squares
<i>SFE</i>	Stochastic Finite Element
<i>SFEM</i>	Stochastic Finite Element Modelling/Model
<i>SG</i>	Sparse Grid
<i>Specification limits</i>	Acceptable limits of a parameter or KPC
<i>TTRS</i>	Technologically and Topologically Related Surfaces
<i>UB</i>	Upper Ball
<i>UQ</i>	Uncertainty Quantification
<i>USL</i>	Upper Specification Limit. The minimum limit of a parameter or KPC.
<i>Yield</i>	Percentage of assemblies which conform to the KPC specification limits

LIST OF SYMBOLS

Parameter	Description
σ	Standard deviation
μ	Mean
γ	Skewness
β	Kurtosis
δ_μ	Difference between estimates of the mean
δ_σ	Difference between estimates of the standard deviation
δ	Influence of additional samples to the change in sample σ
N	Number of terms, samples, or integration points
a_N	Linear constants
d	Dimension
m	Dimension index $m = 1 \dots d$
f	Response function
x	Part or assembly parameter
x_j	Sampling or integration point
$E[f(x)]$	The expected value or population mean
$w(x)$	probability density function
$\langle y^n \rangle$	The n^{th} statistical raw moment (i.e. moment about zero)
i	Summation or product index
j	Summation or product index
$p_i(x)$	Polynomial of degree i
α_i	Polynomial basis coefficients
k	Maximum order of the polynomial
$H_k(x)$	The Hermite polynomial series
ξ_N	Collocation point
s	Point collocation oversampling factor
N_c	number of collocation points
$N_{\text{Complete grid}}$	The total number of terms in a complete product grid
$N_{\text{sparse grid}}$	The total number of terms in a sparse grid
Δ	The sum of the squares of the difference between the expansion of order k and the response function f
ρ_m	Precision level in each dimension $m = 1 \dots d$
Q_{l_m}	interpolatory quadrature rule for variable $m = 1 \dots d$
w_j	Quadrature rule weight
l_m	Level of unidimensional quadrature rules Q_{l_m} with associated l_m for variable $m = 1 \dots d$.
L	Sparse grid level
$A(L, d)$	A sparse grid of level L (for $L \geq 0$) and dimension d
\vec{l}	Vector of unidimensional quadrature rule levels l_m in each dimension $m = 1 \dots d$.
$ \vec{l} $	Product level
\otimes	Tensor product
O	Growth rule associated with a quadrature rule Q_{l_m}
r	Indicator of the smoothness of an integrand

Parameter	Description
C_p	Process capability index which measures the potential of a process to produce outputs within the specification limits
C_{pk}	Process capability index which measure the ability of a process to produce an output that is centred and within the specification limits
C_{pm}	Process capability index which measure the ability of a process to produce an output that is at an arbitrary target and within the specification limits
C_{npk}	Process capability index measuring the performance of processes with non-normal distributions
τ	Target nominal value
\bar{m}	The median of a distribution
ζ	Number of possible interactions in an assembly
g_0	Minimum threshold tolerance cost
κ	Quality loss function weighting constant
T_0	Minimum threshold tolerance of cost-tolerance curve
Z	Cost-tolerance curve fitting parameter derived from experimental data
ϕ	Cost-tolerance curve fitting parameter derived from experimental data
T_{min}	Minimum economically feasible tolerance
T_{max}	Maximum economically feasible tolerance
T	Tolerance value of cost-tolerance curve
$g(T)$	Tolerance cost for a specific component
$G(T)$	Total tolerance cost of an assembly
t	Minimum bore wall thickness
$ID_{measure}$	Clearance between the internal diameter of the spring and the spigot wall
$OD_{measure}$	Clearance between the outer diameter of the spring and the spigot wall
OD_{pocket}	Outside diameter of pocket
ID_{pocket}	Inside diameter of pocket
D_{wire}	Diameter of spring wire
D_{mean}	Mean diameter of spring
H	Spring height
P	Spring pitch
E	Young's modulus of spring
R_{switch}	Switch radius
R_{ball}	Ball radius
A	Angle of ramp face
Θ	Yaw angle of ramp face
F	Spring preload
K	Spring rate
μ_{switch}	Switch-detent dynamic friction coefficient
μ_{slider}	Slider-detent dynamic friction coefficient
ζ	Shortest link in a four-bar linkage
λ	Longest link in a four-bar linkage
ϑ, φ	Intermediate length links in a four-bar linkage

1 INTRODUCTION

1.1 Background and industry collaboration

This research program was conducted in collaboration with tier-one automotive component manufacturers, namely SMR Automotive Australia and Futuris Automotive Interiors, with federal government support through the Australian Cooperative Research Centre for Advanced Automotive Technology (AutoCRC). The research program was initiated to investigate technological solutions for maximising the functionality of automotive seating and automotive actuator assemblies. Extensive consultation with the industry, and rigorous review of existing literature identified deficiencies in the understanding and management of the effects of manufacturing variation on the functionality of complex mechanical assemblies. Addressing these deficiencies provides a significant opportunity for improving manufacturing efficiency, product reliability and quality. Specific opportunities for novel research were subsequently identified and addressed in this dissertation.

1.2 Introduction and motivation

In the process of engineering design, the cost of implementing changes to design decisions typically increases non-linearly as the design progresses. This non-linear cost increase is attributed to progressively accumulating commitments to high-capital resources, such as detailed design efforts, production plans, tooling, prototyping and testing (Pahl *et al.* 2007). Consequently, a high proportion of the cost of engineering and delivering a product can be attributed to the decisions made during the early stages of design. In response to these observed relationships, engineering design philosophy advises that available design and analysis resources should be focused towards the early stages of the project; this maximises knowledge of the design problem, and the expected performance of any design embodiments, while the flexibility to enact changes is high, and accrued costs are low (Pugh 1991; Baumgartner 1995).

Design analysis and refinement techniques provide an efficient means of increasing knowledge of the design problem, and expected performance, early in the project timeline. Such design analysis and refinement techniques include: sensitivity analysis; Design Of Experiments (DOE) studies; tolerance/robustness analysis; and, optimization methods.

These design analysis and refinement techniques allow for: effective selection and refinement of design embodiments; evaluation against technical and economic criteria; identification of errors; and, evaluation of cost effectiveness. This capability allows the designer to make informed decisions regarding design improvement while there is sufficient design flexibility to act without undue expense.

Despite the high benefit of analysis and refinement early in the design process, in practice it may be difficult to achieve as many influential technical and economic properties remain undefined or uncertain. This design uncertainty results in a broad design space in which feasible regions and optimum performance can be difficult to identify efficiently without imposing significant design analysis expense. Research efforts into effective ways of addressing design uncertainty are ongoing (Smith *et al.* 1997; Thompson *et al.* 1999; Krishnan *et al.* 2001; Tomiyama *et al.* 2009; Ebro *et al.* 2012).

Stochastic manufacturing variation is a particularly significant source of uncertainty as it has a high influence on the ability of manufactured products to achieve specified performance requirements. Stochastic manufacturing variation effects in mechanical assemblies are managed by the specification of tolerances. Tolerances denote the permissible variation of parameters such that required assembly functionality is achieved. Identification of the effects of parameter variation on assembly functionality, and the specification of optimal tolerances, are referred to as tolerance analysis and tolerance synthesis, respectively. These are challenging problems involving the competing objectives of manufacturing cost and product quality, as well as constraints imposed by product and manufacturing process requirements (Shah *et al.* 2007).

Addressing the effects of manufacturing variation in early design can reduce the costs of managing poor quality later in the manufacturing stage when the ability to enact change is limited (Bergman *et al.* 2009; Ebro *et al.* 2012). In particular, design analysis and refinement based on tolerance analysis of concept design embodiments can provide insight into the sensitivity of alternative concepts to manufacturing variation, and facilitate concept selection with quantitative measures of robustness. This early increase of design knowledge allows the designer to make informed decisions addressing the effects of manufacturing variation, while there is sufficient design flexibility to act without much expense. Estimating the effects of variation on assembly functionality is typically achieved with tolerance analysis based on a computational assembly tolerance model (Chase 1988). However, traditional statistical tolerance analysis methods typically require a large number of evaluations of the assembly tolerance model which imposes high computational costs.

These computational costs are difficult to accommodate early in design where analysis budgets for individual concept designs are limited (Chase 1988; Soderberg *et al.* 1999; Pahl *et al.* 2007; Shah *et al.* 2007; Singh *et al.* 2009).

Tolerance analysis requires the specification of assembly parameters which indicate whether a given manufactured assembly will conform to the intended functional requirements of the design. The parameters of particular relevance to functionality are referred to as Key Product Characteristics (KPCs), and are typically geometric, such as clearances or nominal dimensions. However, the complexity which arises in product assemblies with many interacting parts and features can make the identification of assembly KPCs a challenging task for the designer due to difficulty in visualizing and understanding variation effects in complex assemblies. Currently there is a lack of an accessible and efficient approach which can aid in the identification of KPCs within the native CAD environment, without imposing significant additional modelling and expertise demands (Thornton 1999; Dahl *et al.* 2001; Zhou *et al.* 2008).

The functionality of mechanical assemblies is often defined in terms of the minimum or maximum allowable proximity between geometric features. However in many mechanical assemblies, functionality is also dependent on loading, including: external or internal forces, temperature changes or electromagnetic interaction. These loads influence assembly functionality through effects such as compliance, dynamics and mechanical wear (Shigley *et al.* 2004; Lovasz 2012). These effects are particularly relevant in, for example: mechanical actuators, automotive seat positioning mechanisms, sheet metal assemblies (such as automotive or aerospace body panels), bolted connections subject to fastener and hole alignment tolerances, and assemblies subject to welding induced thermo-mechanical distortion. The ability to accommodate the effects of loading in tolerance analysis allows for a more realistic prediction of assembly behaviour in the presence of manufacturing variation. Analytical and numerical methods have been proposed for addressing tolerance analysis and synthesis problems in complex mechanical assemblies. However, current approaches are limited in their ability to comprehensively accommodate tolerance analysis problems in which assembly functionality is dependent on the effects of loading. Limitations include (Liu *et al.* 1997; Merkley 1998; Shiu *et al.* 2003; Lee *et al.* 2009; Pierre *et al.* 2009):

- Reliance on specific, custom simulation codes with limited implementation in practical and accessible tools, as well as the need for significant additional expertise in formulating specific assembly tolerance models and interpreting results.

- Accommodation of only specific loading scenarios (such as sheet metal compliance or welding-distortion).

Additionally, Computer Aided Tolerancing (CAT) software tools have been developed which offer practical tolerance analysis and synthesis capabilities. However, current commercial CAT tools generally lack the ability to accommodate tolerance analysis of assemblies whose functionality is dependent on various loading effects (Salomons *et al.* 1998; Prisco *et al.* 2002; Chiesi *et al.* 2003; Zhengshu 2003; Shen 2005; Shah *et al.* 2007). As such, there is currently a lack of an accessible approach to tolerance analysis of assemblies subject to loading, which integrates into an established CAD/E design frameworks.

Manual iteration of tolerance analysis can be ineffective at identifying tolerances which achieve optimum manufacturing cost and yield targets. Tolerance synthesis improves the ability to identify optimal tolerances by utilising optimization algorithms. However, the ability of available CAT tools to effectively address sophisticated optimization problems (such as tolerance synthesis in complex assemblies) with many competing objectives and constraints is relatively limited compared to dedicated optimization tools. Furthermore, tolerance synthesis requires that tolerance analysis be iterated, thereby compounding computational costs, especially when numerical modelling of the effects of loading on mechanical assemblies is required. The cost of such tolerance synthesis is often seen as computationally impractical and not warranting the associated benefits (Hong *et al.* 2002). A major reason for the high computational cost is associated with the estimation of yield in tolerance analysis based on Uncertainty Quantification (UQ) methods. The traditional approach to UQ in statistical tolerance analysis is reliant on sampling based UQ methods such as Monte Carlo (MC) sampling. MC sampling is typically applied due to its inherent robustness and broad applicability. However MC sampling has poor efficiency and requires a large number of model evaluations for accurate results, which can impose high computational costs with demanding models (Nigam *et al.* 1995).

The observations summarised above identify a number of active areas of research, and limitation in existing knowledge, which can be categorically grouped according to three research themes. A summary of the identified limitations associated with each theme is presented below:

Theme 1: Design analysis and refinement accommodating uncertainty in early design stages

- Identifying Key Product Characteristics (KPCs) is challenging due to difficulty in visualizing and understanding variation effects in complex assemblies without imposing significant additional modelling and expertise demands.
- Traditional statistical tolerance analysis imposes high computational costs, which are difficult to accommodate early in design where analysis budgets are limited for individual concept designs.
- Early design stages are often associated with a vast design space in which feasible regions and optimum performance are difficult to identify.

Theme 2: Tolerancing of assemblies subject to loading

- There is a lack of an accessible approach for tolerance analysis of assemblies subject to general loading effects, which integrates into an established CAD/E design frameworks.
- Current Computer Aided Tolerancing (CAT) systems are limited in their ability to accommodate a general class of tolerance analysis and synthesis problems requiring simulation of the effects of loading on mechanical assemblies.
- Compared to dedicated optimization software, CAT tools have a narrower ability to address sophisticated tolerance synthesis optimization problems.

Theme 3: Efficient uncertainty quantification in tolerance analysis and synthesis

- The cost of tolerance analysis, and in particular tolerance synthesis, involving demanding assembly models (particularly assemblies under loading) can often be computationally impractical. The high computational cost is mainly associated with traditional statistical tolerancing Uncertainty Quantification (UQ) methods reliant on low-efficiency Monte Carlo (MC) sampling.

The identified limitations and gaps in domain knowledge provide the motivation for the research undertaken in this dissertation. The associated research objectives and scope are presented in the following section.

1.3 Research scope and objectives

The motivation discussed in the previous section identified a number of active areas of research and limitations in domain knowledge associated with three research themes. Specific opportunities for addressing the identified limitations define the research scope and objectives of this dissertation and are outlined below under each associated research

theme. Additionally, a thesis map is provided in Figure 1.1 which identifies the research scope and objectives as well connections between associated research topics.

Theme 1: Design analysis and refinement accommodating uncertainty in early design

To accommodate limited design analysis budgets, design analysis and refinement techniques need to offer rapid implementation, low analysis cost, as well as reliable outcomes. Furthermore, to accommodate multidisciplinary in design modelling, integration with disparate CAD/E tools is required for effective design analysis and refinement; this is an active research focus of Multi-disciplinary Design Optimization (MDO) engineering methods (Sobieszczanski-Sobieski *et al.* 1997). MDO has resulted in the emergence of a range of Process Integration and Design Optimization (PIDO) software tools capable of facilitating interdisciplinary CAD/E tool integration to enable: automated parametric studies, DOE, statistical analysis, and, multi-objective optimization (Kodiyalam 1998; Malone *et al.* 1999; Padula *et al.* 1999; Simpson *et al.* 2008; Flager *et al.* 2009; Adams 2011).

The emerging design analysis and refinement capabilities of PIDO tools offer novel opportunities for addressing the identified limitations associated with design analysis and refinement accommodating uncertainty in early design stages (Section 1.2).

This research aims to develop novel PIDO tool based methods for managing parameter uncertainty in early stages of design, based on design analysis and refinement techniques such as: sensitivity analysis, tolerance/robustness analysis, DOE and optimization methods.

The associated research objectives include:

- Development of a visualization method for aiding designers in identifying assembly KPCs within native CAD models. The CAD/E tool integration capabilities of PIDO tools offer an opportunity to enable visualization of assembly behaviour under expected manufacturing variation within native CAD models, which are often readily available at the concept embodiment design stage. This capability may thereby aid in the identification of KPCs with low additional modelling effort requirements.
- Development of methods for computationally efficient manufacturing sensitivity analysis in early design stages. To reduce modelling expense, the method should enable the reuse of CAD/E models created as part of the standard design process.
- Development of method for rapidly identifying optimal regions in the early design space with PIDO based DOE analysis and optimization and CAE tool integration, and efficient reuse of design models.

These expected outcomes of these objectives are contributions which can be directly applied to improve the design of mechanical assemblies involving uncertainty or variation in design parameters, in the early stages of design.

Theme 2: Tolerancing of assemblies subject to loading

The ability of PIDO tools to facilitate CAD/E tool integration, automated parametric studies, DOE and statistical analysis, allows novel opportunities for resolving tolerance analysis problems requiring numerical modelling of the effects of loading on mechanical assemblies.

The research objective associated with this theme is the development of a computationally efficient, PIDO based approach for tolerance analysis of assemblies subject to loading, within the modelling environment of existing standalone CAD/E tools. Specific objectives include:

- Use of CAD/E models created as part of the standard design process for parametric CAD/E based tolerance analysis to reduce the need for additional modelling tools and expertise.
- Modelling of the effects of a broad range of loading scenarios on mechanical assemblies with the use of dedicated tools such as FE modellers.
- Validation with practical, industry relevant tolerance analysis case studies.

The expected outcome is an approach which extends the capabilities of traditional CAT tools by enabling tolerance analysis of assemblies subject to general range of loading effects.

Theme 3: Efficient uncertainty quantification in tolerance analysis and synthesis

A variety of alternative analytical UQ techniques have recently been proposed which, under certain conditions, can offer significantly higher efficiency than methods such as MC sampling (Lee *et al.* 2009). These analytical techniques have the potential to significantly improve the practical feasibility of tolerance analysis and synthesis, particularly involving assemblies under loading. A particularly efficient and attractive analytical UQ method is Polynomial Chaos Expansion (PCE), however, its applicability and effectiveness in tolerance analysis and synthesis is not fully known (Xiu *et al.* 2003).

The objectives associated with this research theme are:

- Assessment of whether alternative UQ methods such as PCE are appropriate for the specific requirements identified in this work, in association with tolerance analysis of assemblies subject to the effects of loading. This requires an analysis of the PCE method identifying working principles, implementation requirements, advantages and limitations.

- Based on the outcome of the assessment, establishing of recommendations for appropriate implementation of PCE in tolerance analysis.
- Potential implementation of PCE into a PIDO based tolerance analysis and synthesis framework.
- Integration of the advanced optimization capabilities of PIDO tools into a tolerance synthesis framework.
- Evaluation of PCE on practical, industry relevant tolerance analysis and synthesis case studies, and validation against reference results obtained using traditional methods.

In summary, this research is focused on enhancing the engineering design of mechanical assemblies involving uncertainty or variation in design parameters, with emerging design analysis and refinement capabilities of PIDO tools. The main research objective is the development of a novel, computationally efficient, PIDO based approach for tolerance analysis and synthesis of assemblies subject to loading, within the modelling environment of existing standalone CAD/E tools. The projected outcome is the successful application of the research outcomes to industry relevant design problems involving complex mechanical assemblies subject to the effects of manufacturing variation.

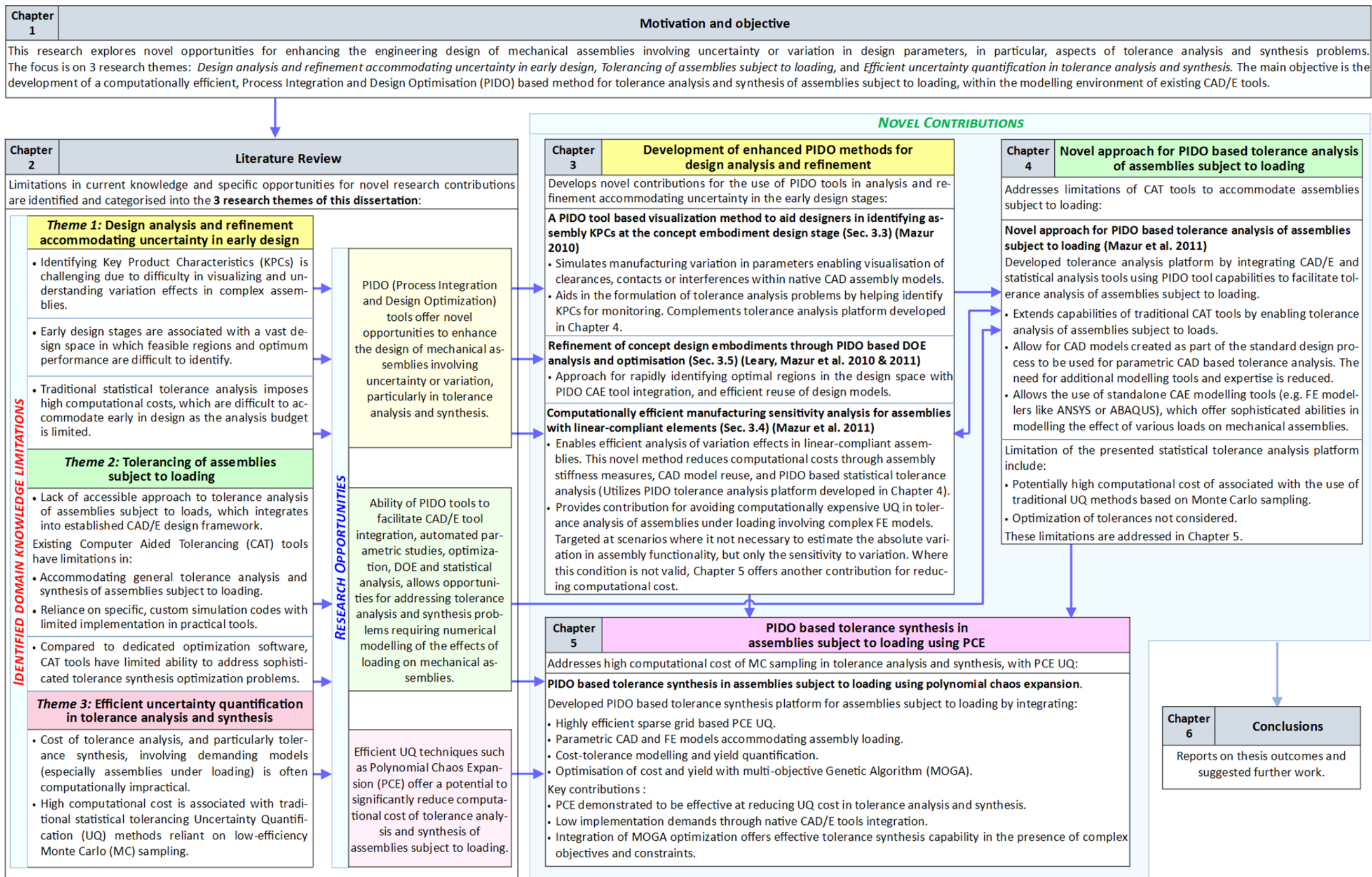


Figure 1.1 – Thesis map

1.4 Research questions

This dissertation is guided by the following key research questions:

1. How can PIDO tools address design problems that involve uncertainty or variation in design parameters?
2. Can the capabilities of PIDO tools be utilised to conduct effective tolerance analysis of assemblies under loading within the modelling environment of existing CAD and CAE software?
3. How can the high computational cost of statistical tolerance analysis and synthesis be reduced, particularly in assemblies under loading?
4. Can analytical UQ methods such as Polynomial Chaos Expansion (PCE) be effectively applied to tolerance analysis and synthesis to improve efficiency without compromising accuracy?

The knowledge base developed by addressing the outlined research questions, will establish the feasibility of effective practical tolerance analysis and synthesis of assemblies subject to loading within a PIDO framework.

1.5 Methodology

The formulated research questions provide a roadmap for successfully addressing the objectives of this research.

This is assisted by the following methodology which identifies milestones required for achieving the research objectives:

1. Review the existing body of knowledge concerning uncertainty in the design of mechanical assemblies; including methods and tools addressing tolerance analysis and synthesis.
2. Investigation of the potential of design analysis and refinement capabilities of PIDO tools to enhance the early stages of design problems involving uncertainty or variation in design parameters.
3. Development of a PIDO based tolerance analysis approach for the general tolerance analysis of assemblies subject to loads within the modelling environment of existing standalone CAD/E tools.
4. Extension of the PIDO based tolerance analysis approach to allow tolerance synthesis guided by multi-objective optimization.

5. Evaluation of the hypothesis that high-efficiency analytical UQ methods can be utilized in tolerance analysis.
6. Integration of analytical UQ methods with PIDO based tolerance analysis and synthesis, pending the successful outcomes of preceding research methodology objectives.
7. Evaluation of the effectiveness of each stage of the methodology with practical industry based design problems.

Additionally, a summary overview of the thesis themes, objectives, contributions, and topic interconnections is presented in the thesis map shown in Figure 1.1. The thesis map outlines chapter topics and general methodology of this dissertation.

This dissertation is organized such that the methodology milestones are addressed sequentially. Validating case studies are presented immediately following the discussion of any developed technique or method in order to demonstrate and highlight any particular associated benefits.

1.6 Key outcomes and contributions:

This research program has resulted in the contributions categorically listed below in summary form according to the relevant research theme. Significant additional detail of key outcomes and contributions is presented in Chapter 6.

Theme 1: Design analysis and refinement accommodating uncertainty in early design stages

- A Process Integration and Design Optimization (PIDO) based visualization method to aid designers in identifying assembly KPCs at the concept embodiment design stage (Section 3.3) (Mazur *et al.* 2010). The method integrates the functionality of commercial CAD software with the process integration, UQ, data logging and statistical analysis capabilities of PIDO tools, to simulate manufacturing variation effects on the part parameters of an assembly and visualise assembly clearances, contacts or interferences. The proposed method has been validated using an industrial case study by enabling the automated identification of unintended component interactions, in the concept design embodiment of an automotive mirror actuator assembly.
- Computationally efficient manufacturing sensitivity analysis for assemblies with linear-compliant elements (Section 3.4) (Mazur *et al.* 2011). An efficient method for analysing the effects of manufacturing variation in linear-compliant assemblies under loading was developed. The method significantly reduces computational costs by utilising linear-compliant assembly stiffness measures, reuse of CAD models created in the conceptual and design embodiment stage, and PIDO tool based statistical tolerance analysis. This method was developed as part of a benchmarking study of alternative automotive seat rail assembly concept embodiments to quantify their sensitivity to manufacturing variation. The benchmarking study identified significant differences in sensitivity to manufacturing variation between alternative designs. This outcome allowed the designers to proceed into the detail design stage with higher certainty of performance and with low additional analysis expense.
- Refinement of concept design embodiments through PIDO based DOE analysis and optimization (Section 3.5) (Leary, Mazur *et al.* 2010; Leary, Mazur *et al.* 2011). This contribution highlights the benefit of exploring the conceptual and embodiment design space through DOE analysis and optimization. This contribution was validated with a case study addressing the conceptual design of automotive seat kinematics consisting of a four-bar linkage system, which, despite its apparent simplicity, is associated with a large design space. An identified Pareto-optimal concept was selected for detail design and manufacture. The selected design was found to offer the best performance in

achieving a vertical seat travel objective with the least number of manual actuations (these are actuations required to lift the seat for a given fixed lift effort). This superior performance against competitors in seat actuation demands was a determining factor for the selection of the design in the seat assembly of the *Tesla Motors Model S* full-sized electric sedan currently on sale in the United States.

Theme 2: Tolerancing of assemblies subject to loading

A novel tolerance analysis platform which integrates CAD/E and statistical analysis tools using PIDO tool capabilities to facilitate tolerance analysis of assemblies subject to loading (Chapter 4) (Mazur *et al.* 2011). Integration was achieved by developing script based links between standalone CAD/E software, through commonly embedded scripting capabilities, and the process integration facilities of PIDO tools. The platform addresses the limitations of CAT tools and offers an accessible tolerance analysis approach with low implementation demands due to integration with the established CAD/E modelling design framework.

The capabilities of the platform were validated with two industry relevant tolerance analysis case studies involving assemblies subject to loading. These include: an automotive actuator assembly consisting of a rigid spigot and complaint spring undergoing compression due to external loading; and an automotive rotary switch in which a resistive actuation torque is provided by a spring loaded radial detent acting on the perimeter of the switch body. In both case studies the developed platform was successfully applied to identify the tolerances required to achieve the required assembly yield.

Theme 3: Efficient uncertainty quantification in tolerance analysis and synthesis

A novel PIDO based tolerance synthesis in assemblies subject to loading using Polynomial Chaos Expansion (PCE). Chapter 5 established that PCE based UQ is feasible in tolerance analysis and can enable significant reduction in computational costs. The resulting computational efficiency enabled the PIDO based tolerance analysis platform developed in Chapter 4 to be further extended to allow multi-objective, tolerance synthesis in assemblies subject to loading. The resultant PIDO based tolerance synthesis platform integrates: highly efficient sparse grid based PCE UQ; parametric CAD and FE models accommodating the effects of loading; cost-tolerance modelling; yield quantification with Process Capability Indices (PCI); and, optimization of tolerance cost and yield with multi-objective Genetic Algorithm (GA). The tolerance synthesis platform can be applied to tolerance analysis and synthesis with significantly reduced computation time while maintaining accuracy.

The effectiveness of PCE in tolerance analysis and synthesis was validated using two case studies, these include: an automotive seat rail assembly subject to compliance due to internal loading; and an automotive switch assembly subject to loading from a spring-loaded detent feature. In both case studies optimal tolerances were identified which satisfied yield and tolerance cost objectives. The implementation of PCE in a PIDO based tolerance synthesis platform resulted in large computational cost reductions without compromising the accuracy achieved with traditional MC methods.

1.7 Thesis Outline

This dissertation is organised into 6 main Chapters. Chapter 1 introduces the research project and summarises the objectives, methodology, and key outcomes. Chapter 2 presents a comprehensive review of literature and technology relevant to this research. Specific opportunities for novel research outcomes are identified.

Chapter 3 identifies opportunities to enhance the conceptual and embodiment stages of design involving uncertainty or variation in design parameters. This is achieved by developing novel methods for the use of PIDO tools in the analysis and refinement of concept design embodiments with sensitivity analysis, tolerance analysis, DOE methods and optimization. Practical conceptual and embodiment design problems are considered and effective solutions developed for a number of industry focused scenarios.

Chapter 4 addresses the limitation of CAT tools to accommodate assemblies subject to loading by developing a novel tolerance analysis platform which integrates CAD, CAE and statistical analysis tools using PIDO software capabilities. To demonstrate the capabilities of the developed platform, examples of practical, industry related tolerance analysis problems involving compliance and multi-body dynamics are presented.

Chapter 5 investigates in detail the integration of highly efficient Polynomial Chaos Expansion (PCE) in tolerance analysis for uncertainty quantification. The PIDO tool based tolerance analysis platform developed in Chapter 4 is subsequently extended to allow multi-objective, tolerance synthesis in assemblies subject to loading, with significantly reduced computational cost. Industry based case studies are presented to demonstrate that the application of PCE based UQ to tolerance analysis and synthesis can significantly reduce computation time while maintaining accuracy.

The final chapter summarizes the outcomes and conclusions of this dissertation and offers recommendations for potential areas warranting further research and development. An appendix containing additional detail on background concepts and methods associated with tolerancing practice concludes the thesis.

2 LITERATURE REVIEW

2.1 Chapter summary

This chapter presents a review of literature and technology relevant to the research outcomes of this work. Specific opportunities for novel research contributions are identified, and further developed in subsequent chapters.

The scope of the literature review is focused on work relating to uncertainty or variation in design parameters, in particular the analysis and synthesis of tolerances in engineering design. The topics considered in this chapter initially address background concepts and methods associated with tolerancing practice as these are extensively utilized in this research. Once the background context is established, the literature review progressively focuses on more active research areas where limitations and gaps in domain knowledge are identified.

Outcomes of the literature review identifying gaps in domain knowledge and limitation in existing methods are presented in section 2.10. A number of associated research opportunities are discussed.

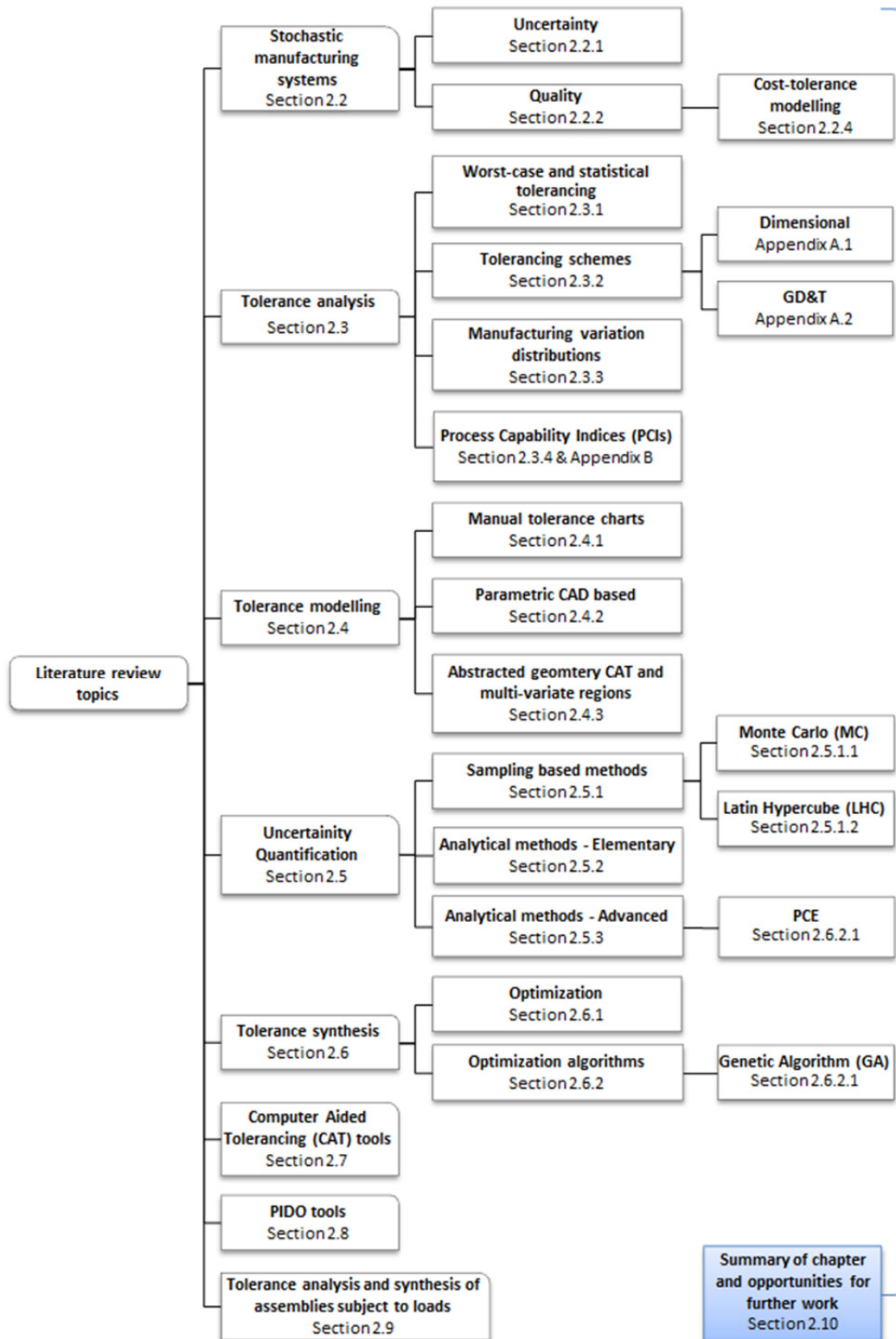


Figure 2.1 – Literature review topic outline

Figure 2.1 categorically outlines the topics addressed in this chapter. The identified fundamental areas of knowledge relevant to this research scope are summarised below, where the relevance of each topic to the research scope is established before subsequent discussion further in the body of this chapter.

Stochastic manufacturing systems (Section 2.2):

Management of the effects of manufacturing variation is inherently associated with the concept of *uncertainty*. Section 2.2.1 considers the nature of uncertainty and the associated aspects of relevance to this research. Uncertainty is linked to the concept of *quality* of manufactured goods, as notions of *high quality* are typically synonymous with high certainty in achieving the specified performance requirements. Section 2.2.2 formally defines the concept of quality as used in this dissertation. Subsequently in Section 2.2.3, methods for formally measuring costs associated with achieving a specified level of product quality are discussed, as they are used in this work as metrics for tolerance analysis and synthesis.

Tolerance analysis (Section 2.3):

Tolerance analysis is the study of the effect of variation of a parameter on the variability in the functionality of a product part or assembly. The parameters of interest in this work are typically dimensional and geometric, and are defined according to conventions of tolerancing schemes. Both Geometric Dimensioning and Tolerancing (GD&T) and Dimensional tolerancing schemes are applied in this research. These are discussed in Section 2.3.2 and Appendix A.

In this research, tolerance analysis is conducted according to statistical tolerancing principles (Section 2.3.1) which require consideration of the probabilistic likelihood that a parameter subject to stochastic manufacturing variation will take on a given value. This likelihood is characterized by the parameter's probability distribution. Probability distributions associated with manufacturing variation relevant to this research are discussed in Section 2.3.3. Quantifying the distribution of a product parameter in terms of the required specification limits is achieved with Process Capability Indices (PCI). PCIs of relevance to this work are defined in Section 2.3.4 and Appendix B and are adopted in this research to provide a measure of manufacturing yield (which is the number of manufactured products which meet specification requirements).

Tolerance modelling (Section 2.4):

Tolerance modelling aims to identify the relationship between the tolerance information associated with part features and assembly functionality. Various approaches to tolerance modelling have been developed which offer different levels of sophistication and capability. These methods are discussed and evaluated in Section 2.4 against the research objectives of this work, namely: suitability for CAD/E integration; and accommodation of assemblies which are subject to loading.

Uncertainty quantification (Section 2.5):

Statistical tolerance analysis requires quantification of the expected manufacturing yield. This can be estimated with Uncertainty Quantification (UQ) methods which characterize the probabilistic response of a system dependent on stochastic variables. UQ methods are discussed in Section 2.5, where limitations of UQ methods traditionally used in statistical tolerancing are highlighted, and recently developed alternative UQ methods with potentially superior performance are identified. The suitability of the alternative UQ methods for tolerance analysis is considered against the requirements imposed by the research objectives of this work, such as: applicability to integration with existing CAD/E and PIDO tools; high efficiency and accuracy; flexibility in accommodating various input parameter distributions; and ability to accommodate high dimensionality problems efficiently.

Tolerance synthesis (Section 2.6):

Tolerance synthesis is the process of optimally allocating part tolerances in a product assembly to maximize assembly yield (or product quality) and minimize tolerance cost. A tolerance synthesis problem requires the integration of a number of analysis and simulation techniques, which are addressed in the identified sections. These include: optimization algorithms (Section 2.6.1); tolerance analysis (Section 2.3); associated UQ method (Section 2.5); and, yield and cost-tolerance estimation approaches (Section 2.2.3.1). A number of tolerance synthesis methods have been proposed with a range of different analysis techniques; these are reviewed in Section 2.9. Limitations in existing methods are identified. Optimization algorithms are compared to identify suitability for tolerance synthesis of assemblies subject to loading, as per the research objectives of this work outlined in Section 1.3.

Computer Aided Tolerancing (CAT) tools (Section 2.7):

Computer Aided Tolerancing (CAT) software tools offer tolerance analysis and synthesis capabilities either as independent software packages, or through integration with commercial CAD systems. A review of existing CAT tool capabilities is presented in Section 2.7 and a number of limitations of relevance to this research are identified. The identified limitations are a key motivation for this research, as discussed in Sections 1.3 and 2.10.

Process Integration and Design Optimization (PIDO) (Section 2.8):

Process Integration and Design Optimization (PIDO) tools are software frameworks for facilitating the integration of diverse, discipline specific CAE analysis tools for process scheduling, design of experiments, optimization and statistical analysis. A review of PIDO tools is presented in Section 2.8. Novel PIDO tool based design analysis and refinement

opportunities are identified for enhancing the engineering design of mechanical assemblies involving uncertainty, or variation in design parameters. These opportunities are exploited in subsequent chapters of this research.

Tolerance analysis and synthesis of assemblies subject to loads (Section 2.9):

Accommodating the effects of loads in tolerance analysis and synthesis is an active research field. A number of methods have been proposed which differ in: the addressed loading effect; the modelling approach; computational expense; and any associated simplifying approximations. Previous contributions to this field are discussed in Section 2.9. Limitations in existing methods are identified and research opportunities formulated.

2.2 Stochastic manufacturing systems

Manufacturing processes are intrinsically subject to stochastic variation. Variation can occur within geometric parameters such as dimensions of a part or assembly feature, within material properties such as yield or fatigue strength, or within other product characteristics.

These variations result in uncertainty in the performance of manufactured goods and require effective management to ensure correct performance. Strategies for management of manufacturing variation have an extensive development history. Prior to mass production, manufacturing was mainly carried out by craftsmen, where the management of variation of the entire product was controlled by the workmanship of the individual (Bijker 1997). Advancements in mass production, such as increased production volumes and efficiency, as well as increased process complexity, were achieved by skill specialisation and automation of labour. Consequently, management of variation was no longer determined by an individual, but was dependent on the workmanship of multiple individuals and the precision of varied machinery. A need arose for a systematic approach to the management of variation in mass manufactured goods, in particular standardised methods for dimensional control and tolerancing (Mitra 1998). Consequently an extensive body of concepts, standards and methods have been developed for effectively managing manufacturing variation. Topics relevant to this dissertation (as outlined in Section 2.1 and Figure 2.1) are discussed in subsequent sections.

2.2.1 Uncertainty

Manufacturing variation is inherently associated with the concept of uncertainty. Uncertainties can be classified as either systematic or stochastic (Kiureghian et al. 2009; Terejanu et al. 2010).

Systematic uncertainties: Result from insufficient data or knowledge about a physical system which can be known in principle, but is unknown in practice. Also referred to as epistemic uncertainties.

Stochastic uncertainties: Result from inherent randomness in the behaviour of a physical system. Also referred to as aleatory uncertainties.

Systematic uncertainties may exist due to factors such as insufficient measurement accuracy, human errors, or modelling simplifications. They can be considered as uncertainties associated with the assessment of a system. These uncertainties can be reduced by collecting additional data, increased measurement precision, or increased understanding of the problem during modelling. Conversely, stochastic uncertainties are nondeterministic and not reduced by the possession of more data or knowledge about the system.

Accommodating uncertainties is the focus of reliability-based design and robust design approaches (Taguchi 1993; Bergman *et al.* 2009; Stapelberg 2009; Pascoe 2011). In general, a robust and reliable system is considered resilient in response to uncertainty. However there is no universal agreement on a distinct definition of the two approaches in the literature, both in terms of meaning and quantifiable criteria. General definitions proposed and adopted in this work are:

Robustness: The ability of a system to satisfy functional requirements in the presence of varying parameters, inputs or environmental conditions. The degree of robustness can be measured by the range of variation under which the system satisfies functional requirements.

Reliability: The ability of a system to perform its requested functions under stated conditions whenever required. The degree of reliability can be measured by the probability of the system failing to perform its function.

Tolerance analysis (introduced in Sections 2.3), which is the focus of this work, can be classified as robust design problems due to the associated intrinsic objective of meeting product functional requirements in the presence of stochastic manufacturing variation.

Tolerance analysis involves both systematic and stochastic uncertainties. Uncertainty in a particular part parameter, such as the stiffness of a coil spring for instance, may be either systematic or stochastic depending on the circumstance. For example, if the desired stiffness value is for a specific spring, then the uncertainty in its stiffness will be *systematic* if the specific spring is tested to quantify its stiffness. Uncertainty in the stiffness value will be subject to the limitation of the measurement equipment and procedures used for assessment, which are reducible with more rigorous testing. However, if the desired

stiffness value is for a batch of springs, uncertainty in the spring parameters will be subject to inherent *stochastic* variation associated with the manufacturing process and cannot be suppressed by more accurate measurements of the springs. Estimating the influence of uncertainty in tolerance analysis is the objective of Uncertainty Quantification (UQ) methods; these form a critical element of this dissertation and are discussed further in Section 2.5.

Uncertainty is linked to the concept of *quality* of manufactured goods, as notions of *high quality* are typically synonymous with high certainty in target performance.

2.2.2 Quality

The term *quality* is often associated with the effect of manufacturing variation on the performance of manufactured goods. A number of definitions of *quality* have been presented in the literature:

- *"The ability of the product to fulfil its intended requirements for technical performance, customer satisfaction, and manufacturing efficiency."* (Juran 1992)
- *"Uniformity around a target value."* (Taguchi 1993)
- *"The loss a product imposes on society after it is shipped."* (Ealey 1988)
- *"Freedom from deficiencies."* (Juran 1992)
- *"Degree to which a set of inherent characteristics fulfils requirements"* where requirements are subsequently defined as *"needs or expectations"* (ISO 2005)
- *"The totality of features and characteristics of a product or service that bears its ability to satisfy stated or implied needs."* (ISO 8402-1986)

The varied definitions are all founded on the same fundamental concepts of quality being a measure of the performance of a product in being free from defects, deficiencies, and significant performance variations. The definition of quality adopted in the specific context of this dissertation is:

Quality: The degree to which a manufactured product achieves target values for parameters of particular importance to the functionality and performance of the product. These parameters of particular importance are referred to as Key Product Characteristics (KPCs).

This concept of quality will be adopted in this dissertation to establish metrics for measuring the expected performance of mechanical assemblies subject to manufacturing variation; these are discussed in the following sections.

2.2.3 Quality loss and cost-tolerance relationships

The costs associated with the quality of a product can be broadly attributed to *quality control* (i.e. achieving defined quality targets) and *quality loss* (i.e. a failure to control quality) (Phadke 1989; Taguchi 1989; Feigenbaum 2012). The costs associated with quality control can be attributed to efforts directed at the detection of defects (appraisal costs) and efforts directed at the prevention of defects (prevention costs). The costs associated with quality loss can be attributed to: internal failure costs (the scrap or repair costs associated with defects identified by the manufacturer) and external failure costs (the cost of an unidentified product defect reaching the customer). Figure 2.2 classifies the quality control and quality loss costs according to their associated sources (Feigenbaum 2012).

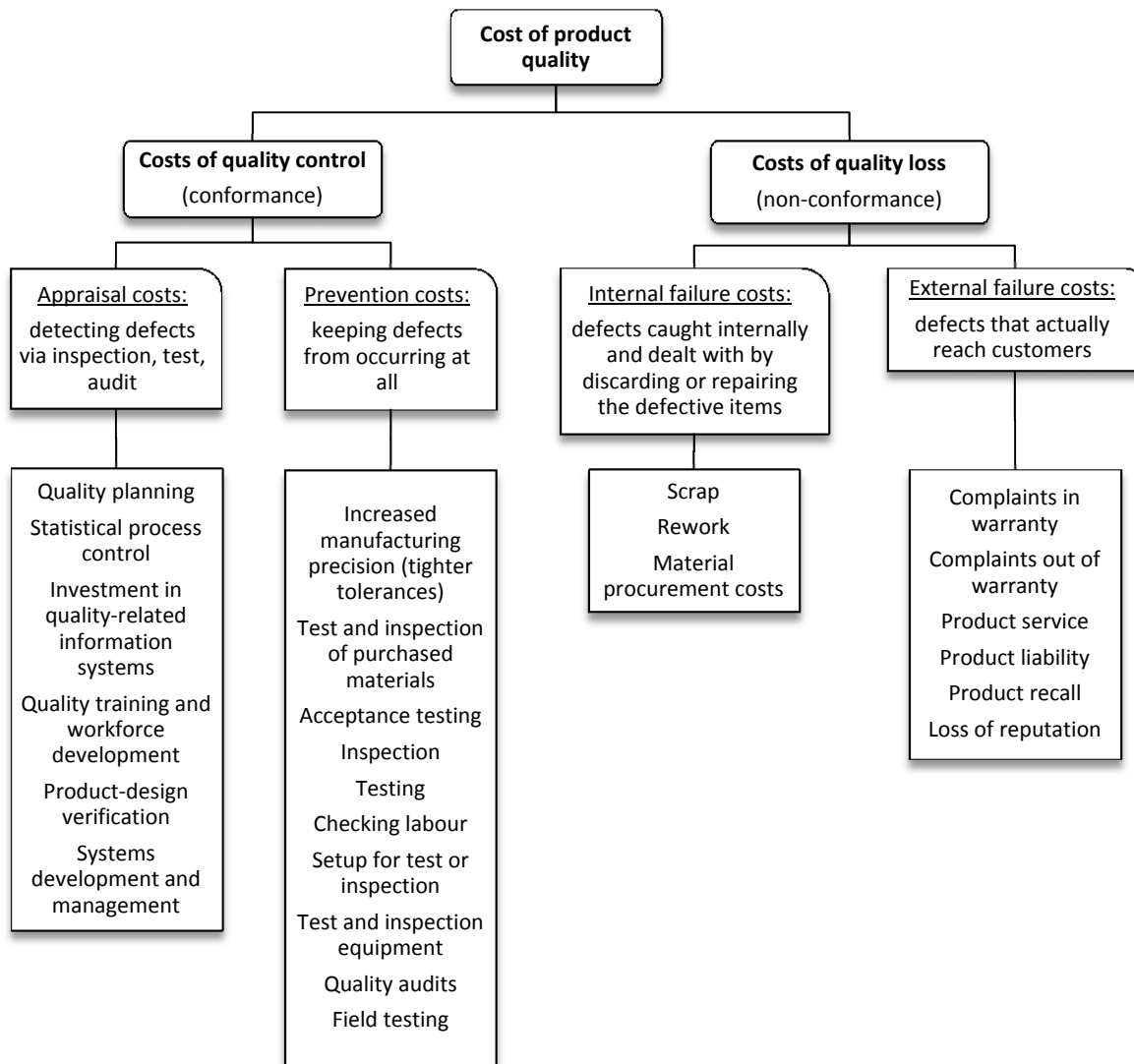


Figure 2.2 - Classification of costs associated with poor quality (Feigenbaum 2012)

The costs associated with quality control and quality loss compete with each other. A product with a high level of defects, deficiencies, and significant performance variations will typically have a low cost of quality control and a high cost of quality loss due to broad variability in key product characteristics. Conversely, a product with a low level of defects will incur a high cost of quality control yet a low quality loss as higher precision typically requires more extensive manufacturing efforts, which in turn, translates into higher production costs. Achieving an efficient balance between quality control and quality loss costs (Figure 2.3) is necessary for mass manufactured goods to be economically competitive (Juran 1992).

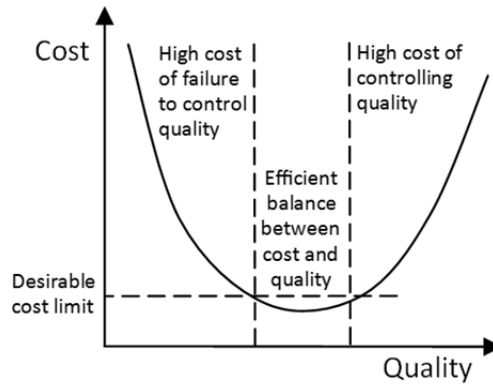


Figure 2.3 – Relationship between quality control and cost (Juran 1992)

In the scope of this work, the costs of controlling quality are attributed to the cost of conforming to specified tolerances, and are modelled using cost-tolerance functions (Section 2.2.3.10). Similarly, the costs of failure to control can be attributed to the number of manufactured assemblies not conforming to specification; these are represented by quality loss functions and process capability indices (Sections 2.2.3.2).

2.2.3.1 Cost-Tolerance models

Manufacturing with reduced variation typically requires added manufacturing effort such as: more precise machinery, increased number of manufacturing steps, higher uniformity in material properties and stricter process control (Feigenbaum 2012). This additional manufacturing effort translates to increased cost. Various functions have been proposed for representing the cost-tolerance (or cost to accuracy) relationship for a range of manufacturing processes. These relationships are summarised in Table 2.1.

Table 2.1 - Proposed cost-tolerance functions (Wu *et al.* 1988; Dong *et al.* 1994).

Cost-Tolerance Function	Reference
Exponential	(Zhang <i>et al.</i> 1993; Dong <i>et al.</i> 1994)
Exponential/Reciprocal power	(Michael 1981)
Linear	(Edel 1964)
Piecewise Linear	(Patel 1980)
Reciprocal	(Chase 1988)
Reciprocal Power	(Sutherland 1975)
Reciprocal squared	(Spotts 1973)

Although the broad applicability of cost-tolerance functions can be limited by difficulties in finding realistic cost models applicable to specific manufacturing scenarios (Hong *et al.* 2002), the cost-tolerance functions serve as a generally reasonable representation of the cost penalty associated with increased manufacturing precision and will be applied in this work to model tolerance cost.

2.2.3.2 Cost of quality loss

The cost incurred by a loss of product quality in a specific KPC can be represented by a quality loss function (QLF) (Taguchi 1989; Cho *et al.* 1997) (Equation (2.1)).

$$QLF = \kappa[\sigma^2 + (\mu - \tau)^2] \quad \text{Where } \mu \text{ and } \sigma^2 \text{ are the mean and variance, respectively, of a KPC} \quad (2.1)$$

with target value } \tau. \kappa \text{ is weighting constant.}

Originally developed by Taguchi (Taguchi 1989), the QLF is based on the theory that any product manufactured outside of the nominal specification will ultimately result in a loss for the manufacturer, customer or society in general on account of effects such as (Taguchi 1989):

- premature wear
- reduced reliability
- increased warranty costs
- reduced brand reputation
- rework costs
- waste due to increased scrap

The quality loss function accrues a loss (representing an associated cost) with any deviation of the relevant KPC from its target value. Both the variance and the mean offset from the target value contribute to a loss in quality. Consequently, the greater the deviation from the nominal value, the higher the loss in quality.

The quality loss function offers a reasonable estimate of customer satisfaction in circumstances where a direct empirical relationship between perceived product quality and the cost associated with customer dissatisfaction is unknown to the manufacturer (Jeang 1999). The QLF has been demonstrated to lend itself well to addressing tolerance analysis and synthesis problems (Jeang 1999; Cho *et al.* 2000; Choi *et al.* 2000; Feng *et al.* 2001).

Similar metrics to the QLF are Process Capability Indices (PCI) which measures the consistency and accuracy of manufacturing process outputs. PCIs are adopted in this work and are discussed in further detail in Section 2.3.4.

2.3 Tolerance analysis

Tolerance analysis is the study of the effect of variation of a parameter on the variability in the functionality of a product part or assembly. The parameters studied are typically dimensional and geometric, and are defined according to conventions of tolerancing schemes (Section 2.3.2).

Parameters which are of particular relevance to functionality are referred to as *Key Product Characteristics (KPCs)* (Lee *et al.* 1996; Zheng *et al.* 2008). The KPCs are defined in terms of the parameters in an assembly by an *assembly response function*. An assembly response function is defined according to methods of tolerance modelling (Section 2.4). The response function may either be explicitly defined by an algebraic expression or may be implicitly captured in a numeric form such as a CAD assembly or CAE model.

The *Upper Specification Limit (USL)* and *Lower Specification Limit (LSL)* are applied to parameters and define the acceptable limits of variation. An assembly with KPCs that all lie within defined specification limits is said to satisfy all functional requirements.

Manufacturing *yield* is defined as the percentage of assemblies that conform to the specification limits of all KPCs. Yield is calculated according to worst-case or statistical tolerancing principles (Section 2.3.1); in the latter case, through the use of *Uncertainty Quantification (UQ)* methods (Section 2.5). These topics are categorically reviewed in the following sections. A summary of the key tolerance analysis nomenclature which will be applied in this work is defined below.

<i>Key Product Characteristic (KPC):</i>	<i>Part or assembly parameter especially critical to product functionality and whose deviation from a target value has a comparatively high loss of quality.</i>
<i>Assembly response function:</i>	<i>The assembly response function defines KPCs in terms of the parameters of an assembly.</i>
<i>Upper Specification Limit (USL) and Lower Specification Limit (LSL):</i>	<i>Define the acceptable limits of variation in a parameter.</i>
<i>Yield:</i>	<i>The percentage of assemblies which conform to the specification limits of all KPCs.</i>
<i>Uncertainty Quantification (UQ)</i>	<i>The process of determining the probabilistic effects of input uncertainties on response metrics of interest in stochastic systems.</i>

2.3.1 Worst-case and statistical tolerancing

Tolerance analysis can be conducted according to two different yield requirements:

- that all manufactured products must satisfy all functional requirements (worst-case tolerancing), or
- a small percentage of manufactured products are permitted to violate functional requirements (statistical tolerancing)

Worst-case tolerancing aims to satisfy the unlikely probability that all parameters within an assembly are concurrently at the unfavourable extremes of their expected distributions. Perfect conformability (100% product yield) is guaranteed, however the approach may require exceptionally tight tolerances resulting in uneconomical production costs.

Statistical tolerancing allows for non-perfect conformability (less than 100% yield), allowing the associated tolerances to be relaxed to enable reduction in manufacturing costs. Due to being more economical in terms of manufacturing costs, statistical tolerancing is typically applied for mass production (Hong *et al.* 2002). Statistical tolerancing is the main focus of this research.

2.3.2 Tolerancing schemes

A tolerancing scheme is a method of defining allowable limits of variation in part or assembly parameters. Two tolerancing schemes are in use; dimensional tolerancing, and Geometric Dimensioning and Tolerancing (GD&T).

Dimensional tolerancing specifies the acceptable size of a part feature and any associated fit between features of mating parts. The size of a feature is specified by a nominal (basic) size, and an associated Lower Specification Limit (LSL) and Upper Specification Limit (USL). Dimensional tolerancing is typically limited to linear dimensions of a part feature. This can often restrict the ability to represent possible types of variation (Wade 1967).

Geometric Dimensioning and Tolerancing (GD&T) is a tolerancing scheme with a comprehensive ability to accommodate a broader range of possible variation types. Geometric tolerancing is based on allowable geometric volumes and allows for the definition of tolerance types which are not limited to linear dimensions of a part feature, but also accommodate geometric characteristics such as variation in surface flatness (Cogorno 2006). Both dimensional and GD&T tolerancing schemes are applied in this work. Additional detail concerning tolerancing schemes is provided in Appendix A.

2.3.3 Manufacturing variation distributions

The stochastic nature of manufacturing results in process outputs that deviate from the intended nominal values. Statistical tolerance analysis often assumes that the variation is distributed according to the normal (Gaussian) distribution (Figure 2.4) (Oakland 2007).

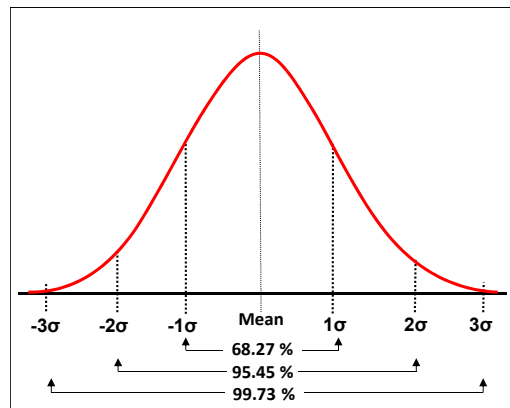


Figure 2.4 - Normal distribution and confidence intervals.

The assumption of a normal distribution can often be valid as such distributions are commonly encountered in manufacturing processes. Furthermore, due to the central limit theorem, normal distributions often arise in mechanical assemblies. The *central limit theorem* states that when populations of means are created from sample data sets of size ζ , drawn from one underlying parent population, then irrespective of the shape of the distribution of the parent population:

- The mean of the population of means will equal the mean of the parent population from which the population samples were drawn.
- The standard deviation of the population of means will equal the standard deviation of the parent population divided by the square root of the sample data sets of size ζ .
- The population of means will exhibit a normal distribution with increasing sample size.
- If a measured variable is a combination of several other uncorrelated variables, all of them subjected to a variation of any distribution, then the measured variable will be subjected to a variation that is normally distributed as the number of combinatorial variables increases.

As such, an assembly parameter that depends on the combination of various part features all subject to some uncorrelated variation, will tend to show a normal distribution with an increasing number of contributing part features regardless of their distribution type (Johnson *et al.* 2004; Miller *et al.* 2010).

In some applications the assumption of a normal distribution may not be valid. For instance, processes with a hard limit will typically show a distribution skewed away from normal and

truncated near a limiting value (Wright 1995). One such example is a hole-drilling process where the distribution is truncated at the drill size diameter. A strategy for handling non-normal data with analysis tools founded on an assumption of normally distributed variables is to transform the data with transformation techniques such as Nataf or Box-Cox (Box *et al.* 1964; Armen Der Kiureghian *et al.* 1986; McRae *et al.* 1995). For instance, a variable with a lognormal distribution can be transformed into a normal by taking its natural logarithm. Similarly, taking the cubed root of a variable with a gamma distribution will transform it to an approximately normal distribution. Approaches for the accommodation of non-normal distributions in tolerancing have been comprehensively documented in the literature (Nigam *et al.* 1995; Zhang *et al.* 1999; Hyun Seok *et al.* 2002; Kharoufeh *et al.* 2002).

In this work, parameters with normally distributions are commonly applied. Where non-normal distributions require consideration, distribution transformation techniques are considered.

2.3.4 Process Capability Indices (PCI)

A manufacturing process output distribution can be quantified by four statistical moments: the mean (μ), standard deviation (σ), skewness (γ) and kurtosis (β). Process Capability Indices (PCI) have been developed to quantify these statistical attributes in terms of the required specification limits (Pearn *et al.* 2006). PCIs are similar metrics to the quality loss function (Section 2.2.3.2) as they measure the consistency and accuracy of manufacturing process outputs. PCI compare the specification limits to the 6σ limits of the manufacturing process distribution (i.e. 99.73% of the predicted population) and nominal target values (Pearn WL 2006). A higher index indicates a more accurate process. Process Capability measurements are subject to three fundamental assumptions (Montgomery 2001):

- The sampled data is representative of the associated population.
- The process is under statistical control – i.e. there are no assignable causes of variation such as machine adjustment or defective materials.
- The process is normally distributed (some PCIs can accommodate non-normal distributions, for example Section B.4).

Additional detail about specific process capability indices is provided in Appendix B. PCI indices are an efficient way of measuring quality loss using a dimensionless metric while giving a directed indication of the expected yield. In this dissertation PCIs are applied to quantify the expected variation in stochastic parameters.

2.4 Tolerance modelling

Tolerance modelling involves the modelling of the relationship between the tolerance information associated with part features and their effect on assembly functionality. The relationship captured by the tolerance model is referred to as the assembly response function.

Various approaches to tolerance modelling have been developed which offer different levels of sophistication and capability. Tolerance modelling is typically achieved using Computer Aided Tolerancing (CAT) tools. The most common types of tolerance modelling in use are:

- Manual tolerance charts (Fortini 1967; Wade 1967)
- Parametric CAT (Nigam *et al.* 1995; Prisco *et al.* 2002)
- Abstracted Geometry CAT (e.g. vector-loop) (Chase *et al.* 1995; Gao *et al.* 1998)
- Multi-variate regions (Roy *et al.* 1998; Houten *et al.* 1999; Mujezinovic *et al.* 2004)

These methods offer varying levels of implementation of the general tolerance analysis process. With the advancement of CAD solid modelling effort have been made to develop tolerance modelling methods which incorporate tolerance information as an intrinsic part of the CAD design process. A number of different tolerance modelling approaches have been suggested, however there has been little consensus towards a standard approach in this area. The research efforts in this field are continuing (Hong *et al.* 2002). A comparison of tolerance modelling approaches is shown in Table 2.2.

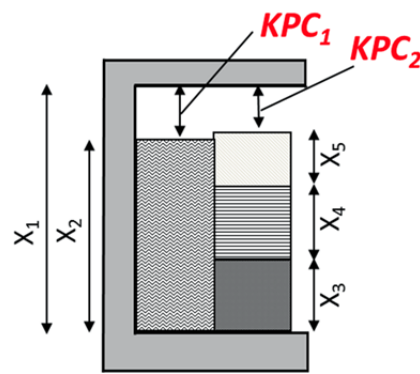
Table 2.2 - Comparison of various Tolerance Analysis methods

Method	GD&T standard support	Tolerancing scheme	External CEA tool integration	Yield requirement	Automation
Tolerance charts	Complete	Dimensional Geometric	Limited	Worst-case	Manual
Parametric CAT	Partial	Dimensional Geometric	Limited	Worst-case Statistical	Automated
Abstracted Geometry CAT	Partial	Dimensional Geometric	Limited	Worst-case Statistical	Automated
Multi-variate regions	Complete	Dimensional Geometric	Limited	Worst-case Statistical	Automated

2.4.1 Manual tolerance charts

Manual tolerance charting is the most elementary system of tolerance analysis. The method is also referred to as liner stack-up analysis and is a manual worst-case procedure based on calculating the extreme values of assembly clearances or interferences of interest in an assembly (these are typically KPCs). A reference coordinate system is established at the extremity of the assembly and the analysed clearance or interference dimension (KPC) is

determined by an arithmetic sum of individual part feature sizes which constitute the assembly. The tolerance chart is a table in which the arithmetic sum is carried out. As an example, Figure 2.5 shows a simple assembly with two clearances as KPCs. The corresponding tolerance chart is shown in Table 2.3. The chart contains the name of the parameter; the corresponding upper or lower specification limits; the difference between upper and lower specification limits; and the sign by which the parameters contribute to the assembly KPC. The resultant value of an assembly KPC is shown in the bottom row where a (+) indicates that the value results in a clearance or (-) if the result is an interference.



Assembly response functions:

$$KPC_1 = f_1(X_1, X_2) = X_1 - X_2$$

$$KPC_2 = f_1(X_1, X_3, X_4, X_5) = X_1 - X_3 - X_4 - X_5$$

Figure 2.5 - Simple mechanical assembly example with all parameters X1 to X5 subject to a dimensional tolerance of +/- 0.1mm

Table 2.3 - Tolerance chart for simple assembly example in Figure 2.5.
All parameters X1 to X5 subject to a dimensional tolerance of +/- 0.1mm

Contributor	KPC1					KPC2				
	Max		Min		Difference	Max		Min		Difference
	USL/LSL	Sign	USL/LSL	Sign		USL/LSL	Sign	USL/LSL	Sign	
X ₁	40.1	+	39.9	+	0.2	40.1	+	39.9	+	0.2
X ₂	36.9	-	37.1	-	0.2					
X ₃						12.9	-	13.1	-	0.2
X ₄						13.9	-	14.1	-	0.2
X ₅						10.9	-	11.1	-	0.2
SUM	3.2	+	2.8	+	0.4	2.4	+	1.6	+	0.8

Manual tolerance charting is comprehensively established within the tolerancing community and is well covered in the literature (Fortini 1967; Wade 1967). The method is easily implemented but limited to worst-case tolerance analysis and simple assemblies for which the assembly response function may be explicitly defined (Chase 1988). Due to these limitations the method is not considered further in this work.

2.4.2 Parametric CAD based CAT

In parametric CAD based Computer Aided Tolerancing (CAD), the constraint equations inherent to CAD part and assembly models are used for tolerance modelling. The modelling approach in typical CAD software is history based. Three-dimensional solid geometric models are created from two-dimensional sketches which are subject to three-dimensional operations such as extrusions, sweeps and lofts. If any part dimensions need to be altered, the model is reverted to the relevant point of change (such as a sketch), the relationships or dimensions are updated, and subsequent operations reapplied in series (Shah *et al.* 1995; Rao 2004).

CAD assemblies are defined by multiple CAD parts whose interaction is constrained to restrict the degrees of freedom between parts. If any part geometry is modified, the assembly constraints are re-evaluated to rebuild the assembly model. Dimensions, relationships and operations can be defined parametrically, providing a means of implementing tolerance analysis by varying individual dimensions, either by the worst-case or statistical approaches (Section 2.5).

Parametric CAD based modelling can be applied to tolerance modelling and analysis with the following methodology (Prisco *et al.* 2002):

1. Creating the nominal model topology of parts with two-dimensional sketches and three-dimensional construction operations. The model topology needs to include all desired geometric elements and their possible variants due to any associated tolerances.
2. Formulating parametric relationships which link the geometric elements of the part model to parametric numerical variables.
3. Defining an assembly from individual part models with parametric interaction relationships between part features. The interaction relationships constrain the degrees of freedom between parts with contact, offset or alignment constraints. Any assembly tolerances need to be accommodated with parametric interaction relationships which allow for possible variants in the assembly configuration due to any associated tolerances.
4. Applying nominal values to all parametric variables.
5. Instructing the CAD software modelling system to apply a general solution procedure to the parametric part and assembly model equations resulting in an evaluated model in which the defined relationships are satisfied.

6. Creating variants of the part and assembly models by changing values of the parametric variables to reflect variation associated with applied tolerances and subsequently re-executing the model solution procedure.

The idealised constraint capabilities of CAD modelling provide an acceptable representation of a product assembly in many cases. However, parameter combinations can exist that do not readily represent realistic mating conditions for a given set of assembly constraints (Shah *et al.* 2007). For example, features which nominally result in a clearance may interfere due to geometric variation, for example Figure 2.6.

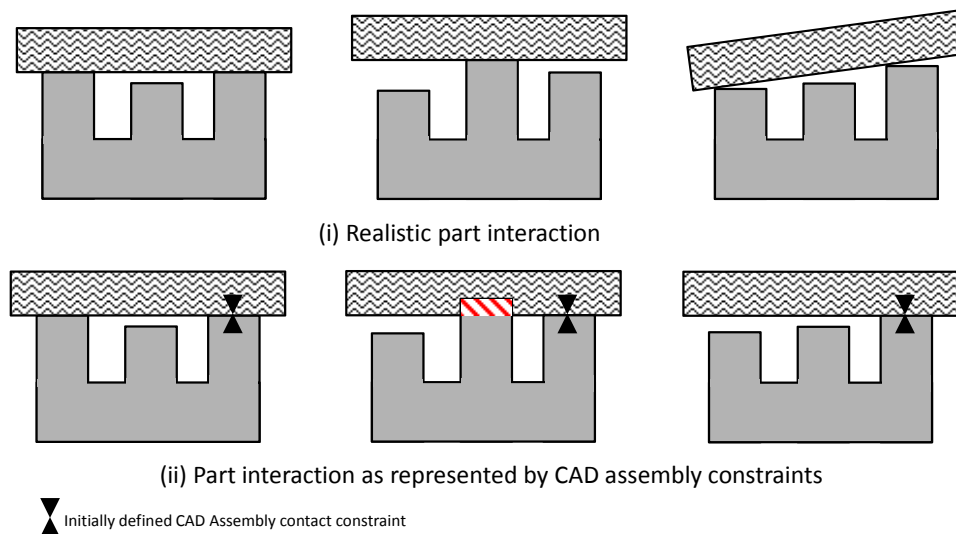


Figure 2.6 - Changing assembly contact conditions due to manufacturing variation of parts. CAD systems can be limited in ability to automatically modify part mating conditions to reflect certain realistic part contacts within an assembly.

To correctly model such a scenario in an automated manner, it is necessary to accommodate intermittent part contact. Such capabilities are may not be readily available within current CAD software in an automated manner. Alternative assembly constraints that represent different contact scenarios may need to be defined and selectively enabled through user input, depending on the KPC under analysis (Eiteljorg *et al.* 2003; Rao 2004; Stroud *et al.* 2011). With such user input it is possible to avoid part interference and unrealistic representation of the physical interaction such as that shown in Figure 2.6.

Additionally, the parametric CAD approach to tolerance modelling is subject to the following limitations:

- Statistical tolerance analysis may require the consideration of a large number of model permutations. Due to their history based nature, parametric CAD models may be computationally expensive for statistical tolerance analysis.

- CAD assembly constraint systems are typically point-to-point constraints. This makes them inconsistent with current tolerance standards which are based on tolerance zones, not point-to-point variation.
- Some forms of geometric variation defined in GD&T standards are not readily accommodated using parametric CAD models and are still under development (Shen 2005).

Despite the identified limitations, the parametric CAD tolerance modelling has advantages which make it an attractive form of tolerance modelling especially when considering assemblies which are subject to loading. The advantages are discussed in Chapter 4. Examples of parametric CAD tolerance modelling are provided in the case studies presented in this work in Chapter 3, 4 and 5.

2.4.3 Abstracted geometry CAT and multi-variate regions

In abstracted geometry CAT systems, an independent geometric model is developed to mitigate the limitations of the parametric CAD approach; in particular the computational expense of history-based CAD model updates. The approach involves the user importing the CAD model into the CAT system and interactively creating a geometry model superimposed on the original CAD data. This abstracted model describes the possible part variation, part mating relationships and resultant assembly response functions without the model rebuild penalty associated with CAD model construction history, for example (Prisco *et al.* 2002; Chiesi *et al.* 2003; Shen 2005).

One example of an abstracted geometry tolerancing modelling is referred to as Technologically and Topologically Related Surfaces (TTRS) (Clément *et al.* 1991). TTRS is based on the concept of pairs of surfaces, associated with a common solid, which are functionally related in an assembly. Interactions between the surfaces of different solids are used to model various tolerance types. The approach classifies the different possible interactions with several distinct surface types and TTRS associations (relative position possibilities of the surfaces). The tolerance zones created by the associated surfaces are represented using torsors or matrices (Clement *et al.* 1993; Desrochers *et al.* 1994). A CAT tool based on the TTRS method has been developed however its applicability is limited to specific tolerance modelling scenarios (Section 2.7) (Salomons *et al.* 1995).

Vector-loop tolerancing is another example of an abstracted geometry tolerancing modelling method (Chase *et al.* 1995; Gao *et al.* 1998). The approach represents part dimensions and clearances between part features within an assembly with vector notation.

Tolerances are represented by variation in the vector magnitude. Mating relationships between parts are defined using relationships based on three-dimensional kinematic joints. These joints define the degrees of freedom associated with part interaction. Assembly response functions are analytically described by considering the accumulation of kinematic joint relationships between vectors - these response functions are referred to as vector-loops. The advantages of this approach when compared with the parametric CAT tolerance modelling are the reduced computation cost associated with: updating model geometry; and, evaluation of the assembly response functions. The CAT software tool CETOL (Sigmetrix 2012) was originally based on the vector-loop tolerancing model. However, the vector-loop method only permits one assembly clearance per vector-loop and has problems in accommodating over-constrained assemblies. These limitations prevent the applicability of the method in more complex tolerance modelling scenarios.

Other abstracted geometry based methods have been developed for CAT analysis with the common objectives of reducing computational cost and extending support for GD&T tolerancing schemes (Prisco *et al.* 2002). One approach presented in the literature is the GapSpace tolerance modelling method (Zou *et al.* 2004). The method considers the kinematics of assembly contacts in order to determine if parts will assemble without interference. The claimed advantage, especially in comparison to parametric CAD based tolerance modelling (Section 2.4.2), is the ability to accurately model intermittent part interaction and offer realistic representation of the physical interaction between assembled parts (Morse *et al.* 2005). However, efforts to implement the method into a software tool which offers comprehensive compatibility with existing CAD modelling software are still ongoing (You 2008).

Another alternative tolerance modelling approach which has been developed is the Attribute Graph Model. The method is a graph-based abstracted CAT approach based on a separate consideration of linear and angular variation and classification of possible variation with abstracted degrees of freedom between points, lines and planes (Shah *et al.* 1992). The model has not seen much practical implementation and the authors have since focused on the development of an alternative model based on hypothetical variation volumes.

The abstracted geometry methods mentioned so far are mostly point-based in that the variation in part geometry is accommodated only at specifically defined point locations. Due to the point-based nature, it is difficult to accommodate all possible variation aspects defined in GD&T standards (Shah *et al.* 2007).

To address limitations of point-based tolerance modelling, research has focused on developing a comprehensive mathematical scheme of representing all possible forms of variation defined in GD&T standards such as (ASME 2009) without the creation of a closed-form solution. The methods in this field are generally classified as Multi-Variate region tolerance modelling. The most notable of these approaches is the T-maps method which utilizes hypothetical variation volumes of all possible locations and variations which can arise in part subjected to GD&T tolerance types (Roy *et al.* 1998; Davidson *et al.* 2002; Shah *et al.* 2007). Overlaying the T-Maps of individual part allows for the assembly response function to be defined. However, the method has currently not been implemented in a practical, readily available CAT software tool.

Despite the many abstracted tolerance modelling methods which have been developed, they share the following limitations:

- Additional expertise, tools and time are required to create the abstracted geometry model and interpret the result of analysis.
- Current abstracted tolerance modelling methods are unable to integrate with external CAE tools for tolerance modelling of assemblies subject to loading.

The CAE integration limitation is especially relevant to the objective of this research of developing tolerance analysis and synthesis methods based within the modelling environment of existing standalone CAD/E tools. This issue is discussed in further detail in Chapter 4.

2.5 Uncertainty Quantification (UQ) methods

The two approaches to yield estimation in tolerance analysis are worst-case and statistical tolerancing. Statistical tolerancing is the approach typically applied for mass production as it results in a more economical choice of tolerances (Section 2.3.1).

The key objective of statistical tolerance analysis is to estimate the assembly yield by quantifying the expected number of manufactured assemblies that will satisfy all KPC requirements for a given set of part and assembly tolerances. An estimate of yield requires that the statistical moments of distributions of the assembly KPCs to be known. These can be estimated by Uncertainty Quantification (UQ) methods.

Uncertainty quantification is the process of determining the probabilistic effects of input uncertainties on response metrics of interest in stochastic systems. The objective of all UQ methods is to characterize the probabilistic response of a system whose behaviour is dependent on stochastic variables. The probabilistic systems response is characterized by its

probability density function (distribution) defined by the associated statistical moments: the mean (μ), standard deviation (σ), skewness (γ) and kurtosis (β).

A number of UQ methods have been demonstrated in literature and can be classified as either sampling based or analytical (Nigam SD 1995; Lee SH 2009) as shown below:

Sampling-based methods:

- Monte Carlo simulation (Hammersley 1975; Rubinstein 1981; Nigam *et al.* 1995; Skowronski *et al.* 1997; Cvetko *et al.* 1998)
- Quasi-Monte Carlo (Niederreiter 1992)
- Latin Hypercube simulation (McKay *et al.* 1979; Keramat *et al.* 1997)

Analytical methods:

- Root Sum of Squares (RSS) (Mansoor 1963)
- Taguchi method (Taguchi 1978; D'Errico *et al.* 1988; Nigam *et al.* 1995)
- Hasofer-Lind index (Parkinson 1982; Lehtihet *et al.* 1991)
- Extended Taylor series approximation (Evans 1975)
- Most probable point (Fiessler *et al.* 1979)
- First and second order reliability (Hohenbichler *et al.* 1987)
- Full Factorial Numerical Integration (Hyun Seok *et al.* 2002)
- Taylor series or perturbation (Ghanem *et al.* 2003)
- Univariate dimension reduction (Rahman *et al.* 2004; Rahman *et al.* 2006)
- Polynomial Chaos Expansion (PCE) (Schoutens 2000; Xiu 2003; Lovett *et al.* 2006)

The application of specific UQ methods depends on the intent and constraints of the problem under consideration, including the:

- Complexity of implementation (simulation based methods for instance are typically trivial to implement in contrast to complex analytical methods such as PCE).
- Computational cost and available computational budget.
- Statistical moments of importance (typically in robust design problems such as tolerance analysis, mean and standard deviation are of greater interest than higher order moments).
- Required statistical moment estimation accuracy (for low precision tolerances, higher moment estimation error may be acceptable).
- Input variable distribution (some UQ methods may not be compatible with non-normal input parameter distributions).

- The model type to be accommodated; where the system response function of the model is either available analytically (explicit) or defined in a numerical model (implicit).

The above issues are considered in the following sections.

2.5.1 Sampling based methods

Sampling based methods are broadly applicable, robust and easily implemented. Furthermore their convergence (number of system evaluations required to achieve a given error in estimating a desired system response) is typically independent of the dimensionality of the problem and the smoothness of the system response function (Gerstner *et al.* 1998). However, sampling methods typically show slow convergence and can be prohibitively computationally expensive when each model evaluation involves lengthy numerical simulations.

One method to address the computational expense associated with simulation methods is by complementing the simulation with Response Surface Modelling (RSM). The real, computationally expensive system model is evaluated a select number of times to map the system response function. A computationally inexpensive surrogate model (meta-model) is subsequently fitted to the evaluated points using RSM techniques (Jeang 1999). A sampling-based UQ method is then applied to the meta-model to obtain approximated estimates of the statistical moments of the system response at a reduced computational cost. This approach however is accompanied with the difficult problem of how to effectively include the meta-model fitting approximations into the statistical moment estimates derived from sampling-based UQ of the meta-model. The result can be highly application dependent and unpredictable requiring an empirical analysis of fitting errors, this limitation narrows the applicability of RSM techniques.

2.5.1.1 Monte Carlo (MC) simulation

Monte Carlo simulation generates a probabilistic estimate of the system response by aggregating the system outputs for a set of input variables randomly selected from their associated probability distributions. The method is simple to implement, and robust against different input parameter distributions. MC simulation statistical moment estimates converge to the exact result at a rate of $O(N^{-0.5})$ where N is the number of simulations and convergence is independent of the problem dimensionality and smoothness of the response function (Frances *et al.* 2005). For example, to reduce the error in the moment estimate by one order of magnitude requires 100 times more data. If greater accuracy is required with

additional samples, already evaluated samples can be reused. MC simulation typically provides a performance baseline for assessment of other UQ methods.

In MC based sampling, the unconstrained random selection of variables can often lead to poor coverage of the distribution of stochastic variables, especially at the tails of the distribution, or when the number of samples is small. For example, achieving a 99% probability of 1% error in sample variance from the desired value, 133,000 random samples may be required (Huntington *et al.* 1998). Distribution tail statistics are especially important for statistical tolerance analysis where interest often lies in estimating yield values near 100%.

A derivative technique is Quasi-Monte Carlo sampling which aims to improve the convergence of the MC method by selecting sampling points with more regular spacing across the parameter space than that achieved with random sampling (Niederreiter 1992). However the rate of improvement over MC can be small in practice (Morokoff *et al.* 1994).

2.5.1.2 Latin hypercube (LHC) simulation

Latin Hypercube (LHC) is a constrained sampling based UQ method in which the probability distribution for stochastic variables is sampled in stratified sections of equal probability. The equal probability strata are defined by the nature of the probability distribution; e.g. for a normal distribution the strata width increases away from the mean due to the associated reduction in probability density (Figure 2.7). For N desired samples, the distribution is sectioned into N strata of equal probability, and a sample is randomly placed in each individual strata. The resulting set of samples avoids clustering (undesirably close proximity of sample points) which and ensures relatively uniform distribution over the probability density function range (McKay *et al.* 1979; Keramat *et al.* 1997).

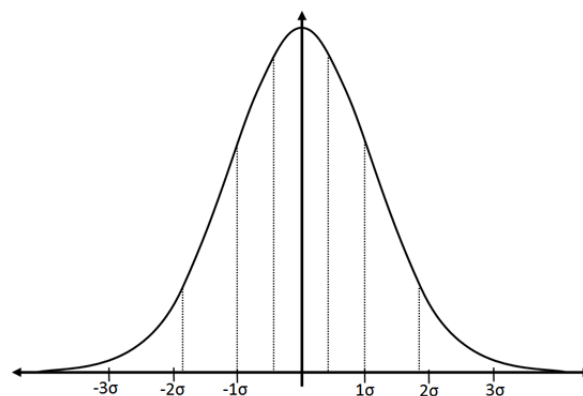


Figure 2.7 - Normal distribution with LHC sampling strata of equal probability ($N=8$)

First and second order LHC statistical moment estimates converge to the ideal result proportionally at a rate of $O(N^{-1})$ where N is the number of simulations. For example, to reduce the error in the moment estimate by one order of magnitude requires ten times more data. However, LHC sampling can result in poor estimates of higher order moments, as the number of independent (uncorrelated) variables increases. Due to the LHC constrained sampling scheme, correlations among variables can occur and high order moments and output probability distribution estimates may not be accurate (Keramat *et al.* 1997; Huntington *et al.* 1998). Due to these potential sources of error, the broad applicability of LHC sampling can be limited.

2.5.2 Analytical methods - Elementary

As sampling based-methods such as MC are typically not founded on simplifying assumptions associated with the UQ problem, they have the advantage of being able to accommodate a broad range of UQ problems with low implementation demands. However, this may also be a disadvantage when valid simplification for UQ problems are possible due to, for instance, input parameters with a single distribution type, or smooth response functions. Analytical UQ methods exploit the extra information available in such UQ problems to significantly improve convergence efficiency.

The analytical UQ methods considered in this work have been categorised as either elementary or advanced based on their associated efficiency, applicability to different problems, simplifying assumptions and complexity of implementation. Elementary methods typically have a comparatively low efficiency, are only compatible with normal parameter distributions and may require the assembly response function to be analytically defined. Advanced methods can accommodate any parameter distribution type and can be applied to implicitly defined assembly response functions while offering higher efficiency.

Some elementary analytical methods widely associated with the field of tolerance analysis include the Root Sum of Squares and Taguchi Methods.

2.5.2.1 Root Sum of Squares (RSS) method

The Root Sum of Squares (RSS) method allows for the analytical computation of the statistical moments if the response function is analytically definable and linearly dependent on the associated parameters i.e. it can be represented in the form of Equation (2.2).

$$f(x_1, x_2, \dots, x_d) = a_1x_1 + a_2x_2 + \dots + a_dx_d \quad \text{Where:} \quad (2.2)$$

x_d are parameters
 a_d are constants
 For d parameters

The RSS method is based on the assumption that x_d are statistically independent and normally distributed (Mansoor 1963). Under these assumptions it is possible to determine the first two statistical moments of the system response from equations (2.3) and (2.4), respectively:

$$\mu = a_0 + a_1\mu_{x_1} + a_2\mu_{x_2} + \dots + a_N\mu_{x_d} \quad (2.3)$$

$$\sigma^2 = a_1^2\sigma_{x_1}^2 + a_2^2\sigma_{x_2}^2 + \dots + a_N^2\sigma_{x_d}^2 \quad (2.4)$$

To apply the RSS method to non-linear response functions, a Taylor's series expansion with truncated high order terms may be applied to linearize the function (Evans 1975). However, the method can be computationally expensive and requires that the response function be explicitly known and differentiable. As the required assembly response functions in tolerance analysis are often difficult or impractical to define analytically, the applicability of the RSS method can be limited in CAD and CAT modelling environments involving complex assemblies.

2.5.2.2 Taguchi method

The Taguchi method of UQ in tolerance analysis is based on Taguchi's Design Of Experiments (DOE) methodology (Taguchi 1978). The assembly response function is evaluated (whether it be analytically defined or implicitly captured with a numerical model such a CAD assembly) with a full factorial, three level experimental design. The Taguchi method is based on the assumption that the assembly response function parameters are statistically independent and normally distributed. The method achieves a computational saving by effectively approximating the mean and standard deviation of the continuous normal distribution of the part parameters with a discrete distribution defined by 3 points (Nigam *et al.* 1995). The three levels for each part parameter x_N of the assembly response function correspond to: the parameter mean μ_{x_N} , a high levels of $\mu_{x_N} + \sigma_{x_N}\sqrt{3/2}$ and a low level of $\mu_{x_N} - \sigma_{x_N}\sqrt{3/2}$. The response function is evaluated at 3^N combination of the levels of each parameter. The resultant is a population of KPC values from which statistical moments can be calculated using standard statistical formulae. The method provides a good estimate of the statistical moment and can also be modified to accommodate non-normal distributions (D'Errico *et al.* 1988). However, the number of sample points required grows exponentially with the number of part parameters and can quickly become impractical. In such cases,

MC methods are a preferable choice as they are not founded on any simplifying assumptions and may provide superior performance (D'Errico *et al.* 1988).

2.5.2.3 Other elementary analytical methods

Some additional UQ methods which can be classified as elementary include:

- Hasofer-Lind index method (Parkinson 1982; Lehtihet *et al.* 1991),
- Extended Taylor series approximation (Evans 1975),
- Most probable point method (Fiessler *et al.* 1979),
- First and second order reliability (Hohenbichler *et al.* 1987).

A number of review articles focused on these methods have been presented (Evans 1975; Parkinson 1982; Lehtihet *et al.* 1991; Lee *et al.* 2009). These elementary analytical UQ methods will not be considered further in this dissertation as their applicability is limited due to their simplifying assumptions (see Section 2.5.2) and as more contemporary advanced analytical methods offer superior performance.

2.5.3 Analytical methods - Advanced

Comparisons of various contemporary analytical UQ methods have been presented in the literature (Haldar *et al.* 2000; Wojtkiewicz *et al.* 2001; Eldred *et al.* 2008; Eldred *et al.* 2009; Lee *et al.* 2009). Based on the outcomes of these comparative studies, Polynomial Chaos Expansion (PCE) offers the most potential for application in tolerance analysis and synthesis problems due to:

- Non-intrusive¹ nature applicable to integration with existing CAD, CAE and PIDO tools
- High efficiency and accuracy
- Flexibility in accommodating various input parameter distributions
- Ability to accommodate high dimensionality problems
- Current high interest in the research community resulting in continual performance improvements of PCE methods

¹ Non-intrusive denotes the ability of the associated UQ method to estimate statistical moments without requiring knowledge of the system function, only the system response for a set of known inputs. In the context of tolerance analysis, a non-intrusive UQ method can be used to estimate the stochastic distribution of assembly Key Product Characteristics (KPCs) from a set of associated stochastic part or assembly parameter values. The assembly response function does not need to be explicitly known in the form of an algebraic expression, but can instead be simply captured as a “black-box” form in a numeric CAD or CAE model. This significantly reduces modelling complexity as in non-trivial assemblies the assembly response function may be analytically intractable.

The PCE method is based on a representation of the response function of a stochastic system as a multi-dimensional, orthogonal polynomial expansion in stochastic variables.

The PCE method offers the potential to be significantly more efficient than sampling based UQ methods such as MC simulation by showing exponential convergence of $O(e^{-N})$ in the estimation error of the mean and standard deviation. Furthermore the method can be applied in a non-intrusive manner to problems where the system response function is implicitly defined.

The PCE method will be considered in further detail in Chapter 5 of this dissertation.

2.6 Tolerance synthesis

There is some ambiguity associated with the usage of the term *tolerance synthesis* in the literature. Tolerance synthesis in its most fundamental form may refer to the process of allocating part tolerances that satisfy the functional requirements of an assembly, without consideration of optimality. The solution procedure can be carried out by manual iteration. A more sophisticated approach is to consider tolerance synthesis as a single-objective optimization problem with the objective of maximizing yield, where the minimum yield requirements acts as a constraint. Alternatively, the single-objective may be to minimise the total cost of allocated tolerances.

Tolerance synthesis may also refer to a more challenging multi-objective optimization problem that is subject to the competing objectives of minimising tolerance cost and maximising yield (or product quality) within the constraints imposed by the product design requirements and manufacturing process characteristics (Hong et al. 2002). The definition of tolerance synthesis adopted in this dissertation is:

Tolerance synthesis: The process of optimally allocating part tolerances in a product assembly to maximize assembly yield (or product quality) and minimize tolerance cost within the constraints imposed by the product design requirements and manufacturing process characteristics

In such a tolerance synthesis problem, a tentative set of tolerances is analysed to determine if the assembly yield requirements are met. If yield targets are not achieved, a more precise set of tolerances needs to be selected. If yield targets are exceeded, a less precise (and therefore less costly) set of tolerances may be selected. An optimization algorithm guides the search for a set of tolerances which offer balanced performance in achieving both the objectives of maximising yield and minimising tolerance cost.

A tolerance synthesis problem requires the application of a number of analysis and simulation techniques, including: optimization algorithms; tolerance analysis and associated UQ method; and, yield and cost-tolerance estimation approaches. A number of tolerance synthesis methods have been proposed with a range of different analysis techniques.

Early tolerance synthesis approaches were based on deterministic optimization algorithms (such as non-linear programming) involving a single cost-tolerance function (Speckhart 1972; Spotts 1973; Wilde *et al.* 1975; Ostwald *et al.* 1977; Parkinson 1982; Parkinson 1985). A comprehensive survey of deterministic tolerance synthesis can be found in (Feng *et al.* 1997). Research has also focused on addressing a discrete tolerance synthesis problem involving the most economical selection of manufacturing process from alternative cost-tolerance functions (Dong *et al.* 1989; Chase *et al.* 1990; Dong *et al.* 1990; Dong *et al.* 1991; Zhang *et al.* 1993; Dong *et al.* 1994; Roy *et al.* 1997; Zhang *et al.* 1997)

Another area of research involves the application of concepts associated with Taguchi's quality loss functions (Section 2.2.3) to tolerance synthesis (Askin *et al.* 1988; Jeang 1994; Anwarul *et al.* 1995; Jeang 1999; Cho *et al.* 2000; Choi *et al.* 2000; Feng *et al.* 2001). Extensions to the concept involve incorporation of customer objectives into the tolerance synthesis problem in addition to manufacturing quality concerns (Soderberg 1993; Soderberg 1994).

To address the limitation associated with deterministic optimization algorithms, such as difficulty in accommodating discrete variables and multiple objectives, as well as poor global optima search performance, a high interest exists in the application of metaheuristic optimization algorithms to tolerance synthesis. Metaheuristic algorithm offer attractive performance as they are typically not limited by assumptions about the problem being optimized (such as smooth objective functions or continuous variables) and can search large spaces of discrete candidate solutions efficiently (Deb 2004) (Section 2.6.1). A number of applications of metaheuristic algorithm have been reported in the tolerance synthesis research community:

- Simulated annealing (Zhang *et al.* 1993; Dupinet *et al.* 1996)
- Particle swarm optimization (Steiner *et al.* 2003; Zhou *et al.* 2006)
- Evolutionary algorithms (Carpinetti *et al.* 1995; Iannuzzi *et al.* 1995; Kanai *et al.* 1995; Ji *et al.* 2000; Forouraghi 2002; Singh *et al.* 2004; Kumar *et al.* 2007; Mazur *et al.* 2011)

Genetic algorithms have been widely adopted due to their robust performance attributes and will be applied in this dissertation for tolerance synthesis (Holland 1992; Bäck 1996; Gen *et al.* 2000; Haupt *et al.* 2004).

The major challenge in realizing effective tolerance synthesis is the impractically large computational cost required as the levels of complexity of the mechanical assembly under analysis increases (Hong *et al.* 2002; Wenzhen *et al.* 2009; Wu *et al.* 2009; Rao *et al.* 2011). Attempts to decrease this computational cost have focused mainly on reducing the solution time of the associated tolerance model with simplifying assumptions, or surrogate approximate models. Introducing such simplifications can, however, limit modelling accuracy with excessively conservative solutions, or limit ability to address more general problems not compatible with the associated approximations (such as linearized assembly response functions, parameter distributions with only a single distribution type or symmetric tolerance specification limits) (Singh *et al.* 2009; Wenzhen *et al.* 2009; Wu *et al.* 2009). However, the overall computational cost of tolerance synthesis can be lowered not only by reducing the solution time of the tolerance model, but also by reducing the number of iterative simulations required as part of the adopted UQ method. There is a potential to exploit this opportunity with the application of more efficient analytical UQ methods which have recently been developed (for example Section 2.5.3). This opportunity is explored in Chapter 5 of this dissertation.

2.6.1 Optimization

The aim of optimization is to select a best solution to a given problem objective from a set of candidate alternatives within any associated constraints. The solution procedure typically involves minimizing or maximizing an *objective function* (which defines the problem under consideration) by systematically evaluating alternative candidates and using the objective function response values to guide a search for a superior solution. A feasible solution that minimizes (or maximizes, if that is the goal) the objective function is referred to as an optimum solution.

An optimization problem is characterized by the following attributes:

1. Design parameters

A design parameter is a controllable input variable which influences the response of the objective function. In tolerance synthesis the design parameters are part feature tolerances. A design parameter may be continuous (such as a nominal part dimension), discrete (such as the cost associated with several alternative cost-tolerance curves for a given tolerance). Problems may involve a mixture of continuous and discrete design parameters. Continuous variables optimization problems are typically less difficult to address (Deb 2004).

2. Constraints

A constraint is a condition that must be satisfied in order for a design to be feasible. An optimization problem may have a closed domain which limits the possible candidates to be evaluated (referred to as a constrained optimization problem) or an open domain where the choice of candidates is unrestricted (unconstrained optimization problem). An example of a tolerance synthesis constraint is a minimum allowable yield requirement for manufactured product assemblies. Constraints can be accommodated explicitly by an optimization algorithm or may be integrated into the objective function using the method of Lagrange multipliers (Avriel 2003).

3. Objectives

An objective is a parameter that is to be maximized or minimized. The objective function describes the relationship between the input and output parameters of the problem under consideration. Depending on the field of application, the objective function may also be referred to as a *cost function* or a *utility function*. In the tolerance synthesis field the objective function is analogous to an assembly response function (Section 2.3). An optimization problem may involve a single objective (such as maximising assembly yield) or multiple objectives (such as maximising assembly yield and minimising tolerance cost). A multi-objective problem typically does not have a single optimum solution due to competing objectives. Instead there exists a best set of solutions, known as Pareto-optimal solutions, which offers equivalently optimal performance, as superior performance for one objective results in a compromise for another other objective (Deb 2004). Furthermore, optimization problem may involve both local and global optimum solutions. A local optimum is a high performing candidate design within a particular region of the design space. However, other regions exist which offer superior overall performance. A solution which maximizes performance over the entire design space is known as a global optimum. Designers are ideally interested in finding global optimum solution (Nocedal *et al.* 1999).

4. Models

The objective function is typically characterized by an explicit or implicit design model. For example, in tolerance synthesis the objective function (assembly response function) is typically characterized by a CAT model of the product assembly (Section 2.7). The comprehensiveness of the model is typically subject to the competing requirements of model fidelity and analysis time.

5. Optimization algorithm

An optimization algorithm aims to intelligently search the feasible design space to identify the best solution from the possible candidates (Section 2.6.2).

A review of optimization algorithms is presented in the following section. The review outlook is on the ability to address the thesis objective of tolerance synthesis of assemblies subject to loading, within the modelling environment of existing standalone CAD/E tools.

2.6.2 Optimization algorithms

Most optimization algorithms follow either deterministic or metaheuristic/stochastic approaches. A number of popular deterministic and metaheuristic optimization algorithms are classified in Table 2.4.

Table 2.4 - Classification of optimization algorithms

Optimization Algorithms						
Deterministic				Metaheuristic/Stochastic		
Direct search	Gradient-Based			Swarm intelligence	Simulated Annealing	Evolutionary algorithms
	Constrained	Unconstrained				
		General	Non-linear least squares			
Nelder-Mead simplicial heuristic (SIMPLEX) (Deb 2004)	Sequential Quadratic Programming/Lagrange-Newton method (Alt 1990)	Steepest descent (Avriel 2003)	Gauss-Newton (Salas Gonzalez <i>et al.</i> 2008)	Particle swarm (Kennedy <i>et al.</i> 1995)	Simulated Annealing (Kirkpatrick <i>et al.</i> 1983)	Evolutionary strategies (Beyer <i>et al.</i> 2002)
Generalized Pattern search (Audet <i>et al.</i> 2006)	Augmented Lagrangian (Schittkowski 1983)	Newton and Quasi-Newton methods (Fischer 1992)	Levenberg-Marquardt (Roweis 1996)	Ant colony (Dorigo <i>et al.</i> 2006)	Parallel Tempering (Earl <i>et al.</i> 2005)	Genetic Algorithms (Holland 1992; Gen <i>et al.</i> 2000; Deb <i>et al.</i> 2002)

Deterministic algorithms are generally based on identify local gradients of the objective function (gradient-based methods) or curvatures (direct search methods) which may lead to a maximum or minimum (Avriel 2003; Audet *et al.* 2006). Deterministic optimization methods are well suited to objective functions which are continuous and smooth (for example, gradient-based methods require the derivative of the objective function to be known). An advantage of deterministic algorithms is efficient local convergence when the search in near a globally optimum point. However deterministic algorithms may dwell near an identified local optimum and have difficulty finding a global optimum (Nocedal *et al.* 1999).

Metaheuristic methods are generally based on a stochastic approach which introduces randomness into the optimization search process in order to explore the design space more comprehensively by prevention of dwelling at local optima. A significant number of metaheuristic methods have been inspired by probabilistic physical phenomena which

exhibit optimization properties. For example, some of the most utilised algorithms are based on swarm intelligence of ants (*Ant colony optimization* (Dorigo *et al.* 2006)), annealing of metal (*Simulated annealing* (Kirkpatrick *et al.* 1983)), and biological evolution (*Evolutionary algorithms* (Holland 1992)). Of the metaheuristic methods, evolutionary algorithms consistently perform well in many optimization problems and have been successfully applied in many fields of engineering (Fonseca *et al.* 1995; Bäck 1996; Zitzler *et al.* 1999). Among the evolutionary algorithm techniques, Genetic Algorithms (GA) show good performance in tolerance synthesis problems as discussed in the following section.

2.6.2.1 Genetic algorithm (GA)

Genetic Algorithms (GA) are popular optimization algorithms inspired by the processes of evolutionary biology. In general GA algorithms work in the following fashion (Holland 1992; Bäck 1996; Gen *et al.* 2000; Haupt *et al.* 2004):

1. A random population of design parameters is initialised and coded into binary string structures referred to as chromosomes.
2. The objective function is subsequently evaluated for the random population of design parameters. The fitness of the design parameters (which is a measure of how well objectives are satisfied) is evaluated.
3. The population of individuals is then improved through manipulations that are analogues for the mechanics of natural selection. Commonly three operators are used: selection, crossover and mutation. The selection operator chooses the best candidates from the previous generation based on their fitness. This selection leads to the formation of an intermediate candidate population, from which a subsequent population (also referred to as a generation) is created. This population (or next generation) is created by applying the crossover operator to the intermediate candidates which combines the binary string structures of two or more candidates (referred to as parents) to form a new candidate (offspring). The crossover process is analogous to reproduction and biological crossover and is based on the notion that the fitness of the offspring candidate has a probability chance of exceeding that of its parents. To ensure comprehensive exploration of the design space by avoiding dwelling at local optima, the last mutation operator aims to slightly perturb the evolution of generations to avoid premature convergence. The mutation is achieved by creating random bit variation in some binary string structures of the coded design parameters.
4. The outcome of the manipulation process is a new population of design parameters, with a commonly increased fitness (although not guaranteed) due to the filtered

selection of best performers in the previous generation. The new population is once again evaluated for fitness and subsequently re-manipulated.

Multiple iterations, or generations, of the process are carried out until a termination requirement is passed such as a limit on the number of generations, or when diversity in the objectives space becomes rare with subsequent iterations.

Genetic Algorithms are well suited to tolerance synthesis problems due to (Iannuzzi *et al.* 1995; Forouraghi 2002; Singh *et al.* 2004; Kumar *et al.* 2007):

- Ability to accommodate both continuous and discrete variables (useful when multiple discrete cost tolerance curves are used).
- Good global optimum search perspective in large objective spaces.
- Multi-objective optimization capability with large number of variables.
- Ability to accommodate implicit objective functions or models (e.g. CAD/CAT assembly models).
- Roust against discontinuities, fluctuations or noise in objective functions or models.

Due to their desirable characteristics GA algorithms will be applied in this work for tolerance synthesis (Chapter 5).

2.7 Computer Aided Tolerancing (CAT) tools

A number of commercial Computer Aided Tolerancing (CAT) tools are available which offer tolerance analysis and synthesis capabilities either as independent software packages, or more commonly through integration with popular commercial CAD systems (Makelainen *et al.* 2001). Some of the available tools include:

- CETOL (Sigmetrix)
- eM-TolMate (Tecnomatix)
- VisVSA (UGS)
- 3DCS (Dimensional control systems)
- Mechanical Advantage (Cognition software)
- TolAnalyst (Solidworks - Dassault Systemes)
- CATIA.3D FDT (CATIA - Dassault Systemes)

A few of the tools are based on the tolerance modelling methods discussed in Section 2.3.2. For example CETOL was originally based on the Vector-Loop method, whereas CATIA.3D FDT is based on the TTRS model (Section 2.4.3); however it is difficult to discern in all cases which methods are applied due to the proprietary nature of these commercial tools. Nevertheless, most CAT tools utilize an independent model abstracted from an underlying

CAD model to represent tolerance variation. A typical CAT software tolerance modelling, analysis and synthesis approach involves (Prisco *et al.* 2002):

1. Definition of CAD models for each part of the product assembly.
2. Importing of the CAD model into the CAT system and interactively creating tolerance modelling geometry superimposed on the original CAD data.
3. Specification of tolerance types for features of interest on each part in the assembly.
4. Definition of part relationships that constitute the assembly such as assembly sequence and mating conditions.
5. Specification of KPCs (e.g. assembly clearances) which must be satisfied in order to fulfil design requirements.
6. Simulation of the effect of part tolerances on KPCs using a stochastic or worst-case tolerance analysis approach.
7. Recording outcomes such as yield and associated tolerance cost.
8. Possible sensitivity analysis to determine most influential part tolerances contributing to variation in assembly KPC.
9. Subsequently, based on analysis outcomes and CAT tool capabilities, re-allocating of part feature tolerances to target the total allowable variation in KPCs. The allocation may be achieved manually, or automated through tolerance synthesis aimed at maximising yield and/or minimising tolerance cost. The manufacturing cost associated with a particular tolerance is typically predicted using cost-tolerance functions (Section 2.2.3.1)

A number of comparative review and survey works of CAT systems have been presented in the literature. Initial works focused on the limitations of the two-dimensional geometry capabilities of the then contemporary systems (Turner *et al.* 1991). Other review works focused on CAT tools developed from a research perspective (Chase *et al.* 1991). A number of recent reviews offer a more detailed overview of the nature of contemporary commercial CAT tools (Salomons *et al.* 1998; Prisco *et al.* 2002; Chiesi *et al.* 2003; Zhengshu 2003; Shen *et al.* 2005; Shah *et al.* 2007). A particularly comprehensive review of some of the most popular CAT tools has noted a number of common capabilities as well as shortcomings (Prisco *et al.* 2002). Additional investigation carried out in association with this dissertation has identified changes in the CAT tool capabilities since the previously published reviews. Furthermore, current limitations associated with uncertainty quantification method capabilities and accommodations of assemblies under loading have been identified. Table 2.5 summarises the results.

Table 2.5 - Comparison of commercial CAT tools.
Limitations in current CAT tools are identified in bold.

Feature	Commercial CAT software tool			
	CETOL	eM-TolMate	VisVSA	3DCS
Tolerancing schemes				
Dimensional	yes	yes	yes	yes
GD&T	yes	yes	yes	yes
Automatic utilisation of CAD model defined GD&T data	no	no	no	no
Tolerance analysis				
Worst-case	yes	yes	yes	yes
Statistical	yes	yes	yes	yes
Sensitivity analysis	yes	yes	yes	yes
Uncertainty Quantification methods				
MC	yes	yes	yes	yes
Analytical (Advanced)	no	no	no	no
Tolerance synthesis capability				
Synthesis capability	yes	yes	yes	yes
Multi-objective optimization	limited	limited	limited	limited
Simplifying assumptions				
Rigid body	yes	yes	yes	partial
Limit on variation size	yes	no	no	no
Integration				
Compatible CAD tools	SolidWorks Pro/E	CATIA, NX I-deas, Pro/E,NX	Operates outside CAD environment on translated models. STEP, IGES	CATIA, Unigraphics, STEP, IGES
Distributed/parallel computing	no	no	no	no
Integration with external CAE modelling tools	no	no	no	no
Accommodation of assembly loads	no	no	no	Limited (compliant sheet metal assemblies)

Despite the extensive capabilities of commercial CAT systems, some notable limitations remain (Table 2.5). For example:

- GD&T data defined in the CAD model is not able to be automatically imported into the CAT system due to limitations with CAD geometry translator standards such as STEP or IGES (ISO 2002).
- None of the currently available tools offer distributed/parallel computing capabilities which can offer reduced analysis times by distributing simulations over multiple computers.
- Lack of ability to accommodate general tolerance analysis and synthesis problems involving assemblies under loading. CAT tools have been identified that accommodate a limited subset of physical phenomena such as deformation of sheet assemblies (3DCS

from Dimensional Control Systems). However, in general the abstracted geometric model employed in current CAT systems become incompatible when dealing with tolerance analysis and synthesis involving a general class of problem requiring the numeric simulation of assemblies under loading conducted on CAE models (such as FEA, CFD, or multi-body dynamics simulations).

Chapters 4 and 5 of this work address some of the identified limitations through the application of Multi-disciplinary Design Optimization (MDO) principals and Process Integration and Design Optimization (PIDO) software tools (Section 2.8) to tolerance analysis and synthesis.

2.8 Process Integration and Design Optimization (PIDO)

Multi-disciplinary Design Optimization (MDO) is an active research field concerning product design problems involving disparate engineering disciplines. In general MDO can be defined as a formal methodology that facilitates the integration of interdisciplinary knowledge and tools to achieve better engineering of overall system design. MDO consists of a number of conceptual elements including; system modelling, design oriented analysis, approximation concepts, optimization procedures, system sensitivity analysis, and human interface (Sobieszczanski-Sobieski *et al.* 1997).

To aid in MDO, a range of Process Integration and Design Optimization (PIDO) software tools have been developed. PIDO tools are software frameworks for facilitating the integration of diverse, discipline specific CAE analysis tools (e.g. FEA or CFD software) for process scheduling, design of experiments, optimization and statistical simulation analysis. Interaction between standalone CAE software tools is achieved with parallel or serial connections and conditional switches, thorough commonly embedded scripting capabilities (based on scripting languages such as JavaScript, Visual Basic, Python or DOS script) (Flager *et al.* 2009). The scripting capabilities of CAE tools allow for autonomous:

- modification of model parameters
- initialisation of simulations
- recording of the obtained simulation results

The available PIDO tools include both commercial as well as research focused software packages, some of these are listed below:

- modeFRONTIER (ESTECO)
- ModelCenter (Phoenix Integration)
- iSIGHT (Engineous Software)

- Epogy (Synaps)
- OPTIMUS (LMS)
- FIDO (developed at NASA)
- MINOS (Stanford Business Software)
- Infospheres Infrastructure (California Institute of Technology)
- DAKOTA (Sandia National Laboratories)

The various tools differ in:

- Degree of interface ability with external CAE software tools and associated models
- Number of possible concurrent interfaces
- Design Of Experiments (DOE) implementations
- Optimization capabilities (single or multi-objective, algorithm implementation)
- Statistical simulation and analysis capabilities
- Data management, exchange, recording, monitoring, visualization and interpretation capability
- Meta-modelling ability (see Section 2.5.1 for additional details about meta-modelling)
- Distributed/parallel computing capabilities
- Level of automation
- Computational overheads
- Accessibility of user interface and learning curve
- Collaborative design support
- User support

Extensive evaluations and comparisons of some of the available tools have been reported in the literature (Sobieszcanski-Sobieski *et al.* 1997; Kodiyalam 1998; Malone *et al.* 1999; Padula *et al.* 1999; Kodiyalam *et al.* 2000; Malone 2001; Piperni *et al.* 2004; Parashar *et al.* 2007; Simpson *et al.* 2008; D. *et al.* 2009; Flager *et al.* 2009; Adams 2011). The published comparisons, in addition to investigations carried out as part of this dissertation, reveal that significant advances have been made by the MDO research community and PIDO tool developers in broadening integration, optimization and statistical analysis capabilities.

The emerging abilities of contemporary PIDO tools to integrate standalone CAD and CAE models with automated parametric control, statistical analysis and multi-objective optimization offer attractive capabilities for design analysis and refinement. These capabilities may offer novel opportunities to enhance the design process, in particular aspects of tolerance analysis and synthesis problems. These opportunities are discussed in further detail in the following chapters.

2.9 Tolerance analysis and synthesis of assemblies subject to loads

The functionality of many real-world assemblies is often defined by how the assembly behaves in response to some applied action, such as a force, temperature change or electromagnetic interaction. These actions are generally referred to as loads. Predominant loads in the design of mechanical assemblies are internally or externally applied forces. External forces are independent of part mass and are applied to the part boundary; for example friction and contact forces. Internal forces occur due to inertial effects and are applied through the centre of mass; for example gravitational and dynamic forces. Internal and external forces typically act to influence assembly dimensions dependent on part compliance or assembly functions dependent on friction and dynamic effects (Bedford *et al.* 2008).

Accommodating the effects of loads in tolerance analysis and synthesis is an active research field. The main focus of research has been on tolerance analysis of compliant assemblies with sheet metal assembly applications in mind. The focus corresponds to the high interest in the quality control of fit and finish of sheet metal body panel assemblies in automotive, aerospace and domestic appliance applications. The need for a different tolerance analysis approach for compliant assemblies was highlighted by researchers attempting to model tolerance stack-up in automotive body panel assembly lines using production data. Common assumptions of part rigidity and linear addition of variance in tolerance analysis were inaccurate and a need for a more realistic modelling approach was required (Takezawa 1980).

The proposed approaches for accommodating forces in tolerance analysis have often adopted Finite Element (FE) models for modelling effects associated with forces such as compliance (Zienkiewicz *et al.* 2005). Pioneering work in tolerance analysis of compliant assemblies focused on the assembly of sheet metal with rigid frames (Liu *et al.* 1995; Liu *et al.* 1996; Liu *et al.* 1997). The approach consisted of modelling the compliance using an approximated FE model of the sheet and frame assembly constructed with the application of the method of influence coefficients (Levy 1953). Uncertainty quantification was carried out using the root sum of squares method (Section 2.5.2.1), applied to an approximating linear response function. The method was later expanded to consider variation in production scenarios involving multi-station assembly systems (Camelio *et al.* 2003).

Another approach involved investigating the use of surrogate polynomial functions for representing surface variation in sheet metal to simplify the modelling of the assembly response function (Merkley *et al.* 1996). The use of surrogate polynomial functions results in

an explicit assembly response function avoiding the need for FE modelling. The approach was later generalised to broader applications such as tolerance analysis of compliant spring, beam and flanged plate assemblies (Merkley 1998). A contribution to this method was also developed for accommodating surface waviness tolerances of sheet parts using spectral analysis techniques (Bihlmaier 1999). This approach reduces the need for computationally expensive FE simulations, however it is founded on a number of specific assumptions such as: small variations in geometry have no effect on the part stiffness, all part compliance is linear, and all tolerances are uniform tolerances. These assumptions can be limiting in broader applications.

A number of additional contributions have been made to tolerance analysis of assemblies under loading for broader application scenarios. One contribution focused on examining the variation in stress and compliance arising in bolted connections subject to fastener and hole alignment tolerances (Gordis *et al.* 1994). The associated solution procedure utilized mapping of assembly variation into the frequency domain, with a reduced representation of the assembled components, to solve a FE frequency domain structural analysis problem. In other work, the variation in static loading behaviour of composite materials subject to manufacturing variation was investigated with composite FE models and Monte Carlo based UQ (Vinckenroy *et al.* 1995). A similar approach was used in investigations of structural behaviour subject to large material property variations (Elishakoff *et al.* 1999). Consideration of tolerances in free form compliant composite surfaces has also been investigated (Polini 2011). More recent contributions include a method of simplifying the geometry of FE models used in tolerance analysis with surrogate models constructed from simplified compliant beam structures (Shiu *et al.* 2003) as well as a linearization FE simplification for tolerance analysis of compliant kinematic linkage mechanisms (Imani *et al.* 2009).

Some additional contributions to the tolerance analysis of assemblies under loading are summarised here:

- The integration of tooling variation into a tolerance analysis problem involving compliant assemblies (Hu *et al.* 2001).
- Consideration of the effect of thermo-mechanical dimensional variation (Pierre *et al.* 2009). The procedure assumes rigid parts with two possible geometrical states – one nominal and one under thermal strain. The thermal strain model is resolved using an FE model. The two different possible states are used in an analytical tolerance analysis procedure.

- Simulation of the effects of welding distortion in tolerance analysis (Lee *et al.* 2009). The approach includes the initial creation of a database of expected variation in welding distortion for different weld parameters using FE welding simulations. The database is utilised during the UQ tolerance analysis process without the concurrent integration of FE model simulations.
- Adaptation of mesh morphing techniques for FE models of compliant parts in tolerance analysis (Franciosa *et al.* 2011). Mesh morphing achieves part geometry changes by reshaping FE mesh elements at the nodal co-ordinate level without requiring underlying CAD model updates. This ability reduces the computational cost associated with parts CAD model rebuilds and re-meshing. Limitations of this approach include restrictions on the allowable magnitude of geometric changes and the continued propagation of any inherent problems or limitations which exist in the original source mesh (Owen *et al.* 2010).

The main challenge in the above approaches to accommodating the effects of loading in tolerance analysis has been the development of a realistic and computationally efficient tolerance model. Research efforts have focused on reducing the computational cost of the tolerance model with simplifying assumption, surrogate FE models of approximated geometry, or with approximating analytical assembly response functions. However, as statistical tolerance analysis involves uncertainty quantification techniques requiring iterative evaluations of the tolerance model (Sections 2.5), the overall computational cost can be lowered not only by reducing the solution time of the tolerance model, but also by reducing the number of iterative simulations required as part of the adopted UQ method. The UQ methods applied in the above approaches have mainly included either linearized UQ techniques (such as root sum of squares (RSS), Section 2.5.2.1) or sampling based methods (such a Monte Carlo simulation, Section 2.5.1.1). The effectiveness of these methods at lowering computational cost is however limited either by their poor efficiency (MC - Section 2.5.1.1) or accuracy (RSS - Section 2.5.2.1). There has been a limited emphasis on investigating the potential for achieving overall computational cost reductions in tolerance analysis with the application of more efficient analytical UQ methods which have recently been developed (for example Section 2.5.3).

Moreover, the tolerance analysis approaches presented in literature for modelling the effects of loading, predominantly focus on a specific problem scenario such as sheet metal compliance or welding distortion. Additionally, they require the use of customised simulation codes and have seen limited implementation in practical tools available for

industry (such as in CAD and FE modelling software). The methods which have been implemented in available tools (such as tolerance analysis of certain sheet metal assembly types in the CAT software 3DCS; Table 2.5) are limited to specific scenarios and cannot accommodate a general class of problem involving variation in assemblies under loading (for example general structural compliance, multi-body dynamics, or kinematics).

As such, there exist limitations in the existing methods for accommodating the effects of loads in the tolerance analysis of assemblies under loading.

2.10 Summary of outcomes and opportunities for further work

This chapter has identified the current state of understanding of the knowledge domains associated with the research scope of this work. Using the expanded understanding that resulted from this literature review, a number of limitations in existing methods, as well as gaps in domain knowledge have been identified. The identified limitations offer a number of research opportunities; these are categorically identified below.

Process integration and design optimization:

Facilitating efficient design analysis and refinement with multidisciplinary integration is an active research focus of Multi-disciplinary Design Optimization (MDO) engineering methods. MDO has resulted in the continually emerging development of a range of Process Integration and Design Optimization (PIDO) software tools. PIDO tools enable interdisciplinary integration of standalone CAD and CAE models to facilitate automated parametric control, DOE, statistical analysis and multi-objective optimization.

A review of available PIDO tools (Section 2.8) reveals that significant advances have been made by the MDO research community and PIDO tool developers in broadening multidisciplinary integration, optimization and statistical analysis capabilities.

These emerging capabilities of PIDO tools may offer novel opportunities to enhance the engineering design of mechanical assemblies involving uncertainty or variation in design parameters, in particular, aspects of tolerance analysis and synthesis problems.

This opportunity will be investigated further in Chapters 3, 4 and 5.

Effects of loads in tolerance analysis:

A number of analytical and numerical methods have been proposed for addressing tolerance analysis problems in complex product assemblies subject to loads. However, a review of these methods has identified a number of limitations, including (Section 2.9):

- Ability to accommodate only single, specific applications (such as sheet metal compliance or welding-distortion).
- Reliance on specific, custom simulation codes for tolerance modelling with limited implementation in practical and accessible software tools.
- Need for significant additional expertise in formulating specific tolerance models and interpreting results.

There remains a lack of a more accessible approach to tolerance analysis of assemblies subject to loads, which can integrate into the established CAD and CAE modelling design framework with lower implementation demands.

Computer aided tolerancing tools:

Numerous Computer Aided Tolerancing (CAT) software tools have been proposed for addressing tolerance analysis and synthesis problems in complex mechanical assemblies (Section 2.7). Despite the extensive capabilities of existing CAT systems, some notable limitations remain. For example:

- Lack of ability to accommodate general tolerance analysis and synthesis problems involving assemblies subject to loading. CAT tools have been identified that accommodate a limited subset of loading effects such as deformation of sheet assemblies. However, in general the abstracted geometric model employed in current CAT systems are incompatible when dealing with tolerance analysis and synthesis involving a general class of problem requiring the numeric simulation of assemblies under loading.
- The ability of CAT tools to effectively address sophisticated optimization problems (such as tolerance synthesis in complex assemblies) with many competing objectives and constraints is relatively limited compared to dedicated optimization tools.
- GD&T data defined in the CAD model is not able to be automatically imported into the CAT system. Consequently, significant additional expertise and effort is required for formulating CAT specific tolerance models and interpreting simulation results.
- None of the currently available tools offer distributed/parallel computing capabilities which can offer reduced analysis times by distributing simulations over multiple computers.

Chapters 4 and 5 of this work focus on addressing these limitations.

Tolerance synthesis and uncertainty quantification:

Tolerance synthesis requires iterations of tolerance analysis which significantly compounds computational costs, particularly if numerical modelling of the effects of loading on mechanical assemblies is required. A main contributor to high computational cost has been the traditional approach to Uncertainty Quantification (UQ) in statistical tolerance analysis which is reliant on robust yet inefficient sampling based UQ methods such as Monte Carlo (MC) sampling. Attempts to decrease this computational cost have focused mainly on reducing the solution time of the associated tolerance model with simplifying assumption,

surrogate FE models of approximated geometry, or with approximating analytical assembly response functions (Sections 2.6 and 2.9). Introducing such simplifications can however limit modelling accuracy and versatility of the method.

However, alternative UQ methods with significantly higher computational efficiency than sampling based methods have recently seen extensive development (Section 2.5.3). A broadly applicable method is Polynomial Chaos Expansion (PCE). Investigation into the utility of these methods in tolerance analysis and synthesis has been limited. There is a potential to exploit this opportunity to significantly reduce the cost of UQ in tolerance analysis, and thereby increase the practical feasibility of tolerance synthesis in complex mechanical assemblies. This opportunity is explored in Chapter 5 of this dissertation.

3 DEVELOPMENT OF ENHANCED PIDO METHODS FOR DESIGN ANALYSIS AND REFINEMENT

3.1 Chapter summary

The early stages of product development typically involve a lack of knowledge or certainty, as influential properties may remain uncertain or poorly defined. This chapter identifies opportunities to enhance the conceptual and embodiment stages of design involving uncertainty or variation in design parameters. This is achieved by developing novel methods for the use of PIDO tools in the analysis and refinement of concept design embodiments with sensitivity analysis, tolerance analysis, DOE methods and optimization. Practical conceptual and embodiment design problems are considered and effective solutions developed for a number of industry focused scenarios. The outcomes allow designers to make informed decisions which positively influence the design early in the design process while cost commitments are low. The additional design knowledge acquired in one industry focused design problem influenced design decisions which resulted in class-leading performance of subsequently commercialised product.

3.2 Introduction

Engineering design is a creative and iterative process focused on the development and implementation of structures, machines or systems. The design process can be represented as a series of interconnected and interdependent stages (Pahl *et al.* 2007) (Figure 3.1), including:

Planning and task clarification:

- Definition of technical criteria such as functional requirements, design objectives and design constraints
- Definition of economic criteria

Conceptual design:

- Establishment of functional structures
- Exploration of feasible solution principles
- Combination of solution principles into concept variants
- Feasibility assessment against technical and economic criteria

Embodiment design:

- Development of concept variants into more comprehensive concept design embodiments (layouts)
- Exploration of the design parameter space for design refinement
- Benchmarking of concept designs
- Selection of best performing concepts

Detail design:

- Detailed specification
- Detail models and drawings
- Specification of production

The first stage of the design process is aimed at clarifying and comprehensively formalising the problem under consideration. A subsequent search for solution principles is carried out and concept variants are established (these are combinations of working principles and structures which may offer a solution to the problem). The feasibility of concept variants is assessed against technical and economic criteria. Feasible concepts are developed further into more comprehensively detailed concept design embodiments (also referred to as layouts) by exploring the design parameter space to identify: regions of desirable performance, design weaknesses or errors, sensitivity to disturbing influences and design refinement opportunities. The refined concept design embodiments can then be subject to further comparative assessment based on performance benchmarking; leading to a final concept being selected for detail design specification and implementation.

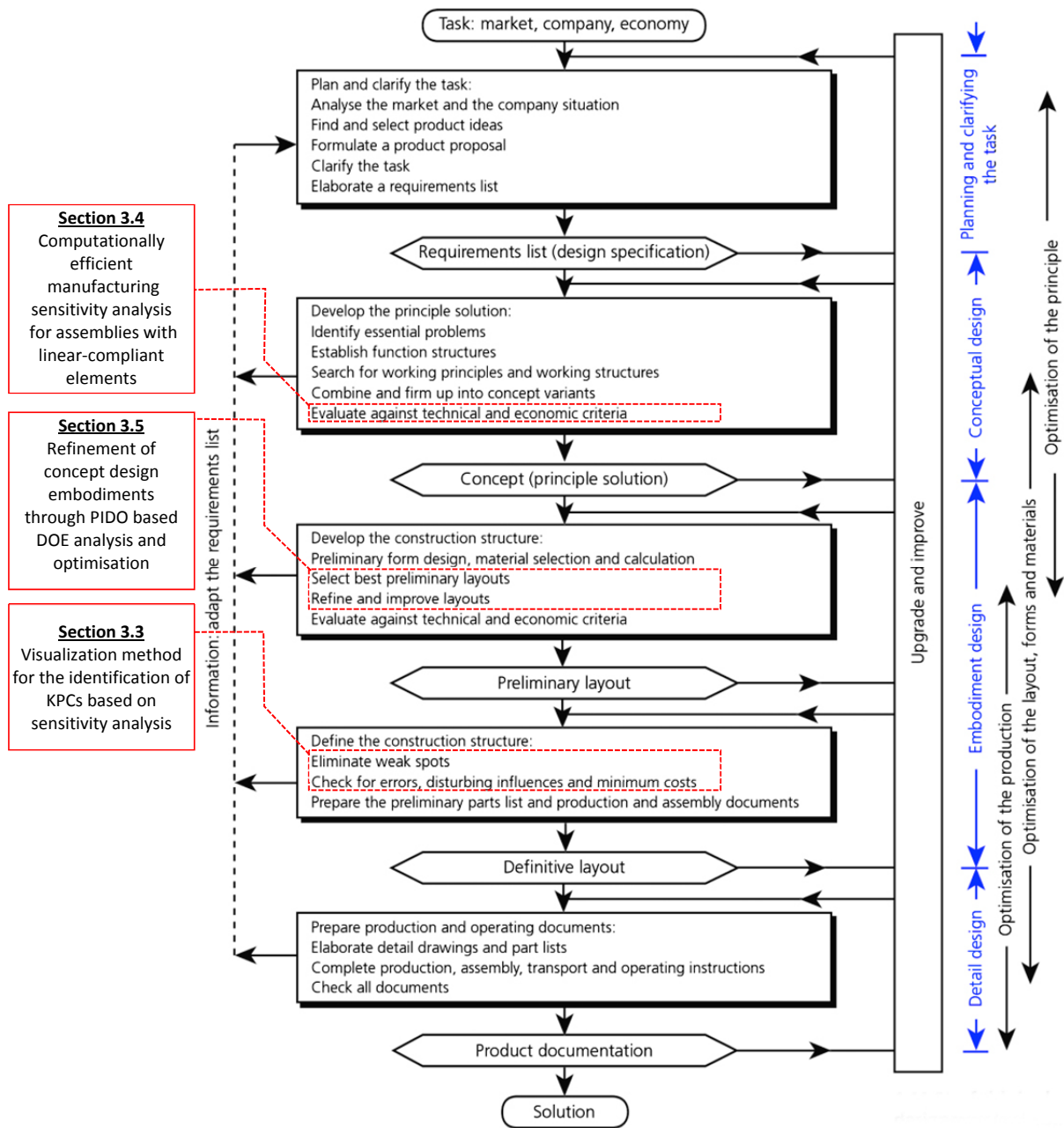


Figure 3.1 - Steps of planning and design process. Reproduced from Pahl and Beitz 2007 (Pahl et al. 2007). Contributions of this chapter are identified in red.

Despite the seemingly serial nature of the design process, it is often iterative in practice (Pugh 1991; Pahl et al. 2007). The conceptual and embodiment stages of product development are typically associated with a lack of knowledge or certainty of concept performance against technical and economic criteria, as many influential properties remain undefined or uncertain (Suh 1990). As the design process progresses and knowledge of concept performance is gathered through design analysis and refinement, the designer may need to reconsider earlier decisions and iterate preceding design process stages.

However, the cost of implementing changes to design decisions increases non-linearly with the design process stages and life of the project (Ullman 2003). This non-linear cost increase is due to progressively accumulating commitments to high-capital resources, such as production plans, tooling, prototyping and testing (Figure 3.2 (ii)). Concurrently, as the commitment to a specific design increases, the flexibility to enact changes to the design diminishes (Figure 3.2 (i)). Consequently, a high proportion of the cost of delivering a product can be attributed to the design decisions made during the conceptual and embodiment design phases. In response to these observed relationships (Figure 3.2), engineering design philosophy advises that available design development and analysis resources should be focused towards the early stages of the design process such as conceptual and embodiment design (Ullman 2003). This emphasis aims to maximise knowledge of the design problem and concept performance when flexibility to enact changes is high, and accrued costs are low. This approach has been referred to as Front End Loading (FEL) (Artto *et al.* 2001; Connor *et al.* 2003; Twigge-Molecey 2003) in reference to the emphasised commitment of design and analysis resources early in the project timeline. FEL is cited as allowing a significant improvements in the ability of a project to meet performance, quality and cost targets (Batavia 2001; Connor *et al.* 2003).

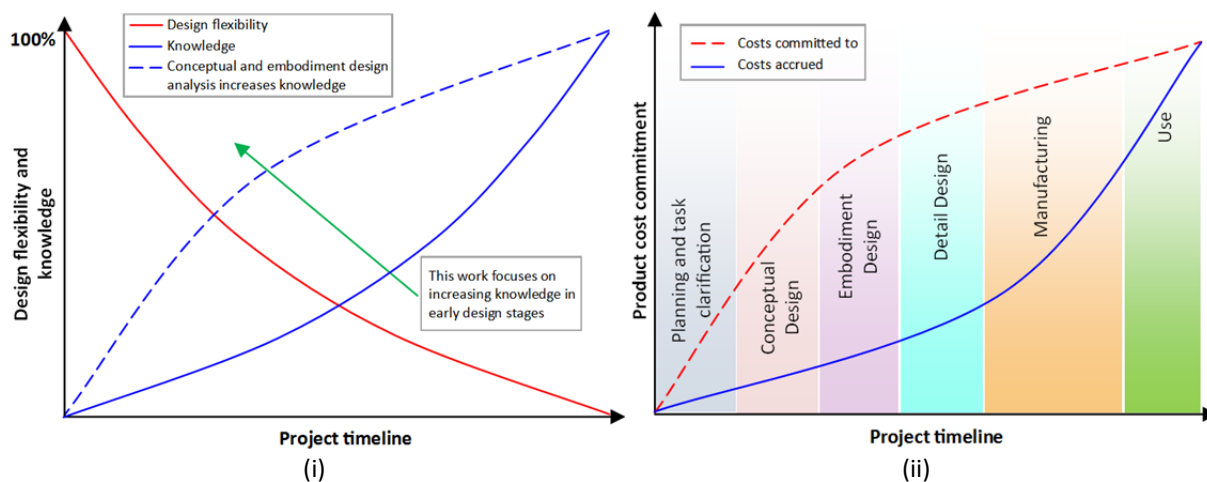


Figure 3.2 - (i) Design flexibility and knowledge versus project timeline
(ii) Cost commitment and accrument during phases of the design process, after (Ullman 2003).

Design analysis and refinement techniques provide an opportunity to increase knowledge of the design problem early in the project timeline (Figure 3.2 (i)); allowing the designer to make informed decisions while there is sufficient design flexibility to act without undue expense (when accrued costs are low i.e. Figure 3.2 (ii)).

Design analysis and refinement techniques include:

- sensitivity analysis;
- tolerance/robustness analysis;
- design of experiments (DOE);
- optimization methods.

Despite the high benefit associated with comprehensive analysis and refinement early in the design process, in practice it may be seen as difficult, time consuming or unreliable to consider at a time where many influential properties remain uncertain (Smith *et al.* 1997; Ebro *et al.* 2012).

This chapter provides contributions to overcome some of the difficulties associated with implementing design analysis and refinement techniques in designs involving uncertainty or variation in design parameters. In particular, the design refinement techniques for the analysis of the effects of manufacturing variation at the conceptual and embodiment design stage, may reduce the undesirable cost of managing poor quality later in the design cycle following the commissioning of manufacturing (Soderberg 1994; Soderberg *et al.* 1999; Taguchi *et al.* 1999). With this objective in mind, tolerance analysis at the conceptual design stage provides insight into the sensitivity of alternative concept designs to manufacturing variation and facilitates concept selection with quantitative measures of robustness (for example Section 3.4). Similarly, sensitivity analysis may be applied to aid in the identification and prioritization of key product characteristics (KPCs) (for example, Section 3.3) which measure the functional performance of the design, and are used for quality control during manufacture (Section 3.2.4).

The benefits associated with the exploration of the parameter space of a design through the utilization of DOE and optimization methods at the conceptual and embodiment design stages are also notable (Askin *et al.* 1988; Sobieszczanski-Sobieski *et al.* 1997; Simpson *et al.* 2008). For instance, DOE based parameter studies may reduce the potentially vast design space of possible conceptual design permutations which can arise from a broad range of design parameters whose feasible limits are yet to be fully defined. Similarly, optimization has the potential to identify desirable regions of local and global optimum performance in the presence of complex constraints and competing design objectives (for example Section 3.5).

Despite the potential benefits of design analysis and refinement techniques, the exploratory nature of the conceptual design stage is often associated with limited analysis time budgets for individual concepts, as time constraints often reserve the expense of comprehensive

analysis efforts for the detailed design stages (Darlington *et al.* 2002; Pahl *et al.* 2007). As such, a justifiable use of design refinement techniques at the conceptual stage needs to offer reasonably rapid implementation, low analysis cost, as well as accurate and reliable outcomes. Furthermore, due to the multidisciplinary nature of CAE modelling tools which may be utilised in conceptual and embodiment design (such as alternative CAD packages or simulation codes), the utilization of design refinement techniques needs to accommodate integration with disparate CAE tools, without excessively burdening the designer with the distraction of software integration.

The outlined requirements for the utilization of design analysis and refinement techniques at the conceptual and embodiment design stages align themselves well with the emerging capabilities of Process Integration and Design Optimization (PIDO) Software tools (Section 2.8).

This chapter identifies opportunities to enhance the conceptual and embodiment stages of design involving uncertainty or variation in design parameters. This is achieved by developing novel methods for the use of PIDO tools in the selection and refinement of concept design embodiments with sensitivity analysis, tolerance analysis, DOE methods and optimization.

The focus of contributions in the context of the design process is identified in Figure 3.1 and described below:

Selection and refinement of concept design embodiments:

Comprehensive exploration of the parameter space is carried out with DOE analysis and optimization to identify feasible and optimal regions of performance. These methods have been developed to identify optimal designs for automotive seat kinematics (Section 3.5).

Evaluate against technical and economic criteria:

The effect of manufacturing variation on the performance of concept design embodiments is achieved with efficient numerical models, tolerance analysis and sensitivity analysis. These methods enable the benchmarking of the relative performance of alternative conceptual automotive seat-rail designs (Section 3.4).

Check for errors and cost effectiveness:

Design weaknesses, sensitivity to disturbing influences and design refinement opportunities are investigated with sensitivity analysis through the identification of the key product characteristics in a complex actuator assembly (Section 3.3).

The outcomes allow designer to make informed decisions to positively influence the design early in the design process while cost commitments are low. Limitations identified in these methods are the basis of the contributions of the following chapters.

3.2.1 PIDO tools

A range of PIDO software tools have been developed which integrate independent CAD and CAE software through commonly embedded scripting capabilities. PIDO tools allow for: autonomous modification of CAD model parameters, initialisation of CAE simulations, and recording of simulation outputs; to facilitate automated parametric studies, statistical analysis and multi-objective optimization (Sobieszczanski-Sobieski *et al.* 1997; Kodiyalam 1998; Kodiyalam *et al.* 2000; Simpson *et al.* 2008). These capabilities are described in detail in section 2.11 and are applied to enhance design analysis and refinement of concept design embodiments.

3.2.2 Accommodating manufacturing variation in conceptual and embodiment design

Addressing the effects of manufacturing variation early in the conceptual and embodiment stages of design can help identify designs that are less sensitive to manufacturing variation and consequently reduce quality costs at the manufacturing stage (Soderberg *et al.* 1999).

The effects of manufacturing variation on product functionality can be investigated with tolerance analysis using virtual models (analytical or numerical) of the product assembly (Section 2.5). However, a tolerance analysis problem requires the definition of assembly parameters which indicate whether a given manufactured assembly will conform to the intended functional requirements of the design. The parameters of particular relevance to functionality are referred to as Key Product Characteristics (KPCs), and are typically geometric, such as clearances or nominal dimensions² (Section 3.2.4). However, the complexity which arises in product assemblies with many interacting parts and features can make the identification of assembly KPCs a challenging task for the designer.

² The concept of KPCs can be extended to include other parameters such as internal or external loads, material characteristics, or mechanical properties (Chapter 4 offers further detail).

3.2.3 Assembly complexity

The complexity of mechanical assemblies can be defined by the number of constitutive components, the number of component interactions and the intricacy of component features. These three aspects correspond to three fundamental elements defining complexity in mechanical engineering design problems (Summers *et al.* 2010):

1. Complexity as size

Complexity may be defined as the size of the problem. For example, in the commonly cited Kolmogorov definition, complexity is defined as the size of the shortest algorithm that can unambiguously define a problem (Stonier *et al.* 1994; Li *et al.* 2008).

2. Complexity as interaction

Complexity may be defined as the degree of interaction within the elements of the problem. This definition of complexity is a function of the interconnectedness between elements, for example (Earl *et al.* 2001; Felgen *et al.* 2005).

3. Complexity as solvability

Complexity may be defined as the number of operations required to identify a solution that satisfies the constraints and objectives associated with the problem. The solvability attribute can be denoted as *computational complexity* (Wang *et al.* 2004).

Attempts at the integration of these inherent aspects of complexity for greater understanding of mechanical assemblies are ongoing (Lesser 2000; Wang *et al.* 2004; Summers *et al.* 2010).

The problem of predicting assembly behaviour subject to stochastic variation is linked to complexity of interaction through the concept of diseconomy of scale; whereby a system becomes unwieldy due to the burden of an increasing number of interrelationships (McAfee *et al.* 1995; Lin *et al.* 2005). As the number of interacting parts increases, uncertainty in the nominal values of assembly parameters can drastically raise the quantity of possible distinguishable states of the assembly.

3.2.4 Key Product Characteristics (KPCs)

The large number of parameters and interacting components in complex product assemblies makes it difficult to know which assembly parameters are indicative of compromised functionality, and how deviations of parameters from the nominal intended values affect the performance of the assembly. As it can be uneconomical to monitor and control all product parameters at the manufacturing stage, key product characteristics are

commonly used to specify parameters especially critical to assembly functionality (Darlington *et al.* 2002). There is no universally standardized definition of a KPC (Zheng *et al.* 2008), and various nomenclature is used to describe nuances of the concept within industry (Lee *et al.* 1996). For instance, Key Characteristic (KC) is a term also commonly used to refer to the concept. Despite the lack of a broadly established consensus, the concept of a KPC is generally understood to be a product parameter whose deviation from a target value is associated with comparatively high loss in product quality. Under common definitions, a KPC is also associated with a requirement for quality monitoring and control of that parameter during manufacturing (Singh 2003). An example of a broad definition of a KPC as used in industry is one applied by General Motors Corporation; *“a product characteristic for which reasonably anticipated variation could significantly affect the product’s safety or compliance with governmental standards or regulations, or is likely to significantly affect customer satisfaction with a product”* (Lee *et al.* 1996). In this work a KPC is defined as: *“A part or assembly parameter especially critical to product functionality and whose deviation from a target value has a comparatively high loss in quality”*.

A generalized implementation of KPCs in industry can be classified into two stages; (i) identification and (ii) control. The identification of KPCs occurs at the design stage of the product and is typically conducted using a top-down approach of product analysis and decomposition (Ertan 1998). The top-down approach entails analysis of product functional requirements and systematically decomposing the product architecture into individual contributing features or parameters. Product parameters with high influence on assembly functionality (parameters with a steep quality-loss function) are classified as KPCs. A quality control plan must subsequently be established for monitoring, verification, and variation reduction of KPCs as the product is transitioned from design to manufacturing.

The identification stage of KPC implementation is particularly challenging. Quantitatively identifying and prioritizing KPCs requires an accessible assembly tolerance model which can be used to establish the range of variation in part parameters for which assembly functionality is not compromised. However, an accurate numerical tolerance model may not be readily available and can be considered excessively difficult to develop, particularly at the conceptual and embodiment design stages (Thornton 1999). An analysis of physical prototypes based on a DOE study can be considered as the only viable alternative (Phadke 1989). This approach however is expensive, slow and impractical, especially when a large number of product parameters are to be considered.

The lack of an accurate assembly tolerance model may lead the designer to a conservative approach to KPC specification. However, over-specifying the number of KPCs may result in uneconomical quality control demands during production. Quality control can become too cumbersome, potentially requiring production personnel to assess an inordinate number of parameters (Lee *et al.* 1996). Conversely, under-specifying the number of KPCs can lead to quality loss (Taguchi 1989).

3.2.5 Assembly response function modelling

Modelling the behaviour of a product assembly requires the definition of an assembly response function which defines the relationship between part and assembly parameters. The assembly response function may be explicitly defined through an algebraic expression however with complex assemblies this may be difficult due to the large number and complex interactions of parts. The assembly response function may, however, be defined implicitly through a numerical model such as CAD assembly or CAE model. CAD based design is well established, and as such, an implicitly defined assembly response function is usually available to the designer through CAD models constructed in the conceptual, embodiment and detail design stage. Inspection of the model using embedded dimension analysis tools allows the designer to identify any geometric assembly parameters of interest.

3.2.6 CAD tools

CAD modelling software is inherently parametric. Operations such as extrusions, sweeps and lofts applied to parametric two-dimensional sketches are used to create geometric three-dimensional solid part models. CAD assemblies are defined by multiple CAD parts with constrained interaction relationships that are re-evaluated if any part parameters are modified.

Commercial CAD tools also feature the ability to execute scripted instructions (i.e. macros) without user input. The CAD software CATIA for instance is able to execute macro instructions programmed in Visual Basic script; SolidWorks can execute Python script instructions. The parametric design and scripting capabilities provide a means of implementing autonomous analysis of CAD model parts and assemblies.

CAD tools commonly provide assembly clash detection capabilities which report the location and magnitude of unintended part contact or interference. This interference detection capability is applied in this work to identify assembly regions where unforeseen part feature interference may violate functional requirements.

3.2.7 Uncertainty quantification strategy

To identify the effects of part parameter variation on the assembly in a virtual model environment, a method of propagating the expected part parameter distributions through the assembly response function is required. A variety of Uncertainty Quantification (UQ) methods have been developed (Section 2.5). Monte Carlo simulation was applied in this work as it is robust and readily implemented. The Monte Carlo method consists of the generation of a feasible set of part parameter values from a random sample of their respective probability distributions, and the evaluation of the resulting assembly response. As the number of evaluations increases, the resulting sample distribution of assembly responses approaches that of the population. Approximately 1000 samples are required to provide acceptable accuracy in an assembly tolerance analysis problem (Gao *et al.* 1995). Monte Carlo simulations of 3000 evaluations were applied in the test case used in this research (Section 3.3.2) to ensure reliable outcomes.

3.3 Visualization method for the identification of KPCs based on sensitivity analysis

Identifying assembly parameters, whose deviation from a nominal value significantly affects assembly functionality, may not be obvious if a large number of parameters and interacting components are present. The ability to identify such key product characteristics (KPCs) early in conceptual and embodiment design increases knowledge about how assembly functionally may be monitored and managed in the presence of manufacturing variation. Design changes which improve the ability to manage variation can then be accommodated at a project stage where design flexibility remains high and accrued cost are low.

Identifying KPCs can however be challenging due to the difficulty in predicting behaviour in complex assemblies without an accessible assembly tolerance model (Section 3.2.4) and the ability to visualize model behaviour under variation (Dahl *et al.* 2001). Although computer aided tolerancing tools (CAT) are available for modelling variation in assemblies and aiding in the identification of KPCs, they require additional tools, modelling and expertise (Section 2.7). The additional effort is associated with the requirement to create an abstracted geometry model separate to any existing CAD model of the concept design before any analysis can be carried out (Prisco *et al.* 2002).

To aid designers in identifying assembly KPCs at the concept stage with low additional modelling effort, a PIDO tool based visualization method has been developed which involves identifying and visualizing unforeseen and unintended part interactions within the native CAD product design environment. The method utilises PIDO tools and functionality commonly available within commercial CAD software to simulate manufacturing variation effects on the part parameters of an assembly and monitor assembly clearances, contacts or interferences. KPCs are identified through design analysis and refinement based on sensitivity analysis

Since it is common practice for designers to carry out design modelling with the use of CAD tools, a numerical CAD model of the design assembly is often readily available at the conceptual and embodiment design stages. If the CAD model has been constructed to be robustly parametric, and if assembly constraints have been defined which ensure the required mating relationships between part features, then the CAD model may be adapted as an assembly tolerance model for aiding in KPC identification with the utilization of PIDO tools.

A method for adapting a CAD model as an assembly tolerance model for aiding in KPC identification with the utilization of PIDO tools is proposed in Figure 3.3. It integrates the

concepts of PIDO tools (Section 3.2.1), assembly response function modelling (Section 3.2.5) CAD tools (Section 3.2.6) and uncertainty quantification (Section 3.2.7).

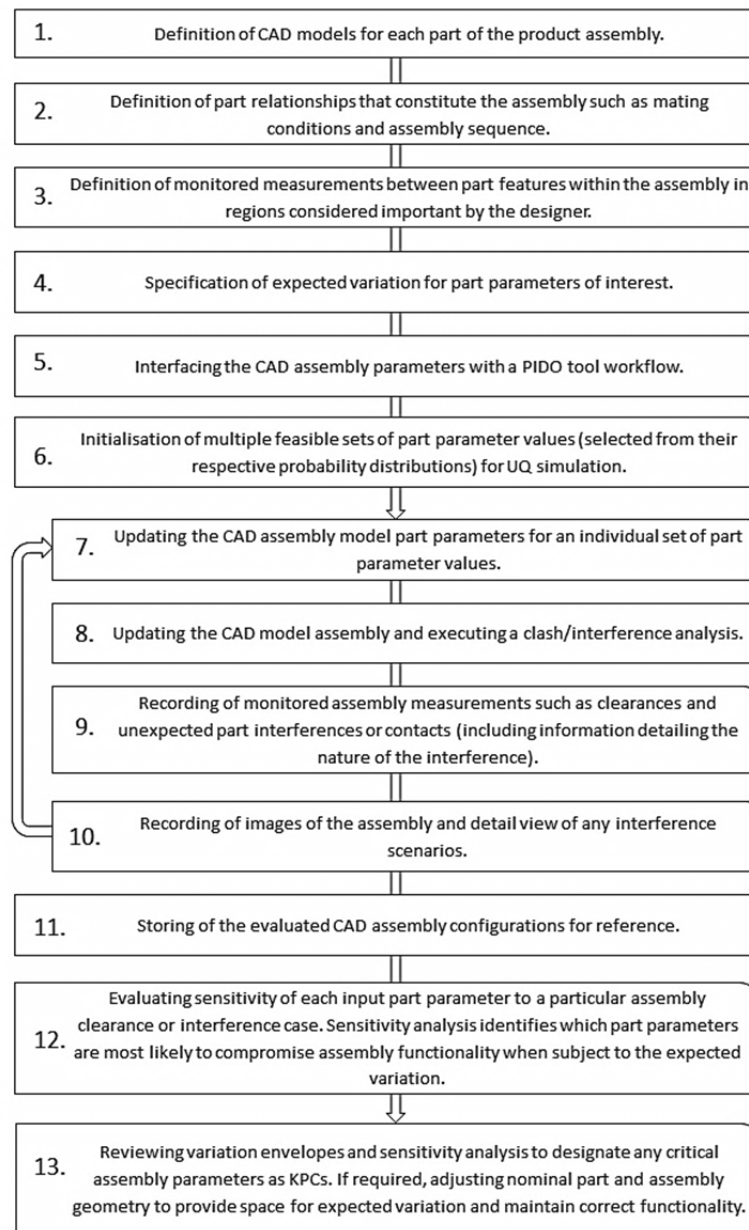


Figure 3.3 - Visualization approach for the identification of KPCs within the native CAD design environment using PIDO tools.

Initially, the CAD part and assembly model parameters are integrated with a PIDO tool workflow. Automated monitoring of assembly parameters potentially relevant to the functionality of the assembly is established with the definition of measurements of assembly dimensions such as clearances (this is facilitated by measurement tools embedded in most CAD software). Model parameters are subsequently subjected to expected manufacturing variation using UQ techniques such as Monte Carlo sampling. For each assembly instance, assembly clash and interference analysis capabilities common in CAD

software are executed using a user script to automatically identify any unexpected part interferences. The variation in model parameters results in variation envelopes of part geometry which represents the potential range of part dimensions and positions within the assembly. The simulated assembly models are automatically stored for reference. A Student's T-test based effect size measure (Jackson 2011) is subsequently used to identify the sensitivity of variation in each part parameter, to the monitored clearances or unexpected interferences in the assembly. The frequency of interference between assembly parts is calculated. The stored assembly models and sensitivity analysis results are subsequently reviewed by the designer to visualize the effects of the variation envelopes and address any identified problems. The identified problems may be corrected by adjusting model geometry to allow space for variation, and monitored by designating the associated assembly parameters as KPCs.

The method improves the general assembly robustness of concept design embodiments by increasing the ability of the designer to monitor and suppress the effects of manufacturing variation from the early concept stage.

3.3.1 Potential limitations

Although the method enables insight into unforeseen and undesirable part interactions, it may suffer from limitations associated with applying parametric CAD for simulating the effect of manufacturing variation. Limitation include such issues as adherence to geometric and dimensional tolerancing standards and problems in simulating intermittent part contact (Section 2.4.2) (Mazur *et al.* 2011).

Commercial Computer Aided Tolerancing (CAT) tools have been developed that can overcome some of these identified issues, however this approach requires the development of a specialised CAT model of the parts and assembly (Makelainen *et al.* 2001). The proposed methodology is applied directly to the CAD models developed for concept design and development, and can be directly integrated with the design process without the need for additional modelling or separate CAT software.

3.3.2 Case Study 3.1 – Visualization method for identification of KPCs in a concept design of an automotive actuator assembly

The visualization method presented in Section 3.3 was applied to a conceptual embodiment of an actuator assembly to aid in the task of identifying unintended part interactions and the associated assembly KPCs. The assembly is an actuator used for automated folding of automotive vehicle side view mirrors. Due to the commercially sensitive nature of the design, some specific details concerning the working of the actuator are not disclosed.

3.3.2.1 Process data

To estimate expected dimensional variations, the existing moulding process used for the manufacture of the test case assembly components was analysed. The manufacturer specifies assembly component dimensional tolerances on injection moulded components according to standard recommended specification limits ((DIN) 1982).

The manufacturer's injection moulding process was analysed by metrological inspection of 1600 production part samples from a commercial component with a comparable material and manufacturing process to the product under analysis. Component samples from four different moulding cavities were measured at five critical locations of equal target dimensions. The results were combined together and process capability indices (Section 2.3.4) were determined for the overall moulding process performance across all components and all cavities (Figure 3.4 and Table 3.1). The measured PCIs were used as input for the test case analysis.

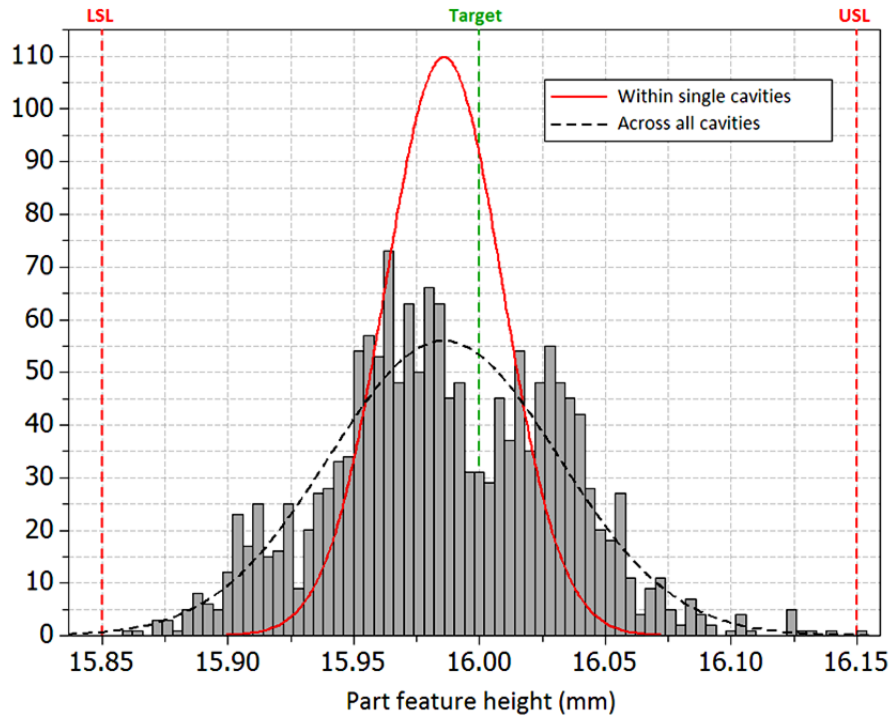


Figure 3.4 - Histogram of measured production component used to establish PCIs

Table 3.1 - Process capability data of measured component (Figure 3.4).

Results based on combined measurements across all locations and from all moulding cavities.

Parameter	Target	Achieved
Mean (mm)	16	15.986
σ (mm)	-	0.0457
LSL (mm)	15.850	-
USL (mm)	16.150	-
C_p	1.00	1.10
C_{pk}	1.00	1.01
C_{pm}	1.00	1.05
% < LSL	0.15 %	0.15 %
% > USL	0.15 %	0.02 %
% Total out of spec.	0.30 %	0.17 %

3.3.2.2 PIDO integration

The functional requirements of the actuator result in a design embodiment involving a sophisticated kinematic interaction of a number of components with functional ramps, each with a number of different relative arrangement scenarios. As such, the conceptual design phase of the actuator required a comprehensive CAD model as a proof of concept of the expected functionality. The parametric CAD assembly model of the concept actuator assembly developed by the designers (Figure 3.5) was interfaced with a PIDO workflow (Figure 3.6) in accordance with the proposed visualization method (Section 3.3). A feasible set of part parameter values was initialised from a random sample of their respective

probability distributions and subjected to a Monte Carlo simulation (3,000 samples were used).

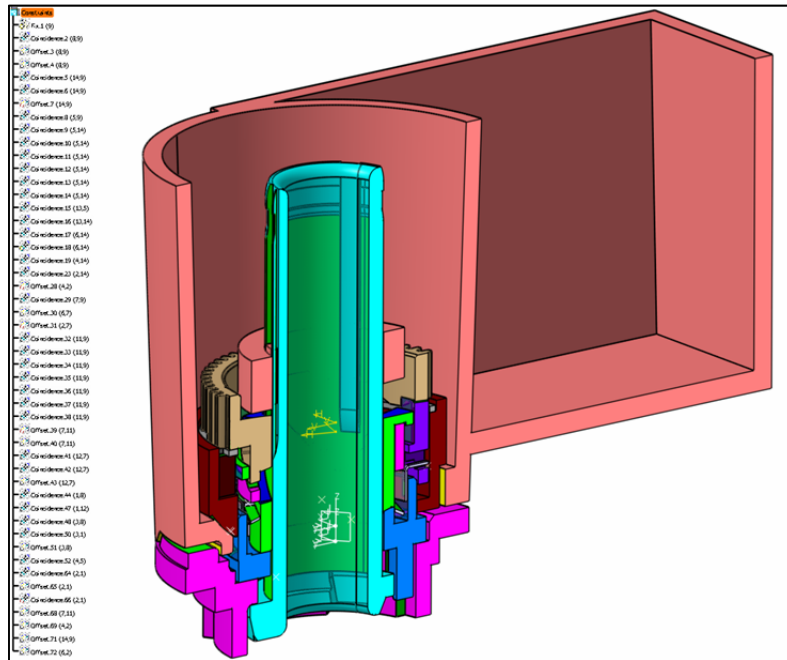


Figure 3.5 - Parametric CAD assembly model of concept actuator design

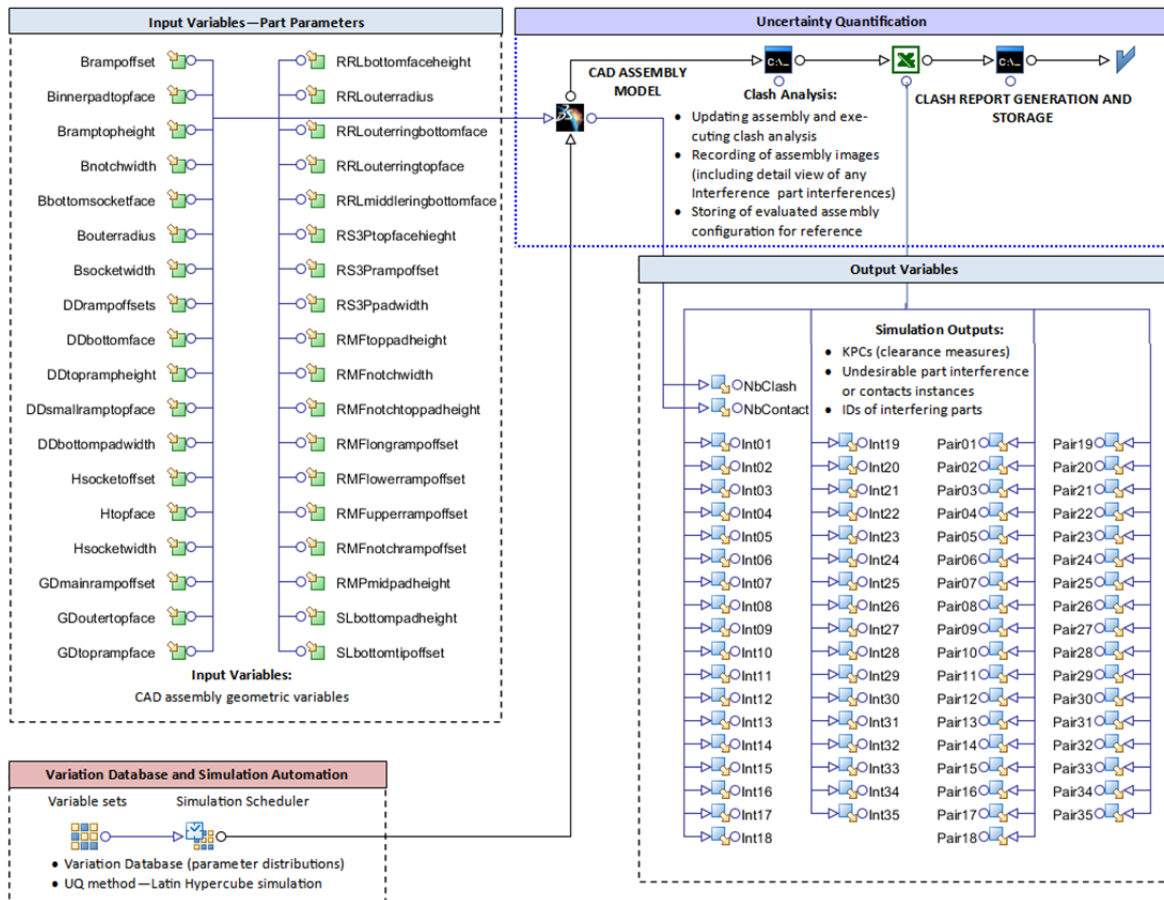


Figure 3.6 - PIDO workflow for visualization methodology for identification of KPCs - Actuator assembly.

3.3.2.3 Results

A number of undesirable part clash and contact instances were identified as part of the simulation. The interference data recorded for each identified scenario detailed the nature of part interactions (whether a contact or clash). Images were recorded for each interaction showing the relevant region of the assembly. The frequency of interference between part pairs was determined (Figure 3.7). A Student t-test was conducted to quantify the sensitivity of part parameter variation to the number of interference scenarios occurring (Figure 3.8). A positive effect size indicates that an increase in the parameter value results in interference, a negative effect size indicates a negative relationship. Sensitivity is indicated by magnitude.

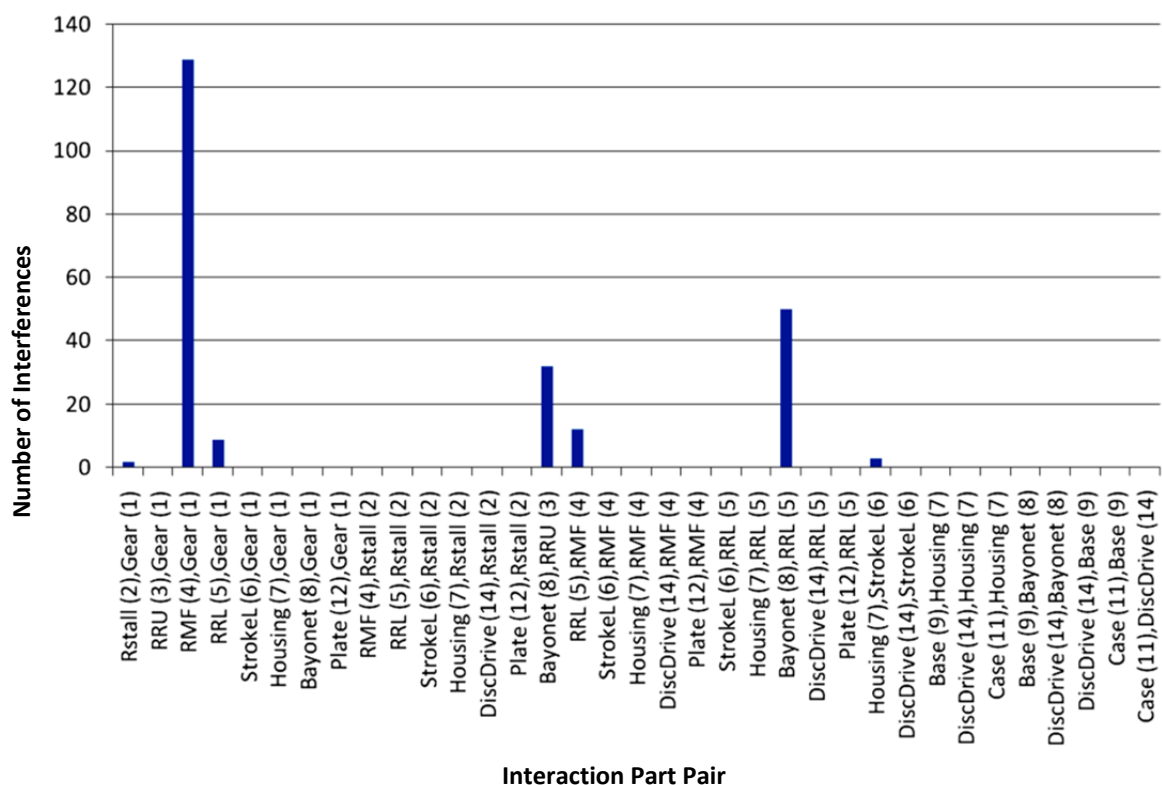


Figure 3.7 - Frequency of interference between assembly parts

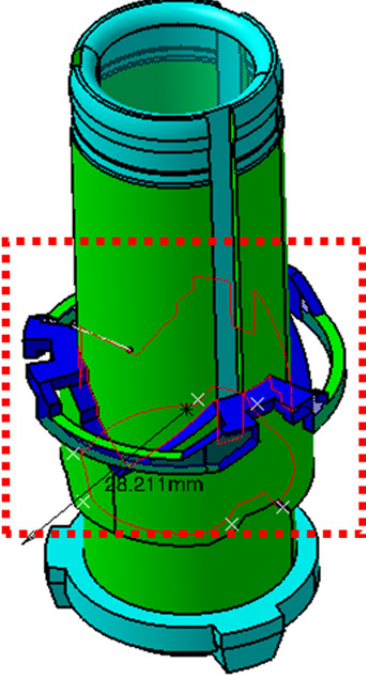
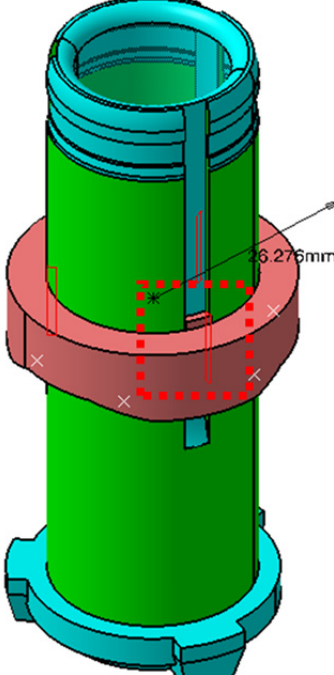
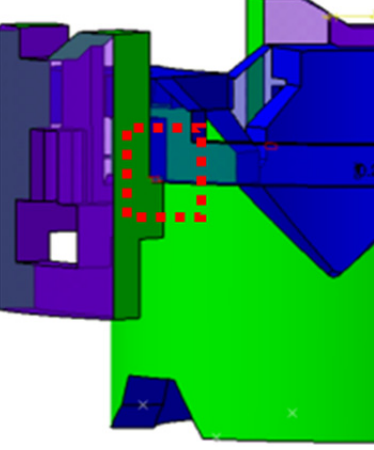
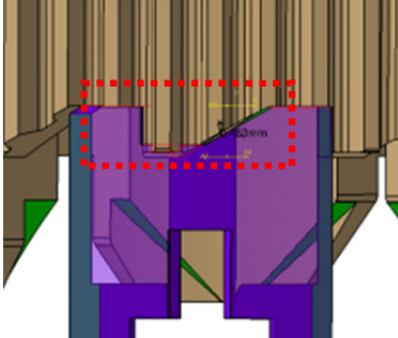
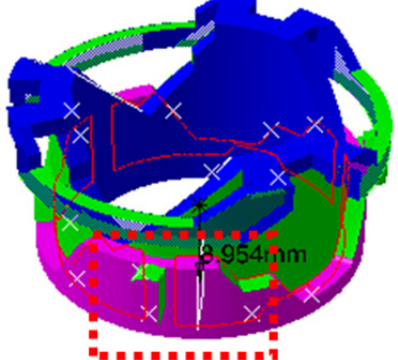
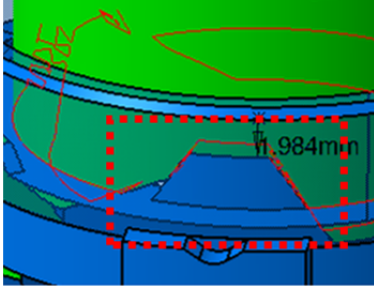
<p>Variation in spigot tube outer diameter and inner diameter of interacting collar can result in an interference that prevents the rotation of the collar around spigot.</p> 	<p>Variation in spigot tube vertical channel width and mating collar notches can result in interference preventing translation of the collar along the spigot.</p> 	<p>Variation in the angular arc length of radial collar ring (blue feature) can result in an interference with functional surfaces of engaging slider (rectangular part) compromising required functionality.</p> 
<p><i>Suggested KPC is an enforced diametral clearance measurement between spigot tube outside diameter and collar inner diameter.</i></p>	<p><i>Suggested KPC is an enforced clearance measurement between spigot tube vertical channel and collar notches.</i></p>	<p><i>Suggested KPC is a measure of collar ring arc length.</i></p>
<p>Excessive horizontal width of vertical ramp face on gear (upper part) can cause contact with vertical ramp faces of engaging slider (lower part). This undesirably reduces the possible vertical travel of engaging ramps.</p> 	<p>Variation in inner and outer diameters of interacting collars can result in interference preventing rotation.</p> 	<p>An excessive depth of collar (top part shown in green) can result in contact of horizontal bottom surface of collar with base preventing functional ramp faces from engaging.</p> 
<p><i>Suggested KPC is measurement of upper ramp width.</i></p>	<p><i>Suggested KPC is an enforced diametral clearance measurement between inner and outer collars.</i></p>	<p><i>Suggested KPC is an enforced clearance measurement between bottom of collar and top of base.</i></p>

Figure 3.9 - Assembly regions identified as being prone to unwanted part interference. KPCs were defined to avoid the identified interference scenarios.

3.3.3 Discussion of results

A PIDO tool based visualization method has been developed to aid designers in identifying assembly KPCs at the concept embodiment design stage. The method integrates the functionality of commercial CAD software with the process integration, UQ, data logging and statistical analysis capabilities of PIDO tools, to simulate manufacturing variation effects on the part parameters of an assembly and visualise assembly clearances, contacts or interferences. KPCs are identified by design analysis and refinement based on sensitivity analysis. The approach has a number of benefits:

- Visualization is carried out using native CAD models, which are often readily available at the concept embodiment design stage, requiring low additional modelling effort requirements.
- Utilization of embedded measurement and interference analysis capabilities in CAD assembly environments offering rapid implementation
- Visualizing variation within the assembly may aid the designer to specify critical assembly dimensions as KPCs for monitoring, as well as adjust nominal dimensions of part and assembly features to provide space for expected variation and maintain correct functionality.
- Addressing the robustness of concept design embodiments to manufacturing variation from the early concept design stages with low additional modelling effort. This can reduce the undesirable cost of managing poor quality later in the design cycle following the commissioning of manufacturing.

The benefit of the proposed method has been validated in an industrial case study by enabling the automated identification of unintended component interactions in a concept embodiment design of an automotive actuator assembly. These interactions had not been anticipated by the industry partner, despite their experience with designs of this type. The increased knowledge enabled the industry partner to establish a series of KPCs that were used to monitor these unintended part interactions early in the conceptual embodiment phase while the associated design flexibility is high and accrued cost commitments are low.

The method has been demonstrated to enhance the design process by offering rapid implementation, low analysis cost as well as accurate and reliable outcomes.

3.4 Computationally efficient manufacturing sensitivity analysis for assemblies with linear-compliant elements

Addressing the effects of manufacturing variation during conceptual and embodiment design can reduce the costs of managing poor quality later in the manufacturing stage when the ability to enact change is limited (Bergman *et al.* 2009; Ebro *et al.* 2012) (Section 3.2.2). In particular, design analysis and refinement based on tolerance analysis of concept design embodiments can provide insight into the sensitivity of alternative concepts to manufacturing variation, and facilitate concept selection with quantitative measures of robustness. This early increase of design knowledge allows the designer to make informed decisions addressing the effects of variation, while there is sufficient design flexibility to act without much expense (Figure 3.2 ii).

Estimating the effects of variation on assembly functionality is typically achieved with tolerance analysis based on a computational assembly tolerance model (Chase 1988). If the functionality of the assembly is subject to applied loads, estimating the effects of variation typically requires computationally expensive Finite Element (FE) simulations to model physical effects such as compliance or stress (Section 2.9). As tolerance analysis requires multiple evaluations of the assembly tolerance model (Section 2.5), the overall computational costs are compounded. With an efficient tolerance model, the computational complexity and expense of quantifying the effects of variation can be reduced allowing a greater number of simulations and analyses in a given time budget. This can increase knowledge early in the design process where analysis time budgets for individual concepts are limited (Section 3.2).

This section presents a method of reducing the computational cost of analysing the effects of variation with an efficient assembly tolerance model, in linear-compliant assemblies under loading. This method:

- Significantly reduces simulation costs by representing linear-compliant elements with a set of equivalent constant rate springs.
- Utilises PIDO tools to allow reuse of CAD models created in the conceptual and embodiment design stages, thereby reducing the cost of creating the assembly tolerance model.

This method is applied to the benchmarking study of alternative automotive seat rail assembly concept embodiments to quantify their sensitivity to manufacturing variation. The additional knowledge gathered as part of the benchmarking study enables designers to

proceed into the detail design stage with higher certainty of performance with low additional analysis expense.

3.4.1 Manufacturing sensitivity analysis of automotive seat rail assemblies

Automotive seating structures are subject to a constrained set of comfort and safety demands requiring the accommodation of anthropometric variation of users while meeting safety standards under crash scenarios (Leary *et al.* 2010). Seat position adjustment in multiple degrees-of-freedom (DoF) facilitates the location of the user within the vehicle cabin in a comfortable and functional seating position. An essential DoF required by all seating structure designs is the fore and aft movement of the seat. As automotive seating structures have evolved over an extended development period, there has been a convergence of practical embodiments. Accordingly, fore and aft movement is typically achieved using a rolling rail assembly consisting of two interlocking rail sections. Due to the stochastic nature of manufacturing processes, rail assembly performance is affected by manufacturing variation. For low cost markets, latitude in manufacturing variation is desirable. For mature markets, predictable and repeatable functional efforts take priority.

Such rail assemblies have historically been designed solely with strength and material use in mind. Consideration of customer perceived quality (such as variation in functional effort) was not prioritized at the conceptual design stage, as it was typically considered as too difficult, and time consuming. However, assessing customer perceived quality later in the design cycle following the commissioning of manufacturing when design flexibility is low, incurs significant cost penalties if the selected concept is sensitive to manufacturing variation. The quality of the customer experience has then to be managed at the manufacturing stage for the life of the product with costly counter measures. Accommodating the effects of manufacturing variation early in the development cycle is important for achieving competitive quality, cost and development time objectives for a range of target markets (Phadke 1989; Park 1996; Wu *et al.* 2000).

This work presents a benchmarking study of alternative conceptual embodiments of automotive seat rail assemblies according to their sensitivity to manufacturing variation i.e. robustness (Figure 3.10 and Table 3.2). All rail assemblies consist of two interlocked steel rail sections (with symmetric or asymmetric profiles) separated by rolling elements (spherical and cylindrical). The upper and lower rail sections are elastically preloaded by an interference fit with the rolling elements. Variation in the geometric parameters of the rail section affects the magnitude of the elastic rail preload and consequently the rolling effort of the rail assembly.

Rolling effort is of significant importance to customer perceptions of product quality, and must be:

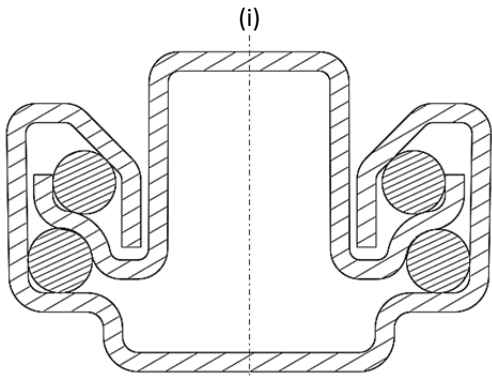
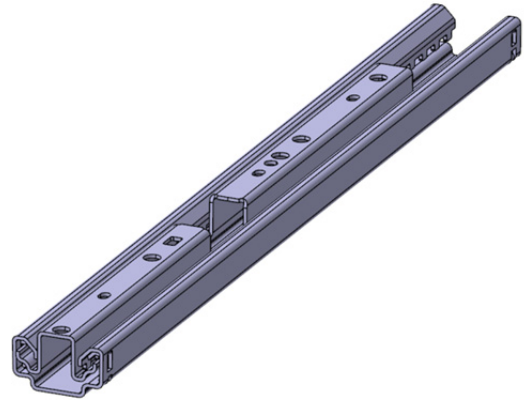
- sufficiently high to avoid chatter in the rail assembly
- sufficiently low to allow the rails to move without excessive effort

Due to these conflicting requirements, rolling effort is highly sensitive to manufacturing variation which results in both large scale batch-to-batch variation between assembly production batches, as well as piece-to-piece variation within single assemblies. Large scale batch-to-batch variation can be accommodated using alternative rolling element diameter increments between batches. Piece-to-piece variation however, is more difficult to accommodate as it requires alternative rolling element diameters for each assembly. The aim of this work is to benchmark alternative rail assembly profiles according to their sensitivity to rolling effort variation in the presence of piece-to-piece manufacturing variation.

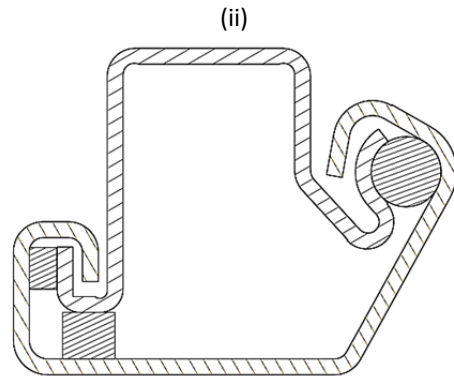
Rolling effort is defined by rolling element clearance, rolling element contact force and the associated coefficient of rolling resistance (Williams 1994). As such, the three benchmarking parameters considered in this study are:

- variation in the coefficient of rolling resistance
- variation in rolling element contact force
- variation in rolling element clearance

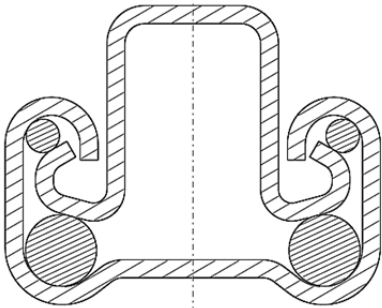
These are discussed in the following sections.



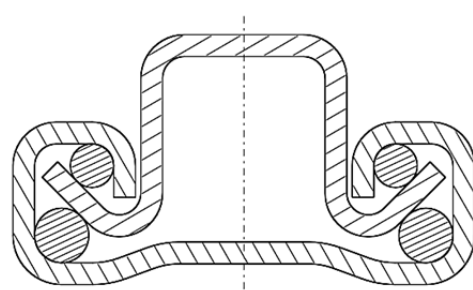
(iii) Rail assembly A



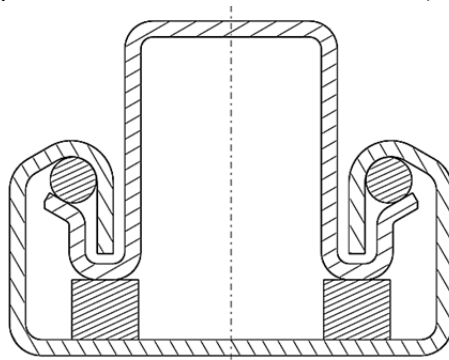
(iv) Rail assembly B



(v) Rail assembly C



(vi) Rail assembly D



(vii) Rail assembly E

Figure 3.10 - (i) Automotive seat (ii) seat rail assembly (iii) - (vii) Alternative rail assembly section views.

Table 3.2 - Rail assembly designs considered in benchmarking analysis.

Rail assembly design	Style	Balls	Rollers
A	Symmetric	2 (upper) 2 (lower)	nil
B	Asymmetric	1 (upper)	1 (lateral) 1 (lower)
C	Symmetric	2 (upper) 2 (lower)	nil
D	Symmetric	2 (upper) 2 (lower)	nil
E	Symmetric	2 (upper)	2 (lower)

3.4.2 Variation in coefficient of rolling resistance

Variation in the coefficient of rolling resistance is characterised by material properties and localised non-elastic effects associated with deformation, surface adhesion, and micro-sliding of the contact surfaces (Williams 1994). The variation in these effects is expected to be similar for alternative rail section profiles due to the use of similar materials, manufacturing processes and surface finish. As such, the variation in coefficient of rolling resistance is negligible and will not be considered in this work.

3.4.3 Variation in rolling element contact force

Due to the complicated geometry of the rail assembly, estimating the rail contact force with a virtual model requires a finite element (FE) simulation of the interference fit of the rail sections with the rolling elements. Quantifying the variation in contact force, which results from the manufacturing distributions associated with geometric rail section parameters, requires a statistical tolerance analysis approach based on uncertainty quantification (UQ) methods (Section 2.5). UQ methods typically require a large number of model evaluations to provide sufficiently accurate distribution estimates (Gao *et al.* 1995). Consequently, estimating the variation in rolling element contact force with FE models and traditional statistical tolerance analysis imposes significant computational costs. Furthermore, there are limited tools available for conducting statistical tolerance analysis of assemblies subject to loading (Section 2.9). The difficulties with analysis tool limitations and high computational cost, in such tolerance analysis problems of assemblies under loading, are addressed in Chapters 4 and 5 of this dissertation. In this chapter however, an alternative approach is developed which avoids these limitations by taking advantage of:

- Linear-elastic behaviour of the folded sheet metal components of the automotive seat rail assembly
- Incompressibility of rolling elements (relative to sheet metal components)

The objective of this work is to benchmark the sensitivity of alternative designs to manufacturing variation, in particular the variation in rail rolling effort. Consequently, it is not necessary to estimate the absolute variation in performance of each design, but only the performance compared to other designs.

Due to the above conditions of rail linear-elasticity and incompressible rolling elements, it is hypothesised that the comparative variation in rolling element contact force between can be assessed by comparing only the stiffness of the rail assembly. As such the assembly tolerance model can be made significantly more efficient.

3.4.3.1 Linear-compliant rail representation

Figure 3.11 depicts the derivation of an efficient contact force variation model for symmetric and asymmetric rail assemblies. Initially the rail assemblies are conceptually simplified to their functional representation, clarifying the underlying loading relationship between the rail sections and rolling elements (Figure 3.11 (1)).

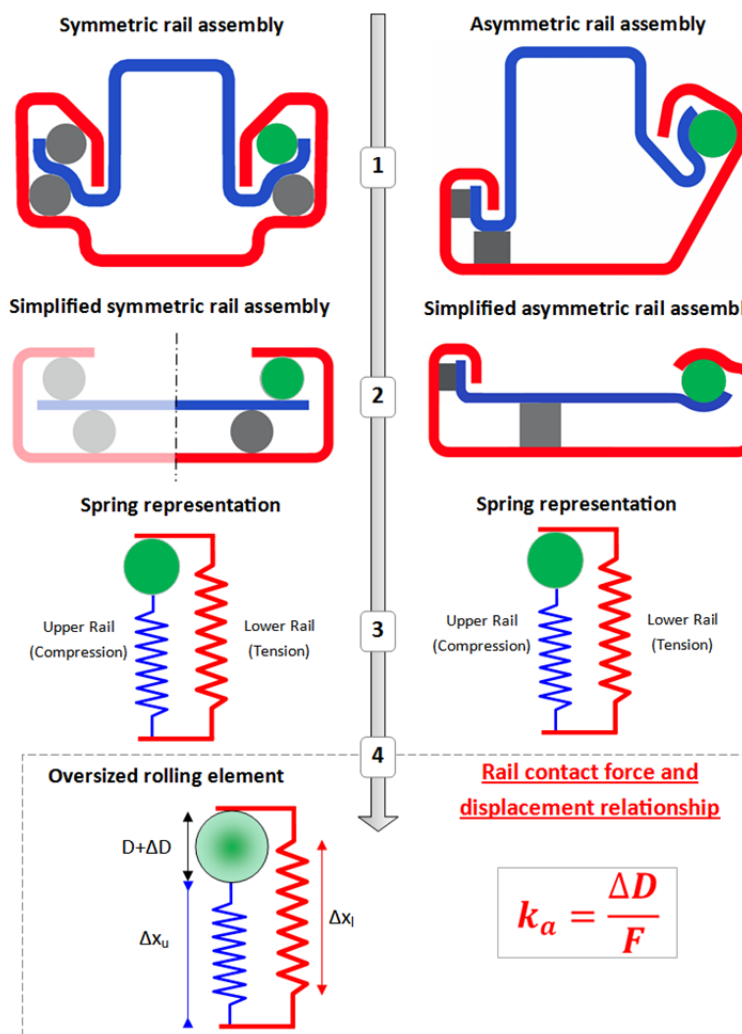


Figure 3.11 - Linear compliant rail simplification.

The rails are deflected upon assembly by rolling elements which are slightly oversized; this deflection is elastic, as validated with a computational mode in Section 3.4.3.2. Due to the elastic loading condition, the relationship between the net contact force applied to the rail section and the associated deflection is linear. The relationship between contact force and deflection is defined by the stiffness, i.e. the rate of change in rolling element preload due to a change in rail section deflection:

$$F = k_a x \quad \text{Where,} \quad (3.1)$$

F: Contact force
k_a: Rail assembly stiffness
x: Deflection

The overall stiffness of the rail assembly (*k_a*) can be determined by measuring the contact force for a known deflection (Figure 3.11 (4)). A known deflection can be imposed by oversizing the rolling elements with a diametral interference amount ΔD , i.e.

$$\Delta D = x_u + x_l = F \left(\frac{1}{k_u} + \frac{1}{k_l} \right) = F k_a \quad \text{Where,} \quad (3.2)$$

x_u, x_l: Deflection of upper and lower rail, respectively
k_u, k_l: Stiffness of upper and lower rail, respectively
D: Rolling element diameter
 ΔD : Rolling element diametral interference

Rearranging (2.2), an expression for the overall rail stiffness is obtained:

$$k_a = \frac{\Delta D}{F} \quad (3.3)$$

Variation in rolling element contact force can therefore be quantified by the stiffness of the rail section assembly. The stiffness can then be used a highly efficient assembly tolerance model of the sensitivity of the rail rolling effort to manufacturing variation. A rail profile which displays a low stiffness is desirable as it accommodates part-to-part variation with little change in rolling effort. To quantify rail assembly stiffness, a Finite Element (FE) simulation was conducted for various rolling element increment sizes.

3.4.3.2 FE contact force model

A parametric Finite Element (FE) model of each rail assembly was constructed to simulate the rail deflection due to an interference fit with the rolling element (Figure 3.12 and Figure 3.13). For symmetric rails the model was constructed to consider one-half of the symmetric rail profile. For asymmetrical profiles the entire rail assembly was considered. An oversized rolling element was initially inserted into the assembly resulting in an interference fit. The associated interference caused an initial state of imbalance in contact force between the rail

sections and rolling elements. A simulation was subsequently initiated in which the rail sections deflected under the contact force imbalance until contact force equilibrium was reached. The resultant equilibrating contact force was integrated over the contact surfaces and recorded. The associated rail deflection corresponded to the amount of initial rolling element interference.

The simulation was carried out for three progressively increasing values of rolling element interference, corresponding to increases of 0.1mm in the diameter of the rolling elements. The three resultant values were used to determine the rail assembly stiffness (Section 3.4.7). The average individual simulation time was approximately 400 seconds on a single-core 3 GHz CPU.

The FE model was also used to validate the linear elasticity assumption of rail compliance as mentioned in section 3.4.3.1. A worst-case condition was simulated consisting of oversizing the rolling element by 1mm and noting the peak stresses in the rail sections. The peak stresses were in the order of 20MPa which was well below the elastic limit of the steel material, validating the linear-compliant rail representation.

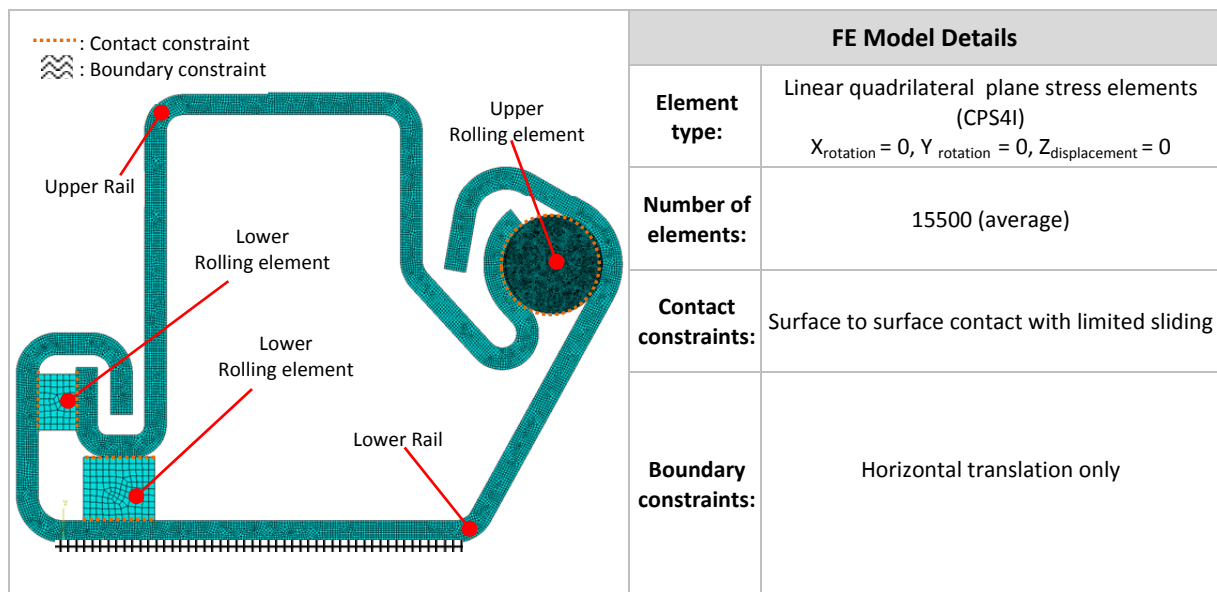


Figure 3.12 - FE model details (rail assembly B). All dimensions in mm.

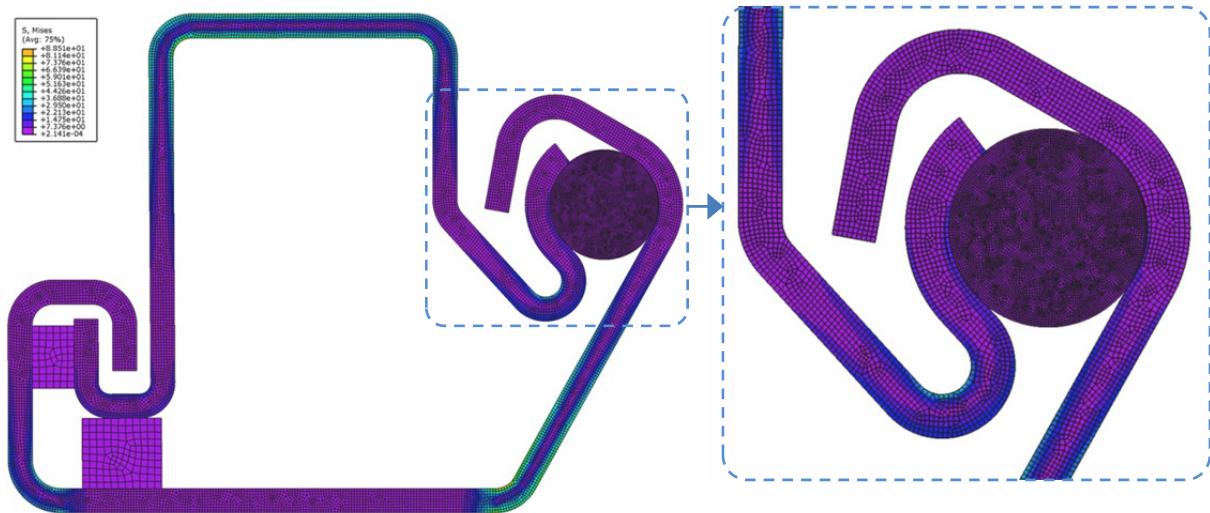


Figure 3.13 - Rail deflection due to interference fit of rolling element (rail assembly B).
Contact area shown in detail.

3.4.4 Variation in rolling element clearance

Variation in rolling element clearance may be assessed by tolerance analysis which accommodates expected manufacturing process capabilities. It is highly desirable that the maximum variation between the upper specification limit (USL) and lower specification limit (LSL) sizes of the rolling elements be small, as it accommodates part-to-part variation within a rail assembly with a small change in rolling effort.

Statistical tolerance analysis was conducted by integrating parametric CAD models of the alternative rail section assemblies with PIDO tool capabilities (Sections 3.2.1 and 2.8). The integration was achieved according to a PIDO tool based tolerance analysis platform (Figure 3.14). This platform is developed in Chapter 4 of this dissertation (Section 4.3). The solution was rapidly implemented, as it allowed the reuse of parametric CAD models constructed in the conceptual and embodiment design, rather than requiring additional models. Utilizing existing CAD data for tolerance modelling significantly reduces modelling expense and the need for additional expertise and tools.

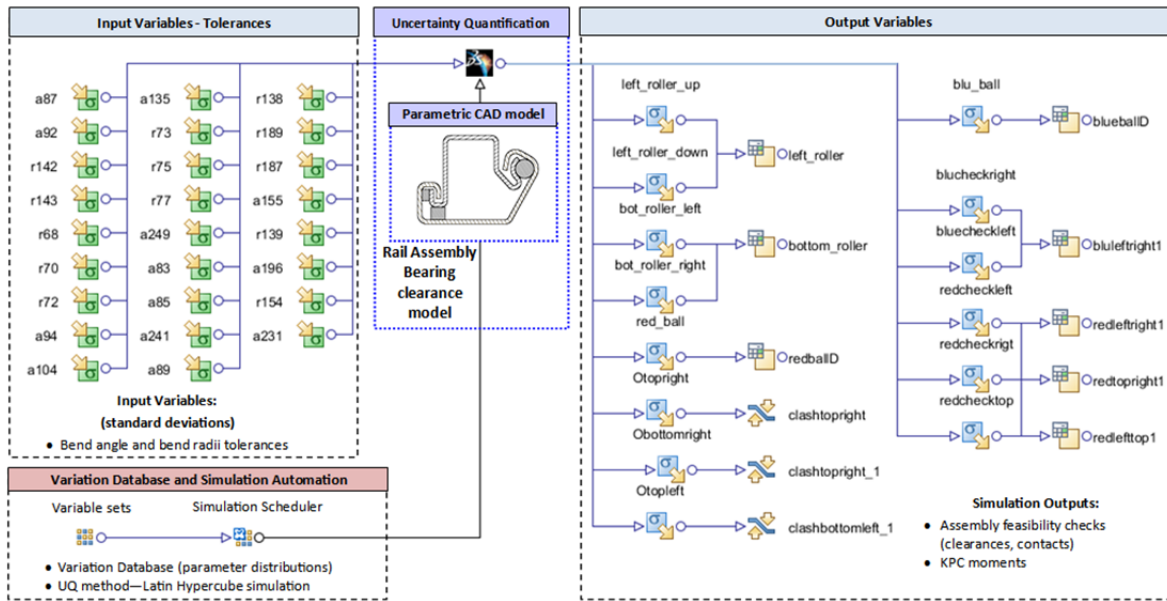


Figure 3.14 - PIDO workflow associated with seat rail benchmarking study.

Estimates of expected variation in the rail section geometries were applied to quantify the expected manufacturing distribution for each parameter. Due to a lack of production process capability data, conservative estimates of expected manufacturing variation in rail sections were provided by the industry partner (Table 3.3). As the focus of the study was to compare sensitivity to manufacturing variation solely based on differences in the geometric configuration of the rail profile, all benchmarked rails were subject to the same manufacturing variation. Variation in linear dimensions and material thickness were not considered.

Table 3.3 - Rail section parameter variation specified by industry partner and used in statistical tolerance analysis

Parameter	Specification limits +/-	C_{pm}	σ
Bend radii	0.1 mm	1	0.033
Bend angle	1°	1	0.333

Parametric models of rail sections were subjected to parameter variation identified in Table 3.3. Each rail assembly was subjected to a statistical tolerance analysis based on a Monte Carlo (MC) simulation of 1000 samples. Studies suggest that 1000 samples provide sufficient accuracy in an assembly tolerance analysis problem (Gao *et al.* 1995). Based on the applied variation, upper and lower specification limits for rolling element diameters were identified in order to achieve a $C_{pm} = 1$.

3.4.5 Assumptions

The conducted analysis was subject to a number of assumptions in order to allow for reasonable scope of analysis within limited analysis time:

- Due to a lack of production process capability data, conservative estimates of expected manufacturing variation in rail sections parameters were applied (no variation in linear dimensions or material thickness was applied).
- Variation in symmetric rail sections was assumed to be equal on either side of the axis of symmetry.
- The plane stress FE model only considers the two-dimensional cross-section of the rail at the rolling element contact location. This simplification results in the estimated magnitude of contact force being based on deformation of the full rail length, rather than point contact. However in reality, the contact scenario is that of a sphere and a surface. The approximation was used to limit the FE model simulation time to a practically manageable size, due to the significant complexity of the more realistic scenario.
- Rail stiffness was assessed at three points. Stiffness shows a linear trend for moderate rail displacement.
- Rail stiffness was assessed for spherical (ball) elements only, not cylindrical elements.

3.4.6 Results

3.4.6.1 Rail assembly A

Rail assembly A is a symmetric design with cylindrical rolling elements (Figure 3.10 (iii)). Contact force was calculated for the scenarios of Table 3.4 and summarized (Section 3.4.7).

Table 3.4 - Ball dimensions used for contact force simulation in rail assembly A

Scenario	Ball interference (mm)	Upper Ball diameter (mm)
Simulation 1	0.1	6.044
Simulation 2	0.2	6.144
Simulation 3	0.3	6.244

A statistical tolerance analysis was conducted for rail assembly A in order to identify the expected clearances at the rolling element locations. A parametric CAD model of the rail profiles was used for the analysis. The separation distance between the vertical extremities of the upper and lower rail was held constant while the rail section parameters were subjected to a MC simulation (Section 3.4.4). The resultant distributions of rail clearances are shown in Figure 3.15 and the identified specification limits in Figure 3.16. The results are summarized in Section 3.4.7.

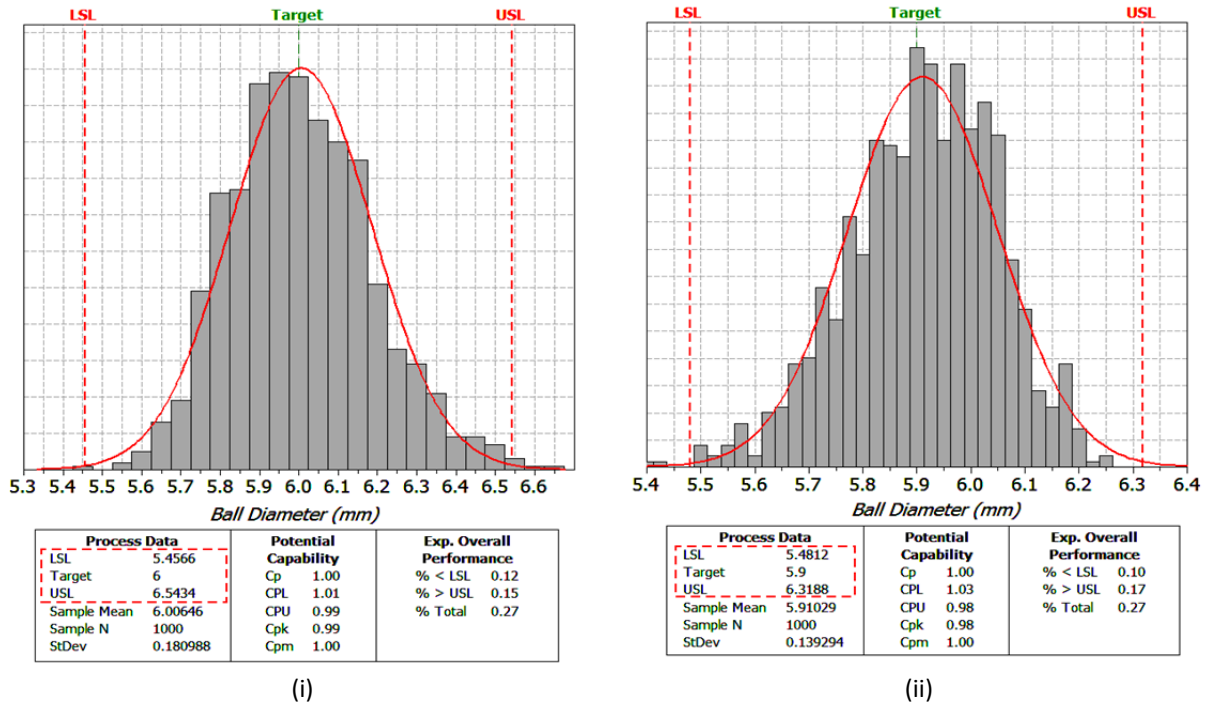


Figure 3.15 - Rail assembly A rolling element clearance distribution. (i) Upper ball (ii) Lower ball.

	UB USL	UB LSL	LB USL	LB LSL
Profiles				
Spec. Limits	6.543 mm	5.457 mm	6.319 mm	5.481 mm

Figure 3.16 - Rail assembly A rolling element specification limits. Shaded profile corresponds to nominal rail dimensions. Upper Ball (UB), Lower Ball (LB).

3.4.6.2 Rail assembly B

Rail assembly B is an asymmetric design incorporating spherical and cylindrical rolling elements (Figure 3.10 (iv)). As the rail assembly has no axis of symmetry, the entire rail profile was considered in the contact force and rolling element clearance analyses. Contact force was calculated for the scenarios of Table 3.5 and summarized in Section 3.4.7. Distributions of rail clearances are shown in Figure 3.17 and the identified specification limits in Figure 3.18. The results are summarized in Section 3.4.7.

Table 3.5 - Ball dimensions used for contact force simulation in rail assembly B

Scenario	Ball interference (mm)	Upper Ball diameter (mm)
Simulation 1	0.1	7.54
Simulation 2	0.2	7.64
Simulation 3	0.3	7.74

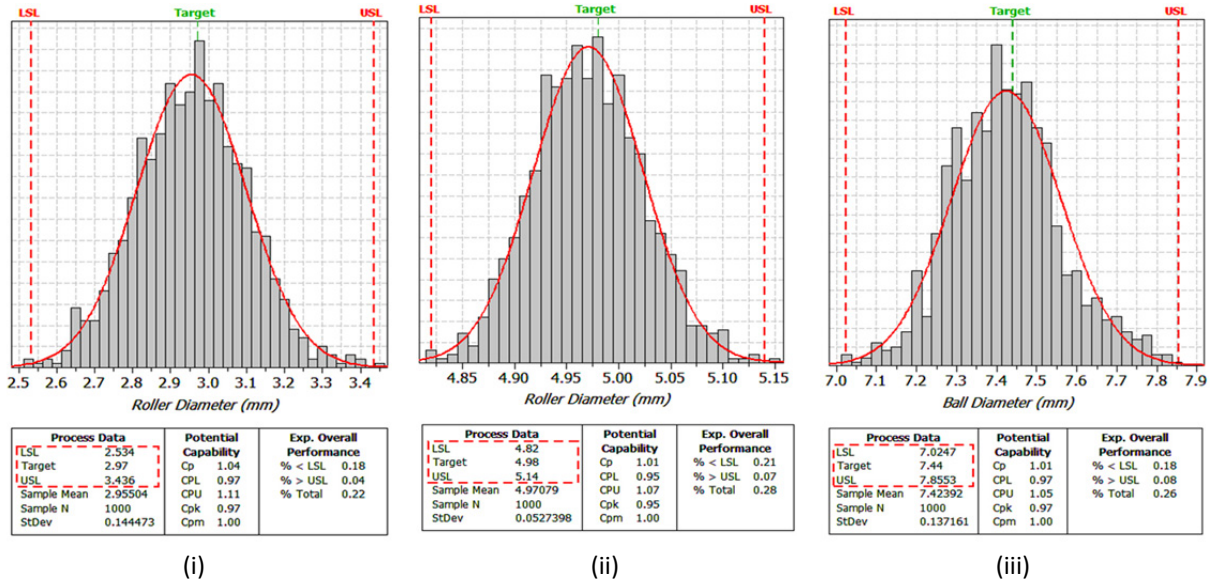


Figure 3.17 - Rail assembly B rolling element clearance distributions.
 (i) Left roller (ii) Bottom roller (iii) Right ball.

	LR USL	LR LSL	BR USL	BR LSL	RB USL	RB LSL
Profiles						
Spec. limits	3.436mm	2.534mm	5.140mm	4.820mm	7.855mm	7.025mm

Figure 3.18 - Rail assembly B rolling element specification limits. Shaded profile corresponds to nominal rail dimensions. Left Roller (LR), Bottom Roller (BR), Right Ball (RB).

3.4.6.3 Rail assemblies C, D and E

Contact force and rolling element clearance analyses for rail assemblies C, D and E were carried as per the procedure demonstrated in sections 3.4.6.1 and 3.4.6.2. The results are summarized in Section 3.4.7.

3.4.7 Benchmarking of designs

The results of the contact analysis conducted for the analysed rails are shown in Figure 3.19. Variation in rolling element contact force is quantified by the stiffness of the rail assembly (Section 3.4.3.1). The stiffness of the rail sections is an indicator of the performance robustness of the nominal rail design. A rail profile showing low variation in contact force with displacement (small gradient) is desirable as it accommodates part-to-part variation with a small change in rolling effort.

Although some rail assemblies show a significantly high and undesirable stiffness (such as rail D) they offer other performance advantages warranting their inclusion within the concept design set, for instance:

- material use efficiency
- ease of pressing
- ease of metrological assessment facilitating simple process control measures

For such designs, although they show poor performance robustness in rolling effort (as is the focus of this benchmarking study) their use may be appropriate for low cost applications where consumer quality expectations are lower.

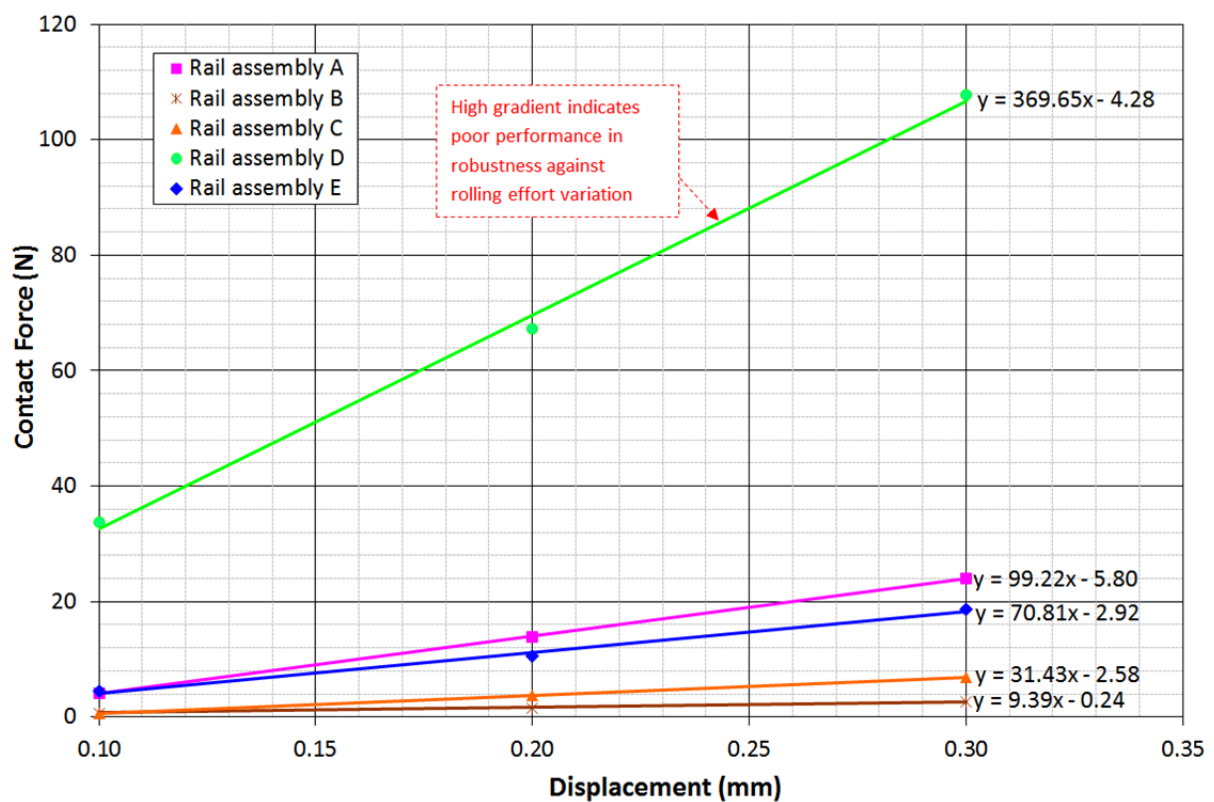


Figure 3.19 - Rolling element contact force versus local rail displacement. Gradient indicates stiffness.

A summary of analysis results for variation in rolling element clearance is shown in Figure 3.20 for the analysed rail assemblies. A rail assembly with minimum variation between the upper and lower specification limits is preferable as this reduces variation in rolling effort.

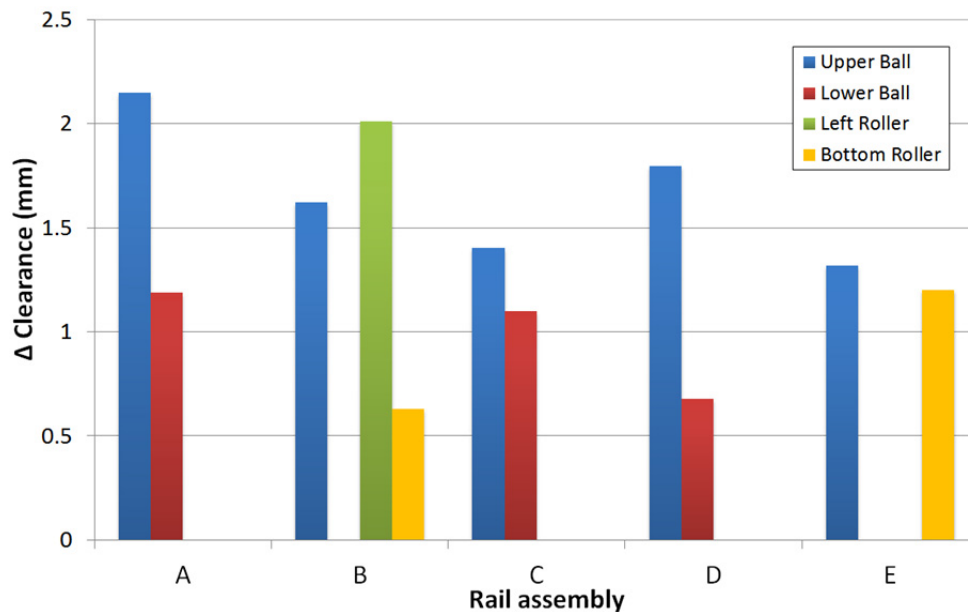


Figure 3.20 - Magnitude of variation in nominal rolling element clearance versus rail assembly design.

The analysed rail assemblies can be benchmarked according to robustness of contact force and rolling element clearance. To provide a global performance ranking it is necessary to assign a weighting to both benchmarking criteria. The appropriate weighting is dependent on the designer's preference to either emphasise individual criteria or pursue a balance.

Due to the linear-elastic characteristic of the rail assembly, variation in rail stiffness and rolling element clearance each influence the rail contact force and subsequently the rolling effort. However, during assembly it is possible to mitigate the effect of clearance variation by allowing a number of ball sizes to be available to assemble with rails as required. Consequently it may be appropriate to assign a greater importance to rail stiffness than to clearance variation.

Table 3.6 shows a ranking of robustness to contact force and rolling element clearance for each of the assessed rail assemblies. These rail assemblies are then ranked globally using a square weighted sum of performance in both analysed categories. The square weighted ranking gives each metric equal importance, but discourages large difference between both performance criteria.

Table 3.6 - Performance ranking of conceptual rail assembly designs.

Rail assembly	A	B	C	D	E
Robustness of contact force	4	1	2	5	3
Robustness of rolling element clearance	5	4	2	3	1
Overall performance rank	5	3	1	4	2

Observing the results of the ranking it is possible to note the following characteristics:

- Rail section designs with reduced spacing between upper and lower rolling elements show higher stiffness (for example A and D). This is due to the closer proximity of opposing contact forces on the upper rail resulting in a shorter effective lever arm associated with rail deflection.
- Rail sections with a higher number of folds leading to the rolling element location show greater variation in rolling element clearance (for example A and D). This is due to the accumulation of variation during each fold.
- Rail sections with a large distance between a fold and a rolling element show high variation in rolling element clearance (for example the right hand side of lower rail B). This high variation is due to the lever arm amplifying variation associated with the fold angle.

3.4.8 Discussion of results

Estimating the sensitivity to manufacturing variation from the early conceptual and embodiment design stages can aid in the management of quality when design flexibility is high. To accurately estimate the effects of variation on the functionality of a design, statistical tolerance analysis based on a computational assembly tolerance model is required. However, the computational cost of statistical tolerance analysis can be prohibitively high, especially when many iterations of FE simulations are necessary to model physical effects such as compliance. Additionally, the ability to carry out tolerance analysis in such scenarios may be limited by the available tools and expertise in formulating the model and interpreting results.

This section provides an efficient method of analysing the effects of manufacturing variation in linear-compliant assemblies under loading. This design analysis and refinement method significantly reduces computational cost by utilising:

- linear-compliant assembly stiffness measures, and
- PIDO tool statistical tolerance analysis based on the reuse of CAD models created in the conceptual and design embodiment stage.

This increase in computational efficiency, allows an estimate of sensitivity to manufacturing variation to be made earlier in the design process with reduced effort.

This approach is validated in a benchmarking study of alternative automotive seat rail assembly concept embodiments to quantify their sensitivity to manufacturing variation. The benchmarking study identified significant differences in sensitivity to manufacturing variation between alternative designs. This outcome assists automotive manufacturers to increase design knowledge early in the design process and proceed into the detail design stage with higher certainty of performance with low additional analysis expense.

The method applied here can be generalised and applied to assess the sensitivity to manufacturing variation in other linear-compliant assemblies whose functionality is dependent on applied loads. Due to high efficiency, application of the method at the conceptual and design embodiment stages is particularly useful for increasing knowledge early in the design process where analysis time budgets for individual concepts can be limited.

Chapter 5 of this dissertation considers the effect of variation on automotive set rail assemblies further by conducting a tolerance synthesis with FE model simulations to identify optimal production tolerances.

3.5 Refinement of concept design embodiments through PIDO based DOE analysis and optimization

The conceptual design and embodiment stages focus on the search for concept variants which offer feasible solutions to the design problem under consideration (Section 3.2). As these stages are early in the project timeline where design knowledge is limited, they can be associated with a vast design space in which feasible regions and optimum performance can be difficult to identify (Askin *et al.* 1988; Thompson *et al.* 1999; Krishnan *et al.* 2001; Simpson *et al.* 2008; Tomiyama *et al.* 2009).

The vast design space may be studied with design and refinement techniques such as design of experiments (DOE) analysis and optimization methods. DOE analysis offers a method to explore the design space by systematically evaluating design parameter combinations in the associated parameter space. Optimization allows for an automated exploration of the parameter space to identify regions of local and global optimum performance, in the presence of complex constraints and competing design objectives.

Design analysis and refinement at the concept stage using DOE analysis and optimization methods provides insight into the design problem while the associated flexibility remains relatively high (Figure 3.2). To minimize overall design time, design analysis and refinement at the conceptual stage with DOE and optimization methods requires rapid implementation and low analysis cost. Implementation is dependent on the integration of DOE and optimization methods with disparate CAE modelling tools which may be required as part of conceptual and embodiment design (such as CAD packages or FE simulation codes). Efficient integration of disparate CAE models for DOE analysis and optimization can be facilitated with the emerging capabilities of PIDO tools (Section 2.8).

This section presents an approach for investigating the design space in the conceptual and embodiment design stages with DOE analysis and optimization methods. The conceptual design of automotive seat kinematics is presented as a highlighting case study.

The capabilities of PIDO tools are utilised to allow CAE tool integration, and efficient reuse of models created in the conceptual and embodiment design stages, to rapidly identify feasible and optimal regions in the design space.

3.5.1 Automotive seat kinematics

The automotive seat structure is required to accommodate the anthropometric variation of users while meeting minimum safety standards under low and high speed crash scenarios.

Seating structures are subject to a stringent set of constraints and objectives, including: allowable envelope of motion, structural integrity, modularity and cost. Within these objectives and constraints, practical embodiments of automotive seating structures have converged to the common solution of a planar kinematic chain. This kinematic chain may exist in several variants, each with their own unique performance attributes (Leary *et al.* 2010). Of the observed kinematic chains, the typical implementation is a four-bar linkage³; “the simplest possible pin-jointed mechanism for single degree of freedom controlled motion” (Norton 2003).

The behaviour of the four-bar linkage is well understood based on the Grashof condition (Figure 3.21) (Barker 1985), which classifies kinematic behaviour based on the length of the shortest, ζ , longest, λ , and other links, ϑ and φ . Depending on which of these links is shortest (Table 3.7), the grounded links will be will behave as a crank (rotary motion), or a rocker (reciprocating motion). Of these permutations, the parallelogram and crank rocker are often observed in automotive seating structures. The latter is typical as it results in induced tilting as the seat lifts – desirable to accommodate different user body dimensions. For example, shorter users typically require a higher seating position and greater seat tilt and vice versa (Leary *et al.* 2010).

Although four-bar linkage kinematics are well understood, a large design space, combined with multiple constraints and objectives, impose significant challenges to their design and optimization in automotive seat structures.

³ Other embodiments include five-bar linkages and independent rocker actuation. The four-bar linkage may include an independent four-bar linkage or crank-slider to enable seat tilting [1].

Table 3.7 - Classification of four-bar mechanisms.

Type	Grashof condition	Shortest link	Behaviour
1	$\lambda + \zeta < \vartheta + \phi$	frame	double-crank
2	$\lambda + \zeta < \vartheta + \phi$	side	crank-rocker
3	$\lambda + \zeta < \vartheta + \phi$	coupler	double-rocker
4	$\lambda + \zeta > \vartheta + \phi$	any	double-rocker
5	$\lambda + \zeta = \vartheta + \phi$	any	double-crank (parallelogram)

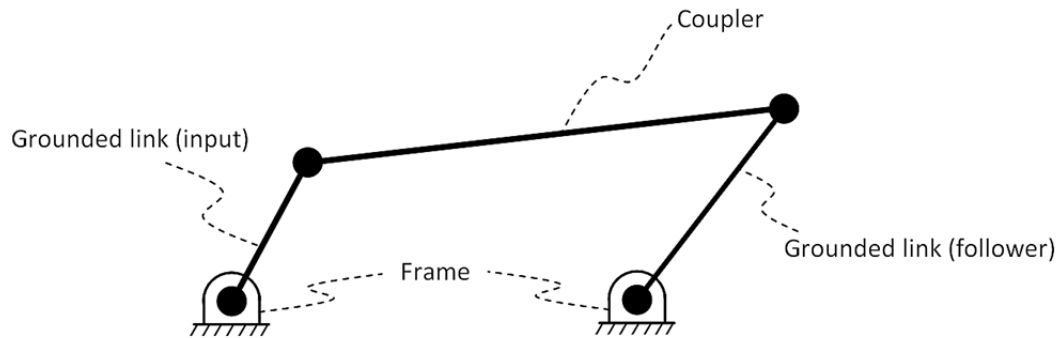


Figure 3.21 - Four-bar linkage and associated nomenclature (Leary et al. 2011).

3.5.2 PIDO based DOE analysis and optimization of the conceptual design of automotive seat kinematics

Despite the apparent simplicity of a four-bar linkage system (Barker 1985) applied in automotive seating structures, the number of input parameters (link lengths and frame position) and associated permutations results in a large possible design space. Furthermore, multiple constraints and objectives hinder systematic optimization efforts. Historically, such problems are solved by inspection, or with graphical (Bastow 1976), or numeric (Norton 2003) aids. This work illustrates a method for resolving these conflicting design requirements at the conceptual design stage by mapping the feasible design space and identifying regions of high performance.

An algebraic model of four-bar linkage kinematics was interfaced with a Process Integration and Design Optimization (PIDO) tool (Figure 3.22). PIDO software has the capability to facilitate automated analysis by the integration of stand-alone CAE tools to enable automated parametric analysis, DOE, multi-objective optimization, and statistical evaluation of system models (Sections 3.2.1. and 2.8). The design refinement and analysis approach consisted of two phases: initial analysis and design refinement.

An initial analysis was developed to explore the design space using a DOE approach. Due to the analytical nature of the kinematic model, the computational cost of each evaluation was sufficiently low to allow a high resolution experiment, providing the designer with a rapid

overview of the feasible regions of the design space, and aiding in the identification of regions of high performance. DOE was carried out using full factorial sampling.

The second phase of design refinement and analysis utilized multi-objective optimization to search the identified feasible design space for optimum designs. A Genetic Algorithm (GA) optimization algorithm was used to search the design space. Stochastic optimization algorithms such as GA are suited to a large search space due to inherent robustness against objective function discontinuity and local optima stagnation. In contrast, deterministic algorithms are more efficient at converging towards an optimum, but are typically only robust within localised regions of the search space and can stagnate at local optima (Section 2.6.2) (Deb *et al.* 2002). For models which exhibit a high computation cost, it may be beneficial to refine the optimization phase with deterministic algorithms prior to stochastic optimization. Due to the low computational cost of the kinematic model used in this work, the direct application of a stochastic GA yielded acceptable results within a reasonable computation time.

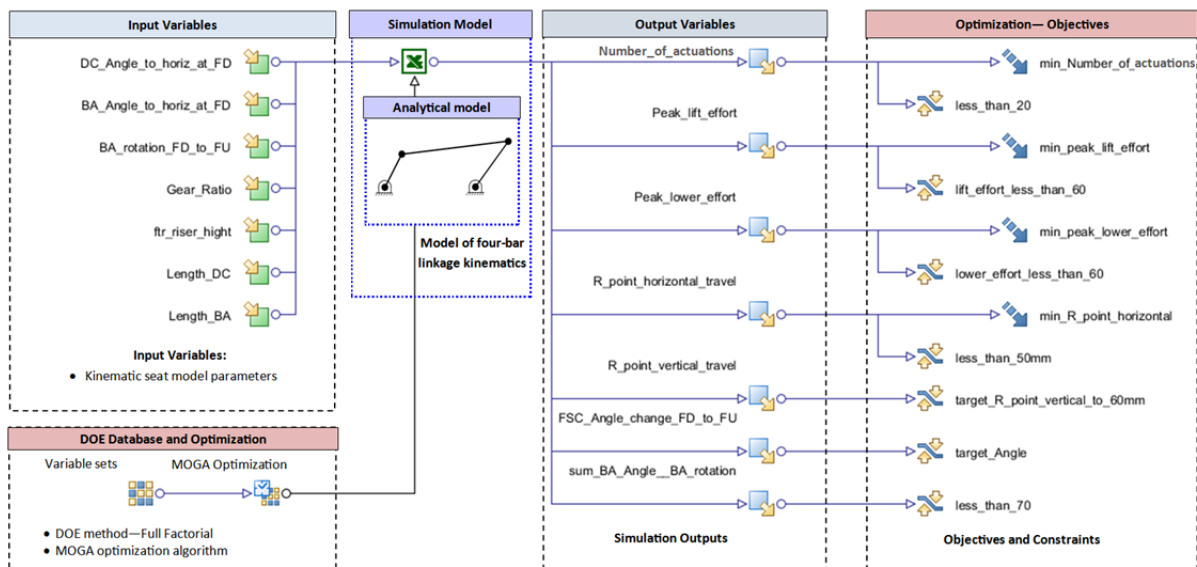


Figure 3.22 - PIDO workflow associated with the second phase of design refinement and optimization of automotive seat kinematic concept designs.

The initial high resolution DOE analysis parameter space was populated using Full Factorial sampling of the model input parameters with an experiment size of 12,888 model evaluations. The resultant design space was used to identify regions of infeasible performance. The subsequent multi-objective GA optimization analysis was initialised with the identified feasible design space. The optimization problem consisted of four competing objectives, and additional constraints. The GA was limited to 10 generations, resulting in a

simulation size of 122,880 model evaluations. The total solution time was 3.5 days on a single-core 3GHz CPU.

Table 3.8 - Model input parameters.

Input parameter	Dimension
Input link length	mm
Follower link length	mm
Height of ground link and frame node	mm
Input link inclination	degrees
Follower link inclination	degrees
Included angle of follower rotation	degrees

Table 3.9 - Model output parameters, dimension and objective.

Output parameter	Dimension	Objective
Vertical travel (at reference point)	mm	Minimise
Horizontal travel (at reference point)	mm	Minimise
Lift effort	N	Minimise
Number of manual actuations to achieve full lift	-	Minimise

3.5.2.1 Results

The simulation identified 20,204 feasible designs with 304 designs being Pareto-optimal (Figure 3.23). Without relative importance weighting of the competing design objectives there is no clearly optimal solution as the set of Pareto-optimal designs offer equal performance in satisfying the design objectives; an improvement in one objective leads to a compromise in others. Designs of interest are identified with associated identification numbers in Figure 3.23:

- Minimum peak force: #105908
- Minimum number of manual actuations to lift seat: #53684, #122063 and #105908
- Minimum horizontal travel: #50560

The other identified designs of Figure 3.23 are balanced compromise between competing objectives.

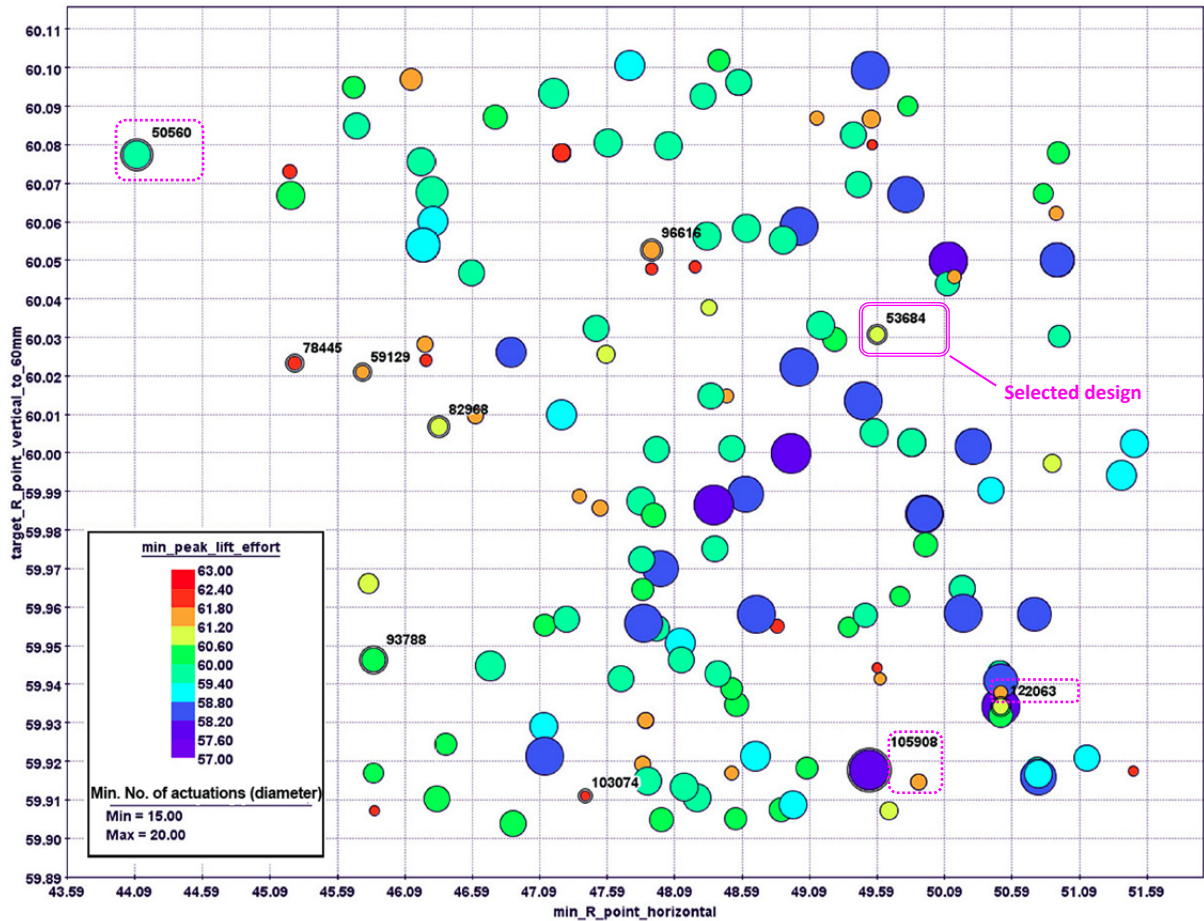


Figure 3.23 - Four-dimensional chart indicating performance of Pareto-optimal solutions in the conceptual design of automotive seat kinematics. Designs referred to in the discussion have been labelled with associated identification numbers.

The industry partner selected design #53684 as offering the most desirable balance of design objectives due to large performance benefits associated with manual actuation efforts. The selected concept design was progressed to the detail design stage and subsequently manufactured as part of a commercial seat assembly. The resultant commercial product was benchmarked against other competing products (Table 3.10).

Table 3.10 - Benchmarking results against other competing products

Competing seat assembly and supplier	Vehicle use	Performance	
		Vertical travel (target 60 mm) [mm]	Number of actuations to achieve full lift (lower is better)
Competitor A	Mazda (Model 2, Model 3)	60	33
Competitor B	Toyota (Yaris, Prius)	60	27
Brose	Volvo C30	60	21
Tachi-S	Honda (Accord, Civic)	60	21
JCI	Ford (Focus, Fiesta)	60	20
Sitech	Volkswagen (Golf, Jetta, Beetle)	60	19
Design #53684	Tesla Model S	60	16

The selected design was found to offer the best performance in achieving the vertical seat travel objective with the least number of manual actuations (these are actuations required to lift the seat for a given fixed lift effort). This superior performance against competitors in seat actuation demands was a determining factor for the selection of the design in the seat assembly of the Tesla Motors Model S full-sized electric sedan currently on sale in the United States (Elders 2011).

3.5.3 Other applications

PIDO based DOE analysis and optimization is a broadly applicable approach for exploring the design space in the conceptual and embodiment design stages. For instance, PIDO based DOE analysis has been used by the author for preliminary investigation of the design space associated with concept wheelchair design (Burton *et al.* 2010; Leary *et al.* 2012).

A numerical, quasi-static wheelchair model was constructed in multi-body dynamics software (Figure 3.24 (i)) and explored using DOE analysis to investigate how wheelchair seating positions influence shoulder and elbow torques in wheelchair users. A large number of feasible wheelchair seat height and fore-aft positions were analysed. The corresponding shoulder and elbow torques required to rotate the wheel through a given range (measured as push progress) were recorded (Figure 3.24 (i) and (ii)). Further analysis is required to identify preferred seating positions and future work is focused on the identification of optimal seat position for specific user parameters. Interested readers are referred to the associated publications for further discussion (Burton *et al.* 2010; Leary *et al.* 2012).

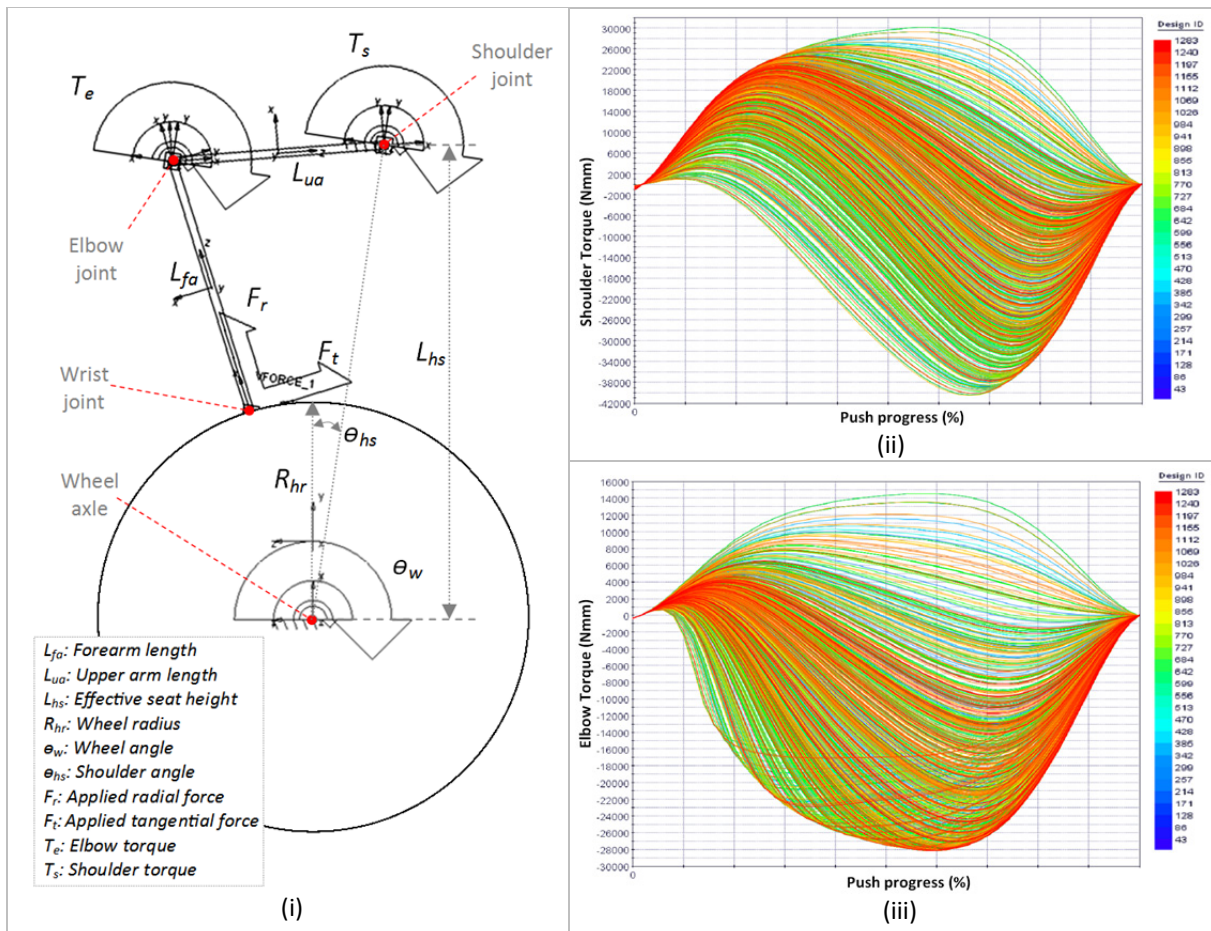


Figure 3.24 - (i) Quasi-static model of users arm and wheelchair wheel interaction (Leary et al. 2012) Shoulder (ii) and elbow (iii) torques corresponding to range of feasible seat height and fore-aft positions. Push progress indicates rotation of the wheel from hand contact until release.

3.5.4 Discussion of results

The conceptual and embodiment stages of the design process can be associated with a vast design space in which regions of desirable performance are difficult to identify. Design analysis and refinement techniques, such as DOE analysis and optimization, allow exploration of the design space and identification of optimum regions in the presence of complex constraints and competing objectives. The resulting increase of understanding of the design space early in the design process, allows for design improvements to be made when overall project cost commitments are low and design flexibility is high.

This section highlights the benefits of searching the conceptual and embodiment design space through DOE analysis and optimization, with a practical case study. The case study addresses the conceptual design of automotive seat kinematics consisting of a four-bar linkage system. Despite the apparent simplicity of the planar four-bar linkage, the large number of input parameters and possible permutations results in a large design space. The capabilities of PIDO tools were utilised to allow CAE tool integration, and efficient reuse of

models created in the conceptual and embodiment design stages, to rapidly identify feasible and optimal regions in the design space. One of the identified Pareto-optimal concepts was selected for detail design and manufacture. Benchmarking has shown the selected design to offer superior performance against commercial competitors in achieving vertical seat travel objectives with the least number of manual seat actuations. The design was subsequently commercialised in the seat assembly of the Tesla Motors Model S full-sized electric sedan.

The PIDO based DOE analysis and optimization approach to exploring the design space in the conceptual and embodiment design stages can be broadly applied. An example is provided focusing on the conceptual design of wheelchairs.

3.6 Summary of research outcomes

This chapter identified opportunities to enhance the conceptual and embodiment stages of design by increasing design knowledge with design analysis and refinement techniques. Novel methods for the use of PIDO tools were developed for the analysis and refinement of concept design embodiments with sensitivity analysis, tolerance analysis, DOE methods and optimization. These methods include:

1. *A PIDO tool based visualization method to aid designers in identifying assembly KPCs at the concept embodiment design stage.*

The method integrates the functionality of commercial CAD software with the process integration, UQ, data logging and statistical analysis capabilities of PIDO tools, to simulate manufacturing variation effects on the part parameters of an assembly and visualise assembly clearances, contacts or interferences.

- Visualizing variation within the assembly may aid the designer to specify critical assembly dimensions as KPCs for monitoring. The nominal dimensions of part and assembly features may then be adjusted to provide clearance for expected variation to maintain correct functionality.
- Visualization is carried out using native CAD models, which are often available at the concept embodiment design stage, requiring low additional modelling effort.
- Utilization of embedded measurement and interference analysis capabilities in CAD assembly environments offers rapid implementation.
- The benefit of the proposed method has been validated in an industrial case study by enabling the automated identification of unintended component interactions, in the concept design embodiment of an automotive actuator assembly. These interactions, which had not been anticipated by the industry partner despite their experience with designs of this type, resulted in the specification of assembly KPCs that would otherwise have been overlooked.

2. *Computationally efficient manufacturing sensitivity analysis for assemblies with linear-compliant elements*

An efficient method of analysing the effects of manufacturing variation in linear-compliant assemblies under loading is presented. The method significantly reduces computational costs by utilising linear-compliant assembly stiffness measures, reuse of CAD models created in the conceptual and design embodiment stage, and PIDO tool based statistical tolerance analysis. This approach is developed as part of a benchmarking study of alternative

automotive seat rail assembly concept embodiments to quantify their sensitivity to manufacturing variation.

- Estimating functionality of the rail assembly requires a FE simulation of the contact force between rail sections and rolling elements. Estimating the variation in functionality with FE models and traditional statistical tolerance analysis imposes significant computational costs, as a large number of FE model evaluations are required to provide sufficient accuracy.
- In this section an alternative approach is developed which increases computational efficiency by taking advantage of the linear-elastic behaviour of the folded sheet metal seat rail assembly, and the relative incompressibility of rolling elements.
- Due to the linear-elastic condition, a measure of assembly stiffness can be used to estimate sensitivity to manufacturing variation. Estimating the stiffness requires only 3 evaluations of the FE model, significantly reducing overall computational expense.
- Due to the high associated efficiency, the method may be applied at the conceptual and design embodiment stages; thereby increasing knowledge early in the design process where analysis time budgets for individual concepts are limited.
- The benchmarking study identified significant differences in sensitivity to manufacturing variation between alternative designs. This outcome allowed the industry partner to proceed into the detail design stage with higher certainty of performance and with low additional analysis expense.
- The method applied here can be generalised and applied to assess the sensitivity to manufacturing variation in other linear-compliant assemblies whose functionality is dependent on applied loads.
- Chapter 5 of this dissertation further considers the effect of variation on automotive seat rail assemblies by conducting a tolerance synthesis with FE model simulations to identify optimal production tolerances.

3. Refinement of concept design embodiments through PIDO based DOE analysis and optimization

This section highlights the benefits of exploring the conceptual and embodiment design space through DOE analysis and optimization, with a practical case study.

- Design analysis and refinement techniques, such as DOE analysis and optimization, allow exploration of the design space to identify optimum regions in the presence of complex constraints and competing objectives.

- The resultant increase of design space knowledge early in the design process, allows for design improvements to be made when overall project cost commitments are low and design flexibility is high.
- The case study addressed the conceptual design of automotive seat kinematics consisting of a four-bar linkage system, which, despite its apparent simplicity, is associated with a large design space.
- The capabilities of PIDO tools were utilised to allow CAE tool integration, and efficient reuse of models created in the conceptual and embodiment design stages, to rapidly identify optimal regions in the design space.
- An identified Pareto-optimal concept was selected for detail design and manufacture. The design was subsequently commercialised in the seat assembly of the Tesla Motors Model S full-sized electric sedan. Benchmarking has shown the selected design to offer the best performance among commercial competitors in achieving the vertical seat travel objective with the least number of manual actuations (these are actuations required to lift the seat for a given fixed lift effort).
- The PIDO based DOE analysis and optimization approach to exploring the design space in the conceptual and embodiment design stages can be broadly applied. An example is provided focusing on the conceptual design of wheelchairs.

The methods presented in this chapter have been demonstrated to enhance the design process by offering rapid implementation, low analysis cost as well as accurate and reliable outcomes. Practical conceptual and embodiment design problems are considered, and effective solutions developed for a number of industry focused scenarios. The outcomes allow designers to make informed decisions which positively influence the design early in the design process while cost commitments are low.

The statistical tolerance analysis conducted in this chapter (Sections 3.4.4) was achieved according to a PIDO tool based tolerance analysis platform. This platform is developed in Chapter 4 of this dissertation.

The method developed in this chapter for analysing the sensitivity to manufacturing variation in linear-compliant assemblies (Section 3.4.3.1) is not applicable to a more general class of problems. In response to this limitation, a novel method for tolerance analysis of assemblies whose functionality is dependent on applied loads is developed in Chapter 4.

Limitations identified in this chapter associated with the high computational cost of uncertainty quantification in statistical tolerance analysis (Section 3.4.8) are addressed further in Chapter 5 of this dissertation.

4 NOVEL APPROACH FOR PIDO BASED TOLERANCE ANALYSIS OF ASSEMBLIES SUBJECT TO LOADING

4.1 Chapter summary

Due to the stochastic nature of manufacturing processes, mechanical assemblies are subject to variation. The influence of variation on assembly functionality can be estimated with tolerance analysis. Numerous Computer Aided Tolerancing (CAT) tools have been proposed that address tolerance analysis problems in complex mechanical assemblies; however in Chapter 2 it was identified that current tools do not accommodate a general class of problem where the functionality of a design is fundamentally dependent on the effects of loads such as external or internal forces (Section 2.10). Such loads influence assembly functionality through effects such as compliance, dynamics and mechanical wear and are particularly relevant in, for example: mechanical actuators, automotive seat positioning mechanisms, and sheet metal assemblies (such as automotive or aerospace body panels). This chapter addresses the limitation of CAT tools to accommodate assemblies under loading by developing a tolerance analysis platform which integrates CAD, CAE and statistical analysis tools using Process Integration and Design Optimization (PIDO) software capabilities. The platform extends the capabilities of traditional CAT tools by enabling tolerance analysis of assemblies in which assembly characteristics are dependent on loads such as external and internal forces. To demonstrate the capabilities of the developed platform, examples of tolerance analysis problems involving compliance and multi-body dynamics are presented.

4.2 Introduction

The stochastic nature of manufacturing processes results in variation which directly affects the functionality and cost of manufactured products. Accommodating the effects of manufacturing variation early in product design is paramount to achieving competitive quality, cost and development time targets. Manufacturing variation is quantified by

tolerances and manufacturing process characteristics. The influence of variation on assembly functionality can be estimated with tolerance analysis. A general tolerance analysis procedure is depicted in Figure 4.1. Tolerances specify the allowable variation around a nominal parameter value (Section 2.3.2). The geometry, size, position and orientation of toleranced features are described according to Geometric Dimensioning and Tolerancing (GD&T) standards (e.g. ISO 1101 (ISO 2005) and ASME Y14.5M (ASME 2009)).

Assembly parameters which are of particular relevance to functionality are referred to as Key Product Characteristics (KPCs) (Section 3.2.4). KPCs are traditionally geometric, such as clearances or nominal dimensions. This work extends the definition of KPCs to any parameter of relevance to assembly functionality (such as a force, pressure, stiffness, coefficient of friction, response time etc.). This broader definition allows this work to be applied to accommodate novel tolerance analysis problems in which assembly functionality is subject to loads. Estimating assembly functionality requires the definition of an assembly response function which defines KPCs in terms of the assembly parameters. The assembly response function may be explicitly defined by an algebraic expression, or may be implicitly defined within a numeric model (e.g. a CAD assembly or CAE model, for example stage 2 and 3 of Figure 4.1). Upper and lower specification limits (USL and LSL, respectively) applied to KPCs define targets beyond which product functionality is compromised (e.g. Figure 4.1, stage 4). The manufacturing yield is defined as the percentage of assemblies which conform to the specification limits of all KPCs (e.g. Figure 4.1, stage 5). The yield requirement can be set according to worst-case or statistical tolerancing principles. Statistical tolerancing allows for component tolerances to be relaxed to enable reduction in manufacturing costs (Section 2.3.1).

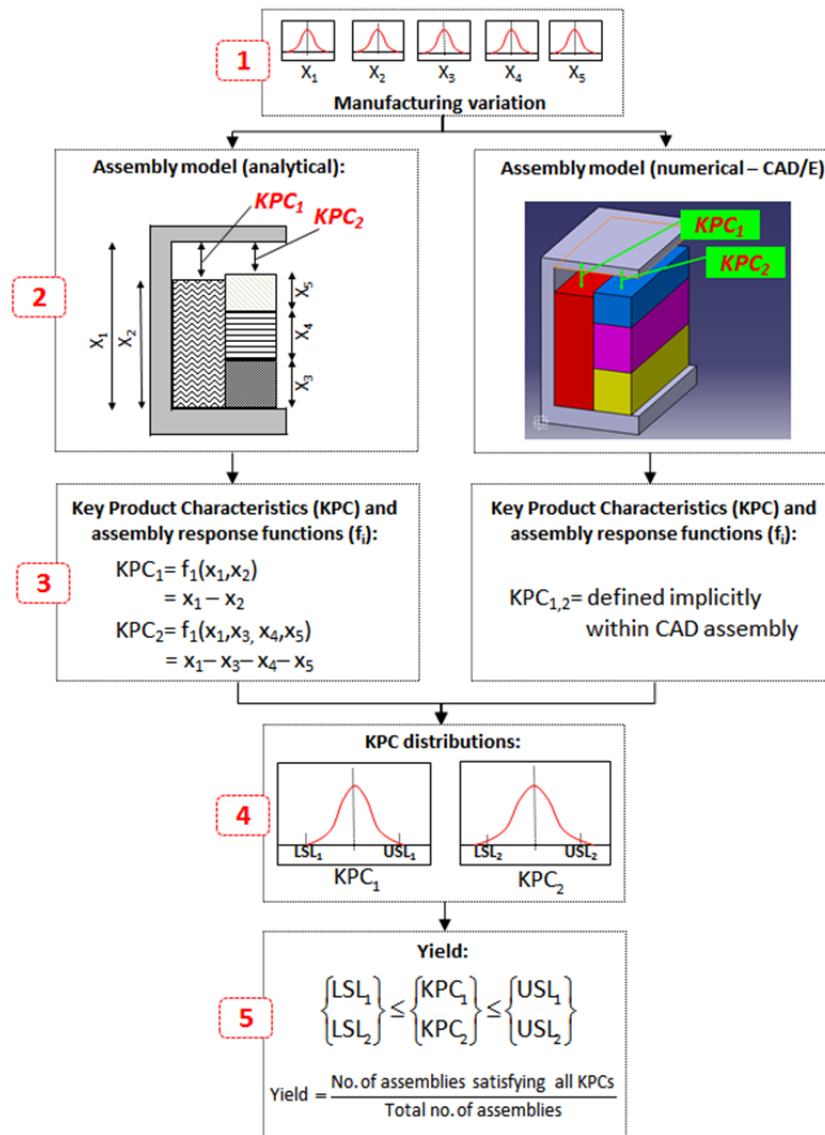


Figure 4.1 - General tolerance analysis of a mechanical assembly. Stages are identified as per Section 4.2.

Identifying the effects of part variation on the functionality of an assembly (tolerance analysis), and allocating acceptable part tolerances (tolerance synthesis) are challenging problems involving the competing objectives of achieving acceptable manufacturing cost and desired product quality, as well as the functional constraints imposed by the product design requirements (Hong *et al.* 2002; Mazur *et al.* 2010). The designer must analyse the influence of individual part tolerances on the functionality of the product assembly in order to determine the expected number of assemblies that conform to functional requirements.

4.3 Effects of loads in tolerance analysis

Assembly functionality can often be sufficiently defined in terms of minimum or maximum clearances. However assembly functionality may also be dependent not only on dimensional characteristics but also by how the assembly behaves in response to some applied action

such as a force, temperature change, or electromagnetic interaction. These actions are generally referred to as loads. Common loads in mechanical assemblies are internally or externally applied forces. External forces are independent of part mass and are applied to the part boundary; for example friction and contact forces. Internal forces occur due to inertial effects, and are applied through the centre of mass; for example gravitational forces and dynamic effects. Internal and external forces act to influence KPCs such as assembly dimensions dependent on part compliance (Section 4.5) or assembly functions dependent on friction and dynamic effects (Section 4.6). The ability to accommodate internal and external forces in tolerance analysis allows for an increased level of capability in estimating the effects of variation on functionality. Examples where assembly functionality is dependent on external and internal forces include: controlled deformation, precise fit requirements, wear of interfacing components, dynamic effects and fluid interactions.

A number of analytical and numerical methods have been proposed for addressing tolerance analysis and synthesis problems in complex product assemblies, in particular for assemblies subject to loads (Sections 2.3.2 and 2.9). However, a review of the existing tolerance analysis methods which aim to accommodate assembly loads ((Merkley 1998; Bihlmaier 1999; Hu *et al.* 2001; Shiu *et al.* 2003; Camelio *et al.* 2004; Imani *et al.* 2009; Pierre *et al.* 2009; Franciosa *et al.* 2011)) has identified a number of limitations, including (Section 2.9):

- Ability to accommodate only single, specific applications (such as sheet metal compliance or welding-distortion);
- Reliance on specific, custom simulation codes for tolerance modelling with limited implementation in practical and accessible software tools;
- Need for additional expertise in formulating specific assembly tolerance models and interpreting results.

Additionally, a number of commercial Computer Aided Tolerancing (CAT) tools have been developed that offer practical tolerance analysis and synthesis capabilities either within independent software packages, or more commonly through integration with commercial CAD systems (Section 2.7). However, current commercial CAT tools generally lack the ability to accommodate tolerance analysis of assemblies whose functionality is dependent on loading. Although the effects of compliance have been addressed by some available CAT tools (particularly within sheet metal assemblies as relevant to automotive or aerospace applications) there remains a lack of ability to accommodate a general class of problem involving assembly loading (Section 2.9).

This chapter presents a novel tolerance analysis platform which integrates the capabilities of CAD, CAE and statistical analysis tools using Process Integration and Design Optimization (PIDO) software. The platform extends the capabilities of traditional CAT tools by enabling tolerance analysis of assemblies which are subject to loads. To demonstrate the capabilities of the developed approach, case study tolerance analysis problems are presented involving compliance and multi-body dynamics. These include:

1. An automotive actuator assembly consisting of a rigid spigot and complaint spring undergoing compression due to external loading. Functional characteristics require that clearance is maintained between the spigot wall and the spring at all times, while minimising overall packaging space.
2. An automotive rotary switch in which a resistive actuation torque is provided by a spring loaded radial detent acting on the perimeter of the switch body. Functional characteristics require that the resistive switch actuation torque be within an ergonomically desirable range.

4.4 PIDO based tolerance analysis platform

To aid in the solution of design problems which involve multidisciplinary engineering disciplines, a number of Process Integration and Design Optimization (PIDO) tools have been developed (Section 2.8). PIDO tools act as software frameworks for facilitating the integration of the standalone capabilities of diverse, discipline specific CAD and CAE analysis tools. The integration enables PIDO tools to also facilitate automated parametric analysis, Design of Experiments (DOE) studies, statistical analysis and multi-objective optimization, in an interdisciplinary setting (Sobieszczanski-Sobieski *et al.* 1997; Hiriyanaiyah *et al.* 2008; Flager *et al.* 2009). Interaction between standalone CAD and CAE software is achieved through commonly embedded scripting capabilities (based on scripting languages such as JavaScript, Visual Basic, Python or DOS script). For example, the CAD software CATIA accommodates the ability to execute Visual Basic language scripts. Scripting capabilities of CAE and CAD tools allow for autonomous:

- modification of CAD model parameters;
- initialisation of CAE simulations;
- recording of the obtained simulation results.

Problem formulation is typically achieved by manually creating a process and logic workflow that describes the intention of the simulation and integrates with the system model to be analysed. The workflow establishes links between external CAE models (through scripting

capabilities), the model input and output parameters, and a simulation procedure so that the model under analysis can be subjected to an automated parametric study. Once the workflow is established, an automated evaluation of the external model for the specified input parameters can be carried out without user input. During a simulation, each of the parameter combinations established as part of the simulation procedure is automatically applied to the external CAE model and any affected model output parameters of interest are read and recorded. At the completion of the simulation, statistical tools available in the PIDO tools can be applied to analyse the recorded results.

The interdisciplinary integration, DOE and statistical data analysis capabilities of PIDO tools can be utilized to address tolerance analysis problems requiring numerical modelling and simulation of the effects of loads on an assembly. The following sections present a PIDO tool based tolerance analysis platform developed for assemblies subject to loads, such as mechanical actuators and automotive seat positioning mechanisms.

4.4.1 Platform flowchart

The proposed PIDO tool based tolerance analysis platform for assemblies subject loads is presented in Figure 4.2. It can be implemented procedurally with the sub-elements briefly defined below (additional detailed discussion is presented in the identified sections):

1. Parametric CAD model (Section 4.4.2)

CAD models for each part of the product assembly are defined, including tolerance types and datums for features of interest as well as part relationships such as assembly sequence and mating conditions. Assembly response functions defining dimensional and geometric KPCs are captured implicitly within the CAD assembly.

2. Physical model simulation (Section 4.4.3)

CAD models are exported to a CAE tool and subjected to a numerical analysis simulating the effect of loads on assembly functionality. Assembly response functions defining KPCs are captured implicitly within the CAE model (e.g. Sections 4.5 and 4.6).

3. Uncertainty Quantification (Section 4.4.4)

An estimate of the assembly yield by statistical tolerance analysis requires that the stochastic variation of part parameters be propagated through the assembly model. Various uncertainty quantification (UQ) methods are available to estimate the statistical moments of the associated KPC distributions. UQ method selection should be according to the specific requirements of the analysis scenario.

4. Variation database (Section 4.4.5)

Distributions of the expected variation in each part parameter are defined in the variation database. The parameters can be dimensional, geometric (GD&T), material or associated with loading. Unique sets of parameter values are selected from the variation database to be used in uncertainty quantifications. Simulations output are recorded within the database.

5. Yield estimation (Section 4.4.6)

Dimensional and geometric KPCs (CAD assembly) and KPCs defined by loading (CAE simulation) are recorded in the variation database. Statistical moments of the associated KPC distributions are evaluated using the applied UQ method. Yield estimates are calculated from the statistical moments of KPCs.

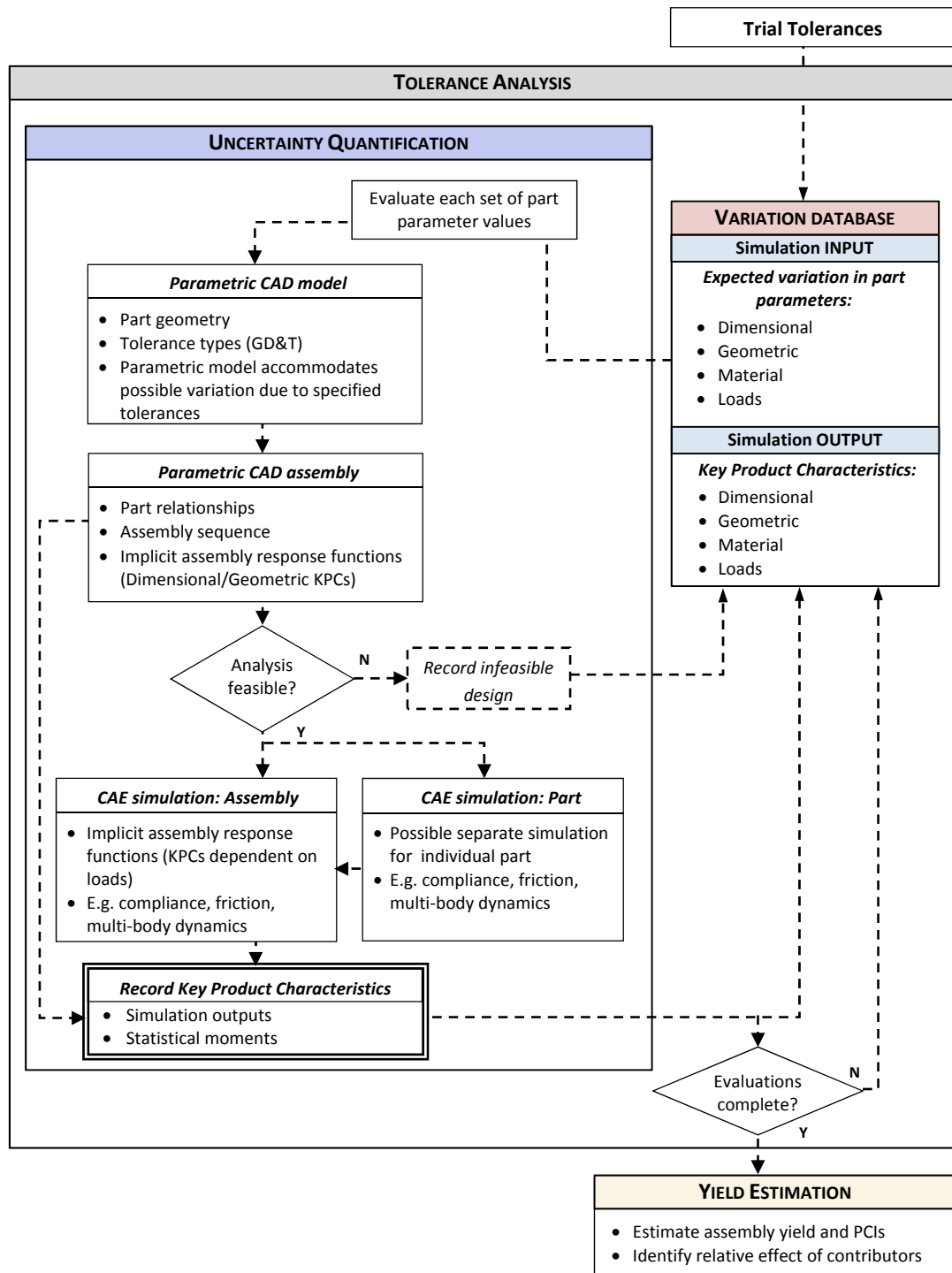


Figure 4.2 - PIDO based tolerance analysis platform

Compared to existing approaches for accommodating loading in tolerance analysis, the proposed platform has the following unique characteristics:

- Tolerance modelling is conducted within existing CAD/E tools using parametric models, and scripting interface enabled by PIDO tool integration. The need for additional modelling tools and expertise is subsequently reduced.

- The use of standalone CAE modelling tools (for example popular FE modellers like ANSYS or ABAQUS), allows sophisticated abilities in modelling the effect of various loads on mechanical assemblies.

These characteristics are discussed in detail in the following sections.

4.4.2 Parametric CAD model

CAD software modelling typically involves a history based approach where three-dimensional solid geometric models are created from two-dimensional sketches subject to three-dimensional operations such as extrusions, sweeps and lofts. CAD assemblies are defined by multiple CAD parts whose interaction is constrained to restrict the degrees of freedom between parts. Changing part geometry requires reverting the model to the relevant point of change (such as a sketch), updating dimensions and relationships, and re-executing subsequent modelling operations in series. If any part geometry is modified, the associated assembly constraints also need to be re-evaluated to rebuild the assembly model. Model dimensions and relationships can be defined parametrically, providing a means of implementing tolerance analysis by varying individual dimensions, either by worst-case or statistical approaches.

Parametric CAD based modelling is however subject to some limitations, such as (Section 2.4.2):

- Due to their history based nature and need to serially re-execute modelling operations for any parameter changes, parametric CAD models may be computationally expensive for statistical tolerance analysis requiring a large number of model evaluations.
- Limitations in representing intermittent part contact (for example Figure 2.6).
- Datum precedence according to GD&T standards can be difficult to accommodate in certain scenarios (Shah *et al.* 2007).

To address some of the limitations of parametric CAD based tolerancing, alternative approaches have been implemented in commercial CAT tools which use independent tolerance models in addition to CAD model geometry (Section 2.4.3). The general approach involves importing the CAD model into the CAT system and interactively creating an abstracted geometry model superimposed on the original CAD data (Chase *et al.* 1995; Salomons *et al.* 1995; Prisco *et al.* 2002; Chiesi *et al.* 2003; Shah *et al.* 2007). The abstracted model describes the possible part variation, part mating relationships and resultant assembly response functions without the rebuild penalty associated with CAD history-based model construction. However, a number of limitations are also associated with the abstracted geometry CAT approach (Section 2.4.3);

- Additional expertise, tools and time are required to define the abstracted geometry model and interpret simulation results.
- Limited ability to accommodate tolerance problems involving assemblies under loading and current inability to integrate with external CAE modelling tools.
- It is difficult to accommodate all possible variation aspects defined in GD&T standards due to the point-based nature of the abstracted geometry systems (Shah *et al.* 2007).

Comparison of the limitations of parametric CAD based and abstracted geometry tolerance modelling shows that the parametric CAD approach is more suited to tolerance modelling of assemblies under loading as the limitations of parametric CAD are not significantly prohibitive in such an application. For instance, CAD software models may be integrated with standalone CAE software through commonly embedded scripting capabilities allowing for modelling of the effects of loading on assembly functionality. The rebuild penalty associated with parametric CAD models is rendered comparatively less significant, within the scope of the proposed platform, as the computational cost of the CAE simulation is typically much greater than the cost of the CAD model update. Additionally, the limitations in representing intermittent part contact can be managed by utilising clash detection capabilities typically featured in CAD software that can report the location and magnitude of any unexpected interference (for example Section 3.3). This capability is utilised in the proposed platform to determine assembly yield where interference violates functional requirements.

Consequently, due to the limitations of abstracted geometry systems, parametric CAD modelling is adopted in this work to represent part feature variation. Example applications of parametric CAD tolerance modelling are shown in the case studies presented in this chapter.

4.4.3 Physical model simulation

The effects loads on mechanical assemblies are typically analysed by CAE simulations, which are not directly compatible with traditional CAT tolerancing tools. To accommodate these effects, PIDO tool can be utilised to integrate the parametric CAD data with CAE analysis tools for modelling of loading. This analysis may be performed on the entire assembly (as in Section 4.6), or on a subset of parts (as in Section 4.5). Computational cost is dependent on the fundamental nature of the analysis and can range from: inexpensive analysis of simple assemblies, where the analysis time is comparable to the time associated with the CAD

model update; to, high fidelity simulations for which the computational time may be orders of magnitude higher than the CAD model update time.

4.4.4 Uncertainty quantification strategy

The objective of statistical tolerance analysis is to provide an estimate of the assembly yield in the presence of manufacturing variation. This yield estimate requires that the statistical moments of the KPC distributions be known. Uncertainty quantification methods can estimate KPC distributions by propagating the expected manufacturing variation in part parameters, through the assembly response function. The CAE methods applied in this platform are based on a numerically defined implicit model, as such it is required that the UQ methods be compatible with an implicit response function.

A number of compatible UQ methods have been presented in the literature (Nigam *et al.* 1995; Lee *et al.* 2009), including: Full Factorial Numerical Integration, Univariate Dimension Reduction, Polynomial Chaos Expansion, Monte Carlo simulation and Taguchi method (Section 2.5). The relative merit of these UQ methods is dependent on the intent and constraints of the engineering design problem, including the: dependence on the dimensionality of the problem, complexity of implementation, computational cost and available computational resources and the required confidence level in the KPC prediction.

The Monte Carlo (MC) simulation is used in this research as it is well understood, robust and easily implemented within the platform (Section 2.5.1.1). Furthermore, the results of the MC simulation can provide a performance baseline for assessing the relative merit of alternate UQ methods which may offer enhanced performance when applied in this platform. Chapter 5 details the application of alternative UQ methods to tolerance analysis and synthesis.

Studies suggest that approximately 1000 samples are required to provide sufficient accuracy in an assembly tolerance analysis problem (Gao *et al.* 1995). These recommendations were applied in the case studies presented in this chapter.

4.4.5 Variation database

The quality of a manufacturing process can be quantified by how consistently and accurately it produces the desired process outputs. The variation in each part is quantified by statistical measurements of the particular manufacturing process output. Tolerances specify the allowable variation around a nominal parameter value between the lower specification limit (LSL) and the upper specification limit (USL). The expected distribution of each part

parameter is defined within the variation database. A set of parameter values is selected from the variation database to be used in the uncertainty propagation simulation (Section 4.4.4).

The ability of a manufacturing process to generate outputs consistently and accurately within the specification limits can be measured using Process Capability Indices (PCI) such as C_p , C_{pk} and C_{pm} indices (Section 2.3.4). These indices compare the specification limits to the 6σ limits of the manufacturing process distribution, i.e. 99.73% of the predicted population, where a higher process index indicates a more accurate process. In this work PCIs are applied to quantify the expected variation distribution for each parameter.

4.4.6 Yield estimation

Yield is calculated from the statistical moments of assembly KPCs estimated with UQ methods. For UQ based on MC simulation, the model is repeatedly evaluated to generate a histogram of the predicted variation in KPCs. Standard statistical techniques are used to calculate the associated moments and resultant assembly PCIs. Contributor analysis based on a Student's T-test is carried out to compute the influence of an individual part parameter on the KPC based on a correlation analysis (Jackson 2011). Correlation coefficients for each parameter are presented hierarchically, for example (Section 4.5.5).

Implementation of the PIDO based tolerance analysis platform involving external and internal forces is presented in the following section using two representative case studies.

4.5 Case study 4.1 - Assembly design subject to external forces

4.5.1 Problem definition

The case study involves a tolerance analysis problem where product functionality is defined by compliance of part geometry due to external forces. It consists of a spring and spigot assembly which is to be used by an industry partner in an automotive actuator mechanism (Figure 4.3). The spigot is an injection moulded polymer component which is assembled with a steel helical compression spring. The spring ends are squared and ground. The design objective is the minimisation of the spigot volume due to strict restrictions imposed on the actuator packaging space. The product specification has imposed a series of rigorous constraints:

- Functionality of the actuator constrains the force-extension characteristics of the spring and consequently its nominal dimensions.
- The minimum bore wall thickness, t , is constrained by structural strength requirements.
- The accuracy of the manufacturing machinery cannot be increased due to strict manufacturing cost targets. Nominal dimensions however can be varied.
- The manufactured spigot and spring assemblies must exceed a C_{pk} of 1. This requirement corresponds to an assembly yield of 99.7%.

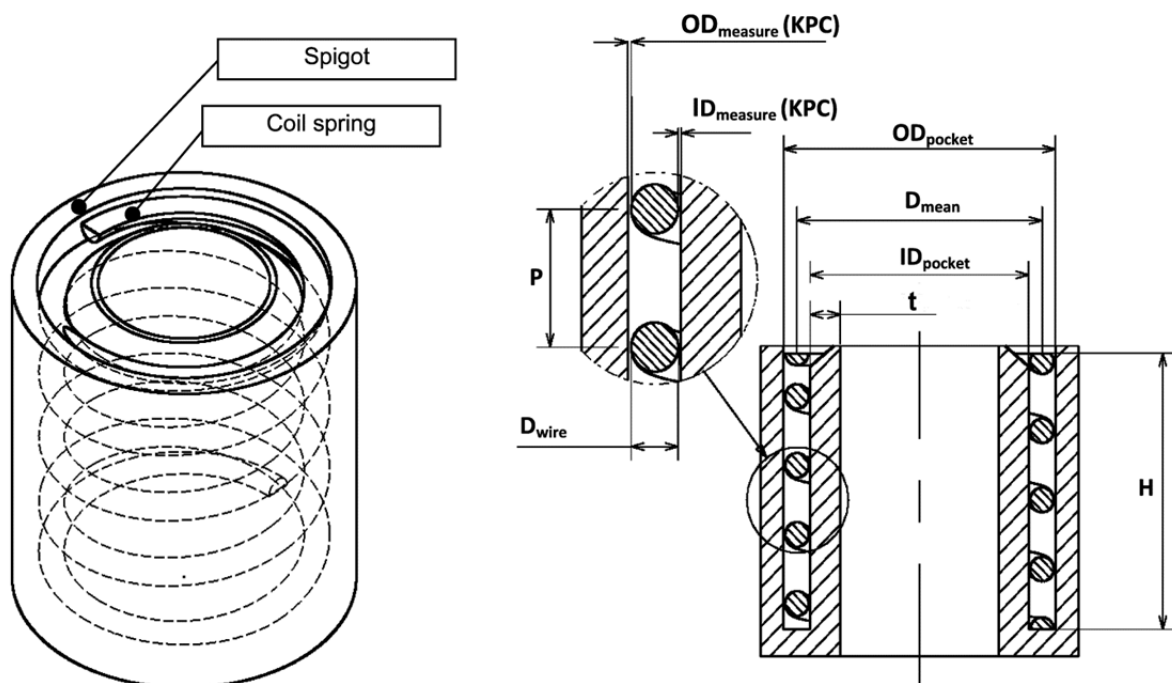


Figure 4.3 - Spring and spigot assembly.

Functional characteristics of the actuator require that clearance is maintained between the spigot wall and the spring. As the spring is compressed from its nominal position, both the inner and outer diameters of the spring increase. Consequently:

- Clearance between the inner diameter of the spring and the spigot wall is minimal when the spring is at free height. The associated assembly response function can be evaluated without modelling external and internal forces.
- Clearance between the spring outer diameter and spigot wall is reduced as the spring compresses. The associated assembly response function cannot be evaluated in a CAD environment without modelling the compliance of part geometry due to external forces. No analytic solution directly applicable to the dilation of a squared and ground compression spring was found in the literature. This problem is therefore a suitable case study for the proposed method as numerical models are necessitated. A solution for an open-coiled spring with ends fixed against rotation is presented in (Wahl 1963). This model was used to validate a FE model comparable to the one used in this case study. The platform proposed in this work is applied to overcome these limitations (Section 4.5.5).

The KPCs for the product assembly in this case study are the minimum clearance between:

- the internal diameter of the spring and the spigot wall ($ID_{measure}$)
- the outer diameter of the spring and the spigot wall ($OD_{measure}$)

The case study objective is to specify a nominal value for the control variable (OD_{pocket}), which minimises packaging space subject to the required yield of 99.7%.

4.5.2 Sources of variation

The product under consideration comprises of polymer injection mouldings and coiled wire, each with unique manufacturing variation characteristics.

4.5.2.1 Variation in injection moulding

Dimensional variation in injection moulded plastics can be attributed to mould characteristics, resin processing and shrinkage. Mould related variation arises from deviation in the mould cavity dimensions, deterioration of the mould with service life, and positional accuracy of movable mould sections. Variation due to the processing of resin can be attributed to resin and mould temperature, clamping pressure, uniformity of resin constitution and humidity levels ((DIN) 1982). When plastic resin is injected into a moulding cavity it is above the resin melting temperature. The resin is then rapidly cooled in the

mould. Once set, the moulding is removed and further cooled to ambient temperature. Due to phase changes of the resin and differential cooling, the final moulded part dimensions are subject to variation ((DIN) 1982; Rosato *et al.* 2000).

4.5.2.2 Variation in spring wire

The performance of coil springs depends on numerous design and manufacturing parameters. Functional requirements typically dictate the required spring rate or force at a specified deflection. These attributes are a function of geometric parameters: wire diameter, mean coil diameter, number of active coils and free length. Spring performance is also dependent on material properties such as strength, shear modulus and plastic formability, which can vary significantly between batches (DeFord 2003). Small variation in the mechanical and surface frictional properties of wire material may significantly affect the manufacturability of the springs and introduce broad variation in the process outputs (Wood 2006). Additional dimensional variation may be introduced during manufacturing by the spring coiling machinery.

The sources of variation present in the manufacture of springs significantly influence their performance and their dimensional envelope under compression, for example (DeFord 2003). Industry standard tolerances exist to limit the effects of such variation, for example ((ASTM) 2007).

4.5.3 Variation data used in simulation

To estimate expected dimensional variation, the existing moulding process used for the manufacture of the spigot was analysed and assessed in terms of its performance. The manufacturer of the spigot assembly specifies dimensional tolerances on injection moulded components according to specification limits recommended by DIN 16901 ((DIN) 1982). The capability of the manufacturer's injection moulding process to generate outputs within the specified limits was determined by metrological assessment of 1600 production part samples of similar geometry to the case study spigot. The production parts are manufactured using multiple moulding cavities, with each having its own variation characteristics. The resultant parts were analysed for variation within a single cavity and across multiple cavities. Process capability indices were determined (Table 3.1) and used as input for the case study analysis. The metrological data was also utilised in Case study 3.1 (Section 3.3.2) due to a common industry partner and manufacturing process.

Table 4.1 - Process capability data of measured component in Test Case 4.1.

Parameter	Target	Achieved
Mean (mm)	16	15.986
σ (mm)	-	0.0457
LSL (mm)	15.850	-
USL (mm)	16.150	-
C_p	1.00	1.10
C_{pk}	1.00	1.01
C_{pm}	1.00	1.05
% < LSL	0.15 %	0.15 %
% > USL	0.15 %	0.02 %
% Total out of spec.	0.30 %	0.17 %

The expected spring tolerances were defined by the spring suppliers own tolerance data (Table 4.2). These specification limits exceed those reported as typical in the literature, e.g. (Hindhede 1983).

Table 4.2 - Spigot and spring assembly parameters and associated variation.
(Note: Spigot specification limits are specified from DIN 16901, C_{pm} from measurements.
Spring specification limits and C_{pm} from supplier's quality data.)

Component	Parameter	Description	Nominal [mm]	Specification Limits +/- [mm]	Min [mm]	Max [mm]	C_{pm}	σ
Spring	D_{wire}	Wire diameter	3.55	0.05	3.50	3.60	1	1.67E-02
	D_{mean}	Mean coil diameter	26.2	0.50	25.70	26.70	1	1.67E-01
	H	Height	25.19	0.12	25.07	25.32	1	4.17E-02
	P	Pitch	11	0.05	10.95	11.05	1	1.67E-02
	E	Young's modulus	2.07E+11	2.070E+08	2.068E+11	2.072E+11	1	6.900E+07
Spigot	OD_{pocket}	Outer diameter of spigot pocket	30.75	0.10	30.65	30.85	1.05	3.03E-02
	ID_{pocket}	Inner diameter of spigot pocket	22.2	0.10	22.10	22.30	1.05	3.03E-02

4.5.4 Simulation model

The tolerance analysis platform presented here utilises CAD and CAE tools for parametric modelling and compliance analysis, respectively. A parametric Finite Element (FE) model of the coil spring was constructed using CATIA CAE software (Figure 4.4). The model consisted of approximately 42 000 3D parabolic tetrahedral elements with 11 000 corresponding nodes. Spring loading conditions were simulated by applying rigid restraints to the base of the spring and a displacement of 8 mm to the top face as per the functional characteristics of the actuator. Individual simulation computation time was approximately 100 seconds on a 1.86 GHz CPU.

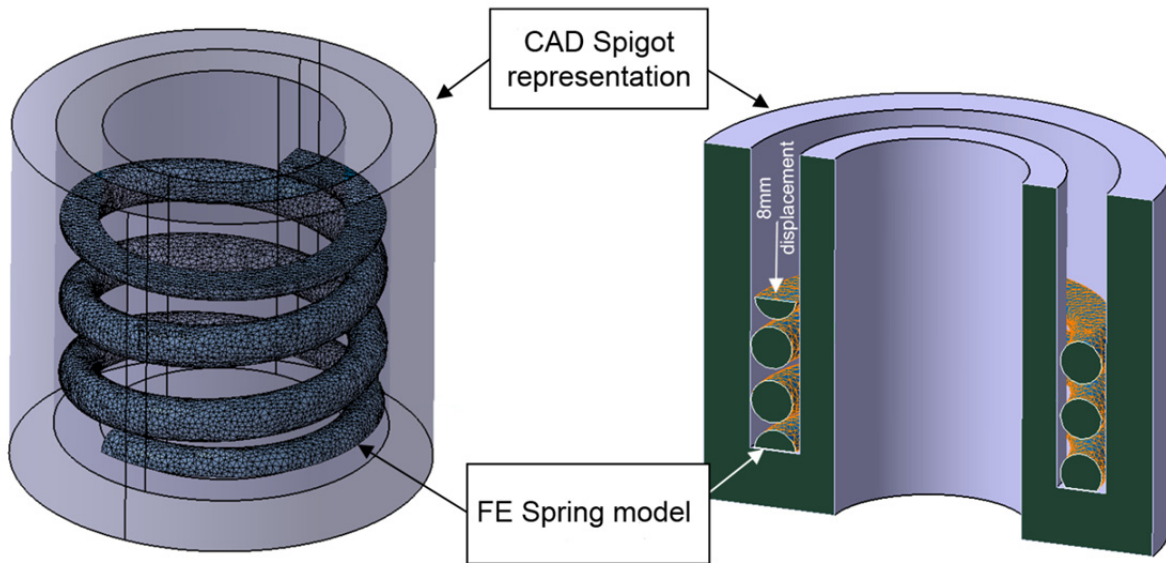


Figure 4.4 - Spring spigot assembly and FE model of spring.

A PIDO tool (ESTECO modeFRONTIER) was interfaced with CATIA CAD and FE tools (Figure 4.5) according to the proposed platform (Figure 4.2). A variation database was initialised from the obtained tolerance data (Table 4.2) and subjected to a Monte Carlo simulation consisting of the following automated stages:

1. CAD models of the spigot and spring were updated.
2. The undeformed spring was assembled with the spigot and a measure of minimum internal diameter clearance was recorded ($ID_{measure}$).
3. A finite element model of the spring was generated and subjected to displacement conditions.
4. The deformed finite element spring model was assembled with the spigot and a measure of minimum outer diameter clearance was recorded ($OD_{measure}$).
5. Clash analysis was conducted to identify unintended interference.

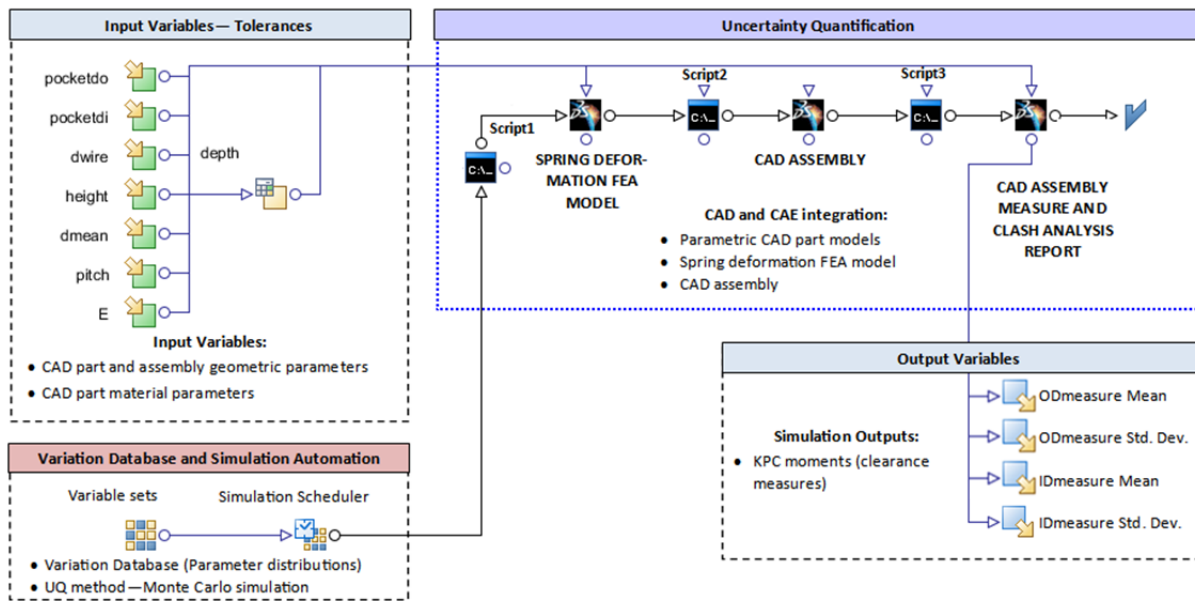


Figure 4.5 - PIDO tolerance analysis workflow for Case study 4.1.

4.5.5 Simulation results

The MC simulation consisted of 1000 assembly variants. A database was generated from clearance measures and clash analysis data obtained for each assembly variant. A normal distribution curve was subsequently fitted to the simulated histograms for both KPCs (Figure 4.6 and Figure 4.7). The theoretical distribution curve predicts the yield of the population of assemblies from the simulated samples, by comparison with the set specification limits (defined for 99.7% yield, Section 4.5.1).

Clearance measurements result from the assembly response function that intrinsically depends on the simulation input parameters. The magnitude of correlation between input parameters and the assembly response function provides insight into the most pertinent input parameters (Figure 4.8). This outcome enables quality control to be applied relative to the importance of the identified contributing factor.

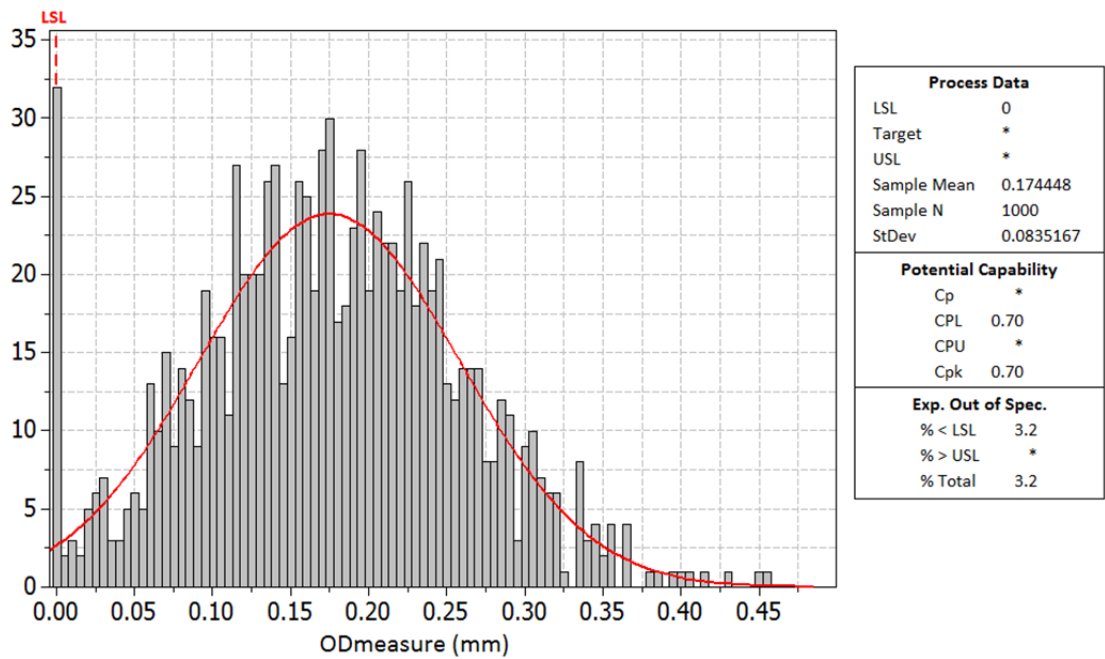


Figure 4.6 - Histogram of clearance measurements for spigot outer diameter ($OD_{measure}$). (Note: Solid line indicates estimated population distribution based on sample results. The initial analysis provided a yield of approximately 96.8 % for the spring outside diameter.)

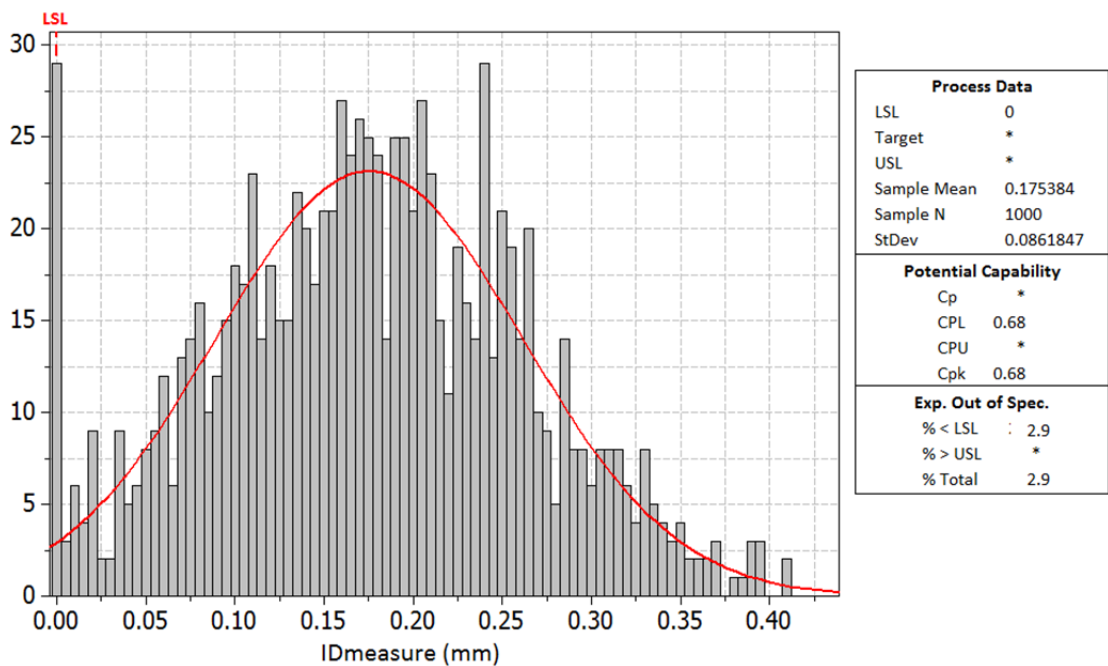


Figure 4.7 - Histogram of clearance measurements for spigot inner diameter ($ID_{measure}$). (Note: Solid line indicates estimated population distribution based on sample results. The initial analysis provided a yield of approximately 97.1 % for the spring inside diameter.)

A Student t-test was conducted to quantify the contribution of part parameter variation to KPC variation. Figure 4.8 and Figure 4.9 summarise the effects of part parameter variation on the KPC ($ID_{measure}$ and $OD_{measure}$). The relative effect of each input parameter on the output is quantified by the effect size. A positive effect indicates a positive relationship

between the input and output variables, a negative effect size indicates a negative relationship.

The simulation results show that mean spring coil diameter D_{mean} , has the highest influence on the clearance between the spring and spigot wall. The outer and inner spigot wall diameters, OD_{pocket} and ID_{pocket} , respectively, have a substantially lower influence. The result can be attributed to the difference in the magnitude of variation between the spring mean diameter, and the spigot wall diameters. As established in Table 4.2, the characteristics of the manufacturing processes result in an expected variation in the spring mean diameter that is substantially higher than that in the spigot diameters.

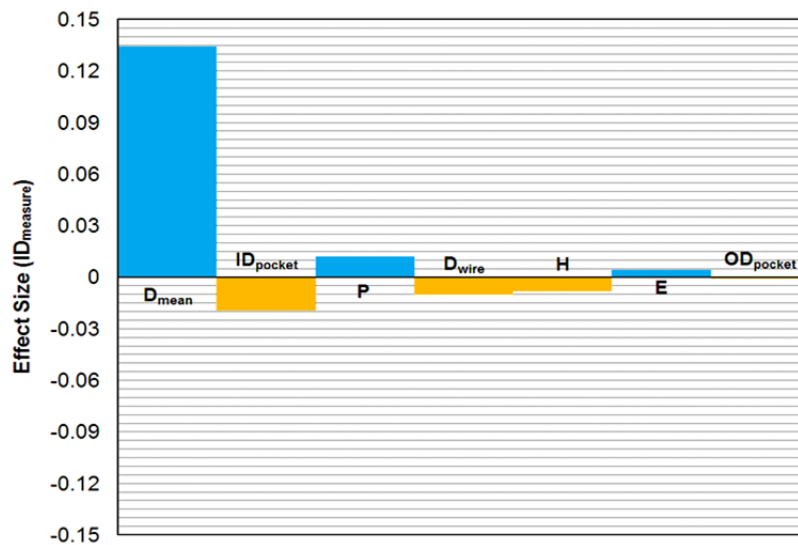


Figure 4.8 - Student chart of $ID_{measure}$
 (Note: A large positive effect size indicates a strong direct correlation; negative values indicate an inverse relation)

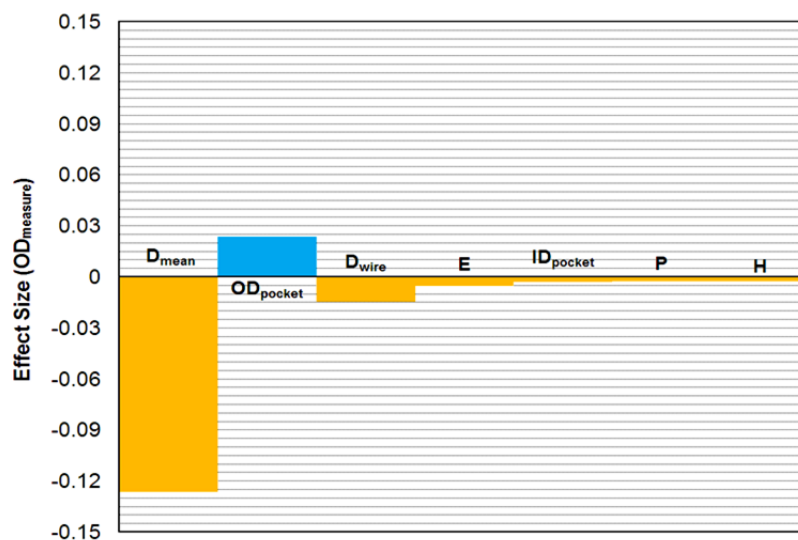


Figure 4.9 - Student chart of $OD_{measure}$
 (Note: A large positive effect size indicates a strong direct correlation; negative values indicate an inverse relation)

4.5.6 Outcomes

The yield requirement for the assembly is 99.7% (Section 4.5.1) implying that the specification limits must occur at 3 standard deviations from the distribution mean. Due to the clearance requirements, the LSL for both of the KPCs $ID_{measure}$ and $OD_{measure}$ is zero. The USL has no restriction as it does not compromise functionality. The simulation results indicate a 97.3% conformance (27 assemblies out of 1000 assemblies result in no clearance) for $ID_{measure}$. The conformance for $OD_{measure}$ is 97.0%. The required yield can however be achieved by adjusting the nominal OD_{pocket} and ID_{pocket} parameter dimension.

Due to the characteristics of the manufacturing process used, the change in standard deviation of the spigot parameters due to a small modification of the nominal parameter values is negligible. Table 4.3 indicates the nominal dimensions required to achieve the target yield of 99.7% (i.e. $USL = \text{mean} - 3\sigma$) as inferred from the simulation outcomes.

Table 4.3 - Initial and required nominal spigot wall dimensions based on simulated clearance measurements.

Parameter	Initial (mm)				Required (mm)			
	Mean _i	σ_i	Mean _i -3 σ_i	Mean _i +3 σ_i	Mean _R	σ_R	Mean _R -3 σ_R	Mean _R +3 σ_R
ID_{pocket}	22.200	0.0303	22.109	22.291	22.283	0.0303	22.192	22.374
OD_{pocket}	30.750	0.0303	30.659	30.841	30.825	0.0303	30.734	30.916
$ID_{measure}$	0.175	0.086	-0.083	0.433	0.258	0.086	0	0.516
$OD_{measure}$	0.174	0.083	-0.075	0.423	0.249	0.083	0	0.498

4.5.7 Potential sources of error

Due to precision limitations of internal CAD software measurement tools as well as geometry approximations due to finite-element tessellation, errors are introduced into the measured KPC values.

KPC values are reported by the measurement tools within the associated CAD environment. These tools may have inherent precision limitations which contribute to uncertainty in the reported outcomes. For the case study applied in this work, the CATIA measure tool was used to measure clearances between assembled parts. Due to internal software characteristics, the CATIA measure tool was able to provide only a close approximation of the exact clearance. To quantify the level of approximation, a MC simulation consisting of 1000 samples was carried out to measure a known clearance. The differences between the measured and known values (Figure 4.10) show that the error introduced by approximations of the CATIA measure tool (mean of 2.25×10^{-3} mm) are more than an order of magnitude less than the smallest associated tolerances (tolerance on parameter D_{wire} of 50.00×10^{-3} mm, Table 4.2) and do not significantly affect the case study results.

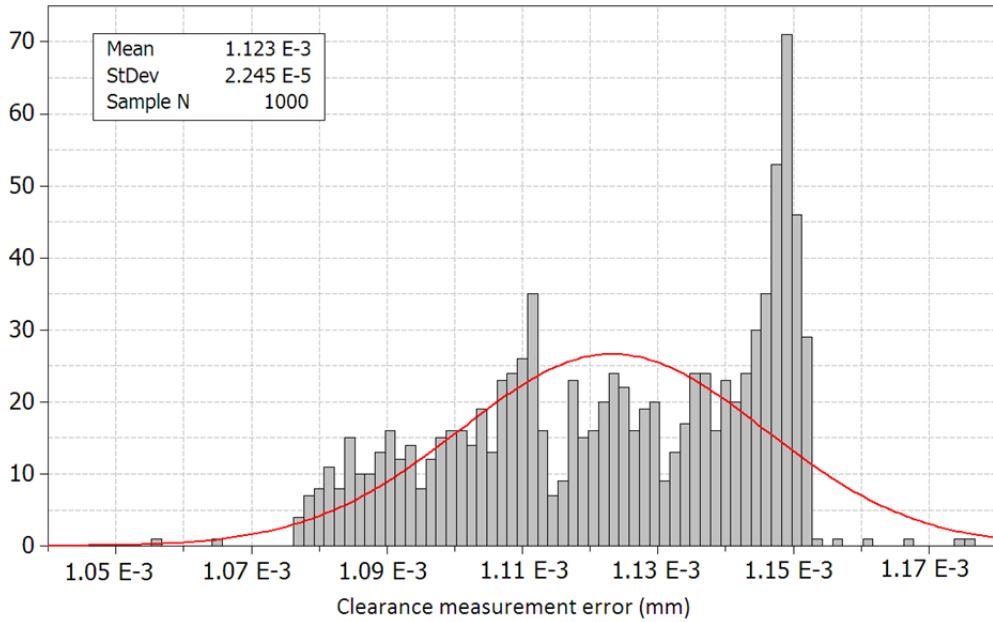


Figure 4.10 - Histogram of clearance measurement error

Finite-element tessellation, also known as faceting, denotes the discrepancy between the finite-element mesh and the actual geometry. This discrepancy can be mitigated by increasing the number of mesh elements until the associated error is sufficiently low. A comparison was made of the ideal and meshed spring models to determine the effect of faceting. Figure 4.11 shows a visual comparison of the ideal and meshed models indicating regions of difference equal to the smallest tolerance range used in the simulation (tolerance on parameter D_{wire} of 50.00×10^{-3} mm, Table 4.2). The result shows that the mesh density results in minimal geometry approximation and does not significantly affect the outcomes of the test case simulation.



Figure 4.11 - Comparison of original and meshed spring geometry. Light shade indicates a difference of mesh geometry from original by 50.00×10^{-3} mm (smallest tolerance used in simulation)

4.6 Case study 4.2 - Assembly design subject to both external and internal forces

4.6.1 Problem definition

This case study involves a tolerance analysis problem where product functionality is defined by both external and internal forces (friction and multi-body dynamics). A rotary switch and spring loaded radial detent assembly (Figure 4.12) is intended to provide positional restraint, with a certain resistive torque, for operational control in a Human Machine Interface (HMI) capacity (such as a headlight control switch in an automobile). The model shown is a simplified representation which omits details not affecting functionality. The cylindrical detent is located in a positioning sleeve within which a helical compression spring biases the cylindrical detent against the switch detent ramp faces.

The peak resistive torque is a KPC of the assembly. The resistive torque depends on:

- the geometry of part features
- internal forces due to part acceleration
- external forces, including the spring force, contact forces between components; and the friction coefficient dependent friction force between components in contact.

A sufficient resistive torque is required to provide ergonomically and functionally adequate positional restraint while providing a positive impression of product quality for the user. Excessive variation in the peak resistive torque of manufactured switch assemblies has a negative impact on perceived product quality. The design variables considered in the simulation are shown in Table 4.

The product requirements dictate a series of constraints:

- A nominal peak resistive torque of 75 Nmm has been experimentally identified as desirable for the intended application.
- The nominal peak resistive torque specification limit has been set at 75 ± 7 Nmm with a process capability requirement of $C_{pm} = 1$, i.e. 99.7% assembly yield.
- The rotary switch, radially acting cylindrical detent and positioning sleeve are all injection moulded polymer components.

The case study objective is to specify required process capability for the part parameters, such that the peak resistive torque (KPC) specification requirements are achieved with an assembly yield of 99.7% ($C_{pm} = 1$). An increase in manufacturing process precision can be accommodated if required to achieve the designated assembly yield.

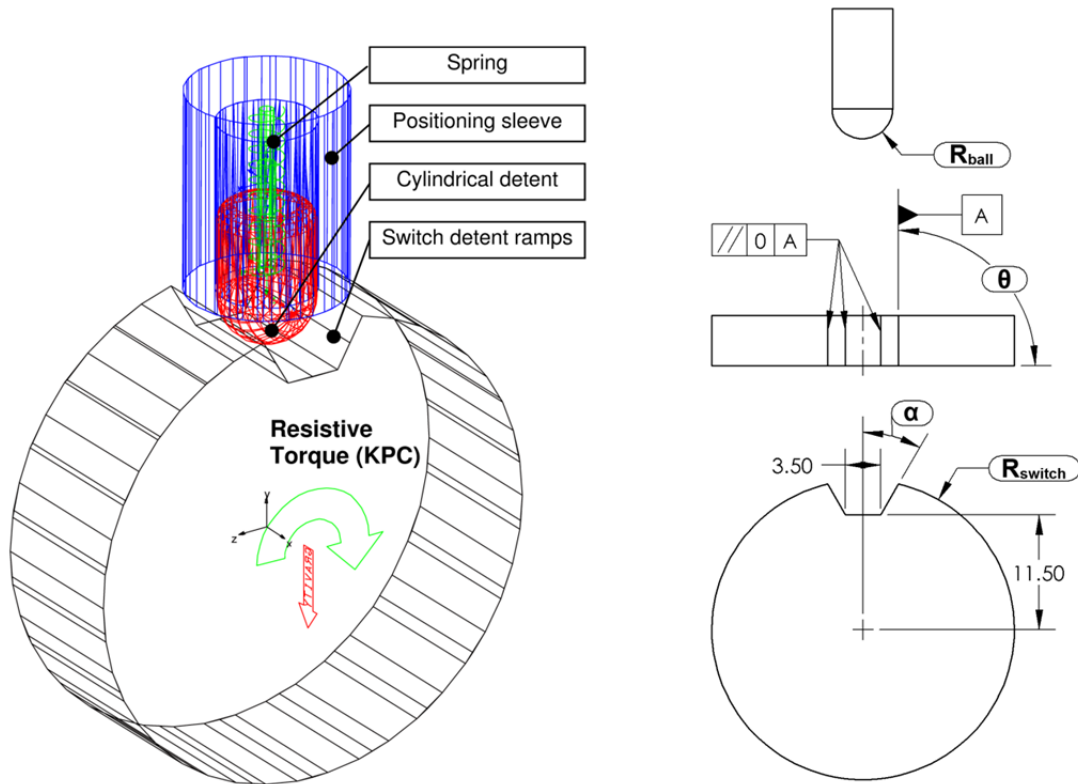


Figure 4.12 - Rotary switch and spring loaded radial detent assembly model used in Case study 4.2
 (Note: Linear dimensions in mm. Variation in non-enclosed dimensions not considered in simulation)

4.6.2 Sources of variation

The product under consideration is comprised of polymer injection mouldings and coiled wire, each with unique manufacturing variation as discussed in sections 4.5.2.1 and 4.5.2.2.

4.6.3 Variation data used in simulation

The relevant design variables considered in the simulation are shown in Table 4.4. The component manufacturer specified tolerances on injection moulded components according to specification limits recommended by DIN 16901, ((DIN) 1982). The specification limits on the spring rate have been estimated from SAE HS-795, (SAE 1997). The required process capability for each parameter was initially set at $C_{pm} = 1$ and the resultant assembly yield was estimated by simulation.

Table 4.4 - Case study 4.2 rotary switch assembly parameters and associated variation.
(Note: Switch and cylindrical detent specification limits are specified from DIN 16901.)

Component	Parameter	Description	Nominal	Specification Limits +/-	Min.	Max.	Initial		Second	
							C_{pm}	σ	C_{pm}	σ
Switch	R_{switch}	Switch radius	15.00 mm	0.25 mm	14.75 mm	15.25 mm	1.00	0.08	1.00	0.08
	α	Angle of ramp face	30.00°	5.00°	25.00°	35.00°	1.00	1.67	2.00	0.83
	θ	Yaw angle of ramp face	0.00°	3.00°	-3.00°	3.00°	1.00	1.00	1	1.00
Spring	F	Spring preload	2.00 N	0.20 N	1.80 mm	2.20 mm	1.00	0.07	2	0.03
	k	Spring rate	0.40 N	0.04 N	0.36 mm	0.44 mm	1.00	0.01	1	0.01
Cylindrical detent	R_{ball}	Ball radius	3 mm	0.19 mm	2.81 mm	3.19 mm	1.00	0.07	2	0.03
	μ_{switch}	Switch-detent dynamic friction coefficient	0.150	0.020	0.130	0.173	1.00	0.008	1	0.008
	μ_{slider}	Slider-detent dynamic friction coefficient	0.150	0.020	0.123	0.173	1.00	0.008	1	0.008

4.6.4 Simulation model

A parametric numerical model of the switch assembly was constructed in MSC ADAMS multi-body dynamics modelling software (Figure 4.12). The model parametrically accommodates the possible variation within geometric and physical parameters (such as spring pre-load, spring stiffness and friction coefficients).

Although a three dimensional assembly model was developed, the simulation was conducted as a two dimensional problem to reduce simulation time. The dimensionality of the problem was reduced by constraining the position of the rotary switch and the cylindrical dial with revolute and translational joints, respectively. Contact between the cylindrical detent and the rotary switch was modelled using a solid-to-solid contact constraint involving Coulomb friction (nominal values: $\mu_{Static} = 0.25$, $\mu_{Dynamic} = 0.15$). Individual simulation computation time was 14 seconds on a 1.86 GHz CPU. No directly comparable algebraic model was identified, however, an approximate model was used to confirm that the predicted results were of a similar magnitude (Canick 1959).

The numerical model was interfaced with a PIDO tool (ESTECO modeFRONTIER) according to the developed platform (Figure 4.14). A variation database was subsequently initialised from the obtained tolerance data (Table 4.4) and subjected to a MC simulation consisting of the following automated stages:

1. Dimensional, spring and friction parameters of models were updated.
2. A rotational velocity of 30 degrees per second was imposed on the rotary switch and the interaction of components simulated for 500 ms.
3. Peak and transient resistive torque were recorded.

Figure 4.13 shows the simulation output for transient resistive torque for 1000 assembly variants. The peak values were used as a KPC for the assembly.

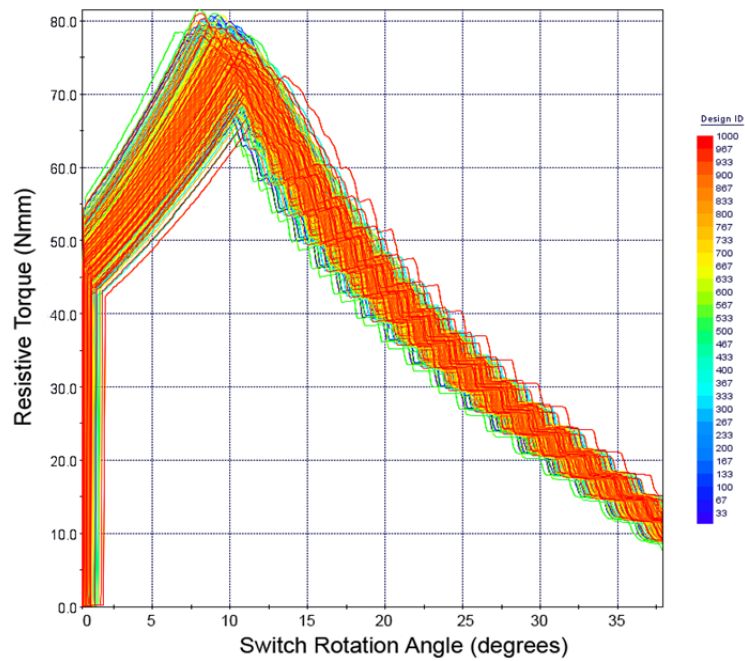


Figure 4.13 - Transient resistive torque for 1000 assembly variants resulting from initial simulation

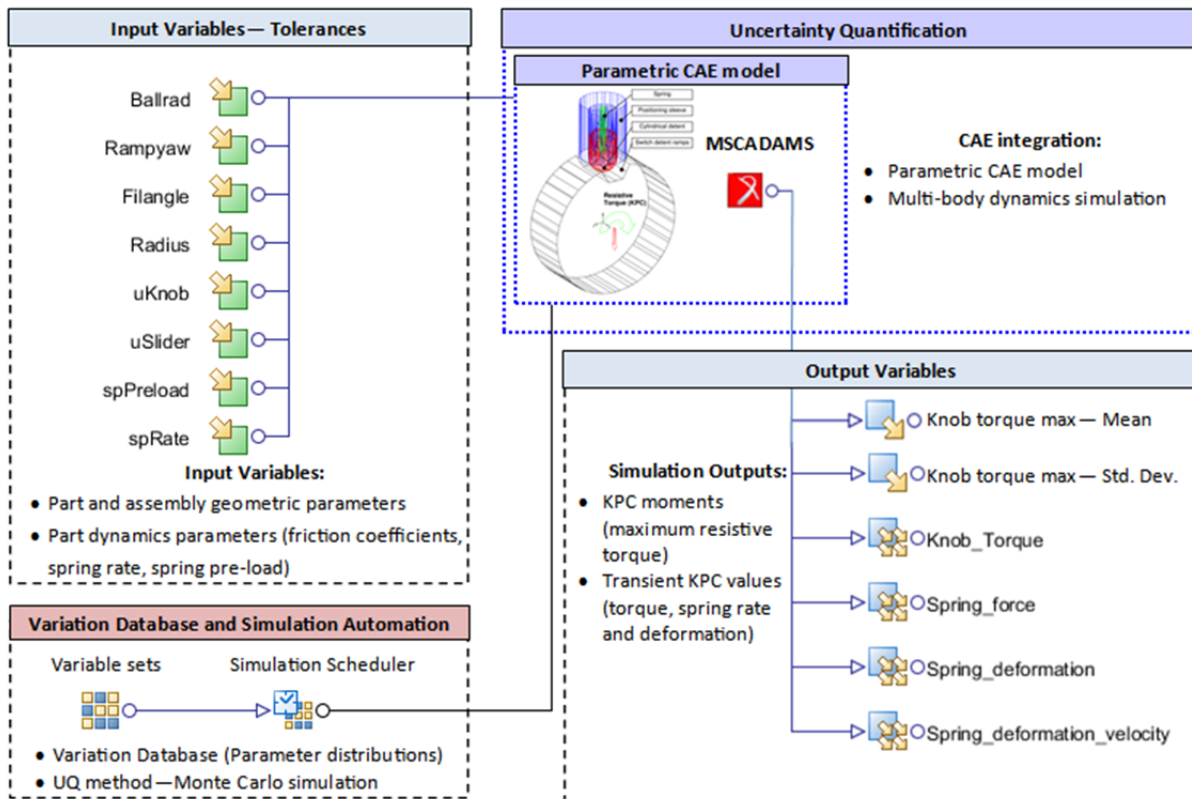


Figure 4.14 - PIDO tolerance analysis workflow for Case study 4.2.

4.6.5 Simulation results and outcomes

4.6.5.1 Initial simulation

Monte Carlo sampling based UQ was conducted with 1000 assembly variant samples. A database was generated of peak resistive torque measurements (KPC) for each assembly variant. A normal distribution curve was subsequently fitted to the simulated KPC histogram (Figure 4.15) and the expected process capability C_{pm} was calculated. The simulation results show that the required assembly yield requirements are not met (achieved $C_{pm} = 0.62$, required $C_{pm} = 1$) with the initially specified process capability requirements for the designated part parameters (Table 4.4).

The peak resistive torque measurements are the result of an assembly response function that intrinsically depends on the simulation input parameters. A Student t-test was conducted to quantify the contribution of part parameter variation to KPC variation. Figure 4.16 summarises the effects of part parameter variation on the KPC (Peak resistive torque). The simulation results show that variation in the ramp face angle A , and the spring preload F , have the highest influence on variation in the peak resistive torque.

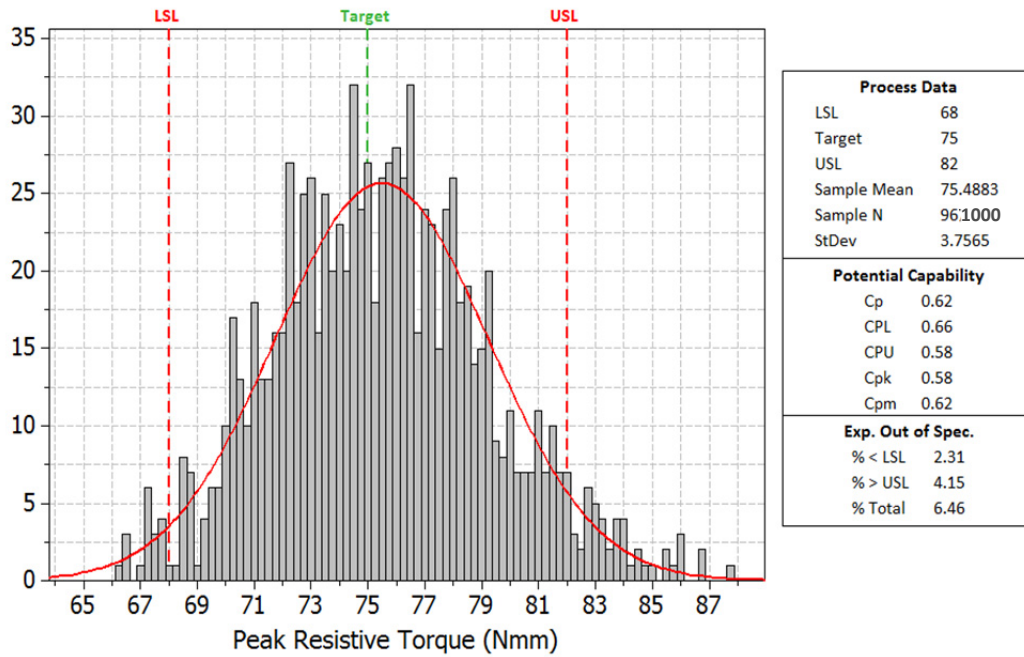


Figure 4.15 - Histogram of peak resistive torques obtained from initial simulation

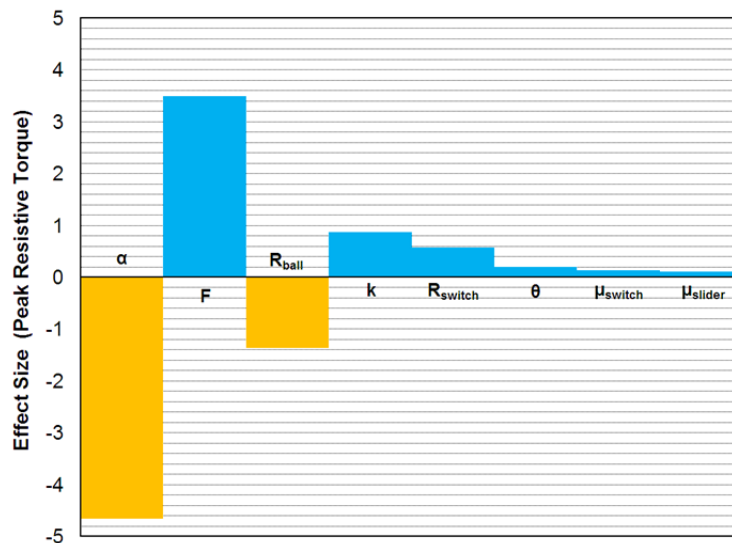


Figure 4.16 - Student chart of peak resistive torque for initial simulation
(Note: A large positive effect size indicates a strong direct correlation; negative values indicate an inverse relation)

4.6.5.2 Second simulation

Based on the outcome of the initial MC simulation, the required process capabilities for the most influential parameters A and F were doubled (Table 4.4) to achieve the required assembly yield. These values were used as input into a subsequent simulation.

A second UQ simulation was conducted with 1000 samples. The simulation results (Figure 4.17) show that the required assembly yield requirements are met (achieved $C_{pm} = 1.11$, required $C_{pm} = 1.15$) with the adjusted process capability requirements for the part

parameters (Table 4.4). The adjusted process capability requirements reduced the contribution of parameters A and F towards variation in the peak resistive torque as seen in the Student chart in Figure 4.18.

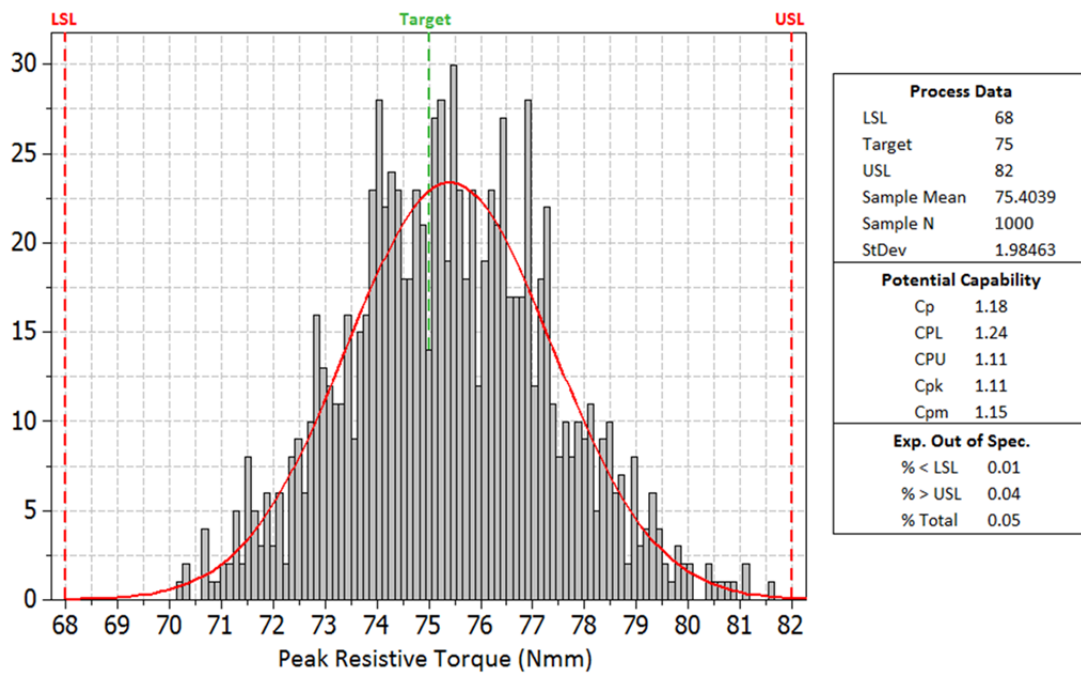


Figure 4.17 - Histogram of peak resistive torques for second simulation.

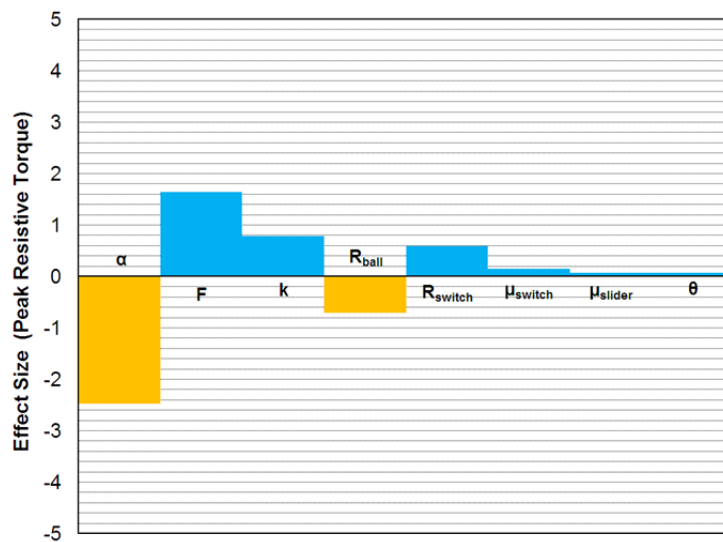


Figure 4.18 - Student chart of peak resistive torque for second simulation
(Note: A large positive effect size indicates a strong direct correlation; negative values indicate an inverse relation)

4.7 Summary of research outcomes

Managing the effects of manufacturing variation on product functionality is paramount to achieving competitive quality, cost and development time targets. The functionality of mechanical assemblies often depends on effects such as compliance and dynamics due to the action of loads on the assembly; commonly external or internal forces. A review of existing methods and tools for addressing tolerance analysis in assemblies subject to loads, has identified a number of limitations, including:

- Accommodation of only single load effect scenarios (such as sheet metal compliance or welding-distortion).
- Need for significant additional expertise in formulating specific assembly tolerance models and interpreting results.
- Reliance on specific, custom simulation codes with limited implementation in practical and accessible Computer Aided Tolerancing (CAT) software tools.

This chapter presented a tolerance analysis platform which overcomes these limitations by providing the capability to accommodate the effects of assembly loads, through integration of CAD, CAE and statistical analysis tools. This is achieved with the interdisciplinary integration capabilities of Process Integration and Design Optimization (PIDO) tools.

To demonstrate the capabilities of the platform, case study tolerance analysis problems involving assemblies subject to loads are presented. These include:

1. An assembly consisting of rigid and compliant components subject to external forces. The tolerance analysis platform was applied to identify that for initially specified tolerances the assembly yield was unacceptable. The nominal dimensions required to achieve the desired assembly yield were subsequently identified.
2. An assembly in which functionality is defined by external forces and internal multi-body dynamics. The platform was applied to identify the tolerances required to achieve the required assembly yield.

Key outcomes of this work are as follows:

- The proposed platform extends the capabilities of traditional CAT tools and methods by enabling tolerance analysis of assemblies which are dependent on loads such external and internal forces. Traditional CAT tools are not able to accommodate a general class of problem involving assemblies under loading.
- The ability to accommodate the effects of loading in tolerance analysis allows for an increased level of capability in estimating the effects of variation on functionality.

- The interdisciplinary integration capabilities of the PIDO based platform allow for CAD/E models created as part of the standard design process to be used for parametric CAD/E based tolerance analysis. The need for additional modelling tools and expertise is subsequently reduced.
- The platform allows the use of standalone CAE modelling tools (for example popular FE modellers like ANSYS or ABAQUS), which offer sophisticated abilities in modelling the effect of various loads on mechanical assemblies. As such, the application of the platform can be extended to accommodate tolerance analysis of assemblies subject to a more general class of loading (for example thermo-mechanics or fluid flow) as well challenging scenarios involving transient or non-linear effects.

Despite the enabling capability of the proposed platform in accommodating tolerance analysis of assemblies under general loading, limitations also exist. These limitations are summarized below and presented in context in the identified sections:

- Computational costs associated with CAD model updates (Section 4.4.2) and the associated CAE simulations (Section 4.4.3) may be significant.
- Parametric CAD may present some limitations (Section 4.4.2) in accommodating all possible variation types defined in GD&T standards, and in representing realistic part interactions for a given set of assembly constraints.
- Approximation errors such as tessellation may be associated with FE models (for example, Section 4.5.7).
- Some CAD and CAE software tools may be limited in certain aspects of their ability to be autonomously controlled through scripting capabilities.

The main limitation of the presented statistical tolerance analysis platform is the potentially high computational cost associated with uncertainty quantification. Traditional UQ methods such as Monte Carlo sampling require a large number of model evaluations to accurately estimate statistical moments of the model response. For tolerance models which are computationally demanding to evaluate (such as FE models of the effects of loads on mechanical assemblies) a large number of model evaluations can significantly compound the overall computational cost. Consequently, for demanding models, statistical tolerance analysis of assemblies subject to loads may be computationally impractical with traditional UQ methods. Additionally, manual iteration of tolerance analysis can be time consuming and ineffective at identifying tolerances which optimally achieve cost and yield targets. Tolerance synthesis can significantly improve this effectiveness by guiding the search for optimal tolerances with an efficient optimization algorithm. However, tolerance synthesis

may require many iterations of tolerance analysis and the computational costs of solving numerical tolerance models and UQ are compounded making tolerance synthesis highly impractical with traditional UQ methods.

Chapter 5 focuses on addressing the limitations of this platform associated with high computational cost of tolerance analysis with traditional UQ methods by investigating the use of recently developed analytical UQ methods with significantly higher efficiency.

5 PIDO BASED TOLERANCE SYNTHESIS IN ASSEMBLIES SUBJECT TO LOADING USING POLYNOMIAL CHAOS EXPANSION

5.1 Chapter summary

Statistical tolerance analysis and synthesis in assemblies subject to loading is of significant importance to optimised manufacturing. Modelling the effects of loads on mechanical assemblies in tolerance analysis typically requires the use of numerical CAE simulations. The associated Uncertainty Quantification (UQ) methods used for estimating yield in tolerance analysis must subsequently accommodate implicit response functions and techniques such as Monte Carlo (MC) sampling are typically applied due to their robustness. Sampling methods require a large number of iterations to accurately estimate associated statistical moments. For non-trivial scenarios, each iteration of the numerical simulation is typically computationally expensive. Consequently, statistical tolerance analysis involving assembly loads is often computationally impractical. Identifying optimum tolerances with tolerance synthesis requires multiple iterations of tolerance analysis, further increasing the computational costs and making tolerance synthesis highly impractical for demanding tolerance models.

A variety of UQ methods have been proposed with potentially higher efficiency than MC sampling. These offer the potential to increase the practical feasibility of tolerance analysis and synthesis of assemblies subject to loading. This chapter investigates the feasibility of Polynomial Chaos Expansion (PCE) in tolerance analysis for uncertainty quantification. A previously developed Process Integration and Design Optimization (PIDO) tool based tolerance analysis platform is further extended to allow multi-objective, tolerance synthesis in assemblies subject to loading. The process integration, Design of Experiments (DOE) and statistical data analysis capabilities of PIDO tools are combined with highly-efficient UQ methods for optimization of tolerances to maximize assembly yield while minimizing cost. Industry-focused case studies are presented which demonstrate that the application of PCE

based UQ to tolerance analysis and synthesis can significantly reduce computation time while maintaining accuracy.

5.2 Introduction

Statistical tolerance analysis and synthesis based on traditional simulation methods is computationally expensive for complex assemblies requiring numerical modelling, in particular when assembly functionality is subject to the effects of loading. Assembly yield is calculated from statistical moments traditionally estimated using sampling-based Uncertainty Quantification (UQ) methods such as Monte Carlo (MC) simulation. The computational cost can be high due to poor efficiency of sampling-based techniques. Addressing a tolerance synthesis problem based on sampling-based UQ further compounds the computation cost as each trial of assembly tolerances requires a computationally expensive MC based yield estimate. Consequently, tolerance synthesis within complex assemblies is often a computationally impractical problem.

Alternative UQ methods have been proposed with significantly higher computational efficiency than sampling-based methods (Section 2.5). A broadly applicable method is Polynomial Chaos Expansion (PCE) which is based on approximating the response function of a stochastic system with orthogonal polynomial basis functions. Implementing the method requires estimation of the polynomial basis function coefficients, for which several approaches exist. Compared to MC simulation, PCE can offer significantly higher computational efficiency with accurate estimation of statistical moments. As such, PCE offers the potential to increase the practical feasibility of tolerance synthesis in complex assemblies. However, the applicability of PCE is affected by:

- the number of design parameters;
- smoothness of the system response function;
- required moment estimation accuracy;
- choice of estimation method for basis function coefficients; and
- allowable computational time.

This chapter investigates the feasibility of PCE based UQ in tolerance analysis and synthesis. The feasibility is assessed through fundamental analysis and the practical evaluation of tolerance synthesis case study problems. The PIDO tool based tolerance analysis platform developed in Chapter 4 is extended to addresses a multi-objective tolerance synthesis problem in assemblies under loading. The process integration, DOE and statistical data analysis capabilities of PIDO tools are combined with highly-efficient PCE based UQ methods

for optimization of tolerances to maximize assembly yield while minimizing cost. Two industry based tolerance synthesis case study problems involving assemblies under loading are presented. These include:

1. Automotive seating rail assembly consisting of interlocked rail sections separated by a series of rolling elements. Functional characteristics require that rolling resistance of the rail assembly be within an ergonomically desirable range. The rolling resistance depends on the compliance of the rail sections.
2. An automotive rotary switch in which a resistive actuation torque is provided by a spring loaded radial detent acting on the perimeter of the switch body. Functional characteristics require that the resistive switch actuation torque be within an ergonomically desirable range.

5.3 Tolerance synthesis

Manual iteration of tolerance analysis can be slow and ineffective at identifying tolerances which optimally achieve cost and yield targets. Tolerance synthesis can significantly improve the manual iteration process by guiding the search for optimal tolerances with an autonomous optimization algorithm. The aim of tolerance synthesis is to optimally allocate part tolerances in a product assembly in order to maximize assembly yield and minimizing tolerance cost, within design and manufacturing constraints. Tolerance synthesis requires an automated iteration of tolerance analysis: trial tolerances are initially analysed to estimate the resultant assembly yield and cost associated with manufacturing to the specified trial tolerances; a new set of tolerances is subsequently selected which aims to achieve improved yield and cost performance in a successive tolerance analysis iteration. The process is repeated until desired performance is achieved. Tolerance synthesis requires the application of a number of analysis and simulation techniques, including: optimization algorithms (Section 2.6.1); tolerance modelling methods (Section 2.4); UQ methods (Section 2.8) and tolerance cost estimation approaches (Section 2.2.3.1).

A number of tolerance synthesis methods have been proposed with a range of different analysis techniques (Section 2.6) (Edel 1964; Spotts 1973; Michael 1981; Chase 1988; Wu 1988; Chase *et al.* 1990; Zhang *et al.* 1993; Skowronski *et al.* 1997; Jeang 1999; Cho *et al.* 2000; Choi *et al.* 2000; Hong *et al.* 2002; Ye *et al.* 2003; Shah *et al.* 2007).

A review of proposed tolerance synthesis methods has however revealed that, the limitations of existing tolerance analysis methods in the inability to comprehensively accommodate the effects of assembly loads (as previously identified in Chapter 4) also exist

in the tolerance synthesis domain. Since tolerance synthesis is an automated iterative extension of tolerance analysis, the common limitations are to be expected.

By extending the tolerance analysis platform developed in Chapter 4 to incorporate optimization and cost-tolerance modelling, it is possible to facilitate tolerance synthesis of assemblies subject to loads within the native modelling environment of CAD/E modelling tools. Such an extended PIDO tolerance synthesis platform is presented in Section 5.4.

However, a significant obstacle to developing practical tolerance synthesis methods, is the impractically high computational cost associated with traditionally applied MC based UQ methods, in combination with computationally expensive assembly tolerance models (Section 2.6). Research efforts have focused on reducing the overall computational cost, by decreasing the solution time of the associated tolerance model with simplifying assumptions (Hong *et al.* 2002; Singh *et al.* 2009). The introduced assumptions can however limit model fidelity and solution accuracy. However, alternative UQ methods with significantly higher computational efficiency than sampling based methods have recently seen extensive development (Section 2.5.3). Investigation of the utility of these methods in tolerance analysis and synthesis has however been limited. A particularly efficient and attractive analytical UQ method is Polynomial Chaos Expansion (PCE) however its effectiveness in tolerance analysis and synthesis is unknown. This opportunity to significantly reduce the cost of UQ in tolerance analysis, and thereby increase the practical feasibility of tolerance synthesis in complex mechanical assemblies, is investigated in Section 5.7 and utilised in the developed PIDO tolerance synthesis platform.

5.4 PIDO based tolerance synthesis

A PIDO tool based tolerance synthesis platform is presented in Figure 5.1. Tolerance synthesis of assemblies subject to loading is enabled by an extension of the PIDO based tolerance analysis platform developed in Chapter 4 (Section 4.4). The tolerance synthesis platform implemented procedurally with the stages defined below (additional detailed discussion is presented in the following sections):

1. A tentative set of trial tolerances is initially selected and applied to an assembly model for tolerance analysis.
2. UQ techniques estimate the statistical moments of assembly KPCs by evaluating the response of a number of assembly models sampled from the design space defined by the trial part tolerances.

3. The assembly response function is implicitly defined using a CAD and CAE based parametric model. For non-trivial assemblies (particularly assemblies under loading) the assembly response is typically too difficult to define explicitly using an analytical model.
4. The assembly yield associated with the trial tolerance set is estimated from the statistical moments of assembly KPCs. The associated tolerance cost is estimated using cost-tolerance curves.
5. An optimization algorithm guides the search for a set of tolerances which offer superior performance in achieving both the objectives of maximising yield and minimising tolerance cost. The estimated assembly yield and tolerance cost are compared to targets. If yield targets are not achieved, a set of tolerances with increase precision is selected.
6. The competing objectives of maximizing yield and minimizing tolerance cost result in a Pareto set of non-dominated designs rather than in a single optimum solution (Deb 2004). The non-dominated set offers equivalently optimal performance, as superior performance for one objective (yield) results in compromise for the other objective (cost). The search can be terminated when an allowable computational time is reached, or when the optimization problem has converged (when diversity in the objectives space becomes rare with subsequent iterations). It is up to the designer to choose the preferred set, which either favours one objective or offers a balance of both.

The tolerance synthesis platform developed in this work provides a comprehensive approach to the tolerance synthesis problem by enabling:

- Tolerance analysis of assemblies under loading.
- Multi-objective optimization of both yield and tolerance cost.
- Large computational cost reduction in UQ enabled by Polynomial Chaos Expansion.
- Application of robust DOE and optimization methods.

The elements unique to this research will be described in greater detail in the following sections.

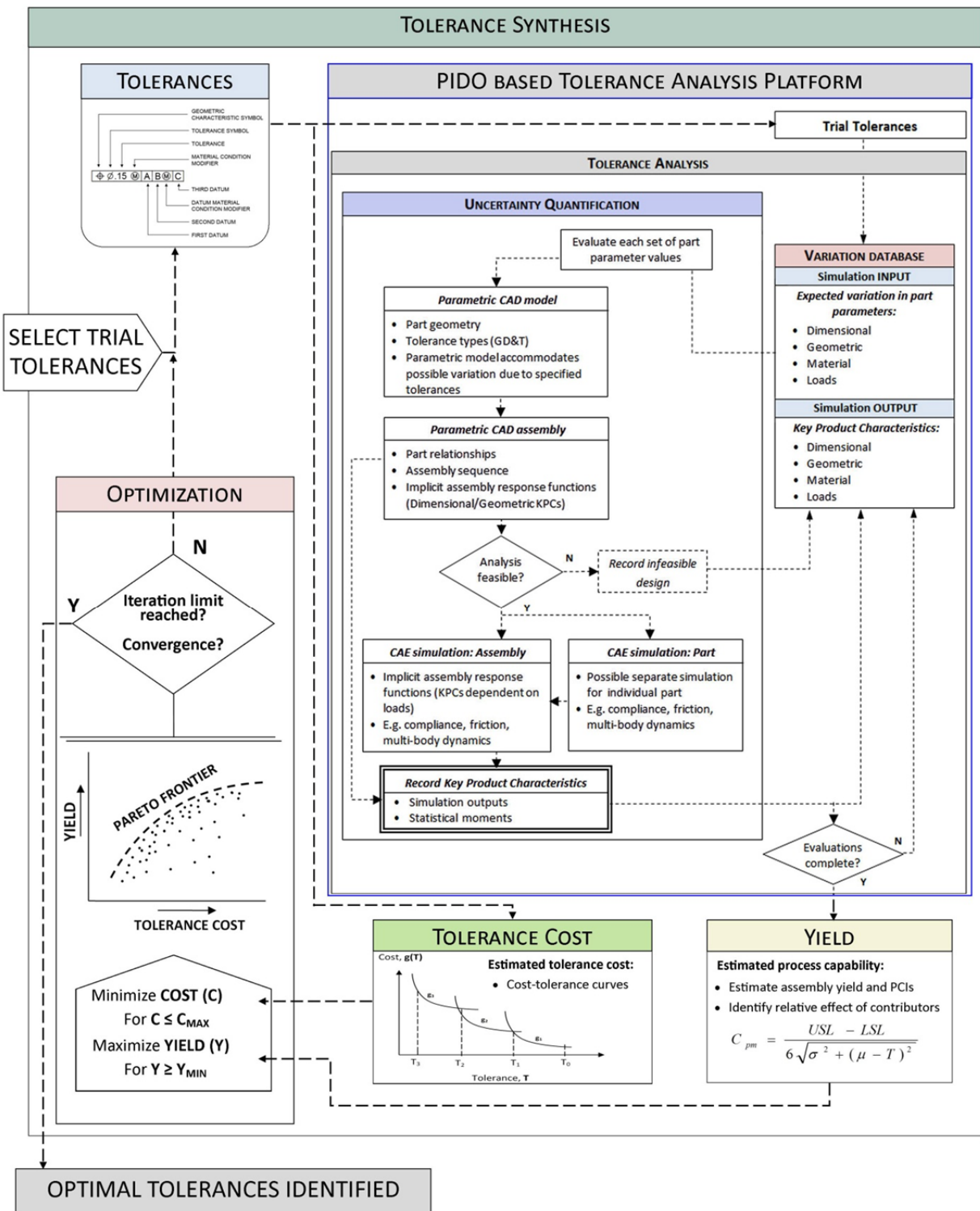


Figure 5.1 - PIDO based tolerance synthesis platform. Extension of the PIDO based tolerance analysis platform presented in Section 4.4. (Figure 4.2).

5.5 Quantification of quality and cost

Quality is defined by the degree to which a manufactured product achieves target values for parameters of particular importance to functionality and performance (Section 2.2.2). The parameters of particular importance are defined as KPCs (Section 3.2.4).

The costs associated with the quality of a product are generally attributable to quality control and quality loss (i.e. a failure to control quality) (Section 2.2.2) (Phadke 1989; Taguchi 1989; Feigenbaum 2012). In this work, the costs of controlling quality are attributed to the cost of manufacturing to specified tolerances, and can be modelled using cost-tolerance functions (Section 5.5.1). Similarly, the costs of failure to control quality can be attributed to the number of manufactured assemblies out of specification (for yield less than 100%) which can be represented by quality loss functions and process capability indices (Section 5.5.2). Achieving a balance between the costs associated with quality control and quality loss promotes manufacturing efficiency (Juran 1992).

5.5.1 Cost-tolerance modelling

Reducing manufacturing variation typically increases manufacturing costs due to demands for higher precision machinery, increased number of manufacturing steps, and stricter process control (Feigenbaum 2012). Various cost-tolerance functions have been proposed for representing the manufacturing cost to tolerance relationship for a range of manufacturing processes (Section 2.2.3.1). The exponential function (Equation (5.5)) and Figure 5.2 (i)) is especially useful due to its applicability to a range of scenarios and will be applied in this work (Wu *et al.* 1988; Chase *et al.* 1990; Dong *et al.* 1990). The exponential function represents the tolerance cost, $g(T)$, for a specific tolerance T , as:

$$g(T) = Ze^{-\phi(T-T_0)} + g_0 \quad \text{Where } T_{min} \leq T \leq T_{max} \quad (5.5)$$

Where:

- T_{min} and T_{max} define an economically feasible tolerance range.
- g_0 and T_0 define minimum threshold cost and tolerances, respectively.
- Z and ϕ are curve fitting parameters derived from experimental data.
- Costs are specified in cost units.

The total tolerance cost of an assembly is the sum of the tolerance cost of each manufacturing process (V) associated with individual constituent components (W) (Figure 5.2 (ii)).

$$G(T) = \sum_{i=1}^W \sum_{j=1}^V g(T_{ij}) \quad \text{Where } V \text{ is the number of manufacturing processes for } W \text{ parts} \quad (5.6)$$

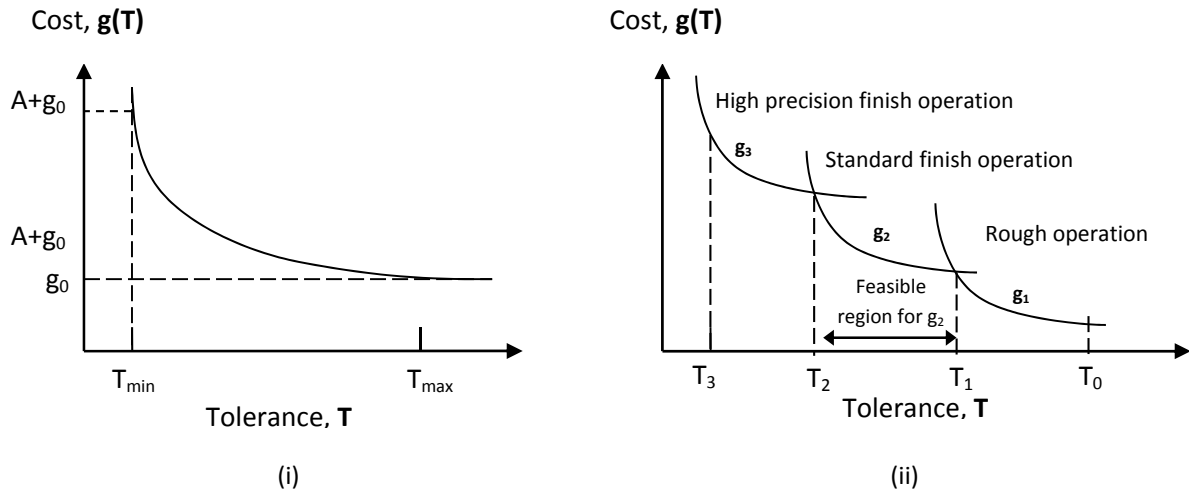


Figure 5.2 - (i) Exponential cost-tolerance relationship, (ii) Chain of cost-tolerance curves for multiple manufacturing processes of varying precision ($V=3$).

5.5.2 Quality loss and process capability

The cost associated with a failure to control product quality can be represented by a quality loss function (QLF) (Taguchi 1989; Cho *et al.* 1997) (Section 2.2.3.2 and Equation A.56).

$$QLF = \kappa[\sigma^2 + (\mu - T)^2] \quad \text{Where } \mu \text{ and } \sigma^2 \text{ are the mean and variance, respectively,} \quad (A.56)$$

of a KPC with target τ . κ is a weighting constant.

The quality loss function increases with any deviation of the relevant KPC from its target value (representing an associated cost). Both the variance and an offset of the mean from the target value contribute to a loss in quality. The QLF has been successfully applied in a number of tolerance synthesis problems (Jeang 1999; Cho *et al.* 2000; Choi *et al.* 2000; Feng *et al.* 2001).

Similar metrics to the QLF are Process Capability Indices (PCI) which measure the consistency and accuracy of manufacturing process outputs (Section 2.3.4). PCIs compare the manufacturing process distribution to the specification limits and nominal target values. Several PCI have been proposed, however a particularly useful index is C_{pm} (Equation A.59) which measures the ability of a process to achieve a target nominal, τ , and the specification limits:

$$C_{pm} = \frac{USL - LSL}{6\sqrt{\sigma^2 + (\mu - \tau)^2}} \quad (A.59)$$

The C_{pm} index was developed to capture a similar intent as the quality loss function while quantifying loss in terms of the intended specification limits. C_{pm} compares the specification limits to the 6σ limits of the manufacturing process distribution, i.e. 99.73% of the predicted

population (which results in C_{pm} of unity). A higher process index indicates higher quality (Feng *et al.* 1997; Feng *et al.* 1999).

C_{pm} is an efficient way of measuring quality loss using a dimensionless metric while giving a direct indication of the expected yield. C_{pm} will be applied as a metric of quality loss in this work.

5.6 Yield estimation by uncertainty quantification

An estimate of assembly yield requires that the statistical moments of distributions of the assembly KPCs be known. These can be estimated by Uncertainty Quantification (UQ) methods. Uncertainty quantification is the process of determining the effects of stochastic input uncertainties on the probabilistic response of a system. The probabilistic systems response is characterized by its probability density function (distribution) defined by four statistical moments: the mean (μ), standard deviation (σ), skewness (γ) and kurtosis (β). A number of UQ methods have been demonstrated in literature and can be classified as either sampling based or analytical (Nigam SD 1995; Lee SH 2009). These alternative UQ methods have been discussed in Section 2.8.

The application of specific UQ methods depends on the intent and constraints of the problem under consideration, including:

- Complexity of implementation (simulation based methods for instance are typically trivial to implement in contrast to difficult to implement analytical methods such as PCE);
- Computational cost and available computational budget;
- Statistical moments of importance (typically in robust design problems such as tolerance analysis, mean and standard deviation are of greater interest than higher order moments.);
- Required statistical moment estimation accuracy (for low precision tolerances, higher moment estimation error may be acceptable);
- Input variable distribution (some UQ methods may not be compatible with non-normal input parameter distributions);
- The model type to be accommodated; where the system response function of the model is either available analytically (explicit) or defined in a numerical model (implicit).

5.6.1 Sampling based UQ methods

Sampling based methods are robust and easily implemented. The most common and robust sampling based UQ method is Monte Carlo (MC) simulation (Section 2.5.1.1). MC simulation is based on estimating the probabilistic system response by aggregating the system outputs for a set of input variables randomly sampled from their specific probability distributions. MC simulation statistical moment estimates converge to the ideal result proportionally at a rate of $O(N^{-0.5})$ where N is the number of simulations. As MC convergence is independent of the problem dimensionality, smoothness of the response function, and type of probability distribution (Kuo FY 2005). MC simulation typically provides a performance baseline for assessment of other UQ methods.

Another sampling based UQ method is Latin Hypercube (LHC) simulation (Section 2.5.1.2). In contrast to MC simulations, LHC uses a constrained sampling approach aimed at avoiding sample clustering and ensures relatively uniform distribution over the probability density function range (McKay MD 1979; Keramat *et al.* 1997). However, the constrained sampling can introduce unintended correlations among input variables and high order moments and output probability distribution estimates may not be accurate.

Sampling methods typically show slow convergence and can be prohibitively computationally expensive when each model evaluation involves lengthy numerical simulations (Huntington *et al.* 1998).

5.6.2 Analytical UQ methods

Sampling based methods such as MC have the advantage of being able to accommodate a broad range of UQ problems as they are not founded on any simplifying assumptions. However, this may also be a disadvantage as efficiency gains can be achieved if valid UQ problem simplifications are possible due to, for instance, input parameters with a single distribution type or smooth response functions. Analytical UQ methods utilize the extra simplifying information available in such UQ problems to significantly improve convergence efficiency.

Detailed comparisons of various analytical UQ methods have been presented in the literature (Haldar *et al.* 2000; Wojtkiewicz *et al.* 2001; Eldred *et al.* 2008; Eldred *et al.* 2009; Lee *et al.* 2009). Based on the outcomes of these comparative studies, Polynomial Chaos Expansion (PCE) is considered to offer the most potential for application in tolerance analysis and synthesis problems due to:

- Non-intrusive nature applicable to integration with existing CAD, CAE and PIDO tools;

- High efficiency and accuracy;
- Flexibility in accommodating various input parameter distributions;
- Ability to accommodate high dimensionality problems;
- Current high interest in the research community resulting in continual performance improvements of PCE methods.

In this research, the PCE method is integrated into a PIDO based tolerance synthesis platform, compared with the Monte Carlo method commonly applied in tolerance analysis, and evaluated on a practical case study. This is achieved by:

- A theoretical analysis of the PCE method identifying working principles, implementation requirements, advantages and limitations (Section 5.7 to 5.7.5).
- Establishing of recommendations for PCE implementation in tolerance analysis including methods of PCE coefficient calculation and approach to error estimation (Section 5.7.6 and 5.7.7)
- Novel implementation in PIDO based tolerance synthesis platform (Section 4.4 and Section 5.4)
- Evaluation on practical tolerance synthesis case studies and validation against reference MC results (Section 5.8 and 5.9).

5.7 Polynomial Chaos Expansion (PCE)

Polynomial Chaos Expansion (PCE) is a method of estimating how input uncertainties in a stochastic system manifest in its outputs, through representation of the system response function using orthogonal polynomial expansions in stochastic variables (*chaos* denotes the associated concept of uncertainty). The historical formulation of stochastic expansion UQ methods such as PCE, is founded on the utilization of mathematical concepts such as weak convergence, orthogonality and projection which are also fundamental to the development of deterministic finite element analysis methods (Ghanem *et al.* 2003).

The orthogonal polynomials of PCE are based on a Weiner-Askey polynomial scheme, which includes various types of orthogonal polynomials bases that are specifically matched to particular probability distributions of the stochastic variables (Weiner 1938; Xiu *et al.* 2003). A basis is a set of functions whose combination can be used to represent all function in a given function space. For example, every quadratic polynomial $ax^2 + bx + c$ can be represented as a linear combination of the basis functions 1, x and x^2 .

For stochastic variables with a normal distribution (as common in tolerancing and quality control fields – Section 2.3.3) the orthogonal polynomial basis is formed by the Hermite

polynomials (Schoutens 2000). The associated density function is the standard normal (Gaussian) distribution. Weighting functions are applied to the polynomial series basis that are probability density functions describing the stochastic input variables. Other distribution types can be accommodated with different weighting function and corresponding orthogonal polynomial bases (Xiu *et al.* 2003). The series is theoretically infinite, however it is truncated in practice. The highest degree of non-truncated polynomial denotes the order of the expansion. The coefficients of the polynomial series may be determined with a number of techniques (Section 5.7.5) and once known, the desired statistical moments of the systems outputs can be rapidly obtained.

The PCE method offers the potential to be significantly more efficient than sampling based UQ methods such as MC or LHC simulation, and can show exponential convergence of $O(e^{-N})$ of the error in estimating the mean and standard deviation. Furthermore the method can be applied in a non-intrusive manner to problems where the system response function is implicitly defined.

However, despite the fact that the convergence of the MC method is independent of the number of parameters of the function under evaluation, the computational cost of PCE methods is dependent on problem dimensionality, smoothness of the system response function, polynomial order, and the polynomial coefficients calculation method; these issue will be considered in the following sections.

5.7.1 Unidimensional Polynomial Chaos Expansion – Derivation of moment expressions

For a stochastic variable x , with a standard normal distribution, the associated probability density function $w(x)$ can be written as (5.7):

$$w(x) = \frac{e^{-\frac{(x-\mu)^2}{2\sigma^2}}}{\sqrt{2\pi\sigma^2}} = \frac{e^{-\frac{x^2}{2}}}{\sqrt{2\pi}} \quad \text{Where for a standard normal distribution } \mu = 0 \text{ and } \sigma^2 = 1 \quad (5.7)$$

The n^{th} statistical raw moment $\langle y^n \rangle$ (i.e. moment about zero) of a real-valued continuous function $f(x)$, is:

$$\langle y^n \rangle = \int (f(x))^n w(x) dx \quad (5.8)$$

The first statistical moment (mean, μ) of a system response function $f(x)$ is therefore:

$$\mu = \langle y^1 \rangle = E[f(x)] = \int f(x)w(x) dx \quad \text{Where } E[f(x)] \text{ is the expected value or population mean} \quad (5.9)$$

(integral of all possible values of a random variable, or any given function of it, multiplied by the respective probabilities of the values of the variable)

Similarly, the second statistical moment (variance):

$$\langle y^2 \rangle = \int f^2(x)w(x) dx \quad (5.10)$$

The standard deviation can be expressed as:

$$\begin{aligned} \sigma &= \sqrt{E[(f(x) - E[f(x)])^2]} = \sqrt{E[f(x)^2] - 2E[f(x)]E[f(x)] + (E[f(x)])^2} \\ &= \sqrt{E[f(x)^2] - (E[f(x)])^2} \quad \text{From the linearity of expected values.} \\ \sigma &= \sqrt{\langle y^2 \rangle - \mu^2} = \sqrt{\int f(x)^2 w(x) dx - \mu^2} \end{aligned} \quad (5.11)$$

The statistical moments can be determined analytically through direct integration if $f(x)$ is known and not prohibitively complex. However, when the system response function is complex, dependent on many variables, or not explicitly defined, an analytical integration is not possible. The statistical moments can however be determined through PCE.

Initially, the response function $f(x)$ is represented with a finite linear combination (5.12) of a subset P of polynomial basis functions $p_i(x)$ (5.13), i.e.:

$$f(x) \equiv \sum_{i=0}^k \alpha_i p_i(x) \quad \text{Where } \alpha_i \text{ are the polynomial basis coefficients} \\ \text{and } k \text{ is the maximum order of the polynomial} \quad (5.12)$$

$$P = \{p_0(x), p_1(x), \dots, p_k(x), \dots\} \quad \text{Where } p_i(x) \text{ is a polynomial of degree } i = (0,1,2 \dots k) \\ \text{up to a maximum order } k \quad (5.13)$$

Substituting (5.12) into (5.8) and expanding the polynomial series, the n^{th} statistical raw moment $\langle y^n \rangle$ of the response function $f(x)$ can therefore be expressed as:

$$\langle y^n \rangle = \int \left(\sum_{i=0}^k \alpha_i p_i(x) \right)^n w(x) dx = \int (\alpha_0 p_0(x) + \alpha_1 p_1(x) + \alpha_2 p_2(x) + \dots + \alpha_k p_k(x))^n w(x) dx \quad (5.14)$$

The moment expression of (5.14) can be simplified by utilizing the unique and useful properties of orthogonal functions. For instance, for $w(x)$ being normal (Gaussian), there exists a unique family of orthogonal polynomials called the Hermite polynomials ($H_k(x)$), which have the following property for the inner product, in the vector space of real functions:

$$\langle p_i(x), p_j(x) \rangle_w \equiv \int p_i(x)p_j(x)w(x) dx = 0 \quad \text{When } i \neq j \quad (5.15)$$

The Hermite polynomial series $H_k(x)$, is described by:

$$H_{k+1}(x) = xH_k(x) - kH_{k-1}(x) \quad \text{Where } H_0(x) = 1 \quad (5.16)$$

Expanding the recursive formula of (5.16), the first ten Hermite polynomials can be written as:

$$\begin{aligned}
H_0(x) &= 1 \\
H_1(x) &= x \\
H_2(x) &= x^2 - 1 \\
H_3(x) &= x^3 - 3x \\
H_4(x) &= x^4 - 6x^2 + 3 \\
H_5(x) &= x^5 - 10x^3 + 15x \\
H_6(x) &= x^6 - 15x^4 + 45x^2 - 15 \\
H_7(x) &= x^7 - 21x^5 + 105x^3 - 105x \\
H_8(x) &= x^8 - 28x^6 + 210x^4 - 420x^2 + 105 \\
H_9(x) &= x^9 - 36x^7 + 378x^5 - 1260x^3 + 945x \\
H_{10}(x) &= x^{10} - 45x^8 + 630x^6 - 3150x^4 + 4720x^2 - 945
\end{aligned} \tag{5.17}$$

Combining the property of (5.15) with the multinomial expansion of the moment expression in (5.14), the following simplification is possible:

$$\langle y^n \rangle = \int \sum_{\substack{i_1=0\dots k \\ i_2=0\dots k \\ \dots \\ i_n=0\dots k}} \alpha_{i_1} \alpha_{i_2} \dots \alpha_{i_n} p_{i_1}(x) p_{i_2}(x) \dots p_{i_n}(x) w(x) dx \tag{5.18}$$

$$= \sum_{\substack{i_1=0\dots k \\ i_2=0\dots k \\ \dots \\ i_n=0\dots k}} \alpha_{i_1} \alpha_{i_2} \dots \alpha_{i_n} \int p_{i_1}(x) p_{i_2}(x) \dots p_{i_n}(x) w(x) dx \quad \text{Due to (5.15)} \tag{5.19}$$

$$= \sum_{i=0}^k \alpha_i^n \int p_i^n(x) w(x) dx \tag{5.20}$$

From (5.20) it is now possible to explicitly define expressions for the statistical moments of $f(x)$, in terms of the polynomial basis coefficients α_i , if $w(x)$ is orthogonal to the polynomial basis $p_i(x)$ (e.g. for $w(x)$ being Gaussian, $p_i(x)$ is given by the Hermite polynomials $H_i(x)$).

The first statistical raw moment (mean) can be expressed as:

$$\mu = \langle y^1 \rangle = \sum_{i=0}^k \alpha_i \int p_i(x) w(x) dx = \alpha_0 \quad \text{As } p_0(x) = H_0(x) = 1 \text{ and } \int p_i(x) w(x) dx = 0 \text{ for every } i > 0 \text{ due to orthogonality} \tag{5.21}$$

Likewise the second statistical raw moment is:

$$\langle y^2 \rangle = \sum_{i=0}^k \alpha_i^2 \int p_i^2(x) w(x) dx \tag{5.22}$$

Also, following from the inner product of two equal functions:

$$\begin{aligned}\langle p_i(x), p_i(x) \rangle_w &= \int p_i(x)p_i(x)w(x) dx \\ &= \int p_i^2(x)w(x) dx \equiv \|p_i(x)\|^2 \quad \text{Where } \|p_i(x)\|^2 \text{ is the norm squared}\end{aligned} \quad (5.23)$$

Therefore:

$$\langle y^2 \rangle = \sum_{i=0}^k \alpha_i^2 \int p_i^2(x)w(x) dx = \sum_{i=0}^k \alpha_i^2 \|p_i(x)\|^2 \quad (5.24)$$

Substituting (5.24) and (5.21) into (5.11), the standard deviation can now be expressed as:

$$\sigma = \sqrt{\langle y^2 \rangle - \mu^2} = \sqrt{\sum_{i=0}^k \alpha_i^2 \|p_i(x)\|^2 - \alpha_0^2} = \sqrt{\sum_{i=1}^k \alpha_i^2 \|p_i(x)\|^2} \quad (5.25)$$

For the Gaussian case, the equation in (5.25) can be further simplified by again utilizing the orthogonality of the Hermite polynomials and noting the following property:

$$\int H_k^2(x)e^{-\frac{x^2}{2}} dx = \sqrt{2\pi}k! \quad (5.26)$$

Consequently, with $w(x)$ being Gaussian (5.7), the norm squared of the Hermite polynomials equates to:

$$\|H_k(x)\|_w^2 = \langle H_k(x), H_k(x) \rangle_w = \int H_k^2(x)w(x) dx = \frac{1}{\sqrt{2\pi}} \int H_k^2(x)e^{-\frac{x^2}{2}} dx = k! \quad (5.27)$$

Substituting (5.27) into (5.25),

The standard deviation can be expressed as:

$$\sigma = \sqrt{\sum_{i=1}^k \alpha_i^2 k_i!} \quad \text{Where } k_i \text{ is the highest order of the polynomial corresponding to each } \alpha_i \quad (5.28)$$

From (5.21) and (5.28) it is possible to determine the mean and standard deviation if the polynomial basis coefficients α_i are known.

For example, by substituting (5.17) into (5.12), with Gaussian input variables and Hermite basis polynomials, the polynomial chaos expansion for a unidimensional, fifth-order case ($d = 1, k = 5$) can be written as:

$$\begin{aligned}f(x) &= \alpha_0 H_0 + \alpha_1 H_1(x) + \alpha_2 H_2(x) + \alpha_3 H_3(x) + \alpha_4 H_4(x) + \alpha_5 H_5(x) \\ &= \alpha_0 + \alpha_1 x_1 + \alpha_2 (x_1^2 - 1) + \alpha_3 (x^3 - 3x) + \alpha_4 (x^4 - 6x^3 + 3) + \alpha_5 (x^5 - 10x^3 + 15x)\end{aligned} \quad (5.29)$$

From (5.21), the mean can then be expressed as $\mu = \alpha_0$. Similarly from (5.28) the standard deviation is given by $= \sqrt{\alpha_1 1! + \alpha_2 2! + \alpha_3 3! + \alpha_4 4! + \alpha_5 5!}$.

Methods for calculating the polynomial coefficients (α_i) are discussed in section 5.7.5.

5.7.2 Multidimensional PCE

When considering a multidimensional UQ problem, it is possible to represent the system response using a multidimensional polynomial chaos expansion:

$$f(x_1, x_2, x_3, \dots) = \alpha_0 p_0 + \sum_{i_1=1}^{\infty} \alpha_{i_1} p_1(x_{i_1}) + \sum_{i_1=1}^{\infty} \sum_{i_2=1}^{i_1} \alpha_{i_1 i_2} p_2(x_{i_1}, x_{i_2}) \quad (5.30)$$

$$+ \sum_{i_1=1}^{\infty} \sum_{i_2=1}^{i_1} \sum_{i_3=1}^{i_2} \alpha_{i_1 i_2 i_3} p_3(x_{i_1}, x_{i_2}, x_{i_3}) + \dots,$$

As in the unidimensional case, the multidimensional expansion is truncated in practice at a finite order k and is applied to finite dimension d , i.e:

$$f(x_1, x_2, x_3, \dots, x_d) = \alpha_0 p_0 + \sum_{i_1=1}^k \alpha_{i_1} p_1(x_{i_1}) + \sum_{i_1=1}^k \sum_{i_2=1}^{i_1} \alpha_{i_1 i_2} p_2(x_{i_1}, x_{i_2}) \quad (5.31)$$

$$+ \sum_{i_1=1}^k \sum_{i_2=1}^{i_1} \sum_{i_3=1}^{i_2} \alpha_{i_1 i_2 i_3} p_3(x_{i_1}, x_{i_2}, x_{i_3})$$

$$+ \dots + \sum_{i_1=1}^k \sum_{i_2=1}^{i_1} \sum_{i_3=1}^{i_2} \dots \sum_{i_d=1}^{i_{d-1}} \alpha_{i_1 i_2 i_3 \dots i_d} p_d(x_1, x_2, x_3, \dots, x_d)$$

The total number of terms in a finite multidimensional polynomial chaos expansion is:

$$N \geq \frac{(k+d)!}{k! d!} \quad \text{Where } N \text{ is the number of terms in the PCE} \quad (5.32)$$

Following the same procedure as for the unidimensional case, leads to expressions for the first and second order moments. Again due to the orthogonality of the polynomial basis, the integral of all basis functions is zero except for the first constant term.

Hence the mean for the multidimensional PCE case is again given by (5.21).

The expression for the standard deviation for the multidimensional case becomes:

$$\sigma = \sqrt{\langle y^2 \rangle - \mu^2} = \sqrt{\sum_{i=0}^k \alpha_i^2 \|p_i(x_1, x_2, x_3, \dots, x_d)\|^2} - \alpha_0^2 = \sqrt{\sum_{i=1}^k \alpha_i^2 \|p_i(x_1, x_2, x_3, \dots, x_d)\|^2} \quad (5.33)$$

Again, with Hermite polynomials H_k as the basis p_i , and by utilizing the orthogonality of the Hermite polynomials and noting the property of (5.27),

The standard deviation for the multidimensional case can be expressed as:

$$\sigma = \sqrt{\sum_{i_1=1}^k \alpha_{i_1}^2 k_{i_1}! + \sum_{i_1=1}^k \sum_{i_2=1}^{i_1} \alpha_{i_1 i_2}^2 k_{i_1 i_2}! + \sum_{i_1=1}^k \sum_{i_2=1}^{i_1} \sum_{i_3=1}^{i_2} \alpha_{i_1 i_2 i_3}^2 k_{i_1 i_2 i_3}! + \dots + \sum_{i_1=1}^k \sum_{i_2=1}^{i_1} \sum_{i_3=1}^{i_2} \dots \sum_{i_d=1}^{i_{d-1}} \alpha_{i_1 i_2 i_3 \dots i_d}^2 k_{i_1 i_2 i_3 \dots i_d}!} \quad (5.34)$$

Where $k_{i_1 i_2 i_3 \dots i_k}$ is the highest order of the polynomial corresponding to each $\alpha_{i_1 i_2 i_3 \dots i_k}$

Assuming that the variables are independently distributed, the multidimensional chaos expansion is formed by the product of the unidimensional polynomials corresponding to each stochastic variable.

For example, for a two dimensional, second order case ($d = 2, k = 2$) with Gaussian input variables and Hermite polynomials, the multidimensional polynomials are:

$$\begin{aligned} p_0(x_1, x_2) &= H_0(x_1)H_0(x_2) = 1 \\ p_1(x_1, x_2) &= H_1(x_1)H_0(x_2) = x_1 \\ p_2(x_1, x_2) &= H_0(x_1)H_1(x_2) = x_2 \\ p_3(x_1, x_2) &= H_2(x_1)H_0(x_1) = x_1^2 - 1 \\ p_4(x_1, x_2) &= H_1(x_1)H_1(x_2) = x_1 x_2 \\ p_5(x_1, x_2) &= H_0(x_1)H_2(x_2) = x_2^2 - 1 \end{aligned} \quad (5.35)$$

Substituting (5.35) into (5.30), the multidimensional polynomial chaos expansion can be written as:

$$\begin{aligned} f(x_1, x_2) &= \alpha_0 H_0 + \{\alpha_1 H_1(x_1) + \alpha_2 H_1(x_2)\} + \{\alpha_{11} H_2(x_1, x_1) + \alpha_{12} H_2(x_2, x_1) + \alpha_{22} H_2(x_2, x_2)\} \\ &= \alpha_0 + \alpha_1 x_1 + \alpha_2 x_2 + \alpha_{11}(x_1^2 - 1) + \alpha_{12} x_1 x_2 + \alpha_{22}(x_2^2 - 1) \end{aligned} \quad (5.36)$$

Now, from (5.21), the mean can then be expressed as $\mu = \alpha_0$. Similarly from (5.34) the standard deviation is given by $\sigma = \sqrt{\alpha_1 1! + \alpha_2 1! + \alpha_{11} 2! + \alpha_{12} 1! + \alpha_{22} 2!}$.

5.7.3 Higher order moments

Expressions for higher order moments of skewness and kurtosis may also be derived however the analytical expressions become quite complex (Berveiller *et al.* 2006). As such higher order moments are often estimated by sampling the PCE. In the scope of tolerance analysis and synthesis, the interest in UQ is predominantly on evaluation of the low-order moments. Furthermore it is important to note that PCE methods are only guaranteed to converge to analytically exact values of the first two moments (mean and variance) and estimation of higher order moments may be erroneous (Xiu *et al.* 2003). This limitation is not overly restrictive in the tolerancing and quality fields, as interest is typically on the mean and standard deviation of a product parameter or process.

5.7.4 Non-normal distributions and correlated variables

Variables with non-normal distributions can be accommodated with the generalized Polynomial Chaos Expansion (gPCE) method (Xiu 2003). The formulation of gPCE closely resembles that shown in sections 5.7.1 and 5.7.2, however a different choice of orthogonal polynomial basis and weighting functions is used to accommodate non-normal variables. The gPCE approach uses the Wiener-Askey scheme in which Hermite, Jacobi, Laguerre and Legendre orthogonal basis polynomials are used to accommodate stochastic variables with a range of different distributions (variables of mixed distribution types in the same UQ problem can also be accommodated). Table 5.1 shows the appropriate polynomial basis and weighting function for various parameter distributions. Additional detail is available in the literature (Xiu 2003; Wan *et al.* 2007; Eldred *et al.* 2008).

Table 5.1 - Generalized polynomial chaos expansion (gPCE) basis and weighting functions for various parameter distributions (Xiu *et al.* 2003; Eldred *et al.* 2008)

Distribution	Probability density function	Orthogonal basis polynomials $p(x)$	Weighting function $w(x)$
Normal (Gaussian), Bounded normal, Lognormal, Bounded lognormal, Gumbel, Frechet, Weibull	$\frac{1}{\sqrt{2\pi}} e^{-\frac{x^2}{2}}$	Hermite	$e^{-\frac{x^2}{2}}$
Uniform, Loguniform, Triangular	$1/2$	Legendre	1
Beta	$\frac{(1-x)^\alpha (1+x)^\beta}{2^{\alpha+\beta+1} \left[\frac{\Gamma(\alpha+1)\Gamma(\beta+1)}{\Gamma(\alpha+\beta+2)} \right]}$	Jacobi	$(1-x)^\alpha (1+x)^\beta$
Exponential	e^{-x}	Laguerre	e^{-x}
Gamma	$\frac{x^\alpha e^{-x}}{\Gamma(\alpha+1)}$	Generalized Laguerre	$x^\alpha e^{-x}$

Another approach for accommodating non-normal variables is based on transformation techniques, such as Nataf or Box-Cox, which transform various distributions into standard normal type (Box *et al.* 1964; Armen Der Kiureghian *et al.* 1986; McRae *et al.* 1995). Comparisons between the gPCE and transformation approaches show that gPCE results in higher moment estimation accuracy, whereas the transformation approach is simpler to implement (Choi *et al.* 2004).

If the input variables associated with PCE formulation are correlated, application of the PCE method requires that they are first transformed into independent uncorrelated variables; specific details are given in (Berveiller *et al.* 2006).

For the unidimensional case, with x being Gaussian, the terms $p_k(\xi_n)$ correspond to the Hermite polynomials, i.e. $p_k(\xi_n) = H_k(\xi_n)$ where H_k are given by (5.16) and (5.17). A similar set of equations can be written for the multidimensional case.

As the response function values $f(\xi_n)$ and basis polynomials terms $p_k(\xi_n)$ are known, by solving the system of linear equations of (5.38) the polynomial chaos coefficients can be determined (Hosder *et al.* 2007). PC is essentially a form of regression analysis in that it aims to determine the relationship between a dependent variable (in this case $f(\xi_n)$) and a series of independent variables (here $p_k(\xi_n)$) formulated in an equation in which the independent variables have parametric coefficients (i.e. α_k). The minimum number of collocation points corresponds to the number of terms in the polynomial chaos expansion (5.32) however oversampling is generally recommended and oversampling factors of $s = 2$ have been suggested (Hosder *et al.* 2007; Xiu 2010). Oversampling does not change the number of polynomial coefficients. As such the number of collocation points is given by:

$$N_c \geq \frac{s(k+d)!}{k!d!} \quad \text{Where } s \text{ is an oversampling factor} \quad (5.39)$$

Table 5.2 indicates the number of required sampling points for a given dimensionality and polynomial order.

Table 5.2 - Minimum number of simulations N required for point collocation based PCE with various expansion order k , and dimensionality d . Oversampling ratio $s = 2$ (as recommended in (Hosder *et al.* 2007)).

$N_c = \frac{s(d+k)!}{d!k!}$		d								
		1	2	3	4	5	10	15	20	50
k	1	4	6	8	10	12	22	32	42	102
	2	6	12	20	30	42	132	272	462	2,652
	3	8	20	40	70	112	572	1,632	3,542	46,852
	4	10	30	70	140	252	2,002	7,752	21,252	632,502
	5	12	42	112	252	504	6,006	31,008	106,260	6.96E+06

As oversampling is recommended, for $s > 1$ the resulting system of linear equations of (5.38) becomes overdetermined (i.e. there are more equations than unknowns) and can be solved using the method of least squares.

The method of least squares is based on the selection of polynomial coefficients which minimize the sum of the squares of the difference (Δ) between the expansion of order k and the response f , over an arbitrary set of trial points $\vec{x} = (\xi_1, \xi_2, \dots, \xi_N)$, e.g. for the unidimensional case:

$$\min_{\Delta} = \sum_{j=1}^N \left[f(\xi_j) - \sum_{i=1}^k \alpha_i p_i(\xi_j) \right]^2 \quad \text{where } \vec{x} = (\xi_1, \xi_2, \dots, \xi_N) \text{ are collocation points} \quad (5.40)$$

Various solution procedures for least squares problems have been documented and can be found in existing literature (Lawson *et al.* 1974; Björck 1996). A PCE specific solution to the multidimensional least squares problem is presented in (Berveiller *et al.* 2006).

For highly dimensional problems, the point collocation method requires a large number of model evaluations (Table 5.3). Furthermore, the least squares approach for calculation of the expansion coefficients may have prohibitively high computational costs (Eldred *et al.* 2008). Consequently, for large multidimensional problems, calculation of expansion coefficients based on stochastic projection using sparse grids methods offers superior performance (Section 5.7.5.4).

5.7.5.2 Stochastic projection

These methods are based on projecting the response function f from (5.12) or (5.31) against each basis function p_i using inner products. The orthogonality between the polynomial expansion basis functions and the weighting functions simplifies the determination of the coefficients. This approach is known as Galerkin projection (Xiu 2007). For the unidimensional case:

$$\langle f(x), p(x) \rangle = \left\langle \sum_{i=0}^k \alpha_i p_i(x), p_i(x) \right\rangle = \sum_{i=0}^k \alpha_i \|p_i(x)\|^2 \quad \text{Due to (5.23) and properties of inner products} \quad (5.41)$$

For an individual coefficient, it can be written as:

$$\langle f(x), p_i(x) \rangle = \langle \alpha_i p_i(x), p_i(x) \rangle = \alpha_i \|p_i(x)\|^2 \quad (5.42)$$

Rearranging:

$$\alpha_i = \frac{\langle f(x), p_i(x) \rangle}{\|p_i(x)\|^2} \quad (5.43)$$

As the denominator in (5.43) is the norm squared and can be solved analytically (as per equation (5.27)), determining the polynomial coefficients is now possible by integrating over the bounds of the weighting function $w(x)$ which, for x being Gaussian and $w(x)$ given by (5.7), the support range is $[-\infty, \infty]$:

$$\langle f(x), p_i(x) \rangle = \int_{-\infty}^{\infty} f(x) p_i(x) w(x) dx \quad (5.44)$$

This integration can be carried out numerically using:

- Sampling (Hosder *et al.* 2007)
- Complete product grid numeric quadrature (Xiu 2007)
- Sparse grid based numeric quadrature (Section 5.7.5.4)

Integration through sampling is based on applying techniques such as Monte Carlo (Kalos *et al.* 2009) based integration to equation (5.44). Advantages of this approach include independence of dimensionality, as well as the ability to accommodate integrand functions which are not smooth. However, as the convergence rates of sampling methods are generally slow (section 5.6.1) a large number of samples will be required for low error, limiting the applicability of the approach.

5.7.5.3 Complete product grid quadrature

Numerical quadrature refers to one-dimensional numerical integration rules. The more advanced of these are interpolatory rules which sample the integrand function at an N number of selected points, to construct and integrate a less complex polynomial interpolation function (Atkinson 2009). The polynomial is constructed over a region $[a, b]$ of the integrand $f(x)$, from monomials (powers of x , shown as a set U in (5.45)) with non-negative coefficients (referred to as weights).

$$U = \{1, x, x^2, x^3, \dots, x^N\} \quad (5.45)$$

Representing $f(x)$ by a series of monomials can be achieved by progressively evaluating the function at a number of points x_j . The points are also referred to as abscissa as they are typically represented as points along the horizontal axis of a one-dimension function plot. Evaluating at two points provides the coefficients of the first two monomials (corresponding to linear representation of $f(x)$). Evaluating a third point provides coefficients for three monomials and a quadratic representation of $f(x)$, i.e.:

$$f(x) \approx c_0 + c_1x + c_2x^2 \quad (5.46)$$

Evaluating $f(x)$ at N points (typically equally spaced) forms an approximating polynomial of degree $N - 1$ which can be integrated exactly as follows:

$$\int_a^b f(x) dx \approx Q_l = \int_a^b u(x) dx = \sum_{j=1}^N w_j f(x_j) \quad \text{Where } x_j \text{ are sampling points, and } w_j \text{ are weights} \quad (5.47)$$

Such an interpolatory quadrature rule Q_l (equation (5.47)) is said to have a *precision* ρ if the highest degree monomial which the rule includes is of degree ρ . The relationship between precision ρ and the number of sampling points N , depends on the quadrature rule. The number of points N , in the quadrature rule, is often referred to as the *order*. Rules based on equally spaced integration points, classed as Newton–Cotes formulae, typically have a precision level $\rho = N - 1$ (Delves *et al.* 1988).

Other rules include Gauss quadrature, which use optimal, unequally spaced integration points with specific weights to increase precision. The specific integration point and weight selection depends on the form of the integrand, resulting in a class of differently tailored Gauss quadrature rules; one of which is Gauss-Hermite quadrature applicable to integrals of the form:

$$\int_a^b f(x)w(x) dx = \int_a^b f(x)e^{-x^2} dx \approx Q_l = \sum_{j=1}^{N_l} w_j f(x_j) \quad \text{Where:} \quad (5.48)$$

N is the number of sampling points
w_j are weights
x_j are sampling points

By using specifically weighted interpolating polynomials that are orthogonal to $w(x)$, and integration points that are the roots of the orthogonal polynomials, it is possible for Gauss quadrature rules to achieve a precision level of $\rho = 2N - 1$; that is to exactly integrate all polynomials up to degree $2N - 1$ using only N integration points (for complete derivation see (Kovvali 2011)). Due to $w(x)$ being Gaussian, the polynomials orthogonal to $w(x)$ in (5.48) are the Hermite polynomials (5.17), where the integration rule domain is conventionally taken as $[a, b] = [-\infty, \infty]$. Since (5.48) is of the form of equation (5.44), Gauss-Hermite quadrature can be used effectively in the stochastic projection based method of determining the PCE coefficients (section 5.7.5.2). Integration of functions with non-normally distributed variables, as in a gPCE UQ problem (section 5.7.4), is possible by applying specifically tailored Gauss–Legendre (uniformly distributed variable), Gauss–Jacobi (Beta distributed) or Gauss–Laguerre (exponentially or gamma distributed) quadrature rules (Epperson 2007).

It is possible to extend a unidimensional quadrature rule to a multidimensional integration problem by taking a product of unidimensional quadrature rules for each dimension. This multidimensional *product rule* is formed from a *tensor product* of unidimensional quadrature rules Q_{l_m} , with associated *level* l_m , for variable $m = 1 \dots d$. The level l_m is an index integer variable which designates the unidimensional quadrature rule in the family of possible rules. The multidimensional product rule is defined as:

$$Q_{l_1,1} \otimes \dots \otimes Q_{l_d,d} = \sum_{j_1=1}^{N_{l_1}} \dots \sum_{j_d=1}^{N_{l_d}} w_{l_1,j_1} \dots w_{l_d,j_d} f(x_{l_1,j_1}, \dots, x_{l_d,j_d}) \quad (5.49)$$

The tensor product of (5.49) is effectively a sum over all possible combinations of the terms in the unidimensional quadrature rules. An increase in the level l_m is associated with an increase in the number of integration points and the precision level ρ of the integration rule; the relationship between these variables is detailed in Section 5.7.5.4.

The multidimensional product rule effectively forms a d dimensional product grid of integration points corresponding to all monomial product combination of the d variables. The total number of monomials in a multidimensional product grid is:

$$N_{Complete\ grid}(l, d) = \prod_{m=1}^d N_{l_m} \quad \text{Where } N_{l_m} \text{ is the number of integration points for variables } m = 1 \dots d \text{ corresponding to a level } l \quad (5.50)$$

For an isotropic product grid where $N_l = N_{l_1} = N_{l_2} = \dots = N_{l_m}$ the total number of monomials is:

$$N_{Complete\ grid}(l, d) = N_l^d \quad (5.51)$$

For increasing dimensionality, the required number of monomials for a multidimensional product rule (5.50) can become very large even for a low number of integration points on the individual variables (and a corresponding precision). For example, for $d = 10$ and $N_{l_1} \dots N_{l_{10}} = 3$, the number of monomials is $N_{Complete\ grid} = 59\ 049$. For an isotropic product grid (5.51), the number of required integration points *grows exponentially* with the dimension. As the number of grid points corresponds to the required number of evaluations of the complex function (in this work that being the typically computationally expensive implicit CAE model of the assembly under tolerance analysis), for larger multidimensional problems, complete product grid quadrature becomes very computationally expensive. However, it has been found that not all the monomials in a complete product grid are required, and more efficient multidimensional quadrature techniques are available.

5.7.5.4 Sparse grid quadrature

The precision of a multidimensional quadrature product rule is limited by the *total degree* of the monomials in the product grid, where the total degree is the sum of the powers of the component variables in a monomial (e.g. the total degree of the monomial $x_1^3 x_2^5$ is 8, which is the sum of the component degrees) (Bungartz *et al.* 2004). Achieving a desired precision ρ_m in each dimension m , requires only monomials for which the total degree does not exceed ρ_m (Smolyak 1963). Table 5.3 shows the monomials for a $d = 2$ product rule with excess monomials highlighted (excess monomial do not add to precision). As the dimensionality increases the excess monomials exponentially dominate the product grid.

Table 5.3 - Monomials for $d = 2$ complete product grid with excess monomials highlighted

Monomials ($d = 2, N_1 = N_2 = 6$)	
5	x_2^5 $x_1x_2^5$ $x_1^2x_2^5$ $x_1^3x_2^5$ $x_1^4x_2^5$ $x_1^5x_2^5$
4	x_2^4 $x_1x_2^4$ $x_1^2x_2^4$ $x_1^3x_2^4$ $x_1^4x_2^4$ $x_1^5x_2^4$
3	x_2^3 $x_1x_2^3$ $x_1^2x_2^3$ $x_1^3x_2^3$ $x_1^4x_2^3$ $x_1^5x_2^3$
2	x_2^2 $x_1x_2^2$ $x_1^2x_2^2$ $x_1^3x_2^2$ $x_1^4x_2^2$ $x_1^5x_2^2$
1	x_2 x_1x_2 $x_1^2x_2$ $x_1^3x_2$ $x_1^4x_2$ $x_1^5x_2$
0	1 x_1 x_1^2 x_1^3 x_1^4 x_1^5
Degree	0 1 2 3 4 5

Based on initial work by Smolyak (Smolyak 1963) methods were developed for eliminating most of the excess monomials by combining low-order (unidimensional or multidimensional) complete product grids to form *sparse grids* (SG) for high-order problems, in which the monomial total degree never exceeds a desired precision (Gerstner *et al.* 1998; Gerstner *et al.* 2003).

A sparse grid $A(L, d)$ of level L (for $L \geq 0$) and dimension d is a weighted, linear combination of the tensor product of unidimensional quadrature rules (equation (5.49)). The sparse grid level L is an index variable which designates the sparse grid from the family of possible grids. The combination is performed according to the Smolyak rule, formally defined as (Gerstner *et al.* 1998):

$$A(L, d) = \sum_{L-d+1 \leq |\vec{l}| \leq L} (-1)^{L-|\vec{l}|} \binom{d-1}{L-|\vec{l}|} \cdot (Q_{l_1,1} \otimes \dots \otimes Q_{l_d,d}) \quad (5.52)$$

Where:

L is the sparse grid level

$\vec{l} = (l_1, \dots, l_d)$ is a vector of unidimensional quadrature rule levels l_m in each dimension $m = 1 \dots d$.

$|\vec{l}| = l_1 + \dots + l_d$ is referred to as the product level

With the binomial coefficient operator given by;

$$\binom{d-1}{|\vec{l}|-L} = \frac{(d-1)!}{(|\vec{l}|-L)!(d-1-|\vec{l}|-L)!}$$

The Smolyak sparse grid construction rule (equation (5.52)) effectively combines multiple unidimensional quadrature rules into a single quadrature rule. The resultant integration points are the set of integration points corresponding to the unidimensional rules. The resultant weights are the unidimensional rule weights multiplied by a coefficient. The condition of the summation in (5.52), referred to as the *selection criterion*, means that the summation is only applied to the terms for which the $|\vec{l}|$ values conform to the inequality. Effectively only the product rules ($Q_{l_1,1} \otimes \dots \otimes Q_{l_d,d}$ as defined in equation (5.49)) are combined whose product levels lie between $L - d + 1$ and L . The terms which are

multiplied with the tensor product in equation (5.49) are referred to as the *combining coefficient* as they determine how the tensor product rules are combined together when forming the sparse grid. The Smolyak combination rule allows each dimension to be treated independently without requiring that the unidimensional quadrature rules (Q_{l_d}) have the same domain or weight function.

The number of points in the sparse grid depends on the sparse grid level L , the unidimensional quadrature rule level l_m , the quadrature rule used, and its associated *growth rule*, O . The growth rule relates the unidimensional quadrature rule level l_m , to the number of sampling points N (often referred to as the order) in the quadrature rule. The type of quadrature rule used typically depends on the distribution type of the stochastic variable under consideration. Different distribution types have preferred quadrature rules (e.g. Gauss-Hermite quadrature is an effective rule for functions with normally distributed variables.) Depending on the quadrature rule used, a number of associated growth rules can be employed which offer a different balance between the number of points (order) and the precision ρ (highest degree polynomial which can be approximated with a given number of sampling points). The rules are classified according to:

- How the number of points increases with the level.
- Whether the sampling points include the interval bounds ($[a, b]$ in equation (5.47)) of the underlying unidimensional quadrature rules which make up the grid. The terms *open* and *closed* designate the exclusion and inclusion, respectively, of points at the bounds.
- Degree of nesting (the number of sampling points from lower level grids which are re-used at higher levels to reduce the total number of unique sampling points).

A common, open, non-linear growth rule with weak nesting (where only the centre point of the quadrature rule is reused in higher levels) for Gauss-Hermite quadrature is $O = 2^{l+1} - 1$. Further details concerning growth rules are provided in specialised literature (Burkardt 2010).

An example of a level 2 sparse grid in 2 dimensions, based on Gauss-Hermite quadrature with a growth rule of $O = 2^{l+1} - 1$, is shown in Figure 5.3. The construction of the sparse grid is based on the Smolyak rule, which for $L = 2, d = 2$ gives:

$$\begin{aligned}
 A(2,2) &= \sum_{2-2+1 \leq |\vec{l}| \leq 2} (-1)^{2-|\vec{l}|} \binom{2-1}{2-|\vec{l}|} \cdot (Q_{l_1,1} \otimes Q_{l_2,2}) \\
 &= 1 \cdot 1(Q_{2,1} \otimes Q_{0,2}) + 1 \cdot 1(Q_{1,1} \otimes Q_{1,2}) + 1 \cdot 1(Q_{0,1} \otimes Q_{2,2}) - 1 \cdot 1(Q_{1,1} \otimes Q_{0,2}) - 1 \cdot 1(Q_{0,1} \otimes Q_{1,2})
 \end{aligned} \tag{5.53}$$

The number of required integration points is reduced from 49 for the full product grid (as given by equation (5.51)), to 17 for the sparse grid, while offering the same precision.

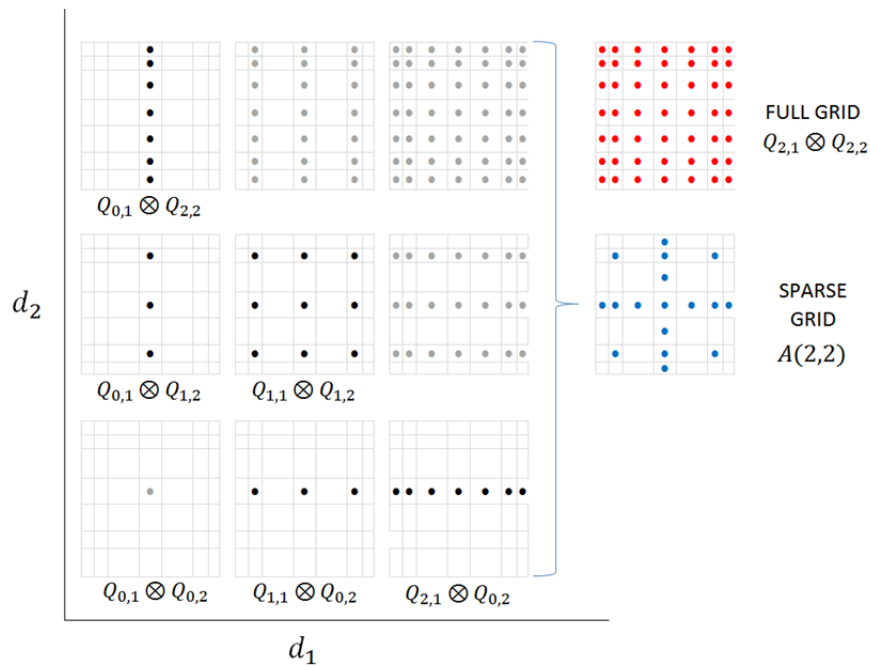


Figure 5.3 - Multidimensional full product and sparse grid Gauss-Hermite Quadrature with level 2 for 2 dimensions and $O = 2^{l+1} - 1$ growth rule.

The size difference between sparse and complete product grids becomes greater with increased dimensionality. Determining the number of points in a sparse grid can be difficult as the associated procedure varies depending on the growth rule, and its level of nesting. Specialised literature on the topic provides further details (Burkardt 2010). To demonstrate one example however, the number of points on an isotropic sparse grid based on Gauss-Hermite quadrature with a $O = 2^{l+1} - 1$ growth rule is given by:

$$N_{sparse\ grid}(l, d) = \sum_{i=0}^l \binom{i+d-1}{d-1} \cdot 2^i \quad (5.54)$$

Table 5.1 demonstrates the significant difference in size between sparse and full product grids for Gauss-Hermite quadrature for higher dimensions and grid levels.

Table 5.4 - Number of points required for isotropic sparse grids and full product grids based on Gauss-Hermite quadrature rules with growth rule $O = 2^{l+1} - 1$, for multiple dimensions and grid levels. Precision indicates the maximum polynomial degree which can be exactly represented by the associated quadrature.

Level L	Precision $\rho = 2O - 1$	Sparse grid							Complete grid						
		d							d						
		1	2	3	4	5	10	20	1	2	3	4	5	10	20
0	1	1	1	1	1	1	1	1	1	1	1	1	1	1	1
1	5	3	5	7	9	11	21	41	3	9	27	81	243	5.9E4	3.5E9
2	13	7	17	31	49	71	241	881	7	49	343	2,401	16,807	2.8E8	8.0E16
3	29	15	49	111	209	351	2,001	13,201	15	225	3,375	5.1E4	7.6E5	5.8E11	3.3E23
4	61	31	129	351	769	1,471	13,441	1.5E5	31	961	2.98E4	9.2E5	2.9E7	8.2E14	6.7E29

The number of points on the sparse grid may be reduced by using slower, linear growth rules such $O = 2l + 1$, however this reduces the precision for a given level. For instance the precision for the non-linear growth rule $O = 2^{l+1} - 1$ is $\rho = 2^{l+2} - 3$, whereas the linear growth rule $O = 2l + 1$ has a precision of $\rho = 4l + 1$. Significant reductions in grid size may also be achieved by utilizing anisotropy of the system model under analysis (Section 5.7.5.5).

To achieve good accuracy, synchronisation is necessary between the PCE expansion order k (Section 5.7.2) and the quadrature rule used in the sparse grid based spectral projection approach for determining the PCE coefficients (Section 5.7.5.4). It has been advised that the PCE expansion order k should be equal to at least half of the quadrature rule precision (rounded down to an integer) (Eldred *et al.* 2008; Crestaux 2009). For example, the precision of Gauss quadrature rules is $\rho = 2N - 1$, (Section 5.7.5.3) which is equivalent to $\rho = 2O - 1$, where O is the quadrature growth rule. For a rule level $l = 1$, with a growth rule of $O = 2^{l+1} - 1$, the precision is $\rho = 5$. Subsequently, the corresponding PCE expansion order is $k = 2$.

The error in the conventional sparse grid implementation is in the order $O(N^{-r}(\log N)^{(d-1)(r+1)})$, where r is an indicator of the smoothness of the integrand. It can be seen that the convergence rate depends only weakly on the dimensionality d , but strongly on the smoothness r . As such, sparse grids require a smooth integrand for accurate results (for smooth integrands where $r \rightarrow \infty$, exponential convergence is possible) otherwise they can be liable to integration errors (Bungartz *et al.* 2004).

5.7.5.5 Anisotropic sparse grids and adaptive PCE

The behaviour of many mechanical systems is often more sensitive to certain parameters than others. Such system anisotropy can be utilized in a sparse grid formulation by using a different unidimensional quadrature rule level l_m , for different grid dimensions $m = 1 \dots d$. Smaller rule levels for less sensitive dimensions require a reduced number of sampling

points; effectively reducing the total number of points used in the sparse grid (and subsequently reducing the number of system model evaluations). The Smolyak sparse grid construction rule (5.52) can facilitate the use of anisotropic sparse grids through modifications to the selection criterion, or the weighting coefficient (defined in section 5.7.5.4) (Burkardt 2010). If the nature of model anisotropy is not known, adaptive methods can be used which progressively increase the rule level in selected dimensions, based on the associated contribution to the system outputs (Jakeman *et al.* 2011). Alternatively the problem may be considered isotropic, in which case the adaptive approach may progressively increase the general sparse grid level and monitor the convergence in the moments of the system output.

Adaptive methods are based on sensitivity analysis (Weirs *et al.*), *a posteriori* error estimates (Liu *et al.* 2011), decay rate of the polynomial coefficients (Foo *et al.* 2008), or are constructed based on the generalized dimension-adaptive sparse grid approach (Gerstner *et al.* 2003). The generalised sparse grid method is especially effective at determining the dimensions and interactions that contribute significantly to the system output variability, and is considered the superior approach. However, additional techniques have recently been proposed which offer further performance improvements (Jakeman *et al.* 2011) Anisotropic sparse grid quadrature is an extensive topic, further consideration of which is not feasible within the scope of this work. For a more detailed examination interested readers are referred to specialised literature (Gerstner *et al.* 1998; Bungartz *et al.* 2004; Burkardt 2010; Jakeman *et al.* 2010; Jakeman *et al.* 2011; Jakeman *et al.* 2011)

5.7.6 Recommendations for calculating PCE coefficients

As demonstrated in the above sections, the applicability of each PCE coefficient determination method depends on the dimensionality of the problem, as well as the order of the PCE expansion; both of which are dictated by the UQ simulation requirements.

In general it is recommended that a sparse grid PCE UQ approach be adopted in tolerance analysis. This is due to superior efficiency (the least number of required model evaluations) in the presence of even relatively low number of parameters (as evident from Table 5.2 and Table 5.4.).

It is important to note however that the number of points (corresponding to model evaluations) required in sparse and complete product grid approaches strongly depends on the selected growth rule (Section 5.7.5.4). In this work an open, non-linear Gauss-Hermite quadrature growth rule with weak nesting of $O = 2^{l+1} - 1$ was used. Although this growth

rule is highly efficient with low polynomial expansion order problems ($k < 3$), other growth rules with higher degrees of nesting may be more efficient for higher expansion orders. In high order problems, Point Collocation or Complete Product quadrature may be more efficient for low dimensionality problems ($d < 5$). Such low dimensionality is however not of high interest in practical tolerance analysis. However, in such cases approximate recommendations for choice of PCE coefficient determination method are presented in (Eldred *et al.* 2008).

5.7.7 PCE error estimates

PCE possess exponential convergence guarantees of $O(e^{-N})$ for estimates of the mean and variance, provided that the basis functions are matched to the stochastic variable distributions (Section 5.7.4) and the system response function is smooth (Xiu *et al.* 2003). Since PCE is based on the representation of a system response function with an infinite polynomial expansion that is truncated in practice, the truncation can lead to an approximation error. The error in the PCE method can be refined in practice by increasing the order k of the polynomial expansion. However it is important to note that selecting a PCE expansion order that is excessively high may lead to over-fitting of the expansion (Congedo *et al.* 2011).

Furthermore, when estimating the PCE coefficients using the spectral projection approach based on sparse grid quadrature (Section 5.7.5.4), accurate estimation of the moments depends on both the truncation error as well as the quadrature error associated with the sparse grid method. However, if the level of sparse grid quadrature is sufficiently high, the associated quadrature error can be negligible compared to the truncation error. To achieve a comparatively low quadrature error the PCE expansion order k should be equal to half of the quadrature rule precision, (rounded down to an integer) (Section 5.7.5.4) (Eldred *et al.* 2008; Crestaux 2009); this recommendation is applied in this work.

A robust indication of error in PCE moment estimates can be obtained with a comparison to a reference MC sampling based moment estimate. Although MC sampling requires a comparatively large number of system evaluations, MC based moment convergence is independent of the problem dimensionality, smoothness of the response function, and type of probability distribution (Section 5.6.1). As such, a MC moment estimate is robust error indicator, despite a potentially high computational cost. Increasing the efficiency of the quantification of the error associated with PCE methods is an active area of research by PCE investigators (Debuschere *et al.* 2005; Congedo *et al.* 2011; Archibald *et al.* 2012).

However, as the associated efforts have not reached a high level of maturity, an MC reference based approach will be applied in this research.

5.8 Case study 5.1

5.8.1 Problem definition

Case study 5.1 is an automotive tolerance synthesis problem in which product functionality is characterized by the compliance of part geometry due to internal equilibrating forces. Automotive passenger seats are required to accommodate anthropometric variation of users while meeting safety standards under crash scenarios (Leary *et al.* 2011). Fore and aft adjustment of seat position is achieved with a rolling rail assembly consisting of interlocked rail sections separated by a series of rolling elements (Figure 5.4). The rail sections are preloaded elastically by an interference fit upon assembly. Manufacturing variation in the geometric parameters of the rail section affects the magnitude of the rolling element contact force and consequently the rolling effort of the rail assembly. It is required that the contact force be sufficiently high to avoid chatter in the rail assembly, while being sufficiently low to allow the rail to move without excessive effort.

Due to these conflicting requirements, contact force is a KPC of significant importance. Minimising the effect of manufacturing variation on elastic rail preload is required to achieve competitive quality, cost and development time objectives. This case study presents a problem of tolerance synthesis in a rail assembly with the objectives of maximising assembly yield (number of rail assemblies which comply with rolling resistance requirement) and minimising the cost of tolerances. The rail assembly selected for the analysis is Rail A (Figure 3.10 (i)) as previously considered in the benchmarking analysis presented in Section 3.4. The benchmarking study compared the sensitivity to manufacturing of various rail section profile designs. Rail assembly A was found to offer high sensitivity to variation, attributable to a large number of section folds and close proximity of rolling elements (Section 3.4.8). The selected rail assembly had the highest number of design parameters among the design alternatives (22 parameters associated with bend angles and radii), and was one of the most challenging for modelling correct rolling element location within the assembly (described further in 5.8.3). Subsequently it presented the most demanding case study both for the PCE UQ method (which is dependent on dimensionality - Section 5.7) and for required tolerance and CAE modelling. As such, outcomes of this case study would provide a worst-case estimates of:

- Performance expected in the simulation capabilities of the tolerance synthesis platform developed in this work (for this application); and,
- the manufacturing tolerances which would be required to achieve desired yield in the most variation sensitive rail assembly design. This was a point of high interest to the industry partner.

Since other rail assembly designs considered in Section 3.4 are less demanding in both of the above aspects, a successful outcome of this case study is expected to ensure similar success if the other rail assembly designs were also subject to tolerance synthesis with the developed platform.

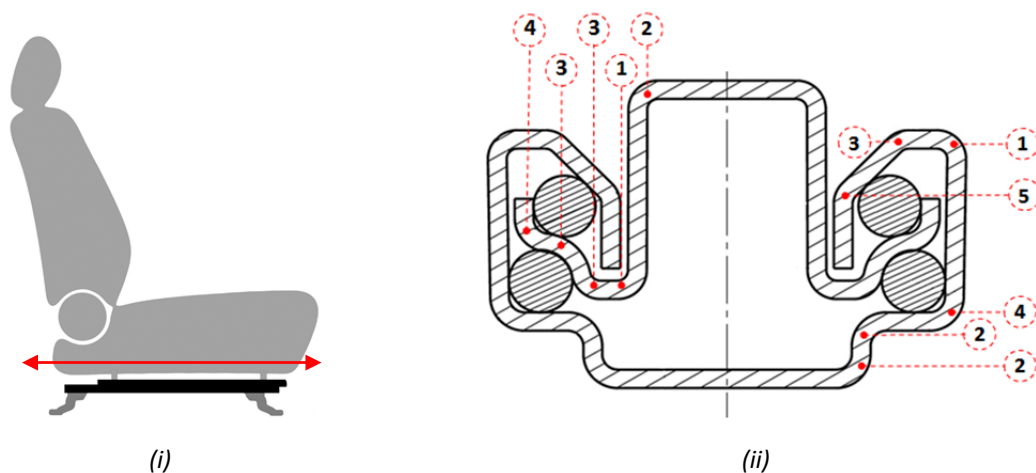


Figure 5.4 - (i) Automotive seat and rail assembly (black) (ii) seat rail assembly section view including die-press folding sequence for upper and lower rails

Variation in rolling resistance can be estimated from the rolling element contact force in the rail section assembly, where the resistance of the rolling element depends on the product of the rolling element contact force and the associated coefficient of rolling resistance (Williams 1994). Each rail assembly has a total of 14 spherical rolling elements, and the coefficient of rolling friction for a physical prototype rail assembly has been experimentally determined to be 0.023.

The following attributes define the design requirements and manufacturing process of the rail assembly:

- A nominal rolling effort force of 35N for a complete seat rail assembly has been identified as desirable with the specification limits set at 35 ± 8 N (corresponding to $C_{pm} = 1$, i.e. 99.7% assembly yield). This rolling effort is for a complete lower seat frame assembly consisting of two seat rail assemblies, with each rail set providing half of the total resistive force.

- The rail sections are manufactured from steel sheet that is progressively folded in die-presses into the desired profile. The required folding sequence for upper and lower rails is indicated in Figure 5.4 (ii). Each folding stage is associated with specific variation in the nominal geometry, in particular the bend angle and bend radii. These variations are quantified in Section 5.8.2. Variation in the sheet thickness is considered negligible in the scope of this work.
- Reduced variation in each fold is possible through stricter control of allowable tool wear, but incurs a cost penalty.
- Controlling variation in the folds is associated with varying level of difficulty on account of:
 - the need to use less precise multi-part dies (which are also fundamentally more expensive than single-part dies)
 - a reduction in freedom to orient the workpiece within the die
 - the need to carry out *free-end* type folds (a fold which is not fully enclosed within a die) which become difficult to control due to spring back effects.

Consequently, the cost-tolerance relationships associated with a fold process is dependent on the difficulty level as well as the allowable tolerance. The folding stages of Figure 5.4 (ii) have been classified in Table 5.6 according to the level of difficulty in controlling associated variation.

- Two alternative die-pressing processes are available, a *standard process* suitable for standard precision tolerances and a *high precision process*. The high precision process can offer a lower tolerance cost than the standard process for high precision tolerances. However, due to increased set-up times, slower operation and higher capital cost, the high precision process imposes a higher cost for standard and low precision tolerance values. There is a limited region of overlap where the two processes offer a similar cost tolerance characteristic.
- Cost-tolerance curves which capture the precision attributes of the die-pressing processes for the rail section bend angle and bend radii parameters are presented in Figure 5.7 and Figure 5.8. The curves were developed in consultation with an industry partner and are based on empirical experience in the analysis of the die-pressing processes used to manufacture similar rail sections. The curves indicate the cost penalty in terms of the standard deviation of the associated part parameter. Each bend may be carried out on either the standard or high-precision process which is determined by the more economical choice for a required tolerance level.

The case study objective is to specify optimal process capabilities for the rail bend angle and radii, such that the following objectives and constraints are addressed (Table 5.5).

Table 5.5 - Case study 5.1 objectives and constraints.

Objective	Description	Constraint
Maximize C_{pm} of assembly KPC	Maximize the number of assemblies conforming to the rolling effort (KPC) specification requirements	The minimum required assembly yield is 99.7% ($C_{pm} = 1$)
Minimize total tolerance cost	Minimise the total cost of the required part tolerances based on cost-tolerance curves (Figure 5.7 and Figure 5.8)	Maximum allowable tolerance cost is 8000 cost units (the cost constraint was set high as it was not certain what tolerance cost would be required to achieve the required yield)

A statistical tolerance analysis simulation was conducted on a numerical model of the assembled rails with bearings under preload, intrinsically capturing the associated assembly response function and quantifying rolling effort variation.

5.8.2 Variation in rail geometry and tolerance costs

To obtain an indication of the variation in production rails, metrological measurement was conducted on rails currently produced by an industry partner with standard precision folding processes (Figure 5.5). The metrological measurements were conducted to provide insight into the expected yield for the case study rail assembly (in Figure 5.4 (ii)) if it were to be manufactured using the same manufacturing processes as the measured rail (Figure 5.5). Furthermore, the manufacturer of the measured rails has found that the variation in rolling effort in production assemblies is unsatisfactorily high. By applying the tolerance synthesis platform developed in this work to a future production designs, the required tolerances and associated cost which achieve an acceptable rolling effort target can be identified.

A rigid mounting fixture was designed, constructed and placed within a Coordinate Measurement Machine (CMM) for metrological assessment (Figure 5.5 (i) and (ii)). A group of 24 upper and 24 lower rails (sampled from different production batches to accommodate batch-to-batch variation) was measured at a number of perimeter points at 18 longitudinally spaced cross-sectional positions (Figure 5.5 (iii)) (resulting in 432 profile sections measurements for both upper and lower rails). The measurement points were used to determine the bend angle and radii for a number of bends within each cross-section. Figure 5.5 (iii) and (iv) show an end view of sample upper and lower rails with measured angles and radii (measured radii shown as superimposed fitted circles).

The resultant overall standard deviation for the measured folds is shown in Table 5.6 along with classification of the level of difficulty in controlling associated variation. The

measurements were conducted until the influence of additional samples on the overall standard deviation was less than 2% (Figure 5.6). The resultant variation was combined into averaged values of standard deviation in bend angle and bend radii associated with both low and high difficulty folds (Table 5.7).

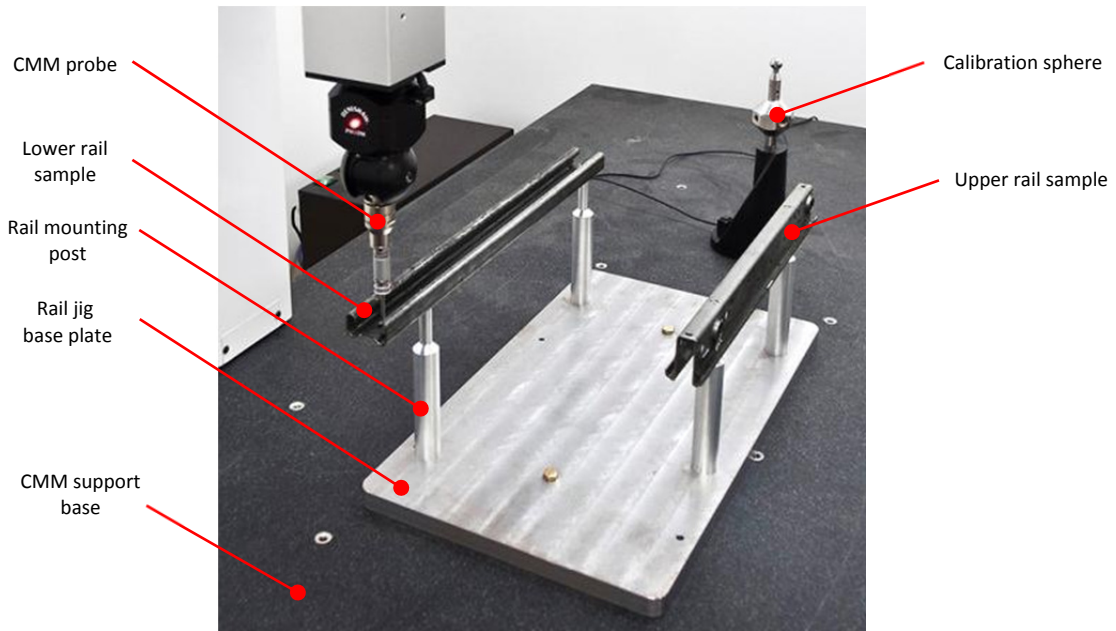
The combined standard deviation values were subsequently used to calibrate the cost-tolerance curves for the folding processes (Figure 5.6 and Figure 5.7). The measured rail sections were manufactured using standard precision folding processes involving both low and high difficulty folds. The cost associated with achieving standard precision was considered approximately equal for all folding stages due to the similarity of tooling, set-up and quality control specifications. The cost was set at the median of the standard process cost unit scale on advice from the industry partner. This reflects the position of the current process precision within the cost-tolerance relationship. However, the precision associated with the equal cost (measured in standard deviation) varied between folding stages as different fold characteristic result in varying levels of difficulty in controlling variation.

Table 5.6 - Standard deviation in measured rail folds. Classification of the level of difficulty in controlling associated variation for both the case study rail (Figure 5.4 (ii)) and the measured rail (Figure 5.5 (iii))

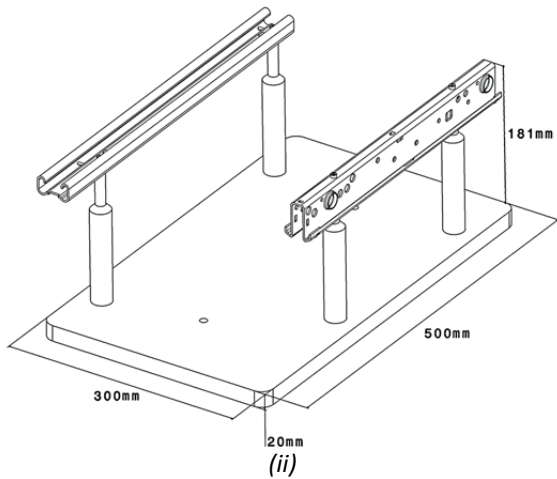
Folding Stage	Case study rail		Measured rail					
	Fold difficulty		Lower Rail			Upper Rail		
	Lower Rail	Upper Rail	Fold difficulty	Standard deviation		Fold difficulty	Standard deviation	
				Angle[deg.]	Radii[mm]		Angle[deg.]	Radii[mm]
1	Low	Low	Low	0.191	-	Low	0.202	0.038
2	Low	Low	Low	-	0.024	High	0.530	-
3	High	High	Low	-	0.078	High	-	0.221
4	High	High	High	-	0.118	High	-	0.205
5	High	-	High	-	-	-	-	-

Table 5.7 - Combined averaged standard deviation associated with low and high difficulty folds for measured rail.

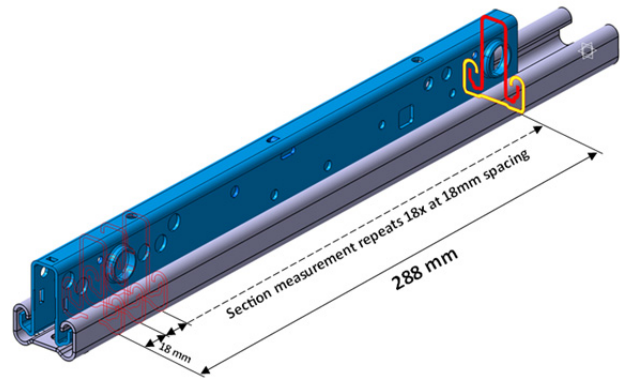
Folding difficulty	Bend angle standard deviation [deg.]	Bend radii standard deviation [mm]
Low	0.197	0.047
High	0.530	0.181



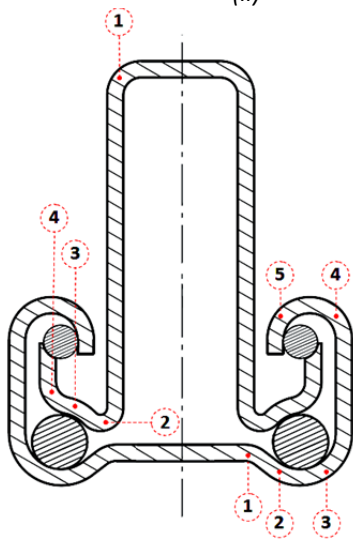
(i)



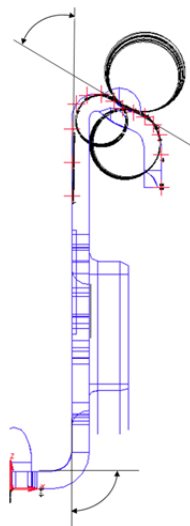
(ii)



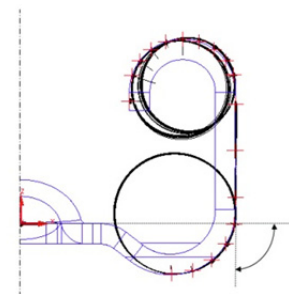
(iii)



(iii)



(iv)



(v)

Figure 5.5 - Measured rail assembly (i) CMM mounting jig and sample rails under measurement
 (ii) general jig dimensions (ii) section measurement locations
 (iii) section view including folding sequence for upper and lower rails
 (iv) sample upper rail variation (v) sample lower rail variation.

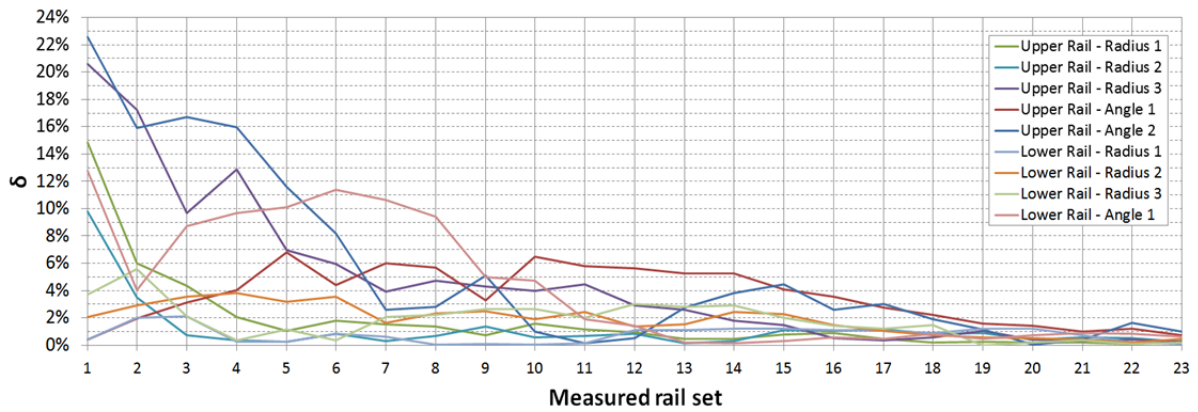


Figure 5.6 - Influence of additional samples to the change in overall standard deviation for a total of 24 measured rail sets. Where $\delta = \left| \frac{\sigma_{RAILSET} - \sigma_{ALLSETS}}{\sigma_{ALLSETS}} \right|$

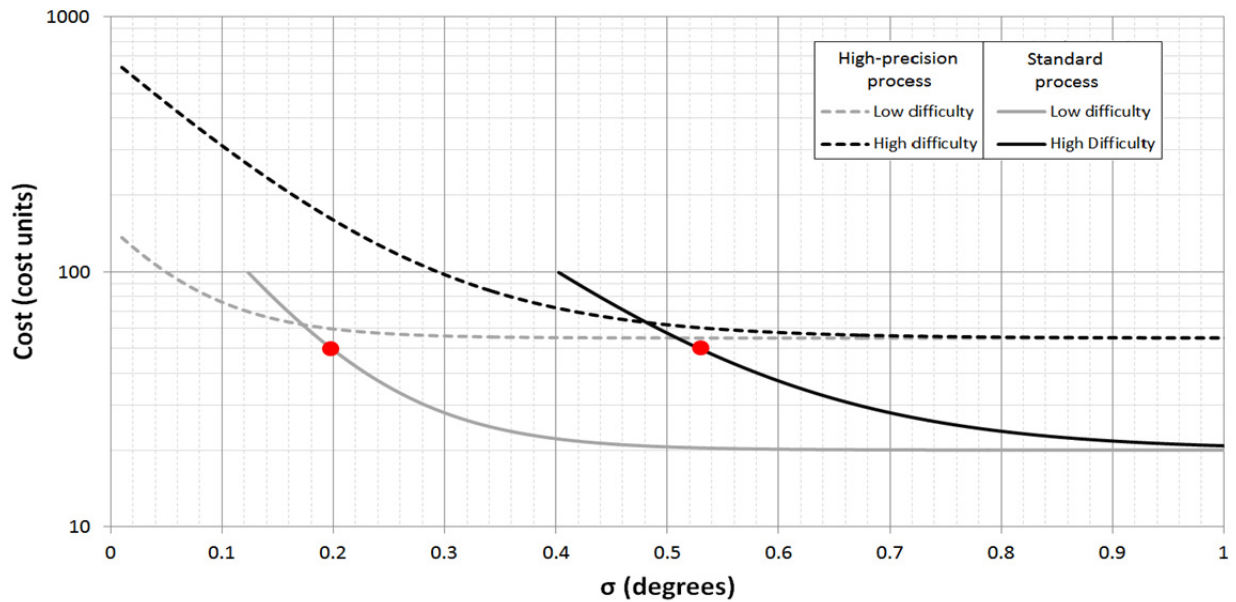


Figure 5.7 - Cost-tolerance curves for rail bend angles for varying levels of variation control difficulty. The process curves are plotted only within the feasible limits of the associated process.

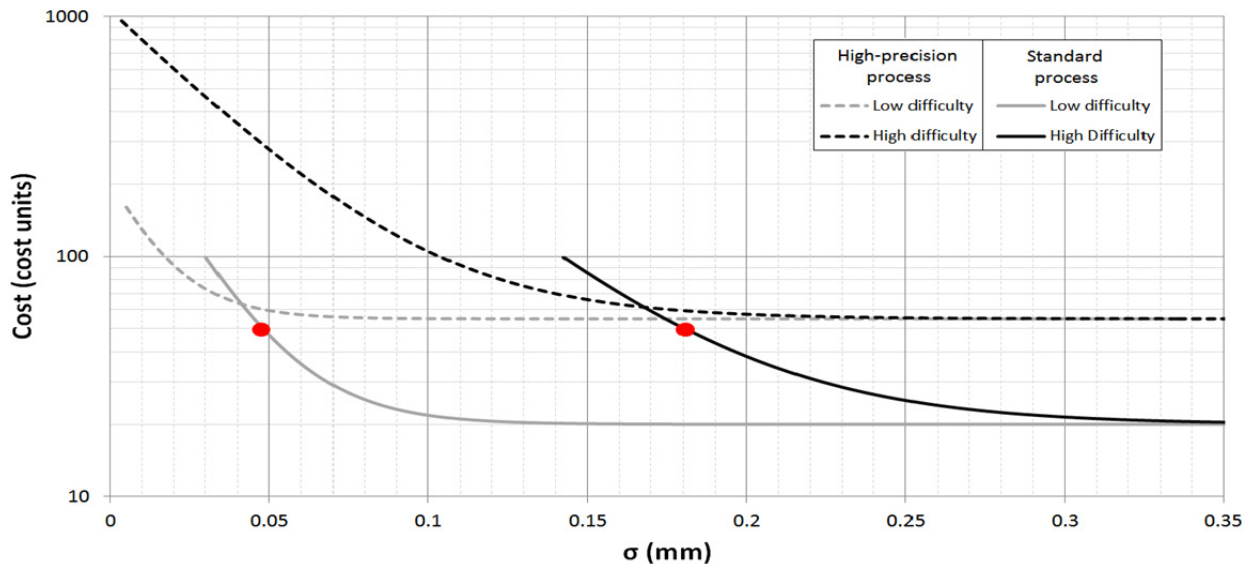


Figure 5.8 - Cost-tolerance curves for rail radii angles for varying levels of variation control difficulty. The process curves are plotted only within the feasible limits of the associated processes.

5.8.3 Simulation models

The effect of variation in rail geometry on rolling effort has been estimated by the integration of two independent numerical models:

- CAD model defining rolling element position, and
- Finite Element (FE) model estimating bearing contact force due to internal loading.

Due to variation in rail geometry, the rolling element size and position which correctly fits within the spacing between assembled rails will vary. Identifying the size and position of the rolling elements required the construction of a comprehensive parametric CAD model, developed using the CATIA software. Due to limitations associated with parametric constraint modelling, the CAD model identified two possible solutions, only one of which is feasible (Figure 5.9 (ii)). The feasible solution was identified by post-processing the CAD output, prior to exporting the correct rolling element position and diameter values to a second, parametric FE model of the rail assembly. ABAQUS FE modelling software was used to simulate the rail deflection due to an interference fit with the rolling elements (Figure 5.9 (iii)). The model was constructed to consider one-half of the symmetric rail profile. The nominally fitting ball for the rail assembly was oversized by 0.1mm in diameter to be representative of the assembled interference fit. The resultant contact force was integrated over the contact surfaces. The average individual simulation time associated with the integrated CAD and FE models was approximately 80 seconds on a quad core 3.2 GHz CPU.

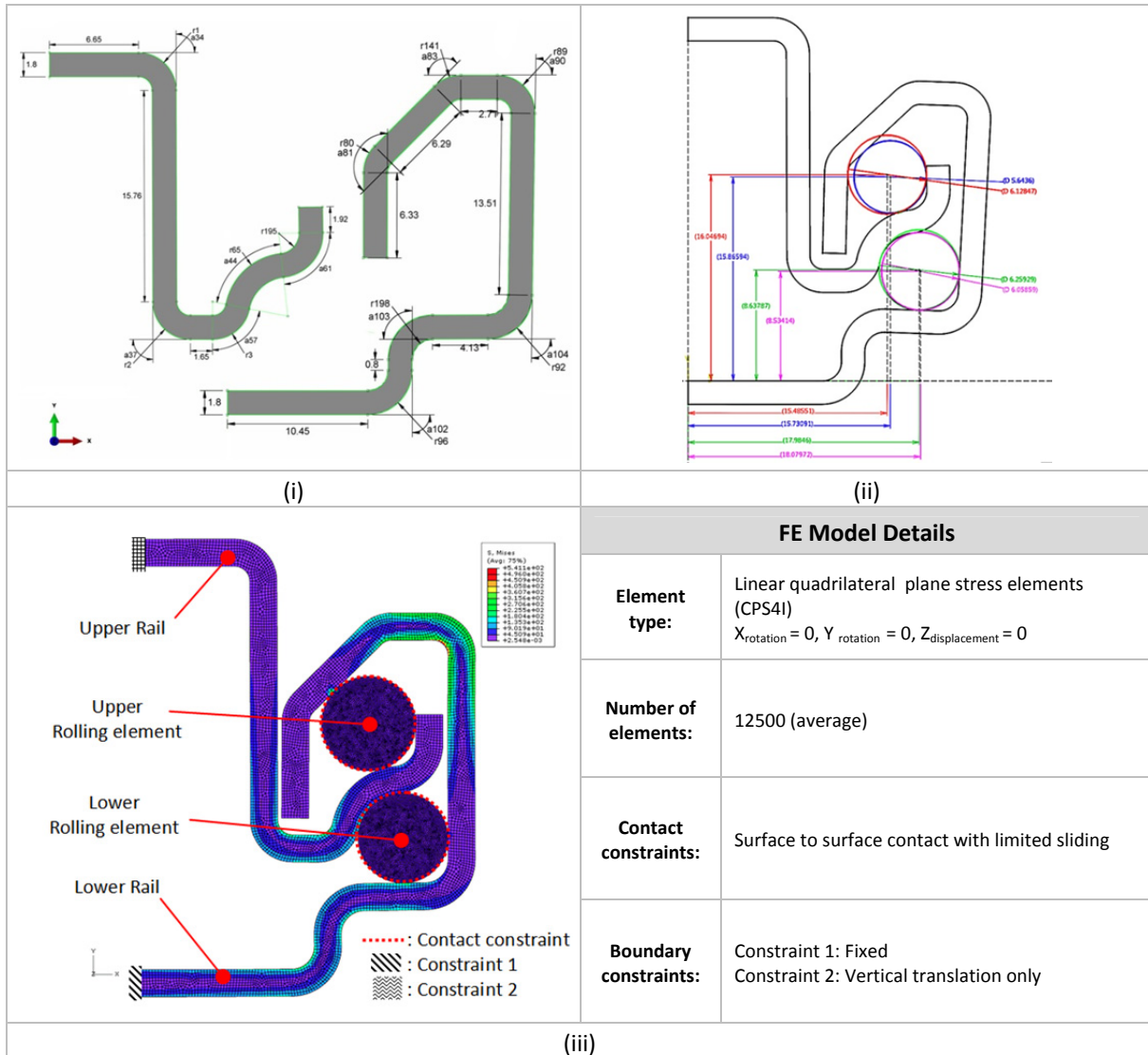


Figure 5.9 - (i) Rail section parameters (alpha numeric label designates stochastic variable – see Table 5.8)
(ii) CATIA model for determining ideal ball size from possible scenarios
(iii) FE model details showing deformation due to interference fit of rolling elements.
All dimensions in mm.

Two PIDO tools were interfaced with the CAD and FE rail models according to a newly developed PIDO tolerance analysis platform (Figure 5.10) (Mazur *et al.* 2011). UQ was conducted using DAKOTA (Adams 2011) and optimization was carried out using ESTECO modeFRONTIER (Figure 5.10). All part parameter distributions were Gaussian. Tolerance synthesis was carried out according to the platform presented in Section 5.4 and consisted of the following stages:

1. Trail standard deviations (i.e. tolerances) for bend angles and bend radii were selected. Initial selection was based on uniformly distributed samples within the design space, subsequent selection was determined by the optimization algorithm defined in Section 5.8.5.

2. The tolerance cost for each bend angle and bend radii pair was calculated for both the standard and high-precision processes. The more economical process was then selected and the total assembly tolerance cost was calculated. If the cost was infeasible (violating maximum cost constraints), a new trial set of tolerances was selected.
3. Trial tolerances were passed to the parametric CAD model to identify the size and position of the correctly fitting rolling elements.
4. Trial standard deviation and correct rolling element size and positions were passed to the UQ tool, which initialised a sparse grid based PCE simulation. For each UQ sampling point, the simulation consisted of:
 - a. The nominally fitting rolling elements were oversized by 0.1mm in diameter which is representative of the interference fit within the rail assembly. A contact simulation was subsequently initialised in which the interference force deformed the rail.
 - b. Resultant peak contact forces were integrated over the contact area.
 - c. Complete rail assembly rolling effort was estimated from the contact forces.
5. Moment estimates for the rolling effort KPC were returned from the UQ tool and C_{pm} was calculated.
6. Objective function fitness was assessed by the MOGA optimization algorithm and new trial standard deviations were generated (return to step 1).

The optimization was terminated at the iteration limit of 45 designs (Section 5.8.5).

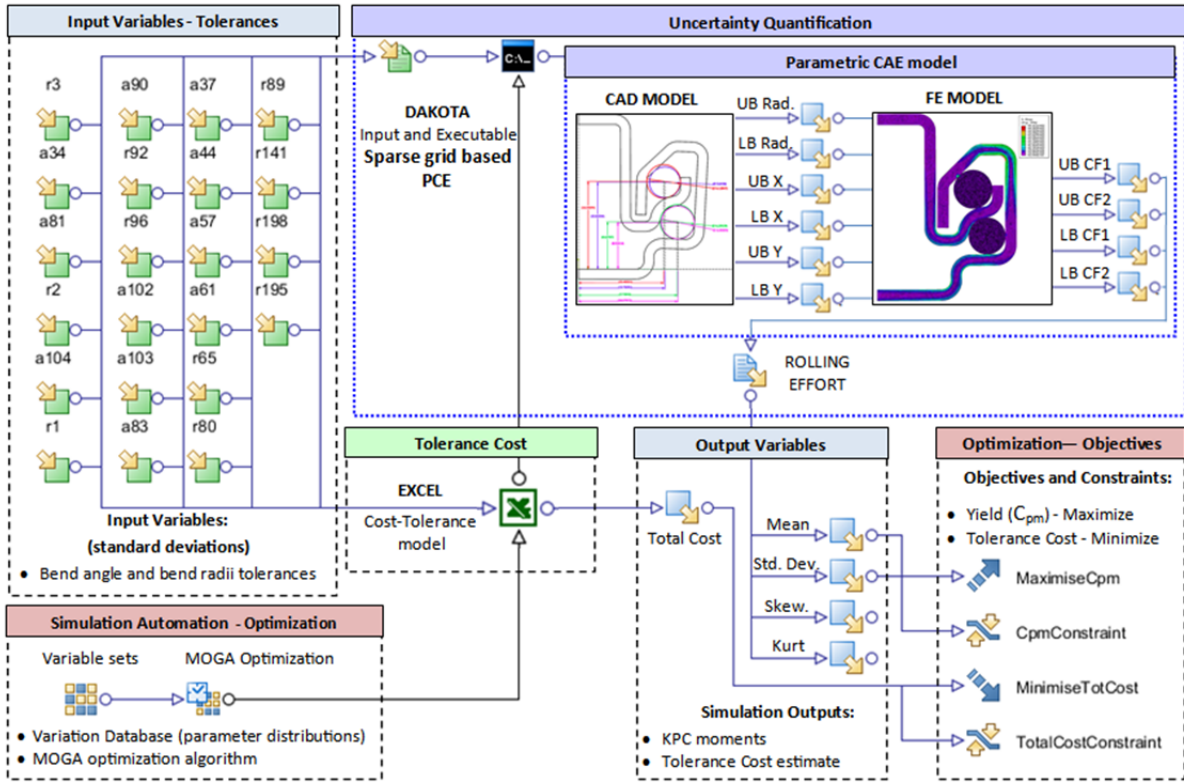


Figure 5.10 - PIDO tolerance synthesis workflow for Case study 5.1.

5.8.4 UQ strategy

Sparse Grid based PCE was incorporated into the PIDO interface for UQ in the rail assembly model. The SG level was selected after comparing PCE moment estimates of rolling effort for the initial design (Section 5.8.7 and Table 5.8) for progressively larger SG levels. An isotropic SG level of 0 was too low to provide reliable moment estimates (corresponds to a single model evaluation). Levels 1 and 2 required 45 and 1101 model evaluations, respectively. The differences between the level 1 and level 2 estimates of mean and standard deviation were approximately $\delta_{\mu} = 0.5\%$ and $\delta_{\sigma} = 2\%$, respectively.

$$\delta_{\mu} = \left| \frac{\mu_1 - \mu_2}{\mu_2} \right| \% \quad \text{Where the subscripts designate the two different moment estimates under comparison. The estimate based on the larger number of model evaluations was taken as estimate 2.} \quad (5.55)$$

$$\delta_{\sigma} = \left| \frac{\sigma_1 - \sigma_2}{\sigma_2} \right| \% \quad (5.56)$$

An anisotropic sparse grid based on the generalized adaptive approach required 85 model evaluations and showed differences of approximately $\delta_{\mu} = 0.8\%$ and $\delta_{\sigma} = 2.3\%$, between the isotropic level 1 grid estimates. The PCE based moment estimates were compared against a MC estimate of 3000 samples. The differences between the SG level 1 and MC estimates of mean and standard deviation are approximately $\delta_{\mu} = 3\%$ and $\delta_{\sigma} = 5\%$, respectively. Based on the small differences between SG based PCE moment estimates at

different grid and adaptivity levels, as well as the small difference between the MC and SG level 1 estimates, an isotropic SG level of 1 was selected for use in tolerance synthesis in order to reduce the number of model evaluations.

5.8.5 Optimization strategy

The optimization algorithm employed was a Multi-Objective Genetic Algorithm (MOGA) with emphasised multi-search elitism which shows good performance in preserving high fitness solutions without compromising a global search by convergence to local optima (Deb *et al.* 2002). The iteration limit is defined by the initial population multiplied by the number of generations. In this work the number of generations was set to 10 and the initial population was 15, resulting in 150 model evaluations. The initial population is a uniformly distributed subset created by applying filtering to a MC sampled base population of 800 designs. The filtering maximizes the separation distance between base points resulting in more uniform sampling of the parameter space.

5.8.6 Assumptions

The conducted analysis was subject to a number of assumptions in order to allow for reasonable scope of analysis within a limited analysis time budget:

- The plane stress FE model only considers the two-dimensional cross-section of the rail at the rolling element contact location. This simplification results in the estimated magnitude of contact force being based on deformation of the full rail length, rather than point contact. However in reality, the contact scenario is that of a sphere and a surface. The approximation was used to limit the FE model simulation time to a practically manageable size, due to the significant complexity of the more realistic scenario.
- Variation in rail sections was assumed to be equal on either side of the axis of symmetry.
- No variation in linear dimensions or material thickness was considered as the industry partners advised that these effects were negligible in comparison with those considered in this work.

The emphasis of this work is on demonstrating the developed PIDO based tolerance synthesis platform based on utilising existing modelling tools. If greater realism is desired, the assumptions may be overcome by more sophisticated models (with greater computational cost) without invalidating the demonstrated applicability of the presented methodology for tolerance synthesis scenarios.

5.8.7 Simulation results and outcomes

Simulation results are shown in Figure 5.11 and Table 5.8. The standard deviations of the bend angle and bend radii for the initial case study designs were set to values corresponding to the measured rails (Table 5.7). The yield and tolerance cost, which would be achieved if the case study rail assembly were to be manufactured with the same process standards as the measured rails, were subsequently estimated. The resultant yield of $C_{pm} = 0.12$ was unsatisfactorily low. The tolerance synthesis platform was able to identify Pareto optimal designs with higher yield (Figure 5.11), however at a significant penalty to the total tolerance cost. This cost penalty indicates that the manufacturing precision of the measured rail assembly is not sufficient to meet the desired yield targets of the case study rail. The rolling effort of the case study rail assembly is particularly sensitive to variation in rail profile parameters that are identified with a comparatively high C_{pm} in Table 5.8 (e.g. C_{pm} approximately greater than 4). The associated high tolerance cost could be reduced by; folding process changes which decrease the tolerance cost of high C_{pm} profile parameters; or re-design of the rail profiles to achieve rolling effort yield requirements without requiring high C_{pm} rail parameters.

From the identified Pareto optimal designs (Figure 5.12) the lowest cost design (Design #114) was selected as the preferred candidate. The selected design offers the lowest tolerance cost while exceeding the yield requirement of $C_{pm} = 1$ by 11%. The higher yield allows for conservatism in the estimated results.

The total number of designs evaluated was 150 (Section 5.8.5). Each evaluation of the rail assembly CAD and FE models required approximately 60 seconds on a quad core 3.2 GHz CPU (Section 5.8.3). The bulk of the analysis time is attributed to the FE solver with process integration overheads amounting to an additional time of approximately 10 seconds per design. The total number of model evaluations was 6750 (i.e. 150 optimization runs, each with a UQ analysis of 45 model evaluations) resulting in a total simulation time of approximately 5.5 days. With additional time resources the selected design could be subjected to a local refinement to explore the objectives space within the vicinity of the selected optimum design with greater resolution.

If UQ was conducted with traditional sampling-based methods, such as MC, with a relatively small sample size of 1000, the total simulation time would be approximately 121 days. This alternative is prohibitively impractical, whereas the sparse grid based PCE method provides a feasible alternate by reducing the computation time by a factor of 22.

The final design (Design ID#114) was validated against a MC reference estimate of 3000 samples. The differences between the PCE and MC estimates of mean and standard deviation was approximately $\delta_{\mu} = 3\%$ and $\delta_{\sigma} = 4\%$, respectively. This difference is considered negligible.

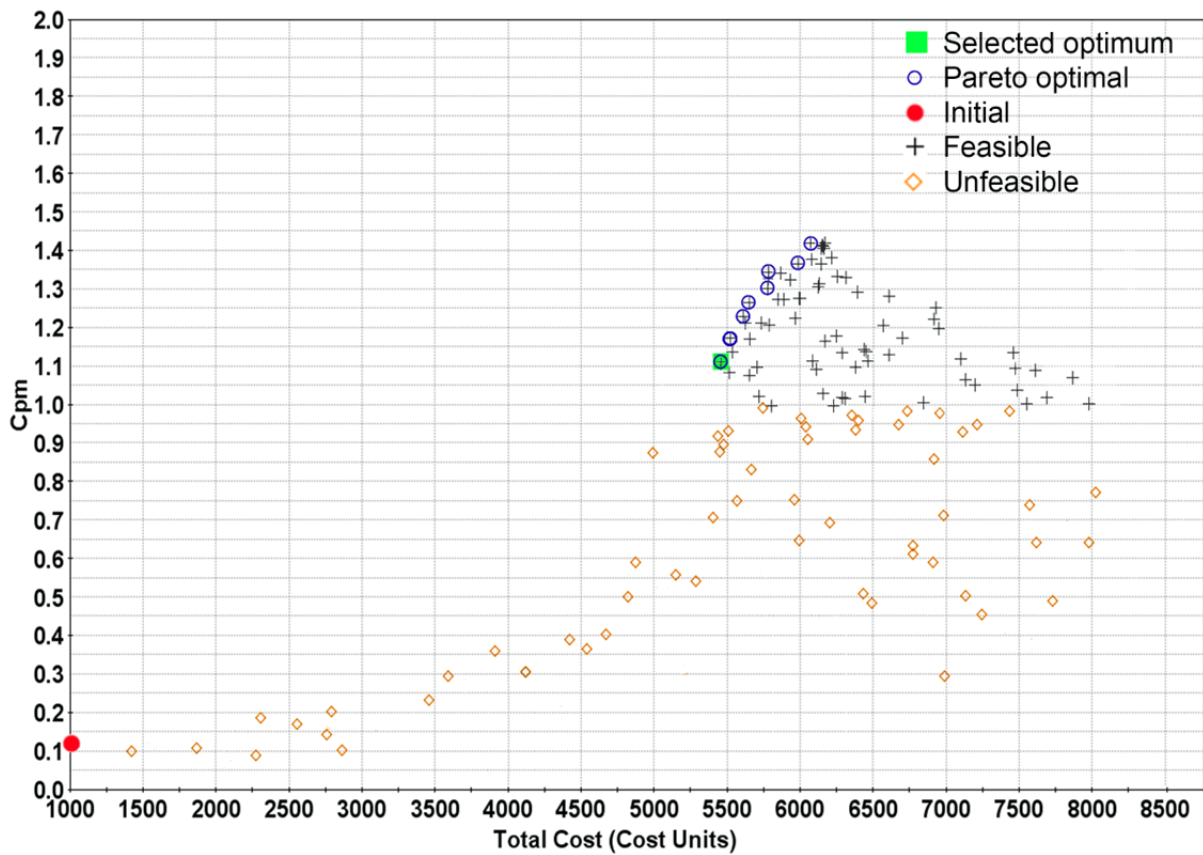


Figure 5.11 - Objectives space of tolerance synthesis for Case study 5.1.

Table 5.8 - Rail assembly parameters and associated variation for initial design and selected optimum.

Component	Parameter		Folding difficulty	Nominal	Spec. Limits +/-	Min.	Max.	Initial design (ID #1)					Optimised design (ID #114)				
								F	σ	C _{pm}	Process (Standard or High-precision)	Tolerance Cost	F	σ	C _{pm}	Process (Standard or High-precision)	Tolerance Cost
Upper Rail	a34	[deg]	L	90	1	89	91	90	0.197	1.69	S	50.6	90	0.023	14.49	H	121.9
	a37	[deg]	L	90	1	89	91	90	0.197	1.69	S	50.6	90	0.026	12.82	H	119.0
	a44	[deg]	H	72.9	1	71.9	74	73	0.530	0.63	S	49.8	73	0.136	2.45	H	241.2
	a57	[deg]	H	79.2	1	78.2	80	79	0.530	0.63	S	49.8	79	0.069	4.83	H	395.4
	a61	[deg]	H	84.7	1	83.7	86	85	0.530	0.63	S	49.8	85	0.093	3.58	H	329.1
	r1	[mm]	L	2.8	0.1	2.7	2.9	2.8	0.047	0.71	S	51.8	2.8	0.034	0.98	H	62.1
	r2	[mm]	L	2.8	0.1	2.7	2.9	2.8	0.047	0.71	S	51.8	2.8	0.043	0.78	H	57.6
	r3	[mm]	H	2.8	0.1	2.7	2.9	2.8	0.181	0.18	S	49.8	2.8	0.031	1.08	H	622.9
	r65	[mm]	H	4.7	0.1	4.6	4.8	4.7	0.181	0.18	S	49.8	4.7	0.025	1.33	H	439.5
	r195	[mm]	H	1.5	0.1	1.4	1.6	1.5	0.181	0.18	S	49.8	1.5	0.051	0.65	H	272.5
Lower Rail	a81	[deg]	H	135	1	134	136	135	0.530	0.63	S	49.8	135	0.093	3.58	H	329.1
	a83	[deg]	H	135	1	134	136	135	0.530	0.63	S	49.8	135	0.092	3.62	H	331.6
	a90	[deg]	L	89	1	88	90	89	0.197	1.69	S	50.6	89	0.079	4.22	H	83.9
	a102	[deg]	L	90	1	89	91	90	0.197	1.69	S	50.6	90	0.055	6.06	H	96.4
	a103	[deg]	L	90	1	89	91	90	0.197	1.69	S	50.6	90	0.033	10.10	H	112.6
	a104	[deg]	H	91	1	90	92	91	0.530	0.63	S	50.6	91	0.043	7.75	H	484.9
	r80	[mm]	H	2.8	0.1	2.7	2.9	2.8	0.181	0.18	S	49.8	2.8	0.043	0.78	H	331.4
	r89	[mm]	L	2.8	0.1	2.7	2.9	2.8	0.047	0.71	S	51.8	2.8	0.005	6.67	H	228.1
	r92	[mm]	H	3.3	0.1	3.2	3.4	3.3	0.181	0.18	S	49.8	3.3	0.047	0.71	H	300.2
	r96	[mm]	L	3.3	0.1	3.2	3.4	3.3	0.047	0.71	S	51.8	3.3	0.006	5.42	H	207.6
	r141	[mm]	H	2.8	0.1	2.7	2.9	2.8	0.181	0.18	S	49.8	2.8	0.105	0.32	H	98.0
r198	[mm]	L	1.5	0.1	1.4	1.6	1.5	0.047	0.71	S	51.8	1.5	0.008	4.17	H	179.4	
Assembly	Rolling effort	[N]		35	8	27	43	32.42	22.19	0.12			34.36	2.31	1.11		
	Total Cost	[Cost units]										1110					5445

5.9 Case study 5.2

5.9.1 Problem definition

The case study presents a significant extension of the tolerance analysis problem presented in case study 4.2 (Section 4.6) in which product functionality is defined by both external and internal loading (friction and multi-body dynamics). The case study is extended to address a tolerance synthesis problem in which an optimal set of part tolerances is identified, minimising manufacturing cost while maximising assembly yield. The product under analysis is a rotary switch assembly used in automotive applications. Positional restraint and a desired resistive switch actuation torque are provided by a spring loaded radial detent acting on the perimeter of the switch body (Figure 5.12). The cylindrical detent is located in a positioning sleeve within which a helical compression spring biases the cylindrical detent against the switch detent ramp faces. The peak resistive torque is a KPC of the assembly and depends on:

- part geometry;
- internal forces due to part acceleration;
- external forces, including the spring force;
- contact forces between components;
- friction coefficient between components in contact.

A sufficient resistive torque is required to provide ergonomically and functionally adequate positional restraint with a positive impression of product quality. Excessive variation in the peak resistive torque of manufactured switch assemblies has a negative impact on perceived product quality. The 8 design variables considered in the simulation are shown in Figure 5.12 and Table 5.10.

The product requirements define a series of constraints and objectives:

- A nominal peak resistive torque of 75 Nmm has been experimentally identified as desirable for the intended application with specification limit set at 75 ± 7 Nmm (corresponding to $C_{pm} = 1$)
- The rotary switch and positioning sleeve are injection moulded polymer components. The radially acting cylindrical detent is machined mild steel. The steel spring is manufactured on dedicated wire coiling machinery (Wahl 1963; Wood 2006; Mazur *et al.* 2011).
- The different materials and manufacturing processes result in specific cost-tolerance characteristics for the associated part parameters. Cost-tolerance curves for each part parameter were specified in consultation with an industrial partner and are presented in

Figure 5.13. The estimated curves indicate the expected cost penalty in terms of the standard deviation of the associated part parameter. The curves are based on a hypothetical estimate due to a lack of empirical data defining the cost-tolerance relationship for the manufacturing processes associated with the assembly components. Lack of process specific empirical data is common problem with cost-tolerance modelling due to broadly varying characteristics of manufacturing process economics (Dong *et al.* 1994; Hong *et al.* 2002). Although cost-tolerance relationships could be defined with dedicated investigation of the industry partners and supplier manufacturing processes, it demands extensive commitments beyond the scope of this research project. As such hypothetical cost-tolerance curves were established which represent the expected relative difficulty in controlling variation in the various assembly parameters.

The case study objective is to specify optimal process capabilities for part parameters, such that the following objectives and constraints are addressed (Table 5.9).

Table 5.9 - Case study 5.2 objectives and constraints

Objective	Description	Constraint
Maximize C_{pm} of assembly KPC	Maximize the number of assemblies conforming to the peak resistive torque (KPC) specification requirements	The minimum required assembly yield is 99.7% ($C_{pm} = 1$)
Minimize total tolerance cost	Minimise the total cost of required part tolerances dictated by part parameter specific cost-tolerance curves (Figure 5.13)	Maximum allowable tolerance cost is 515 cost units. This corresponds to the cost of the best design identified in prior work through manual allocation of tolerances (Original identified in Section 4.6.5.2 and shown for reference in Table 5.10 and Figure 5.15).

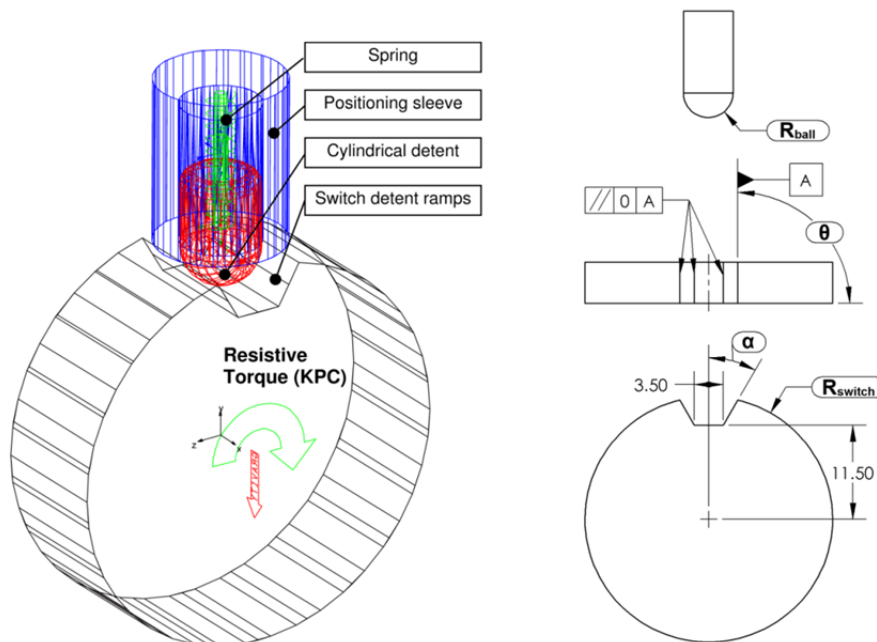


Figure 5.12 - Rotary switch and spring loaded radial detent assembly model used in Case study 5.2 (Note: Linear dimensions in mm. Variation in non-enclosed dimensions not considered in simulation)

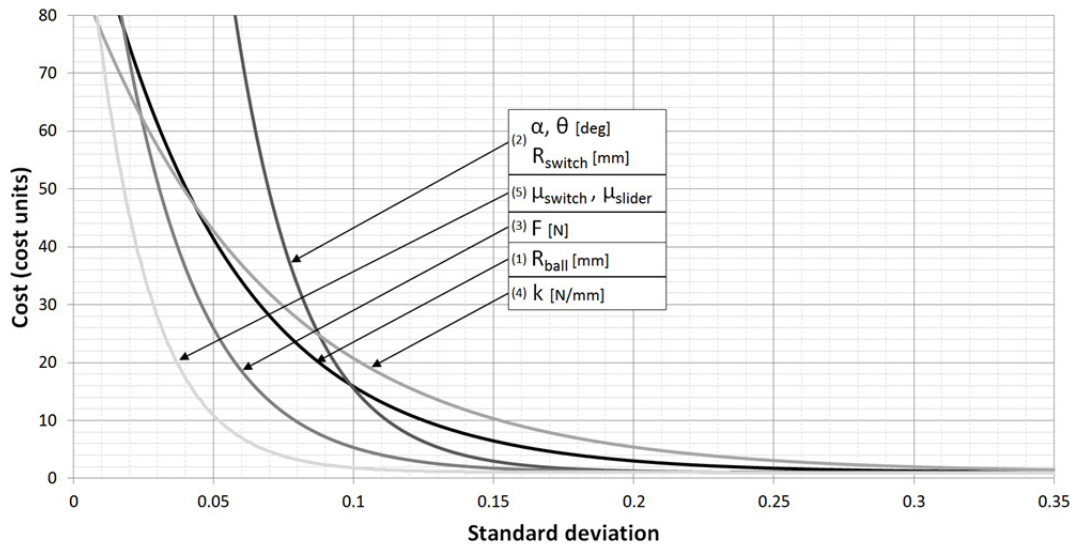


Figure 5.13 - Cost-tolerance curves for part parameters of radial detent assembly

5.9.2 Simulation model and optimization

A parametric numerical model of the switch assembly was constructed using MSC ADAMS Multi-Body Dynamics modelling software (Figure 5.12) (Section 4.6.4) accommodating the possible variation within geometric and physical parameters (such as spring pre-load, spring stiffness and friction coefficients).

Two PIDO tools were interfaced with MSC ADAMS software according to the developed PIDO tolerance synthesis platform (Section 5.4). UQ was conducted using DAKOTA (Adams 2011) with process scheduling and optimization carried out using ESTECO modeFRONTIER (Figure 5.14). All part parameter distributions were assumed to be Gaussian. Tolerance synthesis was carried out according to the platform presented in Section 5.4 and consisted of the following stages:

1. Trial standard deviations (i.e. tolerances) for stochastic dimensional, spring and friction parameters of models were selected.
2. Total assembly tolerance cost was calculated and checked for feasibility against established cost constraints.
3. Trial standard deviation were conducted with sparse grid based PCE simulation. For each UQ sampling point the CAE simulation consisted of:
 - a. A rotational velocity of 30 degrees per second was imposed on the rotary switch and the interaction of components simulated for 500 ms.
 - b. Peak and transient resistive torque were recorded.
4. Moment estimates for the peak resistive torque KPC were returned from the UQ tool and C_{pm} was calculated.

- Objective function fitness was assessed with a MOGA optimization algorithm (Section 5.9.4) and new trial standard deviations were generated (return to step 1).

The optimization was terminated at the iteration limit of 300 designs (Section 5.9.2).

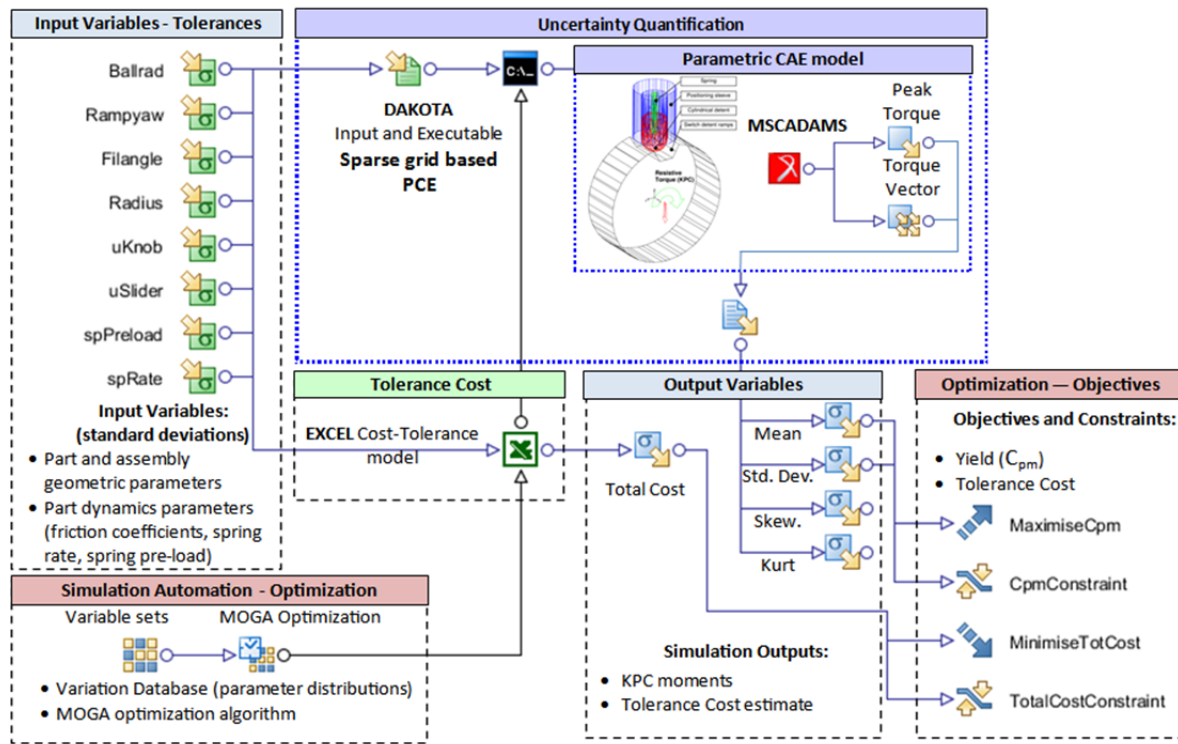


Figure 5.14 - PIDO tolerance synthesis workflow for Case study 5.2.

5.9.3 UQ strategy

Sparse grid based PCE was incorporated into the PIDO interface for UQ in the switch assembly CAE model. The PCE method of UQ drastically reduced the number of model evaluations required for estimation of the first and second moments of the assembly KPCs. The SG level was selected after comparing PCE moment estimates of resistive torque for the initial design (Section 5.9.5 and Table 5.10) for progressively larger SG levels. Level 1 required 17 model evaluations whereas level 2 required 177. The differences between the level 1 and level 2 estimates of mean and standard deviation were approximately $\delta_{\mu} = 1\%$ and $\delta_{\sigma} = 3\%$ (where δ_{μ} and δ_{σ} are defined in (5.55) and (5.56), respectively). The PCE based moment estimates were compared against a MC estimate of 5000 samples. The differences between the SG level 1 and MC estimates of mean and standard deviation are approximately $\delta_{\mu} = 2\%$ and $\delta_{\sigma} = 4\%$, respectively. Based on the small differences between SG based PCE moment estimates at different grid levels, and the small difference between the MC and SG level 1 estimates, an isotropic SG level of 1 was selected for use in tolerance synthesis simulation to reduce the overall number of model evaluations required.

5.9.4 Optimization strategy

The optimization algorithm employed was a Multi-Objective Genetic Algorithm (MOGA) with emphasised multi-search elitism (Deb *et al.* 2002). The number of generations was 15 with an initial population size of 20. The initial population is a uniformly distributed subset created by applying filtering to a MC sampled base population of 800 designs. The filtering maximizes the separation distance between base points resulting in more uniform sampling of the parameter space.

5.9.5 Simulation results and outcomes

Simulation results are shown in Table 5.10 and Figure 5.15. The tolerance synthesis platform was able to identify a design (design #540) with significantly superior performance to the previous best identified in tolerance analysis case study 4.2 (Section 4.6.5.2). Compared to the previous best, design #540 achieves a cost reduction of 40% and an increase in C_{pm} of 59%. Each evaluation of the CAE model took 8 seconds on a quad core 3.2 GHz CPU. Process integration overheads amount to a time of approximately 10 seconds per design. The total number of model evaluations was 5100 (17 for UQ and 300 for optimization) resulting in a total simulation time of approximately 14.2 hours. If UQ was conducted through traditional sampling methods such as MC with a relatively small sample size of 1000, the total simulation time would be a comparatively impractical 35 days. With additional time resources the selected design could be subjected to a local refinement to explore the objectives space within the vicinity of the selected optimum design with greater resolution.

The final design (Design ID#540) was validated against a MC reference estimate of 5000 samples. The differences between the PCE and MC estimates of mean and standard deviation were approximately $\delta_{\mu} = 1\%$ and $\delta_{\sigma} = 5\%$, respectively. This difference is considered negligible.

Table 5.10 - Case study 5.2 assembly parameters, associated variation and tolerance synthesis outcomes

Component	Switch			Spring		Cylindrical detent			Assembly	
Parameter	R _{switch} [mm]	A [deg]	Θ [deg]	F [N]	K [N/m m]	R _{ball} [mm]	μ _{switch}	μ _{slider}	Torque [Nmm]	Total Cost [Cost units]
Description	Switch radius	Angle of ramp face	Yaw angle of ramp face	Spring preload	Spring rate	Ball radius	Switch-detent dynamic friction coefficient	Slider-detent dynamic friction coefficient	Nominal peak resistive torque (KPC)	Total Tolerance cost of assembly
Nominal	15	30°	0°	2	0.400	3	0.150	0.150	75	
Specification Limits +/-	0.250	5°	3°	0.200	0.040	0.190	0.020	0.020	7	
Min.	14.750	25°	-3°	1.800	0.36	2.810	0.130	0.123	68	
Max.	15.250	35°	3°	2.200	0.440	3.190	0.173	0.173	72	
Initial										
μ	15	30°	0°	2	0.400	3	0.150	0.150	75.488	
σ	0.083	1.667	1	0.067	0.013	0.063	0.008	0.008	3.756	
C _{pm}	1	1	1	1	1	1	1	1	0.620	
Tolerance Cost	73.104	1	1	13.499	70.536	98.381	112.264	112.264		482.047
Manual allocation										
μ	15	30°	0°	2	0.400	3	0.150	0.150	75.404	
σ	0.083	0.833	1	0.033	0.013	0.032	0.008	0.008	1.985	
C _{pm}	1	2	1	2	1	2	1	1	1.150	
Tolerance Cost	77.818	1	1	41.137	70.536	98.381	112.264	112.264		514.399
Optimised (Design ID #540)										
μ	15	30°	0°	2	0.400	3	0.150	0.150	75.178	
σ	0.145	0.169	2.767	0.027	0.008	0.023	0.019	0.038	1.261	
C _{pm}	0.573	9.890	0.361	2.449	1.671	2.784	0.370	0.222	1.832	
Tolerance Cost	79.201	4.228	1	50.655	76.355	9.244	62.771	25.721		309.175

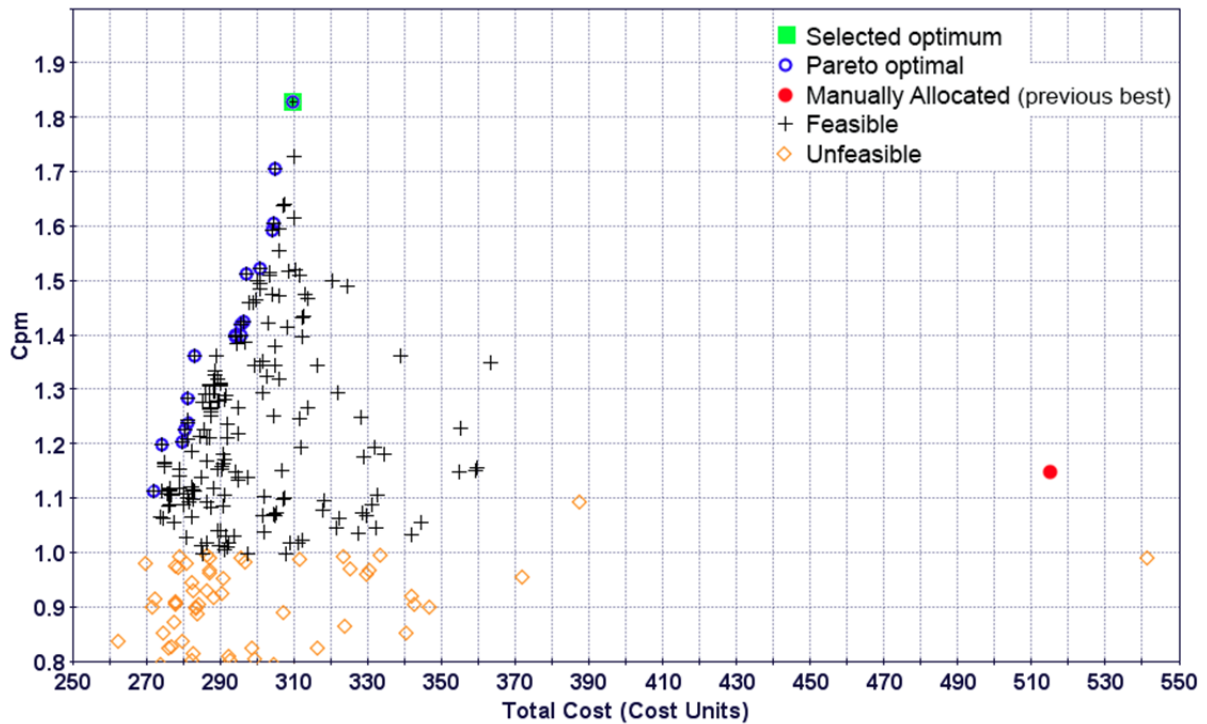


Figure 5.15 - Objectives space of tolerance synthesis for Case study 5.2.

The computational time could further be reduced by conducting a sensitivity study to assess if the influence of any part parameters on the assembly KPC is negligible. Parameters with low influence could be held fixed during UQ to reduce the number of required integration points. However this was deemed unnecessary, as the objective of this work is to demonstrate the significant computational cost reduction in tolerance analysis and synthesis through application of sparse grid based PCE even in the case of high dimensional problems.

5.10 Summary of research outcomes

Tolerance synthesis in complex mechanical assemblies can impose impractically high computational cost demands, particularly when numerical modelling of the effects of loading on assembly functionality is required. A main contributor to computational expense is the traditional use of robust, yet inefficient Monte Carlo (MC) sampling for uncertainty quantification in statistical tolerance analysis. This computational expense is compounded significantly in tolerance synthesis as it involves iteration of tolerance analysis. Previous methods for computational expense reduction in tolerance synthesis, have mainly focused on reducing the complexity and evaluation time of the associated assembly tolerance model with simplifying model approximations. These approximations can however compromise the fidelity of the tolerance model and introduce additional uncertainties.

In this chapter the feasibility of a proposed novel approach was investigated which addresses the high computational cost of MC sampling in tolerance analysis and synthesis, using Polynomial Chaos Expansion (PCE) uncertainty quantification. Compared to MC sampling, PCE results in significant reductions in the number of model evaluations required for statistical moment estimates.

The feasibility of PCE based UQ in tolerance analysis and synthesis was established with:

- A theoretical analysis of the PCE method identifying working principles, implementation requirements, advantages and limitations (Section 5.7 to 5.7.5).
- Establishing of recommendations for PCE implementation in tolerance analysis including methods of PCE coefficient calculation and approach to error estimation (Section 5.7.6 and 5.7.7)
- Novel implementation in PIDO based tolerance synthesis platform (Section 5.4)

The resultant PIDO based tolerance synthesis platform (Section 5.4) integrates:

- Highly efficient sparse grid based PCE UQ (Section 5.7).
- Parametric CAD and FE models accommodating the effects of loading (Section 4.4).
- Cost-tolerance modelling based on exponential functions (Section 5.5.2).
- Yield quantification with Process Capability Indices (PCI) (Section 5.5.2).
- Optimization of tolerance cost and yield with multi-objective Genetic Algorithm (GA) (Section 5.8.5).

The developed PIDO based tolerance synthesis platform was validated using two industry based case studies. The case studies include:

- An automotive seat rail assembly consisting of compliant components subject to loading by internal forces (Section 5.8).
- An automotive switch assembly in which functionality is defined by external forces and multi-body dynamics (Section 5.9).

In both case studies optimal tolerances were identified which satisfied desired yield and tolerance cost objectives. The addition of PCE to the tolerance synthesis platform resulted in considerable computational cost reductions without compromising accuracy compared to traditional MC methods (Sections 5.8.7 and 5.9.5). With traditional MC sampling UQ the required computational expense is impractically high.

Key outcomes of this research are as follows:

- The tolerance synthesis platform has been shown to overcome the impractical computational expense limitations associated with the tolerance synthesis of assemblies under loading.
- PCE has been demonstrated to be effective in significantly reducing the cost of UQ in tolerance analysis and synthesis.
- The developed platform enables tolerance analysis and synthesis integration within native CAD and FE modelling tools, thereby imposing low implementation demands.
- The PIDO based integration of multi-objective GA optimization offers effective tolerance synthesis capability in the presence of competing objectives and constraints. In contrast the optimization capabilities of CAT tools can be limited (Section 2.7).
- Due to the use of dedicated CAE modelling tools (such as ANSYS or ABAQUS FE modellers) the platform allows sophisticated abilities in modelling the effect of various loads on mechanical assemblies. As such, the platform could be applied to accommodate tolerance analysis of assemblies subject to a more general class of loading (such as fluid flow or thermo-mechanics).

Despite the enabling capability of the proposed platform, there are some limitations associated with the approach:

- PCE truncation error may be difficult to predict (Section 5.7.7).
- Parametric CAD and FE may include fundamental limitations in: accommodating all possible variation types defined in GD&T standards; and in representing realistic part interactions for a given set of assembly constraints.
- Accuracy errors associated with physical models used as part of CAE simulations such as modelling simplifications.

6 CONCLUSION

6.1 Chapter Summary

Achieving high manufacturing efficiency requires effective management of the effects of stochastic manufacturing variation on the performance of mechanical assemblies, particularly in the early design process where the potential to enact change is high. However, predicting and addressing the effects of manufacturing variation in mechanical assembly design poses significant challenges due to influences such as: complex part interactions, multiple variation types, loading effects, as well as competing manufacturing process cost and capability constraints. Tolerance analysis and synthesis methods for the management of manufacturing variation have seen extensive research and development efforts; however specific gaps in domain knowledge and limitations in existing methods were identified in this research. This dissertation sought to address these limitations, and develop methods for enhancing the engineering design of mechanical assemblies involving uncertainty or variation in design parameters. The research strategy for achieving this objective was directed at exploiting the potential of the emerging design analysis and refinement capabilities of Process Integration and Design Optimization (PIDO) tools. The main research objective was the development of a computationally efficient, PIDO based approach for tolerance analysis and synthesis of assemblies subject to loading, within the modelling environment of existing standalone CAD/E tools. The objective was successfully achieved through contributions in three research themes:

- Design analysis and refinement accommodating uncertainty in early design;
- Tolerancing of assemblies subject to loading; and,
- Efficient Uncertainty Quantification (UQ) in tolerance analysis and synthesis.

This chapter presents a summary of the outcomes of this research program and identifies associated novel contributions according to each research theme. Recommendations for potential areas warranting further research and development are also presented.

6.2 Contributions

The contributions of this work are presented below according to the associated research theme.

6.2.1 Design analysis and refinement accommodating uncertainty in early design (Chapter 3)

This research identified that a number of specific difficulties are encountered by designers when accommodating uncertainty and variation in early design stages. These difficulties include:

- The identification of Key Product Characteristics (KPCs) in mechanical assemblies (which are required for measuring functional performance) without imposing significant additional modelling and expertise demands;
- Accommodating the high computational cost of traditional statistical tolerance analysis in early design where analysis budgets are limited; and,
- Identifying feasible regions and optimum performance in early design stages within the associated large design space.

To address these difficulties a number of novel contributions were developed in Chapter 3 of this research. These contributions are categorically outlined below.

A PIDO tool based visualization method to aid designers in identifying assembly KPCs at the concept embodiment design stage (Section 3.3) (Mazur et al. 2010)

The developed method integrates the functionality of commercial CAD software with the process integration, UQ, data logging and statistical analysis capabilities of PIDO tools, to simulate manufacturing variation effects on the part parameters of an assembly and visualise assembly clearances, contacts or interferences. Visualizing variation within the assembly assists the designer in specifying critical assembly dimensions as KPCs for monitoring.

The method is implemented using a scripting interface between a CAD assembly model and a PIDO tool workflow. Automated monitoring of assembly parameters potentially relevant to the functionality of the assembly is established with the definition of measurements of assembly dimensions such as clearances (this is facilitated by measurement tools embedded in CAD software). Model parameters are subsequently subjected to expected manufacturing variation using UQ techniques such as MC sampling. For each assembly instance, assembly clash and interference analysis capabilities common in CAD software are executed using a

user script to automatically identify any unexpected part interferences. Images of the assembly instances including detailed views of any interference scenarios are automatically recorded for review by the designer. The evaluated CAD assembly model instance is stored for reference. Utilization of embedded measurement and interference analysis capabilities in CAD assembly environments offers rapid implementation. Visualization is carried out using native CAD models, which are often available at the concept embodiment design stage, thereby requiring low additional modelling effort.

The benefit of the proposed method has been validated using an industry based case study. The method enabled the automated identification of unintended component interactions in the concept design embodiment of an actuator used for automated folding of automotive side view mirrors (Section 3.3.2). Key outcomes are:

- The application of the developed PIDO visualization method identified a number of undesirable part clash and contact interactions in the actuator assembly model, after it was subjected to the expected manufacturing variation (Section 3.3.2.3). The frequency of interactions between associated part pairs was determined, along with the sensitivity of part parameter variation to the number of occurring interaction scenarios (Figure 3.8).
- Six specific assembly regions particularly prone to unwanted part interference were subsequently identified (Figure 3.9).
- These interactions, which had not been anticipated by the designers despite their experience with designs of this type, resulted in the specification of assembly KPCs that would otherwise have been overlooked.

The method developed in this research can be effectively applied to aid in the identification of KPCs without imposing significant additional modelling and expertise demands.

Computationally efficient manufacturing sensitivity analysis for assemblies with linear-compliant elements (Section 3.4) (Mazur et al. 2011).

Estimating the sensitivity of a design to manufacturing variation in the early design stages with statistical tolerance analysis, can reduce the costs of managing poor quality later in the manufacturing stage when the ability to enact change is limited. However, the computational cost of statistical tolerance analysis can be prohibitively high, especially when many evaluations of computationally demanding models (such as FE simulations) are necessary to model physical effects such as compliance. Additionally, the ability to carry out

tolerance analysis efficiently may be limited by the available tools and expertise required for formulating tolerance models and interpreting tolerance analysis results.

In this research an efficient method for estimating sensitivity to manufacturing variation was developed which significantly reduces computational cost, and imposes low implementation demands, in linear-compliant assemblies under loading. Reduction in computational cost are achieved by utilising linear-compliant assembly stiffness measures, reuse of CAD models created in the conceptual and embodiment design stages, and PIDO tool based tolerance analysis. The associated increase in computational efficiency, allows an estimate of sensitivity to manufacturing variation to be made earlier in the design process with low additional effort.

This method was developed as part of a benchmarking study of alternative automotive seat rail assembly concept embodiments aimed at quantifying their sensitivity to manufacturing variation (Section 3.4.1). The seat rail assemblies consist of two interlocking rail sections separated by a series of rolling elements. An interference fit upon assembly elastically preloads the rail sections which results in compliance effects due to the associated internal loading. Estimating functionality of the rail assemblies requires an FE simulation of the contact force between rail sections and rolling elements. Estimating the variation in functionality with FE models and traditional statistical tolerance analysis imposes significant computational costs, as a large number of FE model evaluations are required to provide sufficient accuracy.

An alternative approach was developed in this research which increases computational efficiency by taking advantage of the linear-elastic behaviour of the rail assembly (Section 3.4.3.1). Due to the linear-elastic condition, a measure of assembly stiffness can be used to estimate sensitivity to manufacturing variation. Estimating the stiffness requires only 3 evaluations of the FE model, significantly reducing overall computational expense. The benchmarking study identified significant differences in sensitivity to manufacturing variation between alternative designs (Section 3.4.7). Rail section designs characteristics which were found to influence sensitivity to manufacturing variation include: spacing between upper and lower rolling elements; the number of section folds leading to the rolling element location; and, the distance between a section fold and a rolling element. Identifying the sensitivity to manufacturing variation allowed the designers to proceed into the detail design stage with higher certainty of performance and with low additional analysis expense.

Due to the high associated efficiency, the method may be applied at the conceptual and design embodiment stages; thereby increasing knowledge early in the design process where analysis time budgets for individual concepts are limited. By measuring assembly stiffness in a similar manner, the developed method can be generalised and applied to assess the sensitivity to manufacturing variation in other linear-compliant assemblies whose functionality is dependent on applied loads. The outcome is a significant reduction in the computational cost of tolerance analysis.

For scenarios in which such a linear-compliant approach is not valid, the contributions in Chapter 5 present an alternative approach to reducing the computation cost of tolerance analysis based on more efficient uncertainty quantification. Associated contributions are summarised in Section 6.2.3.

Refinement of concept design embodiments through PIDO based DOE analysis and optimization (Section 3.5) (Leary, Mazur et al. 2010; Leary, Mazur et al. 2011)

The conceptual and embodiment stages of the design process can be associated with a vast design space in which regions of desirable performance are difficult to identify. In this research a design analysis and refinement approach, based on DOE analysis and optimization with PIDO tools, was presented which allows effective exploration of the design space and identification of optimum regions in the presence of complex constraints and competing objectives. The resulting increase of understanding of the design space early in the design process, allows for design improvements to be made when overall project cost commitments are low and design flexibility is high.

The conceptual design of automotive seat kinematics was presented as a highlighting case study. Automotive seat kinematics systems are associated with a large design space due to the number of design parameters (link lengths and frame position) and associated permutations (Section 3.5.1). Furthermore, multiple constraints and objectives hinder systematic optimization efforts. Historically, such problems were solved by inspection, or with graphical, or numeric aids. This research has presented an approach for resolving these conflicting design requirements at the conceptual design stage by mapping the feasible design space and rapidly identifying regions of high performance.

The capabilities of PIDO tools were utilised to allow CAE tool integration, and efficient reuse of models created in the conceptual and embodiment design stages, to rapidly identify optimal regions in the design space (Section 3.5.2). The design refinement and analysis approach consisted of two phases: initial analysis and design refinement. The initial phase

involved a high resolution DOE analysis which identified regions of infeasible performance in the design space. Subsequent refinement was carried out with a multi-objective GA optimization analysis initialised with the identified feasible design space. The optimization problem involved a complex set of four competing objectives and seven constraints. The total simulation size involved 122,880 model evaluations in which 20,204 feasible designs were identified with 304 designs being Pareto-optimal (Figure 3.23). Designer preference objective weighting was applied and the Pareto-optimal design space was reduced to three designs of interest which offered a balanced compromise between competing objectives.

An identified Pareto-optimal concept was selected for detail design and manufacture by the industry partner. The selected design was found to offer the best performance in achieving a vertical seat travel objective with the least number of manual actuations (these are actuations required to lift the seat for a given fixed lift effort) (Table 3.10). The superior performance against competitors in seat actuation demands was a determining factor for the selection of the design in the seat assembly of the *Tesla Motors Model S* full-sized electric sedan currently on sale in the United States.

The presented PIDO based DOE analysis and optimization approach to exploring the design space in the conceptual and embodiment design stages can be broadly applied. An example of conceptual wheelchair design was used to demonstrate the benefits of the developed approach (Section 3.5.3) (Burton *et al.* 2010; Leary *et al.* 2012).

This contribution has highlighted the benefits of investigating the conceptual and embodiment design space through DOE analysis and optimization, with a practical case study. The outcome has resulted in the successful commercialisation of an automotive seat kinematics design.

The novel contributions presented in Chapter 3 have been demonstrated to enhance the design of mechanical assemblies involving uncertainty or variation in design parameters, in the early stages of design. The contributions have addressed the domain knowledge limitations identified in research associated with: the identification of KPCs; accommodation of the high computational expense of tolerance analysis; and, identification of optimal regions in broad design spaces. Practical conceptual and embodiment design problems were considered, and effective solutions developed for a number of industry relevant scenarios. The use of PIDO tools and native CAD/E models developed as part of an established design modelling procedures enables these contributions to be applied with low additional modelling effort. The outcomes allow designers to make informed decisions which positively influence the design early in the design process while cost commitments are low.

6.2.2 Tolerancing of assemblies subject to loading (Chapter 4)

Despite the extensive capability of existing analytical and numerical methods in addressing tolerance analysis problems in complex mechanical assemblies, this research identified that key limitations remain. Particular limitations are associated with the ability to comprehensively accommodate tolerance analysis problems in which assembly functionality is dependent on the effects of loading (such as compliance or multi-body dynamics). Current methods are limited by: the ability to accommodate only specific loading effects; reliance on custom simulation codes with limited implementation in practical and accessible software tools; and, the need for additional expertise in formulating specific assembly tolerance models and interpreting results.

Computer Aided Tolerancing (CAT) tools were identified that accommodate a limited subset of loading effects such as deformation of sheet assemblies (Section 2.7). However, in general the abstracted geometric tolerance models employed in current CAT systems are incompatible with tolerance analysis involving a general class of problem requiring numeric simulation of assemblies under loading. As such, this research identified that there is a lack of an accessible approach to tolerance analysis of assemblies subject to a general class of loading effects, which integrates effectively into the established CAD/E design framework.

These limitations were addressed in Chapter 4 of this work through the development of a novel tolerance analysis platform which integrates CAD/E and statistical analysis tools, using PIDO tool capabilities, to facilitate tolerance analysis of assemblies subject to loading (Section 4.4). Integration was achieved by developing script based links between standalone CAD/E software, through commonly embedded scripting capabilities, and the process integration facilities of PIDO tools. This integration allows for tolerance analysis through:

- Definition of a parametric CAD assembly model, including tolerance types and datums, for features of interest as well as part relationships such as assembly sequence and mating conditions (Section 4.4.2).
- Numerical simulation of the effect of loads on assembly functionality by integration of CAD models with CAE tools such as FE modellers (Section 4.4.3).
- Uncertainty quantification (Section 4.4.4) and yield estimation (Section 4.4.6) with the statistical simulation capabilities of PIDO tools.
- Storage of simulation inputs and results in a variation database (Section 4.4.5).

Key contributions of this research are:

- The proposed platform extends the capabilities of traditional CAT tools and methods by enabling tolerance analysis of assemblies which are dependent on the effects of loads.

- The ability to accommodate the effects of loading in tolerance analysis allows for an increased level of capability in estimating the effects of variation on functionality.
- The interdisciplinary integration capabilities of the PIDO based platform allow for CAD/E models created as part of the standard design process to be used for tolerance analysis. The need for additional modelling tools and expertise is subsequently reduced.
- The use of specialised CAE modelling tools such as FE modellers (for example ABAQUS or ANSYS) or multi-body dynamics simulation codes (such as MSC ADAMS) allows sophisticated abilities in modelling the effect of various loads on mechanical assemblies. As such, the application of the platform can be extended to accommodate tolerance analysis of assemblies subject to a more general class of load (for example thermo-mechanics or fluid flow) as well as challenging scenarios involving transient or non-linear response.

To demonstrate the capabilities of the developed platform, industry based case study tolerance analysis problems involving assemblies subject to loading were presented. The specific outcomes of those case studies are summarised below.

Case study 4.1: An automotive actuator assembly in which functionality is defined by compliance of part geometry due to external loading (Section 4.5).

- This case study addressed a tolerance analysis problem involving an automotive actuator assembly consisting of a rigid spigot and complaint spring undergoing compression due to external loading. Functional characteristics required clearance between the spigot wall and the spring at all times (while minimising overall packaging space) and that manufactured assemblies achieve this requirement with a yield of $C_{pk} = 1$ (i.e. 99.7%). The objective was to specify nominal spigot diametral dimension (parameter OD_{pocket} in Figure 4.3) such that the required assembly yield is achieved when the assembly parameters are subjected to the expected manufacturing variation.
- No analytic solution directly applicable to the dilation of the squared and ground compression spring used in the actuator was found in the literature (Section 4.5.1). This problem was therefore a suitable case study for the proposed platform as numerical models are required. The platform proposed in this work was applied to overcome these limitations.
- To estimate the expected manufacturing variation associated with the spigot and spring components, existing manufacturing process data for similar components was analysed and used as input into subsequent tolerance analysis simulations (Section 4.5.3).

- Parametric CAD and FE models of the spigot and compliant spring were developed (Figure 4.4) and interfaced using a PIDO tool according to the proposed platform (Figure 4.5). The resulting model was used to estimate expected assembly yield with a Monte Carlo UQ simulation based on a sample size of 1000.
- The tolerance analysis platform was applied to identify that for initially specified tolerances the assembly yield was unacceptable at $C_{pk} = 0.68$ (97%). The nominal diametral pocket dimension OD_{pocket} required to achieve the desired assembly yield were subsequently inferred from the simulation outcomes, thereby successfully satisfying the case study objectives.

Case study 4.2: An automotive switch assembly in which functionality is defined by external loading and internal multi-body dynamics (Section 4.6).

- The second case study involved an automotive rotary switch in which a resistive actuation torque is provided by a spring loaded radial detent acting on the perimeter of the switch body. Functional characteristics required that the peak resistive torque for switch actuation be within an ergonomically desirable range. As such, assembly functionality is defined by both frictional and multi-body dynamics loading effects. The case study objective was to specify detent and spring parameter tolerances, such that a peak resistive torque specification limit of 75 ± 7 Nmm be achieved, with a yield requirement of $C_{pm} = 1$, (i.e. 99.7%).
- A parametric numerical model of the switch assembly was constructed in MSC ADAMS multi-body dynamics modelling software (Figure 4.12) accommodating the possible variation within geometric and physical assembly parameters (such as spring pre-load, spring stiffness and friction coefficients). No directly comparable algebraic model for the switch assembly was identified, however, an approximate model was used to confirm that the numerically predicted results were of a similar magnitude (Section 4.6.4).
- Existing manufacturing process data for similar components was used as input into subsequent tolerance analysis simulations (Section 4.6.3).
- The numerical model was interfaced with a PIDO tool according to the developed platform (Figure 4.14) and subjected to Monte Carlo UQ simulation with a sample size of 1000. The simulation results showed that the required assembly yield requirements were not met (achieved $C_{pm} = 0.62$, required $C_{pm} = 1$) with initially specified part parameter tolerances (Table 4.4).
- Based on the outcome of the initial MC simulation, the required process capabilities for the most influential parameters were increased (Table 4.4). A subsequent simulation

successfully identified the part parameter tolerances required to achieve the required assembly yield (Section 4.6.5.2).

The presented case studies demonstrated that the PIDO based tolerance analysis platform developed in this research has proven benefit in solving practical tolerance analysis problems, involving assemblies subject to various loading effects. The platform offers an accessible tolerance analysis approach with low implementation demands due to integration with the established CAD/E modelling design framework. It provides capability and flexibility which is not otherwise available with existing CAT tools. However an associated limitation is the potentially high computational cost of traditional uncertainty quantification with tolerance models which are computationally demanding to evaluate (such as FE models of the effects of loads on mechanical assemblies). The contributions of Chapter 5 respond to this limitation.

6.2.3 Efficient uncertainty quantification in tolerance analysis and synthesis (Chapter 5)

The cost of tolerance synthesis involving demanding assembly models (particularly assemblies under loading) can often be computationally impractical. The high computational cost is mainly associated with traditional statistical tolerancing Uncertainty Quantification (UQ) methods reliant on low-efficiency Monte Carlo (MC) sampling.

Chapter 5 responded to the hypothesis that Polynomial Chaos Expansion (PCE) based UQ is feasible in tolerance analysis, and that the significant reduction in computational costs associated with PCE can enable the PIDO based tolerance analysis platform developed in Chapter 4 to be extended to allow multi-objective, tolerance synthesis in assemblies subject to loading. This hypothesis was assessed and the feasibility of using PCE for UQ in the developed PIDO tolerance analysis and synthesis platform was subsequently established. This was achieved by:

- A theoretical analysis of the PCE method identifying working principles, implementation requirements, advantages and limitations (Section 5.7 to 5.7.5). This analysis identified that the PCE method meets the requirements for implementation in tolerance analysis in the context of this research, namely: non-intrusive nature that is applicable to integration with existing CAD/E and PIDO tools; high efficiency and accuracy; flexibility in accommodating various input parameter distributions; and ability to efficiently accommodate problems with high dimensionality.
- Identification of a preferred method for determining PCE expansion coefficients in tolerance analysis. A number of methods were assessed (Section 5.7.5). It was found

that the effective applicability of each PCE coefficient determination method depends on the dimensionality of the problem, as well as the order of the PCE expansion; both of which are dictated by the UQ simulation requirements. It was concluded that a sparse grid based stochastic projection technique for determining PCE coefficients be adopted in tolerance analysis and synthesis (Section 5.7.6). This is due to superior efficiency (the least number of required model evaluations) for a broad range of problem dimensionality (as demonstrated in Table 5.2 and Table 5.4.).

- Formulation of an approach for the validation of PCE moment estimates (Section 5.7.7). It was found that a reference MC moment estimate is currently the most broadly applicable and robust indicator of PCE moment estimates for implicit systems. It is recommended that MC estimates be used to validate initial and final designs carried out as part of tolerance synthesis. This approach was successfully adopted in the case studies considered in this work and showed that PCE moment estimates closely match those obtained with traditional MC simulation.

PCE based UQ was subsequently implemented in a PIDO based tolerance synthesis platform for assemblies subject to loading (Section 5.4). This was achieved by extending the tolerance analysis platform developed in Chapter 4, with the additional development of the script based links between standalone CAD/E software to include additional PCE implementation codes and cost-tolerance models. The resultant PIDO based tolerance synthesis platform (Section 5.4) integrates: Highly efficient sparse grid based PCE UQ (Section 5.7); Parametric CAD and FE models accommodating the effects of loading (Section 4.4); Cost-tolerance modelling (Section 5.5.2); Yield quantification with Process Capability Indices (PCI) (Section 5.5.2); and, Optimization of tolerance cost and yield with multi-objective Genetic Algorithm (GA) (Section 5.8.5).

The PIDO tolerance synthesis platform incorporating PCE UQ was validated using two industry relevant case studies. The specific outcomes of those case studies are summarised below.

Case study 5.1: An automotive seat rail assembly consisting of compliant components subject to internal loading (Section 5.8).

- This case study significantly extended the work of Section 3.4 and addressed a tolerance synthesis problem involving an automotive seat rails assembly consisting of two interlocking rail sections separated by a series of rolling elements. The rail sections are preloaded elastically by an interference fit upon assembly and are subject to compliance effects as a result of the associated internal loading. The objectives of tolerance

synthesis were to identify optimal rail section bend angle and bend radii tolerances, which: maximize the number of assemblies meeting a rail rolling effort force requirement of 35 ± 8 N with a corresponding minimum required assembly yield of $C_{pm} = 1$ (i.e. 99.7%); and, minimize the associated total tolerance cost with a maximum allowable cost of 8000 cost units.

- A rail assembly tolerance model was constructed consisting of: a CATIA based CAD model defining rolling element position; and, an ABAQUS FE model estimating bearing contact force due to internal loading (Section 5.8.3). Tolerance cost was modelled using cost-tolerance curves developed in conjunction with an industry partner (Figure 5.7 and Figure 5.8). This was based on CMM metrological measurements conducted on 24 rail assembly sets currently produced by the industry partner (Section 5.8.2).
- The tolerance models were interfaced according to the developed PIDO tolerance synthesis platform (Figure 5.10). UQ was conducted using a sparse grid based PCE approach (Section 5.8.4).
- Initial tolerance analysis revealed that the yield, which would be achieved if the case study rail assembly were to be manufactured with the same process standards as the measured rails, were unsatisfactorily low at $C_{pm} = 0.12$. Tolerance synthesis was subsequently conducted and a number of Pareto optimal designs with higher yield were identified. From the identified Pareto optimal designs (Figure 5.12) the lowest cost design (Design #114) was selected as the preferred candidate. The selected design offers the lowest tolerance cost while exceeding the yield requirement of $C_{pm} = 1$ by 11% (achieved $C_{pm} = 1.11$). The higher yield allows for conservatism in the estimated results.
- The associated PCE based moment estimates for the initial and final designs were compared against a reference MC estimate of 3000 samples. The differences for the initial design between PCE and MC estimates of mean and standard deviation were approximately $\delta_{\mu} = 3\%$ and $\delta_{\sigma} = 5\%$, respectively (Section 5.8.4). For the final design (Design ID#114) the differences between the PCE and MC estimates of mean and standard deviation was approximately $\delta_{\mu} = 3\%$ and $\delta_{\sigma} = 4\%$, respectively (Section 5.8.7). This difference is considered negligible.
- The implementation of sparse grid based PCE for UQ reduced the computational cost of tolerance synthesis by a factor of 22, compared to a traditional MC based approach (Section 5.8.7). The computational cost associated with the tolerance synthesis would be impractically high if conducted using traditional MC based UQ, whereas the sparse grid based PCE method provides a feasible alternative.

Case study 5.2: An automotive switch assembly in which functionality is defined by external forces and internal multi-body dynamics (Section 5.9).

- The case study focused on the allocation of tolerances in rotary switch assembly subject to loading. This presented a significant extension of the tolerance analysis problem presented in case study 4.2 by address a tolerance synthesis problem in which an optimal set of part tolerances is identified, minimising manufacturing cost while maximising assembly yield. The objectives were to specify detent and spring parameter tolerances, which: maximize the number of assemblies conforming to the peak resistive torque specification requirements of 75 ± 7 Nmm (corresponding to $C_{pm} = 1$); and, minimise the total cost of required part tolerances with a maximum allowable tolerance cost of 515 cost units. Tolerance cost was modelled using cost-tolerance curves developed in conjunction with an industry partner (Figure 5.13).
- A parametric numerical model of the switch assembly (Section 4.6.4) was interfaced with the developed PIDO tolerance synthesis platform (Section 5.4). Tolerance synthesis was subsequently conducted and a number of Pareto optimal designs were identified.
- The tolerance synthesis platform was able to identify a design (design #540 in Table 5.10 and Figure 5.15) with significantly superior performance to the previous best identified in tolerance analysis case study 4.2 (Section 4.6.5.2). Compared to the previous best, design #540 achieves a cost reduction of 40% and an increase in C_{pm} of 59%.
- The associated PCE based moment estimates for the initial and final designs were compared against a reference MC estimate of 5000 samples. The differences for the initial design between PCE and MC estimates of mean and standard deviation were approximately $\delta_{\mu} = 2\%$ and $\delta_{\sigma} = 4\%$, respectively (Section 5.9.3). For the final design (Design ID#540) the differences between the PCE and MC estimates of mean and standard deviation was approximately $\delta_{\mu} = 1\%$ and $\delta_{\sigma} = 5\%$, respectively (Section 5.9.5). This difference is considered negligible.
- The implementation of sparse grid based PCE for UQ reduced the computational cost of tolerance synthesis by a factor of 59, compared to a traditional MC based approach (Section 5.9.5). The computational cost associated with the tolerance synthesis would be impractically high if conducted using traditional MC based UQ

In both case studies optimal tolerances were identified which satisfied yield and tolerance cost objectives. The addition of PCE to the tolerance synthesis platform resulted in large computational cost reductions without compromising the accuracy achieved with traditional MC methods.

This research has contributed to addressing the high cost of UQ with the novel integration of highly efficient Polynomial Chaos Expansion (PCE) based UQ with tolerance analysis and synthesis. The resulting significant reduction in computational costs enable the PIDO based tolerance analysis platform developed in Chapter 4 to be further extended to allow multi-objective, tolerance synthesis in assemblies subject to loading. The resulting tolerance synthesis platform can be applied to tolerance analysis and synthesis with significantly reduced computation time while maintaining accuracy.

Key contributions of Chapter 5 are:

- The tolerance synthesis platform has been shown to overcome the impractical computational expense limitations associated with traditional, low-efficiency Monte Carlo based UQ tolerance synthesis of assemblies under loading.
- PCE has been demonstrated to be effective in significantly reducing the cost of UQ in tolerance analysis and synthesis.
- The developed platform enables tolerance analysis and synthesis integration within native CAD and FE modelling tools, thereby imposing low implementation demands.
- Due to the use of standalone CAE modelling tools, the effect of various loads on mechanical assemblies can be accommodated by broadening the application of the platform.
- The PIDO based integration of multi-objective GA optimization offers effective tolerance synthesis capability in the presence of competing objectives and constraints. In contrast the optimization capabilities of CAT tools can be limited (Section 2.7).

6.3 Future work

This research developed novel PIDO based methods that have the capacity to improve the design of mechanical assemblies involving uncertainty or variation in design parameters. The main contribution focused on efficient tolerance analysis and synthesis of assemblies subject to loads, within the native CAD/E modelling environment, using a PIDO tool based platform. The effectiveness of the research outcomes of this work is validated with a number of practical, industry related case studies. Although the contributions are well established, further research prospects exist. This section provides a list of potential avenues for future work associated with the general research objectives of this project.

- Significant additional reductions in the computational cost of UQ associated with tolerance analysis can be achieved, if the assembly response functions exhibits pronounced anisotropic sensitivity to the associated part parameters. Such system

anisotropy can be exploited with anisotropic sparse grid quadrature PCE techniques. These techniques use a different univariate quadrature rule level for different sparse grid dimensions, effectively reducing the total number of points used in the sparse grid (and subsequently reducing the number of system model evaluations) (Section 5.7.5.5). However in complex systems (such as mechanical assemblies with many parts and features) the nature of anisotropy is often not known *a priori*, and as such, an active research focus of PCE based UQ has been the development of effective anisotropic approaches with automated adaptivity. Adaptive techniques aim to automatically discern the system anisotropy by progressively increasing quadrature rule levels in selected dimensions, and monitoring the associated influence on the system outputs. Recent advances in the effectiveness of these techniques offer promising prospects for further UQ cost reduction in tolerance analysis and should be investigated further (Jakeman *et al.* 2011; Jakeman *et al.* 2011; Liu *et al.* 2011).

- Recent advances have been made in the development of tools for facilitating grid/distributed computing capabilities with standalone CAD/E software. Grid computing has the capability to accelerate simulation times by enabling sharing of computational resources over multiple computers networked through conventional interfaces, such as Ethernet (Rawat *et al.* 2009; Mo *et al.* 2010; Pan *et al.* 2010). The capabilities allow the computer workstation infrastructure available in typical engineering design office environments to be utilised for simulation during times when it is idle (such as overnight). A central distributed scheduling tool installed on one main workstation coordinates multiple simulation instances over a number of workstations in the grid network; simulation outputs are subsequently compiled on the main workstation. The CAD/E software tools required for simulation need to be installed locally on each workstation, along with a grid communication module. As multiple CAD/E workstation software licences are a common scenario in engineering design environments, this approach can increase utilization of available resources with low implementation demands. The PIDO tolerance analysis and synthesis platform developed in this research is compatible with grid computing tools. This capability offers an interesting opportunity for further research.
- A number of *Mesh morphing* methods have been developed for directly modifying FE model dimensions without requiring geometric changes to associated underlying CAD models (Owen *et al.* 2010; Franciosa *et al.* 2011). Changes in geometry are achieved by directly reshaping the mesh elements at nodal co-ordinate levels. Reducing the need for CAD model updates can decrease overall computational cost of tolerance analysis of

assemblies requiring FE models to quantify the effects of loading. The feasibility of incorporating mesh morphing into the tolerance analysis and synthesis platform developed in this work offers interesting prospects for future research.

APPENDICES

A. TOLERANCING SCHEMES

A.1 Dimensional tolerancing

Dimensional tolerancing specifies the acceptable size of a part feature and any associated fit between features of mating parts. The size of a feature is specified by a nominal (basic) size, and an associated Lower specification limit and Upper Specification Limit (LSL and USL⁴, respectively). The tolerances that can be specified are limited to an allowable plus or minus variation on the linear dimensions of a feature. The dimensional tolerancing method is straightforward and used extensively, but is subject to a series of deficiencies (Voelcker *et al.* 1993; Voelcker 1998; Cogorno 2006):

1. Dimensional tolerancing methods typically result in rectangular tolerance zones which may not capture the intended assembly functionality. For example, rectangular tolerance zones are not well suited for tolerancing cylindrical features.
2. The interaction between tolerances is not accommodated. This may result in scenarios where a tolerance is unnecessarily stringent.
3. Dimensional tolerancing does not accommodate the relative importance of datums.

A.2 Geometric Dimensioning and Tolerancing (GD&T)

To overcome the deficiencies of dimensional tolerancing, a more robust tolerancing scheme was developed based on allowable geometric volumes. Geometric tolerancing allows for the definition of tolerance types which are not limited to linear dimensions of a part feature, but also accommodate geometric characteristics such as variation in surface flatness. This tolerancing scheme, known as Geometric Dimensioning and Tolerancing (GD&T) was developed and standardised based on conventions developed from an accumulation of

⁴ The terminology Maximum Material Condition (MMC) and Least Material Condition (LMC) are also applied (ASME 2009). The MMC is associated with the largest allowable component volume, and is therefore dependant on the dimension type. For example, holes remove material and the MMC is equivalent to the LSL hole diameter; cylindrical features add material and the MMC occurs for the USL hole diameter. USL and LSL will be used in this work as they are associated with the dimension magnitude and are independent of whether the dimension increases or decreases part volume.

empirical knowledge and engineering practice within industry over many decades (Voelcker *et al.* 1993; Voelcker 1998; Shah *et al.* 2007).

The GD&T approach defines tolerance zones within which a feature is allowed to vary. In addition to the capabilities of dimensional tolerancing, a geometric tolerancing approach accommodates specific types of geometric variations in feature parameters such as orientation, location, form, profile and runout. The specific types of geometric tolerances are classified according to their functionality:

- Orientation – specifies the permitted rotation of a feature relative to a datum.
- Location – specifies the allowable deviation in the location of a feature from a desired nominal location specified by a datum.
- Form – specifies the amount a surface of a feature is allowed to deviate from the desired nominal. The nominal surface is taken as the datum.
- Profile – comparable to form tolerances but are specified to a datum external to the feature.
- Runout – defined in terms of the radial variation from a true datum circle measured at one axial location of cylindrical feature (circular runout), or by the circular runout measured along the entire axis of the cylindrical feature (total runout).

The variation types are represented with standardised symbols and notations (Table A.1). Additional concepts such as virtual and resultant condition boundaries and material condition modifiers are also defined in GD&T tolerancing schemes. These are formalised in numerous drawings standards such as:

- ASME Y14.5 - 2009 Dimensioning and Tolerancing (ASME 2009)
- ISO 1101:2005 Geometrical Product Specifications (GPS). Tolerancing of form, orientation, location and run-out (ISO 2005).
- ISO 5458:1998 Geometric Product Specifications (GPS). Positional tolerancing (ISO 1998).
- ISO 286-1:1988 ISO system of limits and fits (ISO 1988)

GD&T standards for three-dimensional CAD include:

- ASME Y14.41-2003 Digital Product Definition Data Practices (ASME 2003)
- ISO 16792:2006 Technical product documentation – Digital product definition data practices (ISO 2006)

Table A.1 - GD&T variation types and standardised symbols (after ANSI Y14.5).

Geometric variation category	Geometric variation type	GD&T Symbol (ANSI Y14.5)
Orientation	Angularity	
	Parallelism	
	Perpendicularity	
Location	Concentricity	
	Positional	
	Symmetry	
Form	Circularity	
	Cylindricity	
	Flatness	
	Straightness	
Profile	Profile of a line	
	Profile of a surface	
Runout	Circular runout	
	Total runout	

The most widely adopted standards are ASME Y14.5 and ISO 1101 which offer a comprehensive specification of GD&T principles. These principles are implemented by the use of a Feature Control Frame (Figure A.1). The feature control frame is a standardised graphical framework which conveys information concerning geometric tolerancing symbols, tolerance values, and datum references. Feature control frames are associated with dimensions, datum references, or features in engineering drawings. Feature Control Frames typically have a standardised GD&T variation type symbols in the first cell, a tolerance value with a zone descriptor and material modifier (if any) in the second cell, followed by cells having Datum references which depend on the design specification that the tolerance definition is intended to convey. For example, the feature control frame in Figure A.1 is to be interpreted as "The position of the axis of a feature when produced within allowable size limits can be off-centre within a diametral tolerance zone of 0.15 when produced at Maximum Material Condition. The feature is primarily located on Datum A, secondarily on Datum Feature B when produced at Maximum Material Condition, and Datum C as Tertiary references."

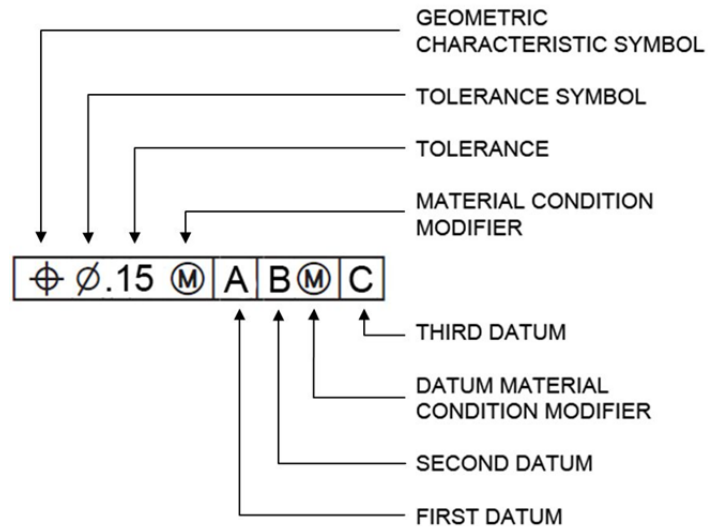


Figure A.1 - GD&T tolerance control frame

GD&T standards overcome the deficiencies of dimensional tolerancing by (Roy *et al.* 1991; Juster 1992; Yu *et al.* 1994; Hong *et al.* 2002; ASME 2009):

1. Rectangular tolerance zones are complemented with geometric tolerance zones compatible with the geometry being manufactured.
2. Where an interaction between tolerances zones exists it is explicitly defined. For example Figure A.2 shows a plate with a semi-circular hole feature with centre position and diameter tolerances. As the hole diameter increases towards its USL (the LMC), the tolerance associated with the centre position may be increased without compromising function. Conversely, when the diameter is at the LSL (the MMC) the centre position tolerance zone is smallest (at 0.1 mm). This relationship can be accommodated using the GD&T datum material condition modifier (circle M).
3. Datum precedence is accommodated. In Figure A.2 the semi-circular hole feature is located relative to both the lower plate edge and side plate edge. When dimensioned with traditional tolerancing methods (Figure A.2 (i)) the priority of dimension locations is ambiguous when a part is subject to manufacturing variation (Figure A.2 (ii) and (iii)). GD&T principles allow the relative importance of datums to be specified to eliminate ambiguity (Figure A.2 (iv)). The feature control frame associated with the hole centre position states that the order of datum precedence is alphabetical i.e. datum A takes precedence of datum B.

Despite overcoming many of the deficiencies of dimensional tolerancing, geometric tolerancing has its own shortcomings. As GD&T is a codification of accumulated empirical knowledge and industrial engineering practice, it is not founded on explicitly defined

mathematical principles, but rather defined through graphics and example scenarios (Shah *et al.* 2007). This lack of mathematical formality can lead to ambiguity in interpretation of GD&T standards and difficulty in integration with CAD modelling tools (Voelcker *et al.* 1993; Voelcker 1998).

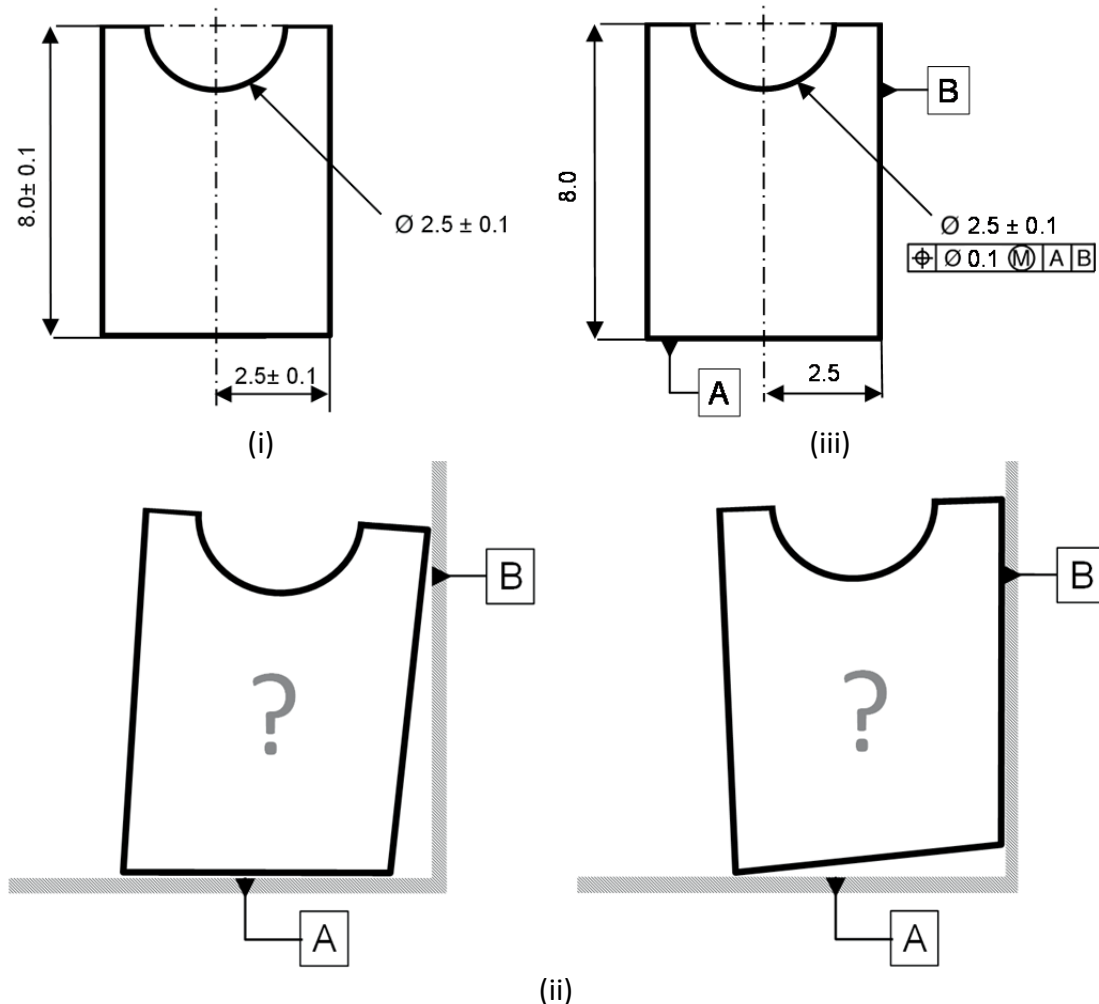


Figure A.2 - Traditional dimensional tolerancing (i). Traditional tolerancing involves datum ambiguity in manufactured parts (ii). GD&T tolerancing including alphabetical datums precedence specification (iii) eliminates ambiguity.

A.3 Vectorial tolerancing

An alternative which aims to address the deficiencies of both dimensional and GD&T based tolerancing schemes is vectorial tolerancing (Wirtz 1993). The vectorial tolerancing scheme aims to define all variation in geometrical parts and assembly parameters in terms of vector models. The vector models are constructed in a manner which is intended to be applicable not only to tolerancing schemes but also to other dimensional control activities such as CAD modelling, CNC machining and metrological measurements with Coordinate Measurement Machinery (CMM) tools (Wirtz *et al.* 1993). The objective is to avoid the ambiguity and

integration problems encountered with GD&T standards by providing a comprehensive dimensional control model based on the same fundamental model.

Despite the potential advantages of the vectorial tolerancing approach, a significant drawback is the lack of compatibility with the syntax and semantics of dimensional and GD&T tolerancing schemes which are broadly established both institutionally and industrially. The substitution of the currently accepted tolerancing schemes, with their long historical tradition, with an alternative model has proven difficult and is the main reason for the lack of adaptation of methods such as vectorial tolerancing (Britten *et al.* 1999)

B. PROCESS CAPABILITY

B.1 Process capability index – C_p

The C_p index measures the potential of a process to produce outputs within the specification limits (Equation (A.57)). C_p increases with a decreasing standard deviation of the process output. Although it is readily calculated, it does not measure whether the process is centred on the specified nominal output value. An output distribution that has a low standard deviation but is skewed towards a specification limit would result in the same C_p index as a distribution that is centred (Figure A.4). Therefore C_p overestimates process capability if the process mean is non-centred, i.e. the nominal and mean values differ (Figure A.3 and Figure A.4). Furthermore the C_p index assumes that the nominal target value is at the midpoint of the specification limits and different target values are not accommodated.

$$C_p = \frac{USL - LSL}{6\sigma} \quad (\text{A.57})$$

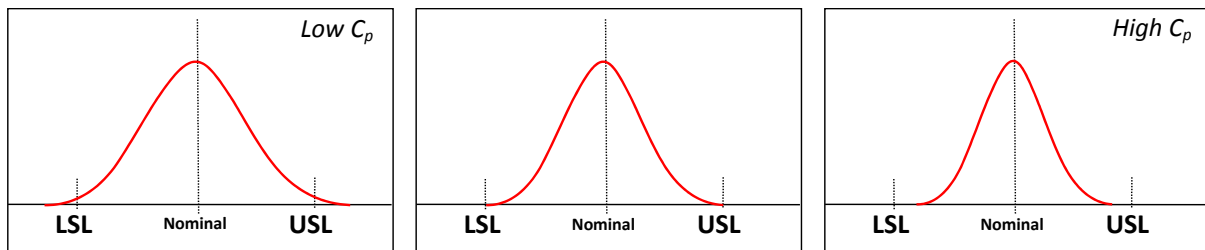


Figure A.3 - Process output distributions with decreasing standard deviation.
 C_p increasing from left to right with decreasing standard deviation.

B.2 Process capability index – C_{pk}

The C_{pk} index is applied to measure both the ability of a process to produce an output that is centred and within the specification limits. C_{pk} reduces the index value if the process is not centred (Equation (A.58)). If the process output mean is skewed away from the nominal target value, C_{pk} becomes smaller than C_p . The C_{pk} index however does not accommodate a process in which the nominal is not at the mid-point of the specification limits, and in such a scenario C_{pk} underestimates process capability. For example, all the distributions in Figure

A.4 have the same C_p index despite a difference in conformance to the specification limits; the C_{pk} index however accommodates the difference due to the mean shift.

$$C_{pk} = \min(C_{pl}, C_{pu}) = \min\left(\frac{USL - \mu}{3\sigma}, \frac{\mu - LSL}{3\sigma}\right) \quad (A.58)$$

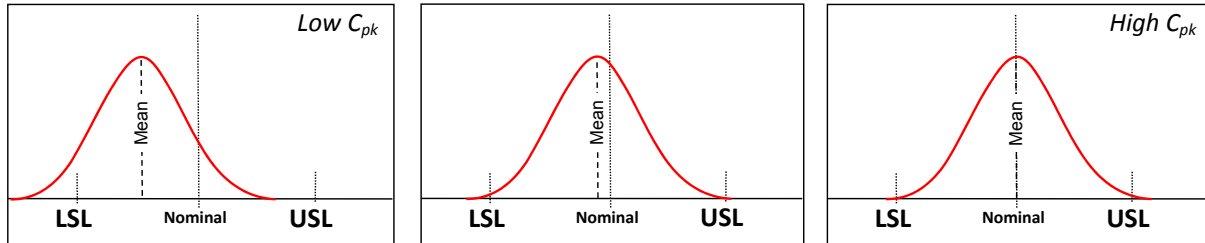


Figure A.4 - Process output distributions of equal standard deviation and increasing centring. C_p is equal for all distributions. C_{pk} increases from left to right with increasing centring.

B.3 Process capability index – C_{pm}

C_{pm} is similar to C_{pk} yet includes the capability to accommodate an arbitrary nominal value, i.e. asymmetric specification limits. The C_{pm} index measures both the ability of a process to achieve an arbitrary target nominal value, τ , and the specification limits (Chan *et al.* 1988) (Equation (A.59)). C_{pm} addresses the drawbacks associated with the C_p and C_{pk} indices however incurs a comparatively higher computational cost. C_{pm} increases as the process mean approaches the target nominal value (i.e. more centred) and as the standard deviation decreases. C_{pm} is particularly useful when the target nominal value is not at the mid-point of USL and LSL i.e. non-symmetric specification limits (e.g. Figure A.5).

$$C_{pm} = \frac{USL - LSL}{6\sqrt{\sigma^2 + (\mu - \tau)^2}} \quad \text{Where } \tau \text{ is the target nominal value} \quad (A.59)$$

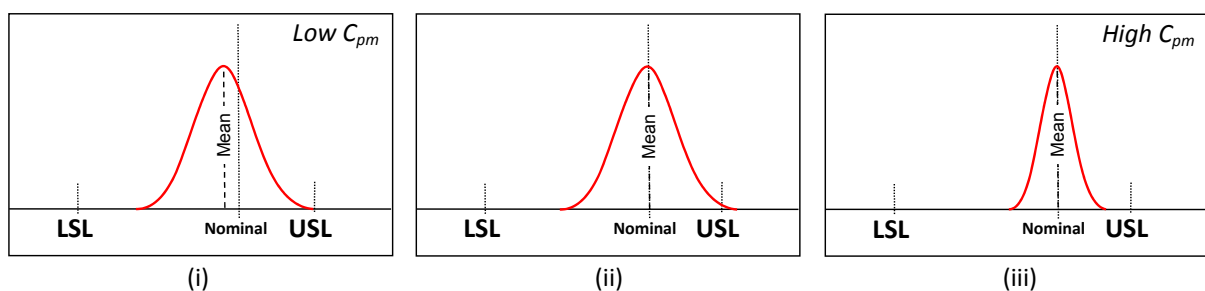


Figure A.5 - Process distributions with non-symmetric specification limits. C_{pm} increasing from left to right:
 (i) large standard deviation, mean not equal to nominal
 (ii) large standard deviation, mean equal to nominal
 (iii) small standard deviation, mean equal to nominal. C_{pk} and C_p underestimate process capability for this case.

B.4 Process capability indices – Non-normal distributions

The above process capability indices are based on the assumption of a normally distributed manufacturing process. Consequently, non-normal distributions can result in an incorrect estimate of the process capability. Non-normal distributions can be correctly accommodated by using distribution transformations to transform the process data into a normal distribution (Section 2.3.3) or applying another set of process indices applicable to non-normal distributions (Somerville *et al.* 1996).

The transformation approach needs to be carried out iteratively. Following a transformation the distribution of the transformed data needs to be tested for normality. If the transformed data is not indicative of a normal distribution then the transformation parameters are modified and the process repeated. When the data is close to normal, the standard process indices applicable to normal distributions can be applied (English *et al.* 1993).

Process indices applicable to non-normal distributions are typically based on finding the equivalent normal distribution which would give the same yield as the non-normal distribution under analysis. An example of a process index applicable to non-normal distributions is the non-parametric capability index C_{npk} given by (McCormack Jr *et al.* 2000):

$$C_{npk} = \min\left(\frac{USL - \bar{m}}{p_{0.995} - \bar{m}}, \frac{\bar{m} - LSL}{\bar{m} - p_{0.005}}\right) \quad \text{Where:} \quad (\text{A.60})$$

\bar{m} is the median of the distribution
 $p_{0.995}$ is the 99.5th percentile of the process data
 $p_{0.005}$ is the 0.5th percentile of the process data

The non-parametric capability index is based on analysis of empirical non-normal distributions which indicates that an interval of acceptance between the 99.5th and 0.5th percentile of the non-normal process data is often equivalent to a normal process with the standard $\pm 3\sigma$ interval of acceptance (corresponding to 99.7% yield). The approach is founded on certain assumptions which need to be considered before application (McCormack Jr *et al.* 2000).

Application of transformation techniques is considered the preferred approach for accommodating non-normal distributions (Chandra 2001).

REFERENCES

- (ASTM), A. S. f. T. a. M. (2007). ASTM A228 / A228M - 07 Standard Specification for Steel Wire, Music Spring Quality. Pennsylvania, American Society for Testing and Materials (ASTM).
- (DIN), D. I. f. N. (1982). DIN 16 901 - Plastics Mouldings - Tolerances and acceptance conditions for linear dimensions. Berlin Deutsches Institut für Normung (DIN).
- Adams, B. M., Bohnhoff, W.J., Dalbey, K.R., Eddy, J.P., Eldred, M.S., Gay, D.M., Haskell, K., Hough, P.D., and Swiler, L.P., (2011). DAKOTA, A Multilevel Parallel Object-Oriented Framework for Design Optimization, Parameter Estimation, Uncertainty Quantification, and Sensitivity Analysis, Sandia Technical Report SAND2010-2183, December 2009. Updated December 2010 (Version 5.1) Updated November 2011 (Version 5.2).
- Alt, W. (1990). "The Lagrange-Newton method for infinite-dimensional optimization problems." Numerical Functional Analysis and Optimization **11**(3-4): 201-224.
- Anwarul, M. and M. Liu (1995). Optimal manufacturing tolerance: The modified Taguchi approach.
- Archibald, R. K., R. Deiterding, C. Hauck, J. Jakeman and D. Xiu (2012). Approximation and error estimation in high dimensional space for stochastic collocation methods on arbitrary sparse samples, Oak Ridge National Laboratory (ORNL); Center for Computational Sciences.
- Armen Der Kiureghian, M. and P. L. Liu (1986). "Structural reliability under incomplete probability information." Journal of Engineering Mechanics **112**: 85.
- Artto, K. A., J. M. Lehtonen and J. Saranen (2001). "Managing projects front-end: incorporating a strategic early view to project management with simulation." International Journal of Project Management **19**(5): 255-264.
- Askin, R. G. and J. B. Goldberg (1988). "Economic optimization in product design." Engineering Optimization **14**(2): 139-152.
- ASME (2003). Y14.41-2003 Digital Product Definition Data Practices
- ASME (2009). Y14.5-2009 - Dimensioning and Tolerancing. New York, American Society of Mechanical Engineers.
- Atkinson, K. E. (2009). An Introduction To Numerical Analysis, 2Nd Ed, Wiley India Pvt. Ltd.
- Audet, C. and J. E. Dennis Jr (2006). Analysis of generalized pattern searches, DTIC Document.
- Avriel, M. (2003). Nonlinear Programming: Analysis and Methods, Dover Publications.
- Bäck, T. (1996). Evolutionary algorithms in theory and practice: evolution strategies, evolutionary programming, genetic algorithms, Oxford University Press, USA.
- Barker, C. R. (1985). "A complete classification of planar four-bar linkages." Mechanism and Machine Theory **20**(6): 535-554.
- Bastow, D. (1976). Kinematic and Dynamic Data for Crank-Rocker and Slider-Crank Link-ages. London, Engineering Sciences Data Unit.
- Batavia, R. (2001). Front-End Loading for Life Cycle Success.
- Baumgartner, G. (1995). Potential Failure Modes and Effects Analysis (FMEA) Reference Manual. Michigan, Automotive Industry Action Group.
- Bedford, A. and W. Fowler (2008). Engineering Mechanics Statics & Dynamics, Prentice Hall.
- Bergman, B., J. De Mare, T. Svensson and S. Loren (2009). Robust Design Methodology for Reliability: Exploring the Effects of Variation and Uncertainty, John Wiley & Sons.
- Berveiller, M., B. Sudret and M. Lemaire (2006). "Stochastic finite element: a non intrusive approach by regression." Revue Européenne de Mécanique Numérique-Volume **15**(1-2).
- Beyer, H. G. and H. P. Schwefel (2002). "Evolution strategies—A comprehensive introduction." Natural computing **1**(1): 3-52.
- Bihlmaier, B. F. (1999). Tolerance analysis of flexible assemblies using finite element and spectral analysis, Brigham Young University. Department of Mechanical Engineering.
- Bijker, W. (1997). Of Bicycles, Bakelites, and Bulbs: Toward a Theory of Sociotechnical Change. Cambridge, MIT.

- Björck, Å. (1996). Numerical Methods for Least Squares Problems, Siam.
- Box, G. E. P. and D. R. Cox (1964). "An analysis of transformations." Journal of the Royal Statistical Society. Series B (Methodological): 211-252.
- Britten, W. and C. Weber (1999). Transforming ISO 1101 tolerances into vectorial tolerance representations - a CAD-based approach. Global Consistency of Tolerances. a. H. K. F. van Houten, University of Twente, Enschede, The Netherlands.: 93-100.
- Bungartz, H. J. and M. Griebel (2004). "Sparse grids." Acta Numerica **13**(1): 147-269.
- Burkardt, J. (2010). 1D quadrature rules for sparse grids, Tech. rep., Interdisciplinary Center for Applied Mathematics and Information Technology Department, Virginia Tech.
- Burkardt, J. (2010). The Combining Coefficient for Anisotropic Sparse Grids. Virginia Tech, Interdisciplinary Center for Applied Mathematics & Information Technology Department.
- Burkardt, J. (2010). Counting Abscissas in Sparse Grids. Virginia Tech, Interdisciplinary Center for Applied Mathematics and Information Technology Department.
- Burton, M., A. Subic, M. Mazur and M. Leary (2010). Systematic design customization of sport wheelchairs using the Taguchi method. 8th Conference of the International Sports Engineering Association.
- Camelio, J., S. J. Hu and D. Ceglarek (2003). "Modeling variation propagation of multi-station assembly systems with compliant parts." Journal of Mechanical Design **125**: 673.
- Camelio, J. A., S. J. Hu and S. P. Marin (2004). "Compliant assembly variation analysis using component geometric covariance." Journal of Manufacturing Science and Engineering **126**: 355.
- Canick, L. (1959). Serrated Clutches and Detents. Product Engineering Design Manual. D. C. Greenwood. New York, McGraw-Hill Book Company Inc.
- Carpinetti, L. and D. Chetwynd (1995). "Genetic search methods for assessing geometric tolerances." Computer Methods in Applied Mechanics and Engineering **122**(1): 193-204.
- Chan, L., S. Cheng and F. Spiring (1988). "A New Measure of Process Capability: Cpm." Journal of Quality Technology **20**(3): 162-175.
- Chandra, J. (2001). Statistical Quality Control, CRC Press.
- Chase, K. W., and Greenwood, W. H. (1988). "Design Issues in Mechanical Tolerance Analysis." ASME Manufacturing Review **1**(1): 50-59.
- Chase, K. W., W. H. Greenwood, B. G. Loosli and L. F. Hauglund (1990). "Least cost tolerance allocation for mechanical assemblies with automated process selection." Manufacturing review **3**(Compendex): 49-59.
- Chase, K. W., G. Jinsong and S. P. Magleby (1995). "General 2-D tolerance analysis of mechanical assemblies with small kinematic adjustments." Journal of Design and Manufacturing **5**(Copyright 1996, IEE): 263-274.
- Chase, K. W. and A. R. Parkinson (1991). "A survey of research in the application of tolerance analysis to the design of mechanical assemblies." Research in Engineering Design **3**(1): 23-37.
- Chiesi, F. and L. Governi (2003). "Tolerance analysis with eM-TolMate." Transactions of the ASME. Journal of Computing and Information Science in Engineering **3**(Copyright 2003, IEE): 100-105.
- Cho, B. R., Y. J. Kim, D. L. Kimbler and M. D. Phillips (2000). "An integrated joint optimization procedure for robust and tolerance design." International Journal of Production Research **38**(Compendex): 2309-2325.
- Cho, B. R. and M. S. Leonard (1997). "Identification and extensions of quasiconvex quality loss functions." International Journal of Reliability, Quality and Safety Engineering. **4**(2): 191-204.
- Choi, H.-G. R., M.-H. Park and E. Salisbury (2000). "Optimal Tolerance Allocation With Loss Functions." Journal of Manufacturing Science and Engineering **122**(3): 529-535.
- Choi, S. K., R. V. Grandhi and R. A. Canfield (2004). "Structural reliability under non-Gaussian stochastic behavior." Computers and Structures **82**(13-14): 1113-1121.

- Clément, A., A. Desrochers and A. Riviere (1991). Theory and practice of 3-D tolerancing for assembly, École de technologie supérieure.
- Clement, A. and A. Riviere (1993). Tolerancing versus nominal modeling in next generation CAD/CAM system.
- Cogorno, G. R. (2006). Geometric dimensioning and tolerancing for mechanical design. New York, McGraw-Hill Professional.
- Congedo, P. M., R. Abgrall and G. Geraci (2011). "On the use of the Sparse Grid techniques coupled with Polynomial Chaos."
- Connor, T., D. Macklin and J. Offutt (2003). "Nontraditional Phillips-Fluor business relationship delivers performance." Pipeline & gas journal **230**(5): 16-18.
- Crestaux, T. (2009). "Polynomial chaos expansion for sensitivity analysis." Reliability Engineering & System Safety **94**(7): 1161-1172.
- Cvetko, R., K. Chase and S. Magleby (1998). New Metrics for Evaluating Monte Carlo Tolerance Analysis of Assemblies. Proceedings of the ASME International Mechanical Engineering Conference and Exposition. Anaheim, CA, ASME.
- D'Errico, J. R. and N. A. Zaino Jr (1988). "Statistical tolerancing using a modification of Taguchi's method." Technometrics: 397-405.
- D'Errico, J. R. and N. A. Zaino Jr (1988). "Statistical tolerancing using a modification of Taguchi's method." Technometrics **30**(Compendex): 397-405.
- D., Z., G. Chen and Y. Gong (2009). "Research of multidisciplinary optimization based on iSIGHT." Mechanical & Electrical Engineering Magazine **26**(12): 78-81.
- Dahl, D. W., A. Chattopadhyay and G. J. Gorn (2001). "The importance of visualisation in concept design." Design Studies **22**(1): 5-26.
- Darlington, M. and S. Culley (2002). "Current research in the engineering design requirement." Proceedings of the Institution of Mechanical Engineers, Part B: Journal of Engineering Manufacture **216**(3): 375.
- Davidson, J., A. MUIEZINOVIC and J. Shah (2002). "A new mathematical model for geometric tolerances as applied to round faces." Journal of Mechanical Design **124**(4): 609-622.
- Deb, K. (2004). Optimization for engineering design: algorithms and examples, Prentice-Hall of India.
- Deb, K., A. Pratap, S. Agarwal and T. Meyarivan (2002). "A fast and elitist multiobjective genetic algorithm: NSGA-II." Evolutionary Computation, IEEE Transactions on **6**(2): 182-197.
- Debuschere, B. J., H. N. Najm, P. P. Pébay, O. M. Knio, R. G. Ghanem and O. P. L. Maître (2005). "Numerical challenges in the use of polynomial chaos representations for stochastic processes." SIAM Journal on Scientific Computing **26**(2): 698-719.
- DeFord, R. (2003). Tolerancing helical springs. Cleveland, OH, Penton Media.
- Delves, L. M. and J. L. Mohamed (1988). Computational Methods for Integral Equations, Cambridge University Press.
- Desrochers, A. and A. Clément (1994). "A dimensioning and tolerancing assistance model for CAD/CAM systems." The International Journal of Advanced Manufacturing Technology **9**(6): 352-361.
- Dong, Z. and W. Hu (1991). "Optimal process sequence identification and optimal process tolerance assignment in computer-aided process planning." Computers in Industry **17**(1): 19-32.
- Dong, Z., W. Hu and D. Xue (1994). "New production cost-tolerance models for tolerance synthesis." Journal of Engineering for Industry (116): 199-205.
- Dong, Z. and A. Soom (1989). Optimal tolerance design with automatic incorporation of manufacturing knowledge.
- Dong, Z. and A. Soom (1990). "Automatic optimal tolerance design for related dimension chains." Manufacturing review **3**(Copyright 1991, IEE): 262-271.
- Dorigo, M., M. Birattari and T. Stutzle (2006). "Ant colony optimization." Computational Intelligence Magazine, IEEE **1**(4): 28-39.

- Dupinet, E., M. Balazinski and E. Czogala (1996). "Tolerance allocation based on fuzzy logic and simulated annealing." Journal of Intelligent Manufacturing **7**(6): 487-497.
- Ealey, L. A. (1988). Quality by design: Taguchi Methods and U.S. industry, ASI Press.
- Earl, C. F., C. M. Eckert and J. Johnson (2001). Complexity in planning design processes. Proceedings of the 13th International Conference on Engineering Design: Design Research – Theories, Methodologies and Product Modelling (ICED'01). Glasgow, UK: 149-156.
- Earl, D. J. and M. W. Deem (2005). "Parallel tempering: Theory, applications, and new perspectives." Physical Chemistry Chemical Physics **7**(23): 3910-3916.
- Ebro, M., T. J. Howard and J. J. Rasmussen (2012). The foundation for robust design: enabling robustness through kinematic design and design clarity.
- Edel, D. H., and T. B. Auer (1964). "Determine the Least Cost Combination for Tolerance Accumulations in a Drive Shaft Seal Assembly." General Motors Engineering Journal **4**: 37-38.
- Eiteljorg, H., K. Fernie and J. Huggett (2003). CAD: a guide to good practice, Oxbow.
- Elders (2011). Elders Limited Annual Report 2011. Australia: pg 18.
- Eldred, M. and J. Burkardt (2009). Comparison of non-intrusive polynomial chaos and stochastic collocation methods for uncertainty quantification, American Institute of Aeronautics and Astronautics, 1801 Alexander Bell Dr., Suite 500 Reston VA 20191-4344 USA.
- Eldred, M., C. Webster and P. Constantine (2008). Evaluation of non-intrusive approaches for wiener-askey generalized polynomial chaos.
- Elishakoff, I. and Y. Ren (1999). "The bird's eye view on finite element method for structures with large stochastic variations." Computer Methods in Applied Mechanics and Engineering **168**(1): 51-61.
- English, J. and G. Taylor (1993). "Process capability analysis—a robustness study." THE INTERNATIONAL JOURNAL OF PRODUCTION RESEARCH **31**(7): 1621-1635.
- Epperson, J. F. (2007). An introduction to numerical methods and analysis, Wiley-Interscience.
- Ertan, B. (1998). Analysis of key characteristic methods and enablers used in variation risk management, Massachusetts Institute of Technology.
- Evans, D. H. (1975). "Statistical Tolerancing: The State of the Art. Part II: Methods for estimating moments." Journal of Quality Technology **7**(1): 1-12.
- Feigenbaum, A. V. (2012). Total Quality Control, 4th Ed.: Achieving Productivity, Market Penetration, and Advantage in the Global Economy, McGraw-Hill.
- Felgen, L., F. Deubzer and U. Lindemann (2005). Complexity management during the analysis of mechatronic systems. Proceedings of the 15th International Conference on Engineering Design (ICED05). W. L. A. Samuel: 409-410.
- Feng, C.-X. and R. Balusu (1999). "Robust tolerance design considering process capability and quality loss." American Society of Mechanical Engineers, Design Engineering Division (Publication) DE **103**(Compendex): 1-13.
- Feng, C.-X., J. Wang and J.-S. Wang (2001). "An optimization model for concurrent selection of tolerances and suppliers." Computers and Industrial Engineering **40**(Compendex): 15-33.
- Feng, C. X. and A. Kusiak (1997). "Robust tolerance design with the integer programming approach." Transactions of the ASME. Journal of Manufacturing Science and Engineering **119**(Copyright 1998, IEE): 603-610.
- Fiessler, B., H.-J. Neumann and R. Rackwitz (1979). "Quadratic limit states in structural reliability." **105**(Compendex): 661-676.
- Fischer, A. (1992). "A special Newton-type optimization method." Optimization **24**(3-4): 269-284.
- Flager, F., B. Welle, P. Bansal, G. Soremekun and J. Haymaker (2009). "Multidisciplinary process integration and design optimization of a classroom building." Electronic Journal of Information Technology in Construction **14**(Copyright 2010, The Institution of Engineering and Technology): 595-612.
- Fonseca, C. M. and P. J. Fleming (1995). "An overview of evolutionary algorithms in multiobjective optimization." Evolutionary computation **3**(1): 1-16.

- Foo, J., X. Wan and G. E. Karniadakis (2008). "The multi-element probabilistic collocation method (ME-PCM): Error analysis and applications." Journal of Computational Physics **227**(22): 9572-9595.
- Forouraghi, B. (2002). "Worst-case tolerance design and quality assurance via genetic algorithms." Journal of Optimization Theory and Applications **113**(2): 251-268.
- Fortini, E. T. (1967). Dimensioning for Interchangeable Manufacture. New York, Industrial Press.
- Frances, Y. K. and H. S. Ian (2005). Lifting the curse of dimensionality.
- Franciosa, P., S. Gerbino and S. Patalano (2011). "Simulation of variational compliant assemblies with shape errors based on morphing mesh approach." The International Journal of Advanced Manufacturing Technology **53**(1): 47-61.
- Gao, J., K. W. Chase and S. P. Magleby (1995). Comparison of assembly tolerance analysis by Direct Linearization and modified Monte Carlo simulation methods. Proceedings of the 1995 ASME Design Engineering Technical Conference, September 17, 1995 - September 20, 1995, Boston, MA, USA.
- Gao, J., K. W. Chase and S. P. Magleby (1998). "Generalized 3-D tolerance analysis of mechanical assemblies with small kinematic adjustments." IIE Transactions (Institute of Industrial Engineers) **30**(Compendex): 367-377.
- Gen, M. and R. Cheng (2000). Genetic algorithms and engineering optimization, Wiley-interscience.
- Gerstner, T. and M. Griebel (1998). "Numerical integration using sparse grids." Numerical algorithms **18**(3): 209-232.
- Gerstner, T. and M. Griebel (2003). "Dimension-adaptive tensor-product quadrature." Computing **71**(1): 65-87.
- Ghanem, R. G. and P. D. Spanos (2003). Stochastic finite elements: a spectral approach, Dover Publications.
- Gordis, J. H. and W. G. Flannelly (1994). "Analysis of stress due to fastener tolerance in assembled components." AIAA journal **32**: 2440-2446.
- Haldar, A. and S. Mahadevan (2000). Probability, reliability, and statistical methods in engineering design, John Wiley.
- Hammersley, J. (1975). Monte Carlo Methods. Norwich, England, Fletcher.
- Haupt, R. L., S. E. Haupt and J. Wiley (2004). Practical genetic algorithms, Wiley Online Library.
- Hindhede, U. (1983). Machine Design Fundamentals: A practical Approach. New York, John Wiley & Sons.
- Hiriyannaiah, S. and G. M. Mocko (2008). "Information Management Capabilities of MDO Frameworks." ASME Conference Proceedings **2008**(43277): 635-645.
- Hohenbichler, M., S. Gollwitzer, W. Kruse and R. Rackwitz (1987). "New light on first- and second-order reliability methods." Structural Safety **4**(4): 267-284.
- Holland, J. H. (1992). "Genetic algorithms." Scientific american **267**(1): 66-72.
- Hong, Y. S. and T. C. Chang (2002). "A comprehensive review of tolerancing research." International Journal of Production Research **40**(Copyright 2002, IEE): 2425-2459.
- Hosder, S., R. W. Walters and M. Balch (2007). Efficient sampling for non-intrusive polynomial chaos applications with multiple uncertain input variables.
- Hosder, S., R. W. Walters and M. Balch (2007). Efficient sampling for non-intrusive polynomial chaos applications with multiple uncertain input variables.
- Houten, F., H. Kals and M. Giordano (1999). Mathematical Representation of Tolerance Zones. Global consistency of tolerances: proceedings of the 6th CIRP International Seminar on Computer-Aided Tolerancing, University of Twente, Enschede, The Netherlands, 22-24 March, 1999, Kluwer Academic.
- Hu, M., Z. Lin, X. Lai and J. Ni (2001). "Simulation and analysis of assembly processes considering compliant, non-ideal parts and tooling variations." International Journal of Machine Tools and Manufacture **41**(15): 2233-2243.

- Huntington, D. E. and C. S. Lyrintzis (1998). "Improvements to and limitations of Latin hypercube sampling." Probabilistic Engineering Mechanics **13**(Compendex): 245-253.
- Hyun Seok, S. and K. Byung Man (2002). "Efficient statistical tolerance analysis for general distributions using three-point information." International Journal of Production Research **40**(Copyright 2002, IEE): 931-944.
- Iannuzzi, M. and E. Sandgren (1995). Tolerance optimization using genetic algorithms: Benchmarking with manual analysis.
- Imani, B. M. and M. Pour (2009). "Tolerance analysis of flexible kinematic mechanism using DLM method." Mechanism and Machine Theory **44**(2): 445-456.
- ISO (1988). 286-1:1988 ISO system of limits and fits
- ISO (1998). 5458:1998 Geometric Product Specifications (GPS). Positional tolerancing
- ISO (2002). ISO 10303: Automation systems and integration - Product data representation and exchange (STEP), ISO.
- ISO (2005). 1101:2005 Geometrical Product Specifications (GPS). Tolerancing of form, orientation, location and run-out
- ISO (2005). ISO 9000:2005, TC 176/SC Quality management systems -- Fundamentals and vocabulary., International Organization for Standardization.
- ISO (2006). 16792:2006 Technical product documentation -- Digital product definition data practices
- Jackson, S. L. (2011). Research Methods and Statistics: A Critical Thinking Approach, Cengage Learning.
- Jakeman, J., M. Eldred and D. Xiu (2010). "Numerical approach for quantification of epistemic uncertainty." Journal of Computational Physics **229**(12): 4648-4663.
- Jakeman, J. D., R. Archibald and D. Xiu (2011). "Characterization of discontinuities in high-dimensional stochastic problems on adaptive sparse grids." Journal of Computational Physics.
- Jakeman, J. D. and S. G. Roberts (2011). "Local and Dimension Adaptive Sparse Grid Interpolation and Quadrature." Arxiv preprint arXiv:1110.0010.
- Jeang, A. (1994). "Tolerance design: choosing optimal tolerance specifications in the design of machined parts." Quality and reliability engineering international **10**(1): 27-35.
- Jeang, A. (1999). "Optimal tolerance design by response surface methodology." International Journal of Production Research **37**(Compendex): 3275-3288.
- Ji, S., X. Li, Y. Ma and H. Cai (2000). "Optimal tolerance allocation based on fuzzy comprehensive evaluation and genetic algorithm." The International Journal of Advanced Manufacturing Technology **16**(7): 461-468.
- Johnson, O. and O. T. Johnson (2004). Information Theory And The Central Limit Theorem, Imperial College Press.
- Juran, J. M. (1992). Juran on Quality by Design. New York, The free Press.
- Juster, N. P. (1992). "Modelling and representation of dimensions and tolerances: a survey." Computer-Aided Design **24**(1): 3-17.
- Kalos, M. H. and P. A. Whitlock (2009). Monte Carlo Methods, John Wiley & Sons.
- Kanai, S., M. Onozuka and H. Takahashi (1995). Optimal Tolerance Synthesis by Genetic Algorithm under the Machining and Assembling Constraint.
- Kennedy, J. and R. Eberhart (1995). Particle swarm optimization, IEEE.
- Keramat, M. and R. Kielbasa (1997). "Latin Hypercube Sampling Monte Carlo estimation of average quality index for integrated circuits." Analog Integrated Circuits and Signal Processing **14**(Compendex): 131-142.
- Kharoufeh, J. and M. Chandra (2002). "Statistical tolerance analysis for non-normal or correlated normal component characteristics." International Journal of Production Research **40**(2): 337-352.
- Kirkpatrick, S., C. D. Gelatt Jr and M. P. Vecchi (1983). "Optimization by simulated annealing." science **220**(4598): 671-680.

- Kiureghian, A. D. and O. Ditlevsen (2009). "Aleatory or epistemic? Does it matter?" Structural Safety **31**(2): 105-112.
- Kodiyalam, S. (1998). "Evaluation of methods for multidisciplinary design optimization (MDO), Phase I." NASA Contractor Report, NASA/CR-1998-208716.
- Kodiyalam, S. and C. Yuan (2000). "Evaluation of Methods for Multidisciplinary Design Optimization (MDO), Part II." NASA Contractor Report.
- Kovvali, N. (2011). Theory and Applications of Gaussian Quadrature Methods, Morgan & Claypool.
- Krishnan, V. and K. T. Ulrich (2001). "Product development decisions: A review of the literature." Management Science **47**(1): 1-21.
- Kumar, M. S. and S. Kannan (2007). "Optimum manufacturing tolerance to selective assembly technique for different assembly specifications by using genetic algorithm." The International Journal of Advanced Manufacturing Technology **32**(5): 591-598.
- Kuo FY, S. I. (2005). "Lifting the curse of dimensionality." Notices of the AMS **52**: 1320–1328.
- Lawson, C. L. and R. J. Hanson (1974). Solving Least Squares Problems, SIAM.
- Leary, M., J. Gruijters, M. Mazur, A. Subic, M. Burton and F. Fuss (2012). "A fundamental model of quasi-static wheelchair biomechanics." Journal of Medical Engineering & Physics **34**(9): 1278-1286.
- Leary, M., M. Mazur, J. Gruijters and A. Subic (2010). Benchmarking and optimisation of automotive seat structures. Sustainable Automotive Technologies 2010: Proceedings of the 2nd International Conference. J. Wellnitz, Springer: 63-70.
- Leary, M., M. Mazur, J. Gruijters and A. Subic (2011). "Benchmarking and optimisation of automotive seat structures."
- Leary, M., M. Mazur, T. Mild and A. Subic (2011). Optimisation of automotive seat kinematics. Sustainable Automotive Technologies 2010: Proceedings of the 2nd International Conference. S. Hung. Greenville, South Carolina, USA, Springer: 139-144.
- Lee, D., K. E. Kwon, J. Lee, H. Jee, H. Yim, S. W. Cho, J. G. Shin and G. Lee (2009). "Tolerance Analysis Considering Weld Distortion by Use of Pregenerated Database." Journal of Manufacturing Science and Engineering **131**: 041012.
- Lee, D. J. and A. C. Thornton (1996). The identification and use of key characteristics in the product development process. The 1996 ASME Design Engineering Technical Conferences and Computers in Engineering Conference August 18-22, 1996, Irvine, California, ASME.
- Lee, S. and W. Chen (2009). "A comparative study of uncertainty propagation methods for black-box-type problems." Structural and Multidisciplinary Optimization **37**(Copyright 2009, The Institution of Engineering and Technology): 239-253.
- Lee SH, C. W. (2009). "A comparative study of uncertainty propagation methods." Struct Multidisc Optim **37**: 239–253.
- Lehtihet, E., E. Gunasena and I. Ham (1991). An update on statistical tolerance control methods and computations.
- Lesser, M. (2000). Analysis of Complex Nonlinear Mechanical Systems: A Computer Algebra Assisted Approach, World Scientific Pub Co Inc.
- Levy, S. (1953). "Structural analysis and influence coefficients for delta wings." J. Aero. Sci **20**(7): 449-454.
- Li, M. and P. M. B. Vitányi (2008). An introduction to Kolmogorov complexity and its applications, Springer.
- Lin, B.-W. and J.-S. Chen (2005). "Corporate technology portfolios and R&D performance measures: a study of technology intensive firms." R&D Management **35**(2): 157-170.
- Liu, M., Z. Gao and J. S. Hesthaven (2011). "Adaptive sparse grid algorithms with applications to electromagnetic scattering under uncertainty." Applied numerical mathematics **61**(1): 24-37.
- Liu, S., S. Hu and T. Woo (1996). "Tolerance analysis for sheet metal assemblies." Journal of Mechanical Design **118**: 62.

- Liu, S. C. and S. J. Hu (1997). "Variation simulation for deformable sheet metal assemblies using finite element methods." Journal of Manufacturing Science and Engineering **119**: 368.
- Liu, S. C., H. W. Lee and S. J. Hu (1995). "Variation simulation for deformable sheet metal assemblies using mechanistic models." TRANSACTIONS-NORTH AMERICAN MANUFACTURING RESEARCH INSTITUTION OF SME: 235-240.
- Lovasz, E. C. (2012). Mechanisms, Transmissions and Applications, Springer London, Limited.
- Lovett, T. E., F. Ponci and A. Monti (2006). "A polynomial chaos approach to measurement uncertainty." IEEE Transactions on Instrumentation and Measurement **55**(Copyright 2006, The Institution of Engineering and Technology): 729-736.
- Makelainen, E., Y. Ramseier, S. Salmensuu, J. Heilala, P. Voho and O. Vaatainen (2001). Assembly process level tolerance analysis for electromechanical products. 2001 IEEE International Symposium on Assembly and Task Planning (ISATP2001), May 28, 2001 - May 29, 2001, Fukuoka, Japan, Institute of Electrical and Electronics Engineers Computer Society.
- Malone, B. (2001). "Building Automated Processes Using ModelCenter." Integrated Enterprise **2**(1): 25-27.
- Malone, B. and M. Papay (1999). ModelCenter: an integration environment for simulation based design. Simulation Interoperability Workshop.
- Mansoor, E. M. (1963). "The application of probability to tolerances used in engineering design." Proceedings of the Institution of Mechanical Engineers **178**: 29-44.
- Mazur, M., M. Leary, S. Huang, T. Baxter and A. Subic (2011). Benchmarking study of automotive seat track sensitivity to manufacturing variation. Proceedings of the 18th International Conference on Engineering Design (ICED11). S. J. H. Culley, B.J.; McAloone, T.C.; Howard, T.J. & Dong, A. Copenhagen, Denmark, The Design Society. **Vol. 10**: 456-465.
- Mazur, M., M. Leary and A. Subic (2010). Automated simulation of stochastic part variation to identify key performance characteristics of assemblies. 6th Innovative Production Machines and Systems 2010 (IPROMS 2010) Conference.
- Mazur, M., M. Leary and A. Subic (2011). "Computer Aided Tolerancing (CAT) platform for the design of assemblies under external and internal forces." Computer-Aided Design **43**(6): 707-719.
- McAfee, R. P. and J. McMillan (1995). "Organizational Diseconomies of scale." Journal of Economics & Management Strategy **4**(3): 399-426.
- McCormack Jr, D., I. R. Harris, A. M. Hurwitz and P. D. Spagon (2000). "Capability indices for non-normal data." Quality Engineering **12**(4): 489-495.
- McKay, M., R. J. Beckman and W. J. Conover (1979). "Comparison of three methods for selecting values of input variables in the analysis of output from a computer code." Technometrics **21**(2): 239-245.
- McKay MD, B. R., Conover WJ (1979). "A Comparison of Three Methods for Selecting Values of Input Variables in the Analysis of Output from a Computer Code." Technometrics (American Statistical Association) **2**(21): 239-245.
- McRae, G. J. and M. A. Tatang (1995). Direct incorporation of uncertainty in chemical and environmental engineering systems, Massachusetts Institute of Technology.
- Merkley, K., K. Chase and E. Perry (1996). An introduction to tolerance analysis of flexible assemblies.
- Merkley, K. G. (1998). Tolerance analysis of compliant assemblies, Brigham Young University.
- Michael, W., and Siddall, J. N. (1981). "The optimization problem with optimal tolerance assignment." J. of Mechanical Design, ASME **103**(Oct. 1981): 842-848.
- Miller, F. P., A. F. Vandome and J. McBrewster (2010). Central Limit Theorem, Alphascript Publishing.
- Mitra, A. (1998). Fundamentals of quality control and improvement, 2nd Edition Prentice-Hall.
- Mo, Z., Y. He, G. Wu and J. Wu (2010). The Application of BP Neural Network in GridGain Grid Computing Environment. Measuring Technology and Mechatronics Automation (ICMTMA), 2010 International Conference on, IEEE.

- Montgomery, D. C. (2001). Introduction to Statistical Quality Control 4th edition. New York, John Wiley & Sons.
- Morokoff, W. J. and R. E. Caflisch (1994). "Quasi-random sequences and their discrepancies." SIAM Journal on Scientific Computing **15**(6): 1251-1279.
- Morse, E. P. and X. You (2005). "Implementation of GapSpace Analysis." ASME Conference Proceedings **2005**(42150): 329-333.
- Mujezinovic, A., J. K. Davidson and J. J. Shah (2004). "A New Mathematical Model for Geometric Tolerances as Applied to Polygonal Faces." Journal of Mechanical Design **126**(3): 504-518.
- Niederreiter, H. (1992). Quasi-Monte Carlo Methods, Wiley Online Library.
- Nigam SD, T. U. (1995). "Review of statistical approaches to tolerance analysis." Computer-Aided Design **27** 6-15.
- Nigam, S. D. and J. U. Turner (1995). "Review of statistical approaches to tolerance analysis." CAD Computer Aided Design **27**(Compendex): 6-15.
- Nocedal, J. and S. J. Wright (1999). Numerical optimization, Springer verlag.
- Norton, R. L. (2003). Design of Machinery: An Introduction to the Synthesis and Analysis of Mechanisms and Machines, McGraw-Hill Higher Education.
- Oakland, J. S. (2007). Statistical process control, Elsevier.
- Ostwald, P. and J. Huang (1977). "A method for optimal tolerance selection." Journal of Engineering for Industry **99**(3): 558-565.
- Owen, S. J. and M. L. Staten (2010). A Comparison of Mesh Morphing Methods for Shape Optimization. Albuquerque, NM, U.S.A, Sandia National Laboratories.
- Padula, S., J. Korte, H. Dunn and A. Salas (1999). Multidisciplinary optimization branch experience using iSIGHT software, Citeseer.
- Pahl, G., K. Wallace and L. Blessing (2007). Engineering Design: A Systematic Approach, Springer.
- Pan, J., Y. Le Biannic and F. Magoules (2010). Parallelizing multiple group-by query in share-nothing environment: a mapreduce study case. Proceedings of the 19th ACM International Symposium on High Performance Distributed Computing, ACM.
- Parashar, S. S. and N. Fateh (2007). Multi-objective MDO solution strategy for multidisciplinary design using modefrontier. Inverse Problems, Design and Optimization Symposium Miami, Florida, U.S.A.
- Park, S. (1996). Robust Design and Analysis for Quality Engineering, Springer.
- Parkinson, D. (1982). "The application of reliability methods to tolerancing." Journal of Mechanical Design: Transactions of the ASME **104**: 612-618.
- Parkinson, D. (1985). "Assessment and optimization of dimensional tolerances." Computer-Aided Design **17**(4): 191-199.
- Parkinson, D. B. (1982). "The application of reliability methods to tolerancing." ASME Transactions. Journal of Mechanical Design **104**: 612-618.
- Pascoe, N. (2011). Reliability Technology: Principles and Practice of Failure Prevention in Electronic Systems, John Wiley & Sons.
- Patel, A. M. (1980). Computer-Aided Assignment of Manufacturing Tolerances. Proc. of the 17th Design Automation Conf, Minneapolis, Minn.
- Pearn, W. and S. Kotz (2006). Encyclopedia and handbook of process capability indices: a comprehensive exposition of quality control measures. New Jersey, World Scientific.
- Pearn WL, K. S. (2006). Encyclopedia And Handbook of Process Capability Indices: A Comprehensive Exposition of Quality Control Measures (Series on Quality, Reliability and Engineering Statistics). New Jersey, World Scientific Publishing.
- Phadke, M. S. (1989). Quality engineering using robust design, Prentice Hall.
- Pierre, L., D. Teissandier and J. P. Nadeau (2009). "Integration of thermomechanical strains into tolerancing analysis." International Journal on Interactive Design and Manufacturing **3**(4): 247-263.

- Piperni, P., M. Abdo and F. Kafyeke (2004). The application of multi-disciplinary optimization technologies to the design of a business jet. Proceeding of the 10th AIAA/ISSMO Multidisciplinary Analysis and Optimization Conference.
- Polini, W. (2011). To Carry Out Tolerance Analysis of an Aeronautic Assembly Involving Free Form Surfaces in Composite Material. Advances in Composite Materials - Ecodesign and Analysis.
- Prisco, U. and G. Giorleo (2002). "Overview of current CAT systems." Integrated Computer-Aided Engineering **9**(Copyright 2003, IEE): 373-387.
- Pugh, S. (1991). Total design: integrated methods for successful product engineering, Addison-Wesley Pub. Co.
- Rahman, S. and D. Wei (2006). "A univariate approximation at most probable point for higher-order reliability analysis." International Journal of Solids and Structures **43**(Compendex): 2820-2839.
- Rahman, S. and H. Xu (2004). "A univariate dimension-reduction method for multi-dimensional integration in stochastic mechanics." Probabilistic Engineering Mechanics **19**(Compendex): 393-408.
- Rao, P. N. (2004). CAD/CAM: Principles and Applications, McGraw-Hill Education (India) Pvt Limited.
- Rao, Y., C. Rao, G. R. Janardhana and P. R. Vundavilli (2011). "Simultaneous Tolerance Synthesis for Manufacturing and Quality using Evolutionary Algorithms." International Journal of Applied Evolutionary Computation (IJAEC) **2**(2): 1-20.
- Rawat, S. and L. Rajamani (2009). Experiments with CPU Scheduling Algorithm on a Computational Grid. Advance Computing Conference, 2009. IACC 2009. IEEE International, IEEE.
- Rosato, D. V. and M. G. Rosato (2000). Injection molding handbook, Kluwer Academic.
- Roweis, S. (1996). "Levenberg-marquardt optimization." Notes, University Of Toronto.
- Roy, U. and Y. C. Fang (1997). "Optimal tolerance re-allocation for the generative process sequence." IIE transactions **29**(1): 37-44.
- Roy, U. and B. Li (1998). "Representation and interpretation of geometric tolerances for polyhedral objects--I. Form tolerances." Computer-Aided Design **30**(2): 151-161.
- Roy, U., C. R. Liu and T. C. Woo (1991). "Review of dimensioning and tolerancing: representation and processing." Computer-Aided Design **23**(7): 466-483.
- Rubinstein, R. (1981). Simulation and the Monte Carlo Method, John Wiley & Sons, Inc.
- SAE (1997). SAE HS-795 - manual on design and application of helical and spiral springs, Society of Automotive Engineers.
- Salas Gonzalez, D., J. Górriz, J. Ramírez, A. Lassi and C. Puntonet (2008). "Improved Gauss-Newton optimisation methods in affine registration of SPECT brain images." Electronics Letters **44**(22): 1291-1292.
- Salomons, O., H. Jonge Poerink, F. Slooten, F. Houten and H. Kals (1995). A computer aided tolerancing tool based on kinematic analogies, Citeseer.
- Salomons, O. W., F. van Houten and H. Kals (1998). "Current status of CAT systems." Geometric design tolerancing: theories, standards and applications: 438-452.
- Schittkowski, K. (1983). "On the convergence of a sequential quadratic programming method with an augmented lagrangian line search function 2." Optimization **14**(2): 197-216.
- Schoutens, W. (2000). Stochastic processes and orthogonal polynomials, Springer.
- Shah, J. J., G. Ameta, Z. Shen and J. Davidson (2007). "Navigating the tolerance analysis maze." Computer-Aided Design and Applications **4**(Compendex): 705-718.
- Shah, J. J. and M. Mäntylä (1995). Parametric and Feature-Based Cad/Cam: Concepts, Techniques, and Applications, Wiley.
- Shah, J. J. and B. C. Zhang (1992). Attributed graph model for geometric tolerancing.
- Shen, Z. (2005). Development of a framework for a set of computer-aided tools for tolerance analysis. PhD Thesis, Arizona State University.
- Shen, Z., G. Ameta, J. J. Shah and J. K. Davidson (2005). "A comparative study of tolerance analysis methods." Journal of Computing and Information Science in Engineering **5**: 247.

- Shigley, J. E., C. R. Mischke and R. G. Budynas (2004). Mechanical Engineering Design, McGraw-Hill.
- Shiu, B., D. Apley, D. Ceglarek and J. Shi (2003). "Tolerance allocation for compliant beam structure assemblies." IIE transactions **35**(4): 329-342.
- Sigmetrix (2012). CETOL. L. CYBERNET SYSTEMS CO.: CAT software tool.
- Simpson, T. W., V. Toropov, V. Balabanov and F. A. C. Viana (2008). Design and analysis of computer experiments in multidisciplinary design optimization: a review of how far we have come or not.
- Singh, J. (2003). Key characteristic coupling and resolving key characteristic conflict, Massachusetts Institute of Technology.
- Singh, P., P. Jain and S. Jain (2004). "A genetic algorithm-based solution to optimal tolerance synthesis of mechanical assemblies with alternative manufacturing processes: focus on complex tolerancing problems." International Journal of Production Research **42**(24): 5185-5215.
- Singh, P. K., P. K. Jain and S. C. Jain (2009). "Important issues in tolerance design of mechanical assemblies. Part 2: Tolerance synthesis." Proceedings of the Institution of Mechanical Engineers, Part B: Journal of Engineering Manufacture **223**(10): 1249-1287.
- Skowronski, V. J. and J. U. Turner (1997). "Using Monte-Carlo variance reduction in statistical tolerance synthesis." CAD Computer Aided Design **29**(Compendex): 63-69.
- Smith, R. P. and S. D. Eppinger (1997). "Identifying controlling features of engineering design iteration." Management Science: 276-293.
- Smolyak, S. A. (1963). "Quadrature and interpolation formulas for tensor products of certain classes of functions." Dokl. Akad. Nauk SSSR **4**: 240-243.
- Sobieszczanski-Sobieski, J. and R. T. Haftka (1997). "Multidisciplinary aerospace design optimization: survey of recent developments." Structural and Multidisciplinary Optimization **14**(1): 1-23.
- Soderberg, R. (1993). Tolerance allocation considering customer and manufacturer objectives. 14th Biennial Conference on Mechanical Vibration and Noise, September 19, 1993 - September 22, 1993, Albuquerque, NM, USA, Publ by ASME.
- Soderberg, R. (1994). "Robust design by tolerance allocation considering quality and manufacturing cost." Advances in Design Automation **69**: 219-226.
- Soderberg, R. (1994). Robust design by tolerance allocation considering quality and manufacturing cost. Proceedings of the 1994 ASME Design Technical Conferences. Part 1 (of 2), September 11, 1994 - September 14, 1994, Minneapolis, MN, USA, ASME.
- Soderberg, R. and L. Lindkvist (1999). "Computer aided assembly robustness evaluation." Journal of Engineering Design **10**(2): 165-181.
- Soderberg, R. and L. Lindkvist (1999). Two-step procedure for robust design using CAT technology, Kluwer Academic Publishers.
- Somerville, S. E. and D. C. Montgomery (1996). "Process capability indices and non-normal distributions." Quality Engineering **9**(2): 305-316.
- Speckhart, F. H. (1972). "Calculation of Tolerance Based on a Minimum Cost Approach." J. of Engineering for Industry, ASME **94**(May 1972): 447-453.
- Spotts, M. F. (1973). "Allocation of Tolerances to Minimize Cost of Assembly." J. of Engineering for Industry, ASME **95**(Aug. 1973): 762-764.
- Stapelberg, R. F. (2009). Handbook of Reliability, Availability, Maintainability and Safety in Engineering Design, Springer.
- Steiner, G. and D. Watzenig (2003). Particle swarm optimization for worst case tolerance design, IEEE.
- Stonier, R. J. and X. H. Yu (1994). Complex systems: mechanism of adaptation, IOS Press.
- Stroud, I. and H. Nagy (2011). Solid Modelling and CAD Systems: How to Survive a CAD System, Springer.
- Suh, N. P. (1990). The principles of design, Oxford University Press New York.

- Summers, J. D. and J. J. Shah (2010). "Mechanical Engineering Design Complexity Metrics: Size, Coupling, and Solvability." Journal of Mechanical Design **132**(2): 021004.
- Sutherland, G. H., and Roth, B. (1975). "Mechanism Design: Accounting for Manufacturing Tolerances and Costs in Function Generating Problems." J. of Engineering for Industry, ASME Conference Proceedings **97**(Feb. 1975): 283-286.
- Taguchi, G. (1978). "Performance Analysis Design." International Journal of Production Research **16**: 512-530.
- Taguchi, G. (1989). Introduction to Quality Engineering. New York, Asian Productivity Organization, Unipub.
- Taguchi, G. (1993). Taguchi on robust technology development: bringing quality engineering upstream, ASME Press.
- Taguchi, G. and S. Chowdhury (1999). Robust Engineering: Learn How to Boost Quality While Reducing Costs & Time to Market, McGraw-Hill.
- Takezawa, N. (1980). "An improved method for establishing the process-wise quality standard." Rep. Stat. Appl. Res., JUSE **27**(3): 63-75.
- Terejanu, G., P. Singla, T. Singh and P. D. Scott (2010). Approximate propagation of both epistemic and aleatory uncertainty through dynamic systems. Information Fusion (FUSION), 2010 13th Conference on.
- Thompson, A., P. Layzell and R. S. Zebulum (1999). "Explorations in design space: Unconventional electronics design through artificial evolution." Evolutionary Computation, IEEE Transactions on **3**(3): 167-196.
- Thornton, A. C. (1999). "A Mathematical Framework for the Key Characteristic Process." Research in Engineering Design **11**(3): 145-157.
- Tomiyama, T., P. Gu, Y. Jin, D. Lutters, C. Kind and F. Kimura (2009). "Design methodologies: Industrial and educational applications." CIRP Annals - Manufacturing Technology **58**(2): 543-565.
- Turner, J. and A. Gangoiti (1991). "Tolerance analysis approaches in commercial software." Concurrent Engineering **1**(2): 11-23.
- Twigge-Molecey, C. (2003). Knowledge, technology and profit, Citeseer.
- Ullman, D. G. (2003). The mechanical design process, McGraw-Hill.
- Vinckenroy, G. V. and W. P. D. Wilde (1995). "The use of Monte Carlo techniques in statistical finite element methods for the determination of the structural behaviour of composite materials structural components." Composite Structures **32**(1): 247-254.
- Voelcker, H. B. (1998). "The current state of affairs in dimensional tolerancing: 1997." Integrated Manufacturing Systems **9**(4): 205-217.
- Voelcker, H. B., C. U. S. S. o. Mechanical and A. Engineering (1993). A Current Perspective on Tolerancing and Metrology, Sibley School of Mechanical and Aerospace Engineering, Cornell University.
- Wade, O. R. (1967). Tolerance Control in Design and Manufacturing. New York, Industrial Press.
- Wahl, A. (1963). Mechanical Springs New York, McGraw-Hill.
- Wan, X. and G. E. Karniadakis (2007). "Multi-element generalized polynomial chaos for arbitrary probability measures." SIAM Journal on Scientific Computing **28**(3): 901-928.
- Wang, H., G. He, M. Xia, F. Ke and Y. Bai (2004). "Multiscale coupling in complex mechanical systems." Chemical engineering science **59**(8): 1677-1686.
- Weiner, N. (1938). "The homogeneous chaos." Amer. J. Math **60**(4): 897--936.
- Weirs, V. G., J. R. Kamm, L. P. Swiler, S. Tarantola, M. Ratto, B. M. Adams, W. J. Rider and M. S. Eldred "Sensitivity analysis techniques applied to a system of hyperbolic conservation laws." Reliability Engineering & System Safety(0).
- Wenzhen, H., T. Phoomboplab and D. Ceglarek (2009). "Process capability surrogate model-based tolerance synthesis for multi-station manufacturing systems." IIE transactions **41**(4): 309-322.

- Wilde, D. and E. Prentice (1975). "Minimum exponential cost allocation of sure-fit tolerances." Journal of Engineering for Industry **97**(4): 1395-1398.
- Williams, J. A. (1994). Engineering Tribology, Cambridge University Press.
- Wirtz, A. (1993). Vectorial tolerancing: a basic element for quality control.
- Wirtz, A., C. Gächter and D. Wipf (1993). "From unambiguously defined geometry to the perfect quality control loop." CIRP Annals-Manufacturing Technology **42**(1): 615-618.
- Wojtkiewicz, S., M. Eldred, R. Field, A. Urbina and J. Red-Horse (2001). "Uncertainty quantification in large computational engineering models." American Institute of Aeronautics and Astronautics **14**.
- Wood, D. A. (2006). "Making better springs using aspects of chaos theory." Proceedings of the Institution of Mechanical Engineers, Part C: Journal of Mechanical Engineering Science **220**(3): 253-259.
- Wright, P. A. (1995). "A process capability index sensitive to skewness." Journal of Statistical Computation and Simulation **52**(3): 195-203.
- Wu, F., J.-Y. Dantan, A. Etienne, A. Siadat and P. Martin (2009). "Improved algorithm for tolerance allocation based on Monte Carlo simulation and discrete optimization." Computers & Industrial Engineering **56**(4): 1402-1413.
- Wu, Y. and A. Wu (2000). Taguchi methods for robust design, ASME Press.
- Wu, Z., W. H. Eimaraghy and H. A. Eimaraghy (1988). "Evaluation of cost-tolerance algorithms for design tolerance analysis and synthesis." Manufacturing review **1**(Compendex): 168-179.
- Wu, Z., W. H. El Maraghy and H. A. El Maraghy (1988). "Evaluation of Cost-Tolerance Algorithms for Design Tolerance Analysis and Synthesis." Manufacturing Review, ASME **1**(3): 168-179.
- Xiu, D. (2007). "Efficient collocational approach for parametric uncertainty analysis." Communications in Computational Physics **2**(2): 293-309.
- Xiu, D. (2010). Numerical Methods for Stochastic Computations: A Spectral Method Approach, Princeton University Press.
- Xiu, D. and G. Karniadakis (2003). "The Wiener-Askey polynomial chaos for stochastic differential equations." SIAM Journal on Scientific Computing **24**(2): 619-644.
- Xiu, D., Karniadakis, G. (2003). "Modeling uncertainty in flow simulations via generalized polynomial chaos." Journal of Computational Physics **187**(Copyright 2003, IEE): 137-167.
- Ye, B. and F. A. Salustri (2003). "Simultaneous tolerance synthesis for manufacturing and quality." Research in Engineering Design **14**(2): 98-106.
- You, X. (2008). GapSpace multi-dimensional assembly analysis, The University of North Carolina.
- Yu, K. M., S. T. Tan and M. F. Yuen (1994). "A review of automatic dimensioning and tolerancing schemes." Engineering with Computers **10**(2): 63-80.
- Zhang, C., J. Luo and B. Wang (1999). "Statistical tolerance synthesis using distribution function zones." International Journal of Production Research **37**(17): 3995-4006.
- Zhang, C. and H. P. Wang (1993). "The discrete tolerance optimization problem." Manufacturing review **6**: 60-60.
- Zhang, C. and H. P. Wang (1993). "Integrated tolerance optimisation with simulated annealing." International Journal of Advanced Manufacturing Technology **8**(Copyright 1993, IEE): 167-174.
- Zhang, C. and H. P. Wang (1997). "Robust design of assembly and machining tolerance allocations." IIE transactions **30**(1): 17-29.
- Zheng, L. Y., C. A. McMahon, L. Li, L. Ding and J. Jamshidi (2008). "Key characteristics management in product lifecycle management: a survey of methodologies and practices." Proceedings of the Institution of Mechanical Engineers, Part B (Journal of Engineering Manufacture) **222**(Copyright 2009, The Institution of Engineering and Technology): 989-1008.
- Zhengshu, S. (2003). "Tolerance analysis with EDS/VisVSA." Transactions of the ASME. Journal of Computing and Information Science in Engineering **3**(Copyright 2003, IEE): 95-99.

- Zhou, C., L. Gao, H. B. Gao and K. Zan (2006). "Particle swarm optimization for simultaneous optimization of design and machining tolerances." Simulated Evolution and Learning: 873-880.
- Zhou, S. and D. Ceglarek (2008). "Variation source identification in manufacturing processes based on relational measurements of key product characteristics." Journal of Manufacturing Science and Engineering **130**: 031007-031001.
- Zienkiewicz, O. C., R. L. Taylor and J. Z. Zhu (2005). The Finite Element Method: Its Basis And Fundamentals, Elsevier Butterworth-Heinemann.
- Zitzler, E. and L. Thiele (1999). "Multiobjective evolutionary algorithms: A comparative case study and the strength pareto approach." Evolutionary Computation, IEEE Transactions on **3**(4): 257-271.
- Zou, Z. and E. P. Morse (2004). "A gap-based approach to capture fitting conditions for mechanical assembly." Computer-Aided Design **36**(8): 691-700.